THE ROLES OF SH2-CONTAINING INOSITOL 5'-PHOSPHATASE 1 (SHIP1) AND SIGNAL TRANSDUCER AND ACTIVATOR OF TRANSCRIPTION 3 (STAT3) IN INTERLEUKIN-10 REGULATION OF ACTIVATED MACROPHAGES

by

Tsz Ying Sylvia Cheung

B.Sc, The University of British Columbia, 2009

A THESIS SUBMITTED IN PARTIAL FULFILLMENT OF THE REQUIREMENTS FOR THE DEGREE OF

DOCTOR OF PHILOSOPHY

in

The Faculty of Graduate and Postdoctoral Studies

(Biochemistry and Molecular Biology)

THE UNIVERSITY OF BRITISH COLUMBIA

(Vancouver)

October 2016

Abstract

Inflammation is a protective mechanism against infection, but it must be appropriately regulated to prevent pathological consequences including inflammatory diseases. Interleukin-10 (IL-10) is a key anti-inflammatory cytokine that inhibits the activation of many immune cell types, including the macrophage, to prevent exaggerated immune responses. Understanding the signalling pathway downstream of IL-10 and IL-10 receptor (IL-10R) is essential in developing therapeutics to treat inflammatory diseases. Canonically, IL-10R signalling is described as solely depending on the activation of the transcription factor STAT3 and the expression of STAT3-response genes. However, our laboratory has previously shown that IL-10 also activates the inositol 5'-phosphatase SHIP1 to mediate its anti-inflammatory responses, such as inhibiting the expression of pro-inflammatory cytokines. Moreover, we have now found that IL-10 is able to inhibit expression of miRNA-155 (miR-155) in macrophages activated by the bacterial product lipopolysaccharide (LPS). This inhibition by IL-10 requires both STAT3 and SHIP1, and occurs at the maturation step, but not at the transcription step, of miR-155. Consistent with SHIP1's involvement in IL-10 function, a previously described SHIP1 activator, AQX-MN100, mimics IL-10 and inhibits LPS-induced miR-155. Next, we investigated the roles of STAT3 and SHIP1 in IL-10 regulation of global gene expression in activated macrophages. Among the genes identified as IL-10 regulated, we have found different subsets of genes potentially to be SHIP1-regulated, STAT3-regulated, and SHIP1-STAT3 regulated.

Considering the importance of SHIP1 activation in IL-10 function, SHIP1 activators provide an alternate way to control inflammation. We have previously shown

that SHIP1 activators bind to SHIP1's C2 domain and regulate SHIP1 enzymatic activity allosterically. Using x-ray crystallography, we obtained the crystal structure of SHIP1's phosphatase and C2 domains, the minimal region necessary for allosteric activation by SHIP1 activators. Analysis of the crystal structure revealed differences between SHIP1 and related phosphatases. Biochemical and biophysical methods have been employed to identify amino acid residues potentially interacting with SHIP1 activators.

Together, this work strengthens the model that STAT3 and SHIP1 work together to mediate the anti-inflammatory function of IL-10. We also described the structure of SHIP1, providing the first step in rational drug design to generate better small molecule SHIP1 activators.

Preface

Contributions:

The design of all research, data analysis and manuscript preparation were completed with the assistance of Dr. Alice Mui. All experiments were performed by the author with the following exceptions:

Chapter 3:

The pGL3- IkBζ promoter luciferase reporter construct was generated by Eva So, who also assisted in performing the luciferase reporter assay. The SHIP1 siRNA, STAT3 siRNA and SCRMB siRNA transduced cell lines were previously generated by Dr. Andrew Ming-Lum and Gary Golds.

Chapter 4:

Experiment using the continuous flow apparatus was performed by Joanna Chan. The J2M KO:SHIP1 WT and J2M KO:SHIP1 Y190F cell lines were generated by Soroush Shakibakho, and the TNF production assays using these cell lines were performed by Kamaldeep Kaur Jawanda. The mRNA microarray was performed by Anne Haegert from the Vancouver Prostate Centre's Laboratory for Advanced Genome Analysis facility.

Chapter 5:

The generation of bacterial expression plasmids, expression and purification of proteins were performed with the assistance of Eun-Jung Kim, Lauren Coombe, Melissa Ng, Alix Thomson, Udit Dalwadi, Lisa Lee and Lucy Mei. The *in vitro* phosphatase assays were performed with the assistance of Alix Thomson, Lisa Lee and Kevin Chung. The crystal structures were solved with the assistance of Dr. Bernd Gardill and Dr. Filip

Van Petegem. The STD-NMR experiments were performed by our collaborators, Dr. Raymond Andersen and Dr. David Williams.

List of Publication:

The data presented in Chapter 3 have been published: Cheung, S.T., So, E.Y., Chung, D., Ming-Lum, A., and Mui, A.L. (2013) Interleukin-10 Inhibits Lipopolysaccharide Induced miR-155 Precursor Stability and Maturation. *PloS ONE* **8**(8): p. e71336.

Ethics Approval:

All biohazardous experiments were performed in accordance with the Health Canada, Laboratory Biosafety Guidelines under protocols B12-0012 and B15-0187. All animal experiments were performed in accordance with the UBC Animal Care Committee guidelines under the following protocols:

SHIP1 KO mouse colony:	A13-0203
Harvest of tissues and cells:	A11-0218

Table of Contents

Abstract ..... **ii**

Preface ..... **iv**

Table of Contents ..... **vi**

List of Tables ..... **ix**

List of Figures ..... **x**

List of Abbreviations ..... **xii**

Acknowledgements ..... **xvi**

Dedication ..... **xviii**

Chapter 1: Introduction **1**

1.1. Inflammation **2**

1.2. Macrophages **5**

1.2.1. Macrophage activation by TLR ligands 6

1.3. Lipopolysaccharide (LPS) **8**

1.3.1. Toll-like receptor 4 (TLR4) signalling 9

1.3.2. Negative regulation of TLR4 signalling 12

1.4. microRNAs (miRNAs) **14**

1.4.1. miRNA biogenesis 15

1.4.2. miRNA functions 20

1.4.3. miRNAs in immune cells 23

1.4.4. miRNA-155 24

1.5. Interleukin-10 (IL-10) **31**

1.5.2. IL-10 signalling 33

1.6. Signal transducer and activator of transcription 3 (STAT3) **36**

1.6.1. STAT3 functions in immune system **36**

1.6.2. STAT3's role in IL-10 signalling **37**

1.7. SH2-containing inositol-5´-phosphatse 1 (SHIP1) **39**

1.7.1. SHIP1 structure 40

1.7.2. SHIP1 functions in immune cells 42

1.7.2.1. SHIP1 function in B cell activation 42

1.7.2.2. SHIP1 function in T cell activation 43

1.7.2.3. SHIP1 function in NK cells function 43

1.7.2.4. SHIP1 function in mast cells 44

1.7.2.5. SHIP1 function in macrophages 44

1.7.3. SHIP1 regulation 45

1.7.4. SHIP1 in diseases 47

1.8. Objectives and aims **49**

Chapter 2: Materials and Methods **52**
2.1 Cells and reagents **53**
2.2 Mouse colonies **54**
2.3 Plasmids **55**
2.3.1 Mammalian expression plasmids 55
2.3.2 Bacterial expression plasmids 56
2.4 Lentivirus production and transduction **57**
2.5 Cell stimulation **57**
2.6 Luciferase reporter analysis **58**
2.7 Fractionation of nuclear and cytoplasmic RNA **58**
2.8 Immunoblot analysis **58**
2.9 RNA extraction and real-time quantitative PCR **59**
2.10 RT-PCR of pri-miR-155 for DNA sequencing analysis **59**
2.11 Measurement of TNFα production level **60**
2.12 Continuous flow system **60**
2.13 *In vitro* pull down assay **61**
2.14 mRNA microarray **61**
2.15 Identification of SHIP1, STAT3 regulated genes **62**
2.16 Protein expression and purification **63**
2.16.1 HEK293T expression system 63
2.16.2 Bacterial expression system 63
2.17 *In vitro* phosphatase assay **65**
2.18 Protein crystallization, data collection, phasing and refinement **66**
2.19 Protein lipid overlay (PLO) assay **68**
2.20 Saturation transfer difference nuclear magnetic resonance (STD-NMR) **69**
2.21 Isothermal titration calorimetry (ITC) **69**
2.22 Statistical analysis **70**

Chapter 3: LPS and IL-10 Regulate miR-155 at the Maturation Step in Macrophages **71**
3.1. Introduction **72**
3.2. Results **74**
3.2.1. IL-10 inhibits LPS-induced pri-miR-155 and miR-155 expression in macrophages 74
3.2.2. LPS and IL-10 do not regulate miR-155 at the level of transcription 75
3.2.3. Pri-miR-155 is constitutively transcribed but maintained at low level via degradation mechanism. 78
3.2.4. LPS and IL-10 do not cause editing of pre-miR-155 79
3.2.5. LPS and IL-10 do not regulate nuclear export of pre-miR-155 79
3.2.6. IL-10 inhibits LPS induction of miR-155 via SHIP1 and STAT3 82
3.3. Discussion **87**

Chapter 4: STAT3 and SHIP1 Work Together to Mediate IL-10 Functions 91
4.1. Introduction..... 92
4.2. Results..... 95
4.2.1 Both STAT3 and SHIP1 mediate IL-10 inhibition of LPS-induced TNFα production. 95
4.2.2 Physical interaction of SHIP1 and STAT3 96
4.2.3 Y190F mutation on SHIP1 abolishes IL-10's ability to inhibit TNFα 97
4.2.4 SHIP1 and STAT3 co-regulate a number of IL-10 regulated genes. 100
4.3. Discussion 124

Chapter 5: Crystal Structure of SHIP1 Fragment Reveals Insight into SHIP1 Activator Binding..... 130
5.1 Introduction 131
5.2 Results..... 133
5.2.1 The minimal enzymatic region of SHIP1 contains the phosphatase and C2 domains. 133
5.2.2 Crystal structure of PAC 139
5.2.1.1 Overall structure 141
5.2.1.2 Phosphatase domain 142
5.2.1.3 C2 domain..... 149
5.2.1.4 Phosphatase-C2 interface 154
5.2.3 Binding of SHIP1 activators to SHIP1..... 158
5.3 Discussion 164

Chapter 6: Conclusions 170
6.1. Conclusions..... 171

References..... 179

Appendices..... 214

List of Tables

Table 1.1: Negative regulation of TLR4 signalling 13

Table 1.2: Regulation of miRNA biogenesis 18

Table 1.3: Validated targets of miR-155 25

Table 4.1: SHIP1-regulated genes identified after 0.5-hour stimulation of LPS and LPS+IL-10 in SHIP1 WT and SHIP1 KO macrophages 102

Table 4.2: Comparison of expression profiles of Lang *et al.* identified IL-10/STAT3-regulated genes in SHIP1 WT and SHIP1 KO cells. 106

Table 4.3: Enriched pathways identified by NetworkAnalyst using Reactome database 111

Table 4.4: Microarray data of previously described SHIP1-regulated genes. 113

Table 4.5: TargetScan analysis of SHIP1, STAT3, SHIP1-STAT3 gene subsets 123

Table 5.1: Data collection and refinement statistics 140

Table A.1: Primers used in qPCR 215

Table A.2: Site-directed mutagenesis primers 217

Table A.3: Ligase-independent cloning primers 218

Table A.4: Results of SERp server 220

List of Figures

Figure 1.1 LPS/TLR4 signalling. 8

Figure 1.2 Biogenesis of miRNA. 17

Figure 1.3 The structure of SHIP1 and its binding partners. 40

Figure 3.1 IL-10 inhibits LPS induction of pri-miR-155 and miR-155 expression in macrophages. 75

Figure 3.2 IL-10 does not regulate miR-155 expression at the transcription level. 77

Figure 3.3 LPS and IL-10 do not cause editing on the pre-miR-155 sequence. 79

Figure 3.4 IL-10 does not affect the export of pre-miR-155 from the nucleus to the cytoplasm. 81

Figure 3.5 SHIP1 mediates IL-10 inhibition of miR-155. 85

Figure 3.6 SHIP1 and STAT3 play additive roles in IL-10 inhibition of miR-155. 86

Figure 4.1 Deficiency in STAT3 or SHIP1 results in impaired IL-10 inhibition in the first peak of TNFα production, but not the second peak. 96

Figure 4.2 His_6-SHIP1 does not bind to Flag-STAT3 in an *in vitro* pulldown assay. . 97

Figure 4.3 Location of the mutated tyrosine in SHIP1 sequence. 98

Figure 4.4 SHIP1 Y190F impairs IL-10 inhibition of TNFα in activated macrophages. 99

Figure 4.5 Identification of candidate SHIP1-STAT3 regulated genes. 108

Figure 4.6 Interacting genes in the SHIP1-regulated gene subset. 110

Figure 4.7 Real time PCR revealed that many of the IL-10 regulated genes require SHIP1 and STAT3. 119

Figure 5.1 PPAC and PAC have similar enzymatic activity as full length SHIP1. ... 135

Figure 5.2 AQX-MN100 is able to enhance the enzymatic activity of PPAC and PAC. 136

Figure 5.3 Calcium reduces basal enzyme activity but enhances activation by SHIP1 activators. 138

Figure 5.4 Structures of wild type PAC2 and PAC1cc. 142

Figure 5.5 Sequence alignments of mouse phosphoinositol-5'-phosphatases. 144

Figure 5.6 Superposition of mouse SHIP1, human INPP5B and human SHIP2 phosphatase domains. 147

Figure 5.7 Position of LC1R and LC2R in mouse SHIP1 or INPP5B phosphatase domains. 149

Figure 5.8 Structures of C2 domains. 150

Figure 5.9 SHIP1 C2 domain does not contain the polybasic cluster as other C2 domains. 153

Figure 5.10 The interface between phosphatase domain and C2 domain. 155

Figure 5.11 Potential AQX-MN100 binding sites in PAC. 157

Figure 5.12 SHIP1 binds to both PI(3,4)P_2 and PI(3,4,5)P_3 through its C2 domain. .. 159

Figure 5.13 Binding of AQX-151 and PI(3,4)P_2 to C2 domain by STD-NMR. 161

Figure 5.14 No binding of AQX-1125 or PI(3,4)P_2-diC8 to PAC1 is detected by ITC. 163

Figure A.1 The BIC promoter reporter is unresponsive to LPS and IL-10. 218

Figure A.2 CHX treatment alters the expression level of GAPDH and actin, but not that of 18S rRNA. 219

Figure A.3 4-HT treatment in the AKT-ER cells increases phosphorylation of GSK3β. 220

List of Abbreviations

4-HT	4-hydroxytamoxifin
AGO	Argonaute
AMBP	alpha-1-microglobulin/bikunin precursor
AML	Acute myeloid leukemia
AMPK	AMP-activated protein kinase
AP-1	Activator protein 1
ARE	AU-rich element
ATF1	Activating transcription factor 1
BCR	B cell receptor
BCR/ABL	Breakpoint cluster region/Abelson virus oncogene
BIC	B cell integration cluster
BMDM	Bone marrow derived macrophage
BRCA	Breast cancer (e.g. BRCA1)
BTK	Bruton’s tyrosine kinase
CBR	Calcium binding region
CCL	C-C motif chemokine ligand (e.g. CCL2)
CD	Custer of differentiation (e.g. CD14)
ChIP	Chromatin immunoprecipitation
CREB	cAMP-responsive-element binding protein
CRLF2	Cytokine receptor-like factor 2
CSF-1	Colony stimulating factor-1
CXCL	Chemokine (C-X-C motif) ligand (e.g. CXCL2)
DAG	Diacylglycerol
DAMP	Damage-associated molecular pattern
DCP	Decapping protein
DGCR8	DiGeorge syndrome chromosoal region 8
DMEM	Dulbecco's Modified Eagle Medium
Dox	Doxycycline
eIF	Eukaryotic initiation factor
ER	Estrogen receptor
Ets	E26 transformation specific
EXP5	Exportin-5
FCS	Fetal calf serum
FcγR	Fcγ-receptor
FOXP3	Forkhead box P3
FZD7	Fizzled class receptor 7
GPR35	G protein-coupled receptor 35

HDAC	Histone deacetylase
IBD	Inflammatory bowel disease
ICAM	Intracellular adhesion molecule
IFN	Interferon
IKK	IκB kinases
IL	Interleukin (e.g. IL-6, IL-10)
ILK	Integrin-linked kinase
IMDM	Iscove's modified Dulbecco's media
IP_3	Inositol-1,3,4-trisphosphate
IP_4	Inositol-1,3,4,5-tetrakisphosphate
IRAK	IL-1-receptor-associated kinase
IRES	Internal ribosome entry site
IRF	Interferon regulatory factor 3
ITAM	Immune receptor tyrosine-based activation motif
ITIM	Immune receptor tyrosine-based inhibition motif
IκB	Inhibitor of κ light chain gene enhancer in B cells
Jak1	Janus kinase 1
JNK	c-Jun N-terminal kinase
KHSV	Kaposis sarcoma-associated herpesvirus
KO	Knockout
KSRP	KH-type splicing regulatory protein
LBP	LPS-binding protein
LC1R	Lipid chain 1 recognition
LIC	Ligase-independent cloning
LPS	Lipopolysaccharide
LysM	lysozyme M
M1	classically activated macrophage
M2	alternatively activated macrophage
MAPK	Mitogen-activated protein kinase
MCH	Major histocompatibility complex
MDSC	Myeloid-derived suppressor cell
MDV	Marek's disease virus
miRNA	microRNA
MyD88	Myeloid differentiation primary response gene 88
NFκB	Nuclear factor κ B
P4IM	P4-interacting motif
PABP	Polyadenylate-binding protein
PAC	Phosphatase-C2

PAMP	Pathogen-associated molecular pattern
PBS	Phosphate buffered saline
Perimacs	Peritoneal macrophages
PH	Pleckstrin homology
PI(3,4,5)P3	Phosphatidylinositol-3,4,5-trisphosphate
$PI(3,4)P_2$	Phosphatidylinositol-3,4-bisphosphate
$PI(4,5)P_2$	Phosphatidylinositol-4,5-bisphosphate
PI3K	Phosphoinositide 3-kinase
PKB	Protein kinase B
PRR	Pattern recognition receptor
PRR	Proline-rich region
PTEN	Phosphatase and tensin homolog
PX	Phox homology
RA	Rheumatoid arthritis
RIP1	Receptor-interacting protein 1
RISC	RNA-inducing silencing complex
RNS	Reactive nitrogen species
ROS	Reactive oxygen species
SDS	Sodium dodecyl sulphate
SH2	Src-homology 2
SHIP1	SH2-containing inositol-5'-phosphatase 1
SMAD	Sma and Mad related protein
SNP	Single nucleotide polymorphism
SOCS1	Suppressor of cytokine signalling 1
SP	Specificity protein (e.g. SP1, SP2)
STAT	Signal transducer and activator of transcription
T2D	Type 2 diabetes
TAB	TAK1-binding protein
TAK1	TGFβ-activated kinase 1
TANK	TRAF family member-associated NFκB activator
TBK	TANK binding kinase
TCR	T cell receptor
TGF	Transforming growth factor
Th	T cell helper (e.g. Th1, Th2)
TIR	Toll/interleukin-1 receptor
TIRAP	TIR domain containing adaptor protein
TLR	Toll-like receptor
TNFα	Tumour necrosis factor alpha

TRAF6	TNF receptor-associated factor 6
TRAM	TRIF-related adaptor molecule
TRBP	Transactivating response RNA-binding protein
Treg	Regulatory T cell
TRIF	TIR-domain-containing adapter-inducing interferon-β
Tyk2	Tyrosine kinase 2
UBC13	Ubiquitin-conjugating enzyme 13
UEV1A	Ubiquitin-conjugating enzyme E2 variant 1 isoform A
UTR	Untranslated region
WT	Wild type

Acknowledgements

This dissertation would not have been possible without the help and support of many people. First and foremost, I would like to express the deepest appreciation to my supervisor, Dr. Alice Mui, who has always believed in me and constantly driven me to go beyond what I thought is the limit. Her persistent encouragement and guidiance are invaluable in my doctoral studies. Secondly, sincere thanks to the members of my supervisory committee, Dr. Filip Van Petegem and Dr. Eric Jan, who provided priceless input and recommendations to my studies throughout the years. An additional thanks to Dr. Filip Van Petegem, who not only made an impact in my graduate studies, but also supported me tremendously in my undergraduate thesis. While Dr. Franck Duong and Dr. Guy Tanantzapf research on fields unrelated to my doctoral studies, I am thankful for having them as my co-op supervisors in my undergraduate years; the time I spent in their labs have inspired me to pursue graduate studies and continue my dream to be a competent scientist.

Thank you to all the past and present members in the Mui lab, especially the undergraduate students (aka, my minions), who tirelessly contributed to reagent preparation and data acquisition, as well as fulfilled my occasional requests for holiday decorations in the lab. My thanks are extended to the members of the Van Petegem lab, who quickly took me as one of them and granted me the title of “honorary lab member”.

To my science friends, your insightful suggestions in my studies have been wonderful, and your endless support and encouragement have helped me through some of the most stressful days in this PhD journey. To my non-science friends, thank you for

being patient and tolerant of my countless “5 more minutes”, and for boosting my confidence and lifting my spirits whenever I doubt myself.

My family is clearly my biggest supporter, to whom I will forever be in debt. They take care of me in every way possible so I can focus all my energy on my studies. Thank you for always loving me, even when I am being unreasonable and unpleasant to live with at times. You are awesome and I love you with all my heart.

Getting a PhD is certainly the hardest things I have ever done, and will be one of the most challenging things I will ever do in my life, but I have no regret about the decision to participate in this path. It has been an eye-opening and inspiring journey. Not only have I grown as a scientist, but I have also grown as a person – a stronger and better person who understands her values and dreams more than ever. Because of this, I thank myself for not giving up and for soldiering on even in the most stressful times.

謹將此博士論文獻給我的外婆

Chapter 1: Introduction

1.1. Inflammation

Inflammation is a complex physiological process involving both the immune and the circulatory systems, whose main activities are to protect the host from invading pathogens, and to repair damaged tissues. The symptoms of inflammation were first described in the first century as pain, heat, redness and swelling, and later in the 1800s, loss of function was added as the fifth symptom [1,2]. Since then, considerable efforts have been put into understanding the source, the process and the resolution of inflammation. Despite being a protective response, deregulated inflammation is associated with various inflammatory/immune disorders and diseases. Today, partly due to a change of lifestyle in developed countries, we see a rise in various inflammation-related diseases such as inflammatory bowel diseases (IBD) and Type 2 diabetes (T2D). Studies have found that westernized lifestyle, such as increased sugar and animal protein intake may increase the risk of developing IBD [3-5], while elevated sugar and fatty acids, along with a sedentary lifestyle, produces a chronic inflammatory state that underlies T2D [6-10]. Thus, understanding the cellular and molecular mechanisms of inflammation has become more urgent than ever.

Inflammatory response involves four stages that are characterized by: (1) inflammatory stimuli, (2) sensor cells, (3) inflammatory mediators produced by the sensor cells, and (4) the affected tissues [11]. Inflammatory stimuli can be categorized into exogenous and endogenous. Examples include pathogen-associated molecular patterns (PAMPs) [12-14] and damage-associated molecular patterns (DAMPs) [15-17]. PAMPs are conserved molecules commonly expressed on specific groups of pathogens, while DAMPs are host molecules, many of which are cytosolic and nuclear proteins that

are only released outside of the cells during tissue injury. PAMPs or DAMPs are sensed by specific receptors on the surface of resident mast cells and macrophages, which become activated and secrete soluble pro-inflammatory mediators that cause vasodilation and increased permeability of the blood vessels in the local area. These mediators include cytokines such as tumour necrosis factor α (TNFα), interleukin-1 (IL-1), IL-6, IL-8 and IL-12, chemokines such as chemokine (C-C motif) ligand 2 (CCL2) and CCL3, as well as other non-protein factors such as histamine, prostaglandins and reactive oxygen and nitrogen species (ROS/RNS) [11]. The consequence is an increase in blood flow to the area and the entrance of blood plasma to the damaged tissue. Concurrently, the expression of adhesion molecules is upregulated on the luminal surface of the endothelial cell layer. Circulating leukocytes including neutrophils and monocytes in the blood establish interaction with these adhesion molecules that slow down their movement, and cause them to roll along the endothelial wall [18]. These leukocytes eventually leave the blood vessels to enter the tissue and migrate to the affected site following a chemotactic gradient [19,20]. The recruited leukocytes are activated by secreted cytokines, mainly TNFα, and together with plasma components such as complement proteins and antibodies, kill the invading pathogens or clear damaged cells. Successful removal of the inflammatory stimuli switches on the tissue repair mechanism, whereas failure leads to the initiation of adaptive immune response [21,22].

Overall, inflammation is beneficial to the host. However, the degree of inflammation needs to be tightly regulated to prevent pathologies from arising. On one hand, too little inflammation impairs the ability of our immune cells to remove harmful stimuli (e.g. bacterial infection) leading to persistent sickness or progressive tissue

destruction. On the other hand, excessive inflammation is destructive. The inflammatory mediators secreted by activated leukocytes are harmful to healthy tissues when persistent. For example, the process of acute systemic inflammation can result in over-accumulation of neutrophils and macrophages in organs causing dysfunctionality and even death [23,24]. Chronic inflammation in the colon causes IBD [25], and that in the joints causes rheumatoid arthritis (RA) [26]. The pathogenesis of atherosclerosis also involves inappropriate inflammation in which macrophages are activated by excess lipid uptake [27,28]. Inflammation must be properly restrained to avoid the development of these diseases. Negative regulation of inflammation occurs at several levels. The first one is the prevention of inflammatory stimuli from interacting with the receptors. For example, PAMPs can be sequestered by the expression of soluble receptors [29-31]. The second level of regulation to terminate the inflammatory signalling pathways is via the production of cytosolic signalling inhibitors [32-34]. The third level involves the inhibition of pro-inflammatory cytokine expression through transcriptional and post-transcriptional controls. Transcriptional control includes the inactivation of transcription factors important in inflammation [35-39], the expression of transcription repressors [40-43], or chromatin remodeling [44,45]. In addition, RNA binding proteins [39,46,47] and microRNAs [48-50] constitute the repertoire of post-transcriptional control. The fourth level of negative regulation includes the production of decoy receptors [51,52] and receptor antagonists [53]; pro-inflammatory cytokines are prevented from initiating inflammatory pathways inside the cells. The next layer of regulation is the production of anti-inflammatory cytokines such as IL-10 and transforming growth factor β (TGFβ) [11]. These negative regulators inhibit inflammation on multiple levels. Examples include the

inhibition of TNFα production by IL-10 [36,46,54-56], and the expression of IL-1 receptor antagonist (IL1Ra) by IL-10 [57,58].

1.2. Macrophages

Macrophages play a key role in inflammation [59-62]. They belong to the innate immune system, and provide an immediate response to invading pathogens in three main ways: phagocytosis and digestion of engulfed pathogens, production of pro-inflammatory cytokines and chemokines that activate and recruit other immune cells to the affected tissues, and presentation of antigens derived from digested pathogens to stimulate T cell activation and proliferation [63-65]. Macrophages also participate in the homeostasis of our body by removing apoptotic cells in the blood such as red blood cells [65].

Different subsets of macrophages have been described. While the first classification divided macrophages into two types depending on their activation states: the "classically" activated (M1) macrophages and the "alternatively" activated (M2) macrophages, it has been greatly revised, and a more complicated and nuanced model exists [65-68]. The M1-M2 paradigm arose from observations that interferon-γ (IFNγ) and IL-4 elicited different reactions from macrophages *in vitro*. Macrophages activated by IFNγ or ligands of Toll-like receptors (TLRs) such as lipopolysaccharide (LPS) express pro-inflammatory cytokines including IL-1, IL-6 and TNFα, as well as ROS and RNS [69]. Originally referred to as M1 type macrophages, these cells also upregulate the expression of major histocompatibility complex class II (MHC II) and antigen presentation molecules on the surface, both of which are essential for activating the adaptive immune system. While M1 macrophages are responsible for the inflammatory response, another type of macrophages is derived by IL-4, IL-13 or glucocorticoid

treatment, and expresses relatively higher level of IL-10 that inhibits inflammation [70,71]. Initially called M2 type macrophages, these cells are associated with antagonizing inflammation and enhancing tissue repair response. However, it has been shown that the M1 and M2 classifications are not mutually exclusive, and that they often co-existed. Added to the complication in macrophage classification is the ability of macrophages to switch between the different activation states [72]. Moreover, a recent non-biased transcriptome based analysis showed that macrophages existed in an activation "spectrum" with M1 (IFNγ treated) and M2 (IL-4 treated) at the two ends, instead of discrete activation states [73]. To this end, two proposals have been suggested to revise and unify the nomenclatures in the macrophage system to reflect the diverse phenotypes that macrophages can adapt [68,74,75]. One proposal suggested the nomenclature to be based on the origin of macrophages, the source of activation and the expression of surface markers [68], and the other proposal suggested an ontology based approach [74,75].

1.2.1. Macrophage activation by TLR ligands

Macrophages express different pattern recognition receptors (PRRs) that recognize different PAMPs and DAMPs. Among PPRs, Toll-like receptors (TLRs) are probably the most studied [76]. There are 10 different TLRs in human (TLR1 to TLR10) and 12 in mouse (TLR1 to TLR9 and TLR11 to TLR14), and each of them recognizes different PAMPs, including lipids, nucleic acids, carbohydrate and peptides, either on their own or in partnership with another TLR [77]. Some TLRs (e.g. TLR1, TLR2 and TLR4) reside on the cell surface, whereas the others are localized at the membranes of endosomes (e.g. TLR3, TLR7, TLR8 and TLR9).

TLRs belong to the interleukin-1 receptor/toll-like receptor superfamily, defined by the presence of a Toll-IL-1 receptor (TIR) domain at the cytosolic side of the receptor [78] (**Figure 1.1**). TLRs also have a leucine-rich extracellular domain and a transmembrane domain. Upon recognition of PAMPs, TLRs recruit different TIR-domain-containing adaptor proteins such as myeloid differentiation primary response 88 (MyD88), TIR-domain-containing adaptor-inducing interferon-β (TRIF), TIR-domain containing adaptor protein (TIRAP) and toll-like receptor 4 adaptor protein (TRAM), and activate downstream molecules that eventually lead to the expression of pro-inflammatory mediators [79]. Depending on the adaptor proteins recruited, these signalling events can be divided into either MyD88-dependent or MyD88-independent pathways. Although both of these pathways lead to the activation of nuclear factor kappa B (NFκB) and mitogen-activated protein kinases (MAPK), the consequence is somehow different. The MyD88-dependent pathway is associated with the expression of pro-inflammatory cytokines, while the MyD88-independent pathway mediates the expression of Type I interferons.

TLRs have a crucial role in macrophage activation and infection control. Macrophages lacking TLRs or the adaptor proteins show hyposensitivity to pathogenic ligands and defective activation [80,81], and TLRs (or MyD88) knockout mice have an inability to clear infections [81-83].

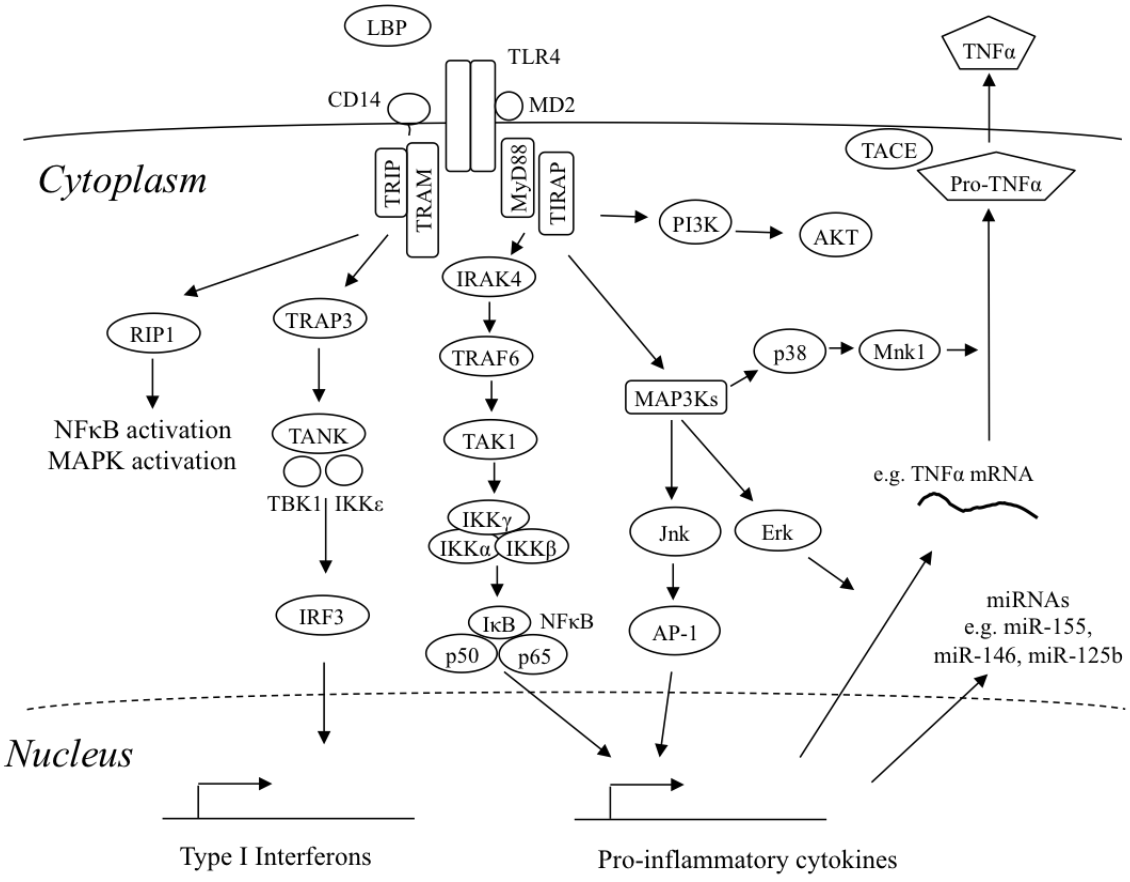

Figure 1.1 LPS/TLR4 signalling.
LPS binding to TLR4 is facilitated by LBP, CD14 and MD2. Both MyD88-dependent and MyD88-independent pathways are activated, leading to the expression of pro-inflammatory cytokines (such as TNFα), Type I interferons, as well as microRNAs.

1.3. Lipopolysaccharide (LPS)

LPS is a major component of the outer membrane of Gram-negative bacteria, and it has a vital role in the viability of the bacteria. LPS contributes to the structural integrity of the bacteria by increasing the negative charge of the membrane and stabilizing the membrane structure, as well as protects the bacterial membrane from certain chemical attacks [84]. Liberated LPS from dying bacteria or multiplying bacteria binds strongly to the TLR4 complex on immune cells such as macrophages, and initiates inflammatory responses [85].

LPS has a molecular mass of 10-20 kDa, and its structure consists of a lipid component called lipid A, a core oligosaccharide and an O antigen [84]. The O antigen is the outermost domain of LPS, and is a repetitive glycan polymer consisting of one to eight glycosyl residues. The composition of the O antigen varies among different bacterial strains. Because the O antigen is exposed to the environment, it can be recognized by host antibodies and confers the immunogenicity of LPS. The core oligosaccharide is attached to the O antigen, and commonly contains sugar such as 3-deoxy-D-mannococtulosonic acid and heptose, as well as non-carbohydrate components including phosphate and amino acids. The lipid A is made up of a phosphorylated glucosamine disaccharide core that is covalently linked to multiple fatty acids. These fatty acids anchor the molecule to the bacterial membrane while the rest of the molecule projects out to the environment. The lipid A moiety is very conserved and is responsible for activating immune cells by binding to TLR4 [85].

1.3.1. Toll-like receptor 4 (TLR4) signalling

LPS does not directly bind to TLR4, but instead requires additional proteins. The first protein that LPS interacts with is the LPS-binding protein (LBP) [86]. LBP is a soluble lipid transferase that transfers LPS to CD14, a glycoprotein anchored into the host cell membrane [87]. CD14 then facilitates the transfer of LPS to the TLR4/MD-2 complex. MD-2 is a soluble protein that non-covalently associates with TLR4 and enables responsiveness to LPS [88]. TLR4 then undergoes oligomerization and triggers a cascade of signalling events via the TIR domain in its cytoplasmic tail [85]. Depending on the identities of the recruited adaptor proteins, TLR4 downstream signalling can be divided into MyD88-dependent and MyD88-independent pathways [89-91] **(Figure 1.1)**.

In the MyD88-dependent pathway, MyD88 and TIRAP are recruited to the activated TLR4 through the TIR domain. MyD88 contains a death domain, and the death domain-containing IL-1-receptor-associated kinase-4 (IRAK-4) is recruited to the membrane where it is phosphorylated and activated [92]. IRAK-4 subsequently recruits and activates additional IRAKs including IRAK1 [93] and IRAK2 [94]. The IRAK4-IRAK1/2 complex dissociates from the receptor and activates TNF receptor-associated factor 6 (TRAF6), which then associates with ubiquitin-conjugating enzyme 13 (UBC13) and ubiquitin-conjugating enzyme E2 variant 1 isoform A (UEV1A) and becomes activated by Lys63-linked polyubiquitin chain [95]. TRAF6 subsequently activates transforming growth factor-β-activated kinase 1 (TAK1) [96]. TAK1 is involved in the activation of NFκB via the induction of IκB kinases (IKKs). IKKα, IKKβ and IKKγ form a complex and phosphorylate inhibitor of κ light chain gene enhancer in B cells (IκB) proteins. Phosphorylated IκB is then ubiquitinated and degraded by the proteasome, leading to the translocation of the transcription factor NFκB to the nucleus [97]. TAK1 also activates the p38 MAPK pathway and the subsequent induction of another transcription factor, activator protein 1 (AP-1) [98]. The activation of these transcription factors controls expression of pro-inflammatory cytokines, such as TNFα.

In the MyD88 independent pathway, TRIF is recruited to TLR4 via the adaptor protein TRAM [99,100]. TRIF then recruits TRAF3, which in turn associates with TRAF family member-associated NFκB activator (TANK), TANK binding kinase 1 (TBK1) and IKKε to mediate the activation of interferon regulatory factor 3 (IRF3) [101]. IRF3 is a transcription factor that controls the expression of Type 1 interferons such as IFNα and IFNβ [37]. TRIF also activates receptor-interacting protein 1 (RIP1) through TRAF3.

RIP1 is not involved in IRF3 activation, but is responsible for the activation of NFκB and MAPK pathways [102].

Figure 1.1 depicts a schematic diagram of TLR4 singalling and includes important signalling mediators in both MyD88-dependent and independent pathways. However, the real picture is more complicated. For example, TRIF interacts with TRAF6 or TBK, and these two interactions differentially regulate NFκB and IRF3 activation [103]. In addition, there are reports showing that TLR4 signalling leads to the activation of phosphoinositide 3-kinase (PI3K), involving MyD88 or TRIF [104-106], although the details of the mechanism are not well defined. Upon activation, PI3K is recruited to the plasma membrane, where it converts phosphatidylinositol-4,5-phosphate, $PI(4,5)P_2$, into phosphatidylinositol-3,4,5-phosphate, $PI(3,4,5),P_3$, which then acts as second messenger and recruits pleckstrin homology (PH) domain or phox homology (PX) domain containing proteins. These include Bruton's tyrosine kinase (BTK) [107], integrin-linked kinase (ILK) [108] and protein kinase B (PKB, also known as AKT) [109-112]. These proteins are then activated and initiate signalling cascades that mediate cell growth, proliferation, activation and motility. The role of PI3K in TLR signalling has been confusing with reports showing positive and negative contributions (reviewed in [113]).

Besides gene transcription, TLR4 signalling also plays a role in the post-transcriptional regulation of these cytokines. For example, the translation of TNFα mRNA is mediated by the TRIF-dependent MAPK pathway [114]. TLR4 activation also stimulates the production of microRNAs (miRNAs), usually via NFκB activation [115-118]. miRNAs are small non-coding RNAs that regulate gene expression via mRNA

stability and degradation, as well as affecting translation [119]. Examples include miR-155 [120-122], miR-146b [123] and miR-21 [49].

1.3.2. Negative regulation of TLR4 signalling

TLR4 signalling is necessary for pathogen clearance, but it also needs to be tightly regulated to prevent excessive signalling that eventually leads to pathological consequences. Numerous negative regulators of TLR4 signalling have been discovered and their modes of actions can be divided into four categories: dissociation of signalling complex, degradation of signalling proteins, transcriptional control, and post-transcription control [124]. These are summarized in **Table 1.1**. Some of these negative regulators are induced by LPS itself through a negative feedback mechanism (e.g. TRIM30a [125], Ah receptor [42]), while others are induced or further induced by anti-inflammatory cytokines, including IL-10 and TGFβ (e.g. miR-146b [48], miR-187 [126]).

Positive regulators of TLR4 signalling can at the same time have negative roles in TLR signalling. For example, TIRAP can associate with IRF7, but not IRF3, and inhibit its activation [127]. The consequence is a specific blockage of TLR3-induced IFNβ production, while TNFα and IL-6 productions are unaffected [127]. Another adaptor protein, TRIF, has been shown to negatively regulate TLR3, 4 and 5 signalling by causing the degradation of TLRs and inhibition of cytokine production [128-130].

Table 1.1: Negative regulation of TLR4 signalling

Regulators	Description	References
Degradation of signalling molecules		
Atg16L1	negatively regulates TRIF-dependent pathway	[131]
Pin1	binds to phosphorylated IRF3 and promotes its proteasomal degradation	[132]
RAUL	directly ubiqutinates IRF3 and IRF7, leading to their degradation	[133]
TAG	required for TLR4 degradation	[134]
TRIM30a	promotes degradation of TAB2-TAB3-TAK1 signal complex via lysosome	[125]
TRIM38	binds to TRAF6 and promotes K48-linked polyubiqutination for proteasomal degradation	[135]
Dissociation of signalling complexes		
A20	removes K63-linked polyubiquitin chains from TRAF6 and inhibits TLR activation; binds to and inhibits IKK activation by TAK1	[32]
BCAP	interacts with MyD88 and TIRAP	[136]
soluble CD14	diminishes monocyte responses to LPS by transferring cell-bound LPS to lipoproteins	[30]
CD33	binds to CD14 to prevent its downstream signalling	[137]
cylindromatosis (CYLD)	removes K63-linked polyubiquitin chains from TRAF6 and TRAF7 to suppress TLR activation	[138]
DUBA	removes K63-linked polyubiquitin chains on TRAF3, and suppresses TLR-induced type 1 IFN production but does not affect NFκB activation	[139]
Fliih	interacts with MyD88	[140]
IRF4	competes with IRF5 for MyD88 causing inhibition of IRF-5 induced gene expression	[41]
NLRC3	interacts with TRAF6, and attenuates K63-linked ubiqutination of TRAF6 to inhibit NKfB activation	[141]
p38γ and p38δ	MAPK isoforms block ERK activation in macrophages and dendritic cells	[142]
RP105	TLR homologue that lacks signalling domain; directly interacts with TLR4 signalling complex to prevent ligand binding	[143]
SARM	bind to TRIF and block TRIF-TRAM complex formation	[144]
SENP6	deSUMOylates IKKγ and allows deubiquitinase CYLD to remove polyubiquitn chain necessary for function	[145]
SHP	inhibits TRAF6 ubiquitination necessary for its function	[146]
SHP2	binds to the kinase domain of TBK1, and inhibits TRIF-dependent type 1 IFN production	[147]
TAG	competes with TRAM for TRIF binding to inhibit TRIF-dependent pathway	[134]
TAK1	negatively regulates p38 activation	[34]
TANK	binds to TRAF6, and inhibits ubiquitination and thus activation of TRAF6	[148]

Regulators	Description	References
TERM2	transduces inhibitory signal to reduce production of TNFα, IL-12 p70, IL-6 and IL-10	[149]
soluble TLR4	sequesters LPS	[29]
TNFAIP8L2 (TIPE2)	binds to caspase 8 and regulates AP-1 and NFκB activation	[150]
USP4	removes K63-linked polyubiquitin chains from TRAF6 and suppress NFκB activation	[38]
Zc3h12a	removes K63-linked polyubiquitin chains from TRAF6 and suppress NFκB activation	[151]
Transcription control		
Ah receptor	interacts with STAT1 and NFκB in IL-6 promoter and reduces IL-6 production	[42]
ATF3	recruits HDAC1 to pro-inflmmatory cytokine gene promoter; histone deacetylation limits access of transcription factors to inflammatory genes	[44]
Bcl-3	prevents p50 ubiquitination and degradation, and occupies NFκB DNA binding site to limit duration of TLR responses	[152]
IκBδ	inhibits NKκB	[35]
MSK1/2	promotes binding of phosphorylated CREB and ATF1 to promoters of anti-inflammatory cytokines such as IL-10 and DUSP1	[153]
Nurr1	interacts with p65, and represses transcription	[40]
Post-transcription control		
miR-21	targets PDCD4 expression, which has pro-inflammatory functions by regulating NFκB activity and IL-10 production	[49]
miR-146b	targets TRAF6 and IRAK1 mRNA	[48]
miR-155	bidirectional, fine tunes TLR signalling; targets MyD88, TAB2 and IKKε, as well as SHIP1	[154]
miR-187	targets TNFα mRNA stability and translation, and indirectly decreases IL-6 and IL-12p40 expression via downregulation of IκBζ	[126]
TTP	binds to AU-rich elements in TNFα mRNA and promotes mRNA degradation	[43]
Zc3h12a	degrades IL-6 and IL-12p40 mRNA	[155]

1.4. microRNAs (miRNAs)

Discovered approximately two decades ago, miRNAs have been recognized as a new class of regulatory molecules in cells. miRNAs are small non-coding RNAs that regulate target mRNA translation and stability in the cytoplasm. This regulation depends on the association of the miRNAs to mostly the 3'-untranslated region (UTR) of the target

mRNAs [119]. It has been found that instead of one miRNA regulating one mRNA, one miRNA can regulate multiple mRNAs, and that each mRNA can be regulated by multiple miRNAs [156]. The intricate web of miRNA-mRNA interactions makes studying the function of a single miRNA difficult. In addition, while the cytoplasm is the major site of action for miRNAs, emerging studies have found that mature miRNAs can be shuttled back to the nucleus and may play a role in pre-mRNA silencing, epigenetic regulation and alternative splicing [157].

1.4.1. miRNA biogenesis

The biogenesis of miRNAs (**Figure 1.2**) starts with the generation of a long primary miRNA transcript (pri-miRNA) transcribed by RNA polymerase II [158] or RNA polymerase III [159]. Majority of the human miRNA genes are located within the introns of protein-coding or non-coding transcripts, but some are encoded by exonic regions [160], indicating that miRNAs may be transcribed in parallel with mRNA transcripts. There are also miRNAs that are expressed as their own transcripts.

Maturation of pri-miRNA is initiated by the microprocessor [161]. The microprocessor complex is composed of the class III RNase Drosha, and DiGeorge syndrome chromosomal region 8 (DGCR8) that binds to Drosha to increase its stability [160]. The size of the pri-miRNAs varies, but they typically contain a stem-loop that upon processing becomes the precursor miRNA (pre-miRNA). Pre-miRNAs can also be directly spliced out of introns, bypassing the microprocessor; these are known as mirtrons [162]. A pre-miRNA is about 65 nucleotides in length.

After Drosha processing, the pre-miRNA is transported from the nucleus to the cytoplasm via a transport complex formed by Exportin-5 (EXP5) and the GTP-binding

nuclear protein, Ran-GTP [163]. GTP is hydrolyzed after translocation of the pre-miRNA, causing the release of pre-miRNA from the complex into the cytoplasm. It has been shown that a 2-nucleotide overhang at the 3'-end of pre-miRNAs is preferred for nuclear export [164]. In additional to exporting pre-miRNA, EXP5 may have a role in protecting pre-miRNA from degradation in the nucleus, since knocking down EXP5 does not cause an accumulation of pre-miRNAs in the nucleus [163].

In the cytoplasm, further processing is carried out by another class III RNase, Dicer, which cleaves away the terminal loop of pre-miRNA to produce an imperfect RNA duplex about 22 nucleotides long [165]. Dicer forms a complex with transactivating response RNA-binding protein (TRBP), recruits Argonaute (AGO), and loads AGO with one of the RNA strands, which becomes the functional miRNA [166]. AGO is part of the RNA-inducing silencing complex (RISC) that functions to regulate mRNA. Inside RISC, miRNA acts as a guide by base pairing with its target mRNAs, and AGO recruits other factors necessary for downstream functions. There are four AGOs in mammals, named AGO1 to AGO4, but only AGO2 has endonuclease activity [167]. The four AGO proteins have overlapping functions [168] and do not show preference for specific sets of miRNAs [168-170].

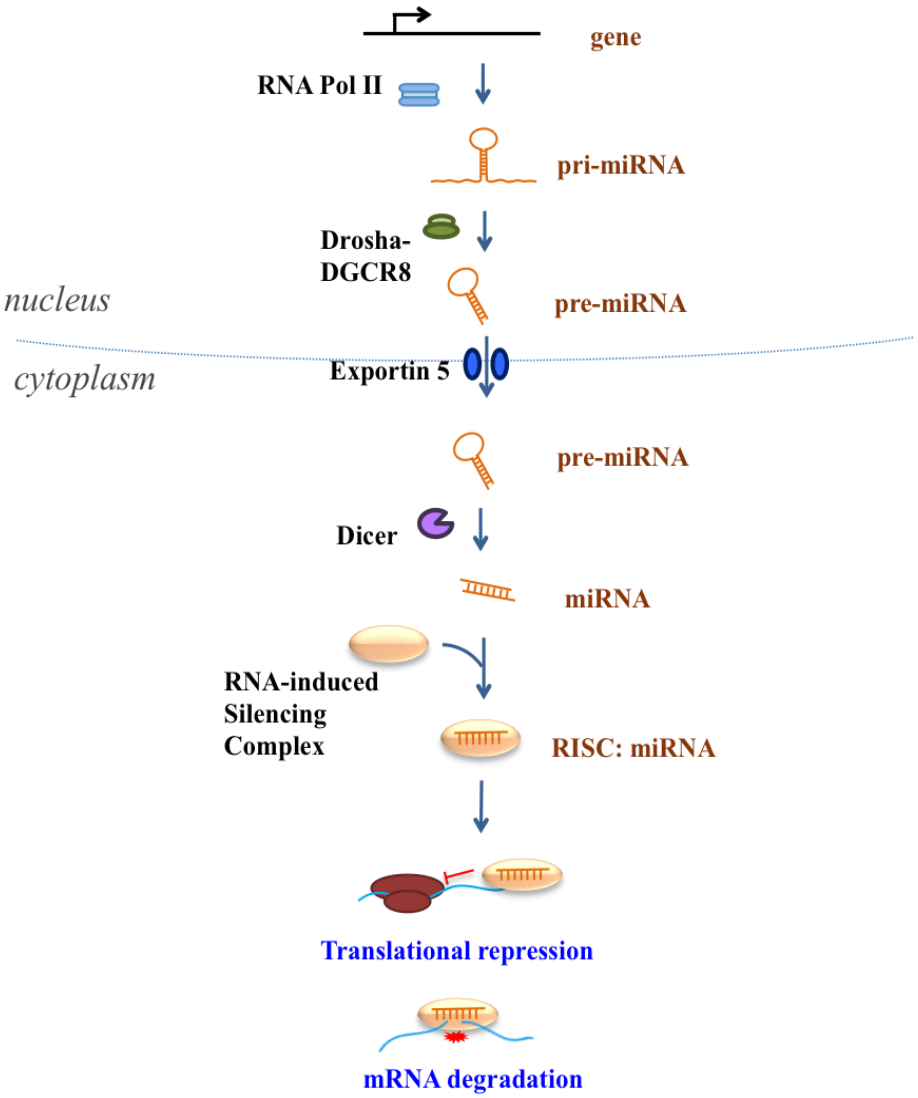

Figure 1.2 Biogenesis of miRNA.
Pri-miRNA is transcribed by RNA Pol II or RNA Pol III, and then processed by the microprocessor complex to generate pre-miRNA. Subsequently, pre-miRNA is transported from the nucleus to the cytoplasm through Exportin-5. In the cytoplasm, Dicer/TRBP complex further processes the pre-miRNA into miRNA duplex. The guide strand is then loaded into RISC to form a functional RISC, which reduces protein expression by translational repression and mRNA degradation.

The biogenesis and function of miRNAs have to be tightly regulated for many reasons, including the fact that more than 60% of human protein-coding transcripts contain at least one conserved miRNA binding site [171] and hence, may be regulated by

miRNAs. Furthermore, dysregulation of miRNA expression is often associated with human diseases [172,173]. Thus, it is not surprising that every step of the miRNA biogenesis is regulated (**Table 1.2**).

Table 1.2: Regulation of miRNA biogenesis

Name	Effect on miRNAs	References
Regulation of miRNA transcription		
DNMT1, DNMT3b	reduces methylation of miRNA-20a promoter in glioma cells	[174,175]
MYC	induces transcription of miR-17~92 and miR-9 but inhibits miR-15a; regulates transcription of Drosha	[119,176-178]
MYOD1	activates transcription of miR-1	[119,176,179]
p53	induces transcription of miR-34 and miR-107	[119]
REST (NRSF)	recruits histone deacetylases and methyl CpG binding protein MeCP2 to inhibit miR-124	[180]
ZEB1 and ZEB2	repress transcription of miR-200	[119,176,181]
Regulators of microprocessor complex-mediated processing		
Drosha	cleaves DGCR8 mRNA leading to its degradation	[182,183]
ERK1/2	phosphorylates DGCR8 to increase its stability	[184]
GSK3b	phosphorylates Drosha; requires for its nuclear localization	[185,186]
HDAC1	deacetylates DGCR8 to increase its affinity to pri-miRNAs	[187]
MECP2	binds to DGCR8 to prevent miRNA processing	[188]
RNA-binding proteins		
ARS2	stimulates Drosha/Dicer processing and maturation of miR-21, miR-155, and let-7	[189,190]
hnRNP A1	component of Drosha complex; binds loop regions of pri-miR-18a and facilitates Drosha-mediated processing	[191,192]
KSRP	binds to terminal loop of miR-198 and facilitates its cleavage by Drosha	[192]
Lin-28	blocks Drosha and Dicer processing of pri/pre-let-7 by interacting with its terminal loop; blocks pre-miR-128 cleavage by Dicer; recruite TUT-4	[193-195]
Nanog	interacts with p68 and Drosha; regulates processing of pri-miR-21	[196]
NF90/NF45	binds to pri-let-7a, pri-miR-15a~16-1, -21, -30a and reduces DGCR8 accessibility	[197]
p68/p72	components of Drosha complex, facilitates Drosha mediated processing of selected pri-miRNAs	[198]

Name	Effect on miRNAs	References
P53	interacts with p68; facilitates Drosha complex assembly and processing of selected pri-miRNAs	[199]
R-SMADs	interacts with p68; facilitates processing of pri-miR-21and pri-miR-199a upon vascular TGFb and BMP stimulation	[200,201]
SF2/ASF	facilitates Drosha-mediated cleavage of pri-miR-7, and possibly pri-miR-221 and -222, independently on its splicing factor activity	[202]
SNIP1	binds to Drosha and regulates maturation of miR-21, miR-22, miR-23, miR-25 and let-7i	[203]
SRp20, SRSF3	binds CNNC motifs on pri-miRNA and increase the processing of human pri-miRNAs (79% of human miRNAs)	[204]
TDP43	interacts with and increases the stability of Drosha; promotes Drosha and Dicer processing	[205,206]
Regulators of Dicer-mediated processing		
BCDIN3D	binds to pre-miRNA and inhibits access of Dicer	[207]
ERK	phosphorylates TRBP; upregulates growth-promoting miRNAs, and downregulates let-7 miRNAs	[208]
FMRP	interacts with Dicer and TRBP, and pre-miRNAs; depletion impairs miRNA biogenesis	[209]
IRE1α	cleaves selected pre-miRNAs during ER stress to release translational repression of the pro-apoptotic caspases 2	[210]
KSRP	binds to terminal loop of pre-miRNA, and facilitates Dicer-mediated processing	[211]
let-7	targets Dicer1 mRNA	[212,213]
MCPIP1	cleaves the terminal loop of the pre-miRNA	[214]
Regulators of RISC activity		
AKT3	phosphorylates AGO2 at Ser38 and enhances localization within the processing bodies	[215]
CP4H	hydroxylizes Pro700 of AGO2, increases the stability of AGO2 and localization within the processing bodies	[216,217]
EGFR	phosphorylates AGO2 at Tyr393, causing dissociation from Dicer	[218]
LIN41	ubiquitylates AGO2 for proteosomal degradation	[219]
MAPKAPK2	phosphorylates AGO2 at Ser387 in response to stress, leads to increased localization within the processing bodies	[220]
PARP	polyADP-ribosylates RISC and inhibits their activity to repress targets	[221]
TRIM71	ubiquitylates AGO2 for proteosomal degradation	[219]

Name	Effect on miRNAs	References
Modification of the RNA molecules		
ADAR1/2	changes the RNA sequence of pri-miR-142, pri-miR-376a and pre-miR-151, and blocks processing by Drosha and Dicer	[222,223]
BCDIN3D	methylates the 5'-end of pre-miRNAs and interferes with Dicer mediated processing	[207]
DIS3L2	recognizes the U tail generated by TUT4 and degrades the RNA	[224,225]
HEN1	adds terminal 2'O-methyl group to stabilize the miRNA	[226]
GLD2	adenylates miR-122 to increase its stability	[227]
PNPT1	degrades miRNAs	[228]
Tudor-SN	interacts and cleaves dsRNA substrates containing multiple IU and UI pairs	[222,229]
XRN1 and XRN2	degrades miRNAs	[230]
Zcchc11 (TUT4)	adds terminal uracil to miRNAs to stabilize or destabilize it	[195,231]

1.4.2. miRNA functions

Target recognition is important in miRNA-mediated gene regulation. In plants, the miRNA-mRNA interaction is almost always near perfect complementarity, resulting in direct endonucleolytic cleavage and mRNA degradation [232]. However, in mammals, mismatches between miRNAs and target mRNAs are common, and target recognition is driven by the following "rules": perfect match of the "seed" region on the miRNA, which spans from nucleotide position 2 to 7 from the 5'-end, to the mRNA target; mismatch in the central region of the miRNA-mRNA duplex; and complementary 3'-sequence to stabilize the interaction [204,233]. Targeting with mismatch at the seed region has also been reported [234-236]. This non-canonical targeting is generally less effective [234]. The most frequent site for miRNA binding is the 3'-UTR of target mRNAs. Targeting within the 5'-UTR [237,238] (e.g. miR-10a [238]) or the coding region (e.g. let-7 in Dicer mRNA [239]) is less frequent as the translation machinery may displace RISC as it

moves along the mRNA. Also, miRNA binding sites are preferentially found in AU-rich (ARE) region in the 3'-UTR [233]. Usually, multiple sites for the same miRNA or different miRNAs are required for efficient repression [240]. The GW182 proteins are an essential factor in RISC [241]. They interact directly with and act downstream of AGO. Tethering GW182 to an mRNA is sufficient for translational repression, even in the absence of AGO1 in Drosophila [242], showing that GW182 is an effector of AGO function.

Recruitment of RISC to the target mRNAs leads to translational repression, as well as mRNA deadenylation and subsequent degradation. There have been much discussions on whether miRNA-mediated translational repression and mRNA degradation act separately, in parallel or in sequence. Accumulating reports have shown that the primary event mediated by miRNAs is translational repression, and that mRNA degradation may occur subsequently [243-247]. However, it is apparent that translation repression is required for miRNA-mediated mRNA degradation [247]. Several kinetic studies have demonstrated that translational repression precedes mRNA degradation [244-246] (**Figure 1.2**).

Translation initiation starts with the recognition of the mRNA 5'-terminal-7-methylguanosine (m^7G) cap by the eukaryotic initiation factor 4F (eIF4F) through one of its subunits, eIF4E [248]. eIF4F also contains eIF4A and eIF4G. eIF4A is an RNA helicase that unwinds the secondary structure of the mRNA 5'-UTR. eIF4G interacts with polyadenylate-binding protein (PABP), which binds to the polyadenylated, or poly(A), tail of the mRNA. This leads to "circularization" of the mRNA, which increases the affinity of eIF4F to the m^7G cap and stimulates translation initiation. eIF4G then

recruits eIF3, which facilitates the association of the 40S ribosomal subunit to the mRNA. The 40S subunit scans the mRNA until it finds the start codon (AUG), followed by the joining of the 60S subunit and the beginning of the elongation step. Initiation can also occur at internal ribosome entry sites (IRES) with some or no initiation factors [249]. Experiments on target mRNA reporters containing either the m^7G cap or different IRES showed that miRNA-mediated translational repression only occurs on mRNAs that have a m^7G cap [247], indicating that the translation initiation step is the major target for miRNA action and that the activity of the eIF4F complex may be affected by the miRNA machinery. In fact, repression can be overcome *in vitro* by an excess amount of eIF4F [243]. It is also reported that eIF4A2 is a key component in the eIF4F complex through which miRNA functions, although the mechanism of action is unclear [247]. Translational repression is usually associated with subsequent mRNA degradation through the recruitment of deadenylase complexes. Two complexes have been described: the CCR4-NOT complex and the Pan2-Pan3 complex [242,250-252], both of which can directly interact with GW182 of RISC. Whether these complexes have redundant or distinct functions is still unclear. In addition, GW182 can interact with PABP to compete for eIF4G binding [253,254], which is required for miRNA-mediated deadenylation of target mRNAs. PABP can also associate with CCR4-NOT directly to initiate deadenylation [253]. The shortening of the poly(A) tail leads to decapping of the target mRNA, which leads to degradation [255]. GW182 has been reported to interact with decapping enzyme complexes DCP1:DCP2 [242,256].

miRNAs can also upregulate gene expression. One of the first reports showed that while miR-369-3p normally represses the expression of TNFα, in quiescent cells,

miR-369-3p can upregulate TNFα translation [257]. miR-155 has also been shown to increase TNFα production after LPS stimulation [120] or alcohol treatment [121] in macrophages. Another example is miR-10a, which binds to the 5'-UTR of ribosomal protein mRNAs to enhance their translation [238].

1.4.3. miRNAs in immune cells

The essential role of miRNA in all biological processes is highlighted by the fact that knocking out Dicer in the mouse germline cells results in embryonic lethality [258]. Therefore, efforts have been made to generate lineage-specific knockout of Dicer in mice. Transgenic mice with conditional Dicer-KO in T cells show a number of immunopathologies including splenomegaly, enlarged intestinal lymph nodes and colitis [259]. T cells isolated from these mice have reduced viability, impaired development and differentiation, as well as abnormal cytokine production [259]. Ablation of Dicer expression in early B cell progenitors blocks the transition from pro-B cells to pre-B cells [260]. In dendritic cells, Dicer is essential for maturation, turnover, and MHC II antigen presentation capacities [261]. Deletion of Dicer in macrophages enhances expression of LPS-induced cytokines, such as IL-1β and IL-10, indicating that miRNAs are important in LPS-induced macrophage activation [262].

miRNAs are crucial in the regulation of both innate and adaptive immunity [263-265]. Within the innate immune system, up to 52% of innate immune genes are predicted to be the targets of miRNAs [156], again pointing to the importance of miRNA-mediated regulation in the immune system. The first step to understanding this regulation is to identify miRNA expression profiles in immune cells. In fact, all immune cells express five specific miRNAs (miR-142, miR-144, miR-150, miR-155, and miR-223) [266].

Cells from different lineages also have unique miRNA expression profiles.

Many of these miRNAs are involved in inflammatory responses, and they are implicated in different human inflammatory diseases including multiple sclerosis [267], rheumatoid arthritis [268,269], systemic lupus erythematosus [270,271], type 1 and type 2 diabetes [272,273], atopic dermatitis [274,275], IgA nephropathy [276], IBD [277], and celiac disease [278]. One of the most studied miRNAs in the immune system is miR-155.

1.4.4. miRNA-155

miR-155 was first identified as the B cell integration cluster (BIC) gene that is induced by a viral promoter insertion in the chicken genome [279]. Later, homologous genes were found in human and mouse, and comparison of these homologs showed a 78% identity over 138 nucleotides [280]. BIC is mapped to chromosome 21 in human (and chromosome 16 in mouse) [280], and miR-155 is mapped within an exon of BIC [281]. miR-155 is highly expressed in the thymus and spleen [280], but also detected in all human tissues [282]. Bioinformatics analysis using TargetScan 7.0 (August 2015) [283] predicted 3297 human transcripts and 2109 mouse transcripts to be miR-155 target candidates. Validated targets are listed in **Table 1.3**, including genes involved in hematopoiesis (e.g. AICDA, ETS1, JARID2, SPI1), inflammation (e.g. SHIP1, SOCS1, MYD88, FADD, BACH1, RIPK1), and tumour suppressor genes (e.g. ZNF652). It is consistent with the observation that high levels of miR-155 are associated with cancer [284].

Table 1.3: Validated targets of miR-155

Gene symbol	Gene name	References
Nuclear proteins		
AID	Activation-induced cytidine deaminase	[285,286]
ARID2	AT rich interactive domain 2	[287]
ARNTL	Aryl hydrocarbon receptor nuclear translocator-like	[288]
BACH1	BTB and CNC homology 1, basic leucine zipper transcription factor1	[287,288]
BCL-6	B-cell lymphoma 6 protein	[289]
C/EBPβ	CCAAT/enhancer binding protein, beta	[287,288]
CUTL1 (CUX1)	Cut-like homeobox 1	[288]
ETS1	v-ets erythroblastosis virus E26 oncogene homologue 1	[290,291]
FOS	FBJ murine osteosarcoma viral oncogene homologue	[292]
HDAC4	Histone deacetylase 4	[292]
HIF	Hypoxia-inducible factor 1	[288,292]
HIVEP2	Human immunodeficiency virus type I enhancer binding protein 2	[287]
MAF	v-maf musculoaponeurotic fibrosarcoma oncogene homologue (avian)	[293]
MEIS1	Meis homeobox 1	[291]
PU.1 (SPI1)	Spleen focus forming virus (SFFV) proviral integration oncogene spi1	[288,294]
SMAD2	SMAD family member 2	[295]
SMAD5	SMAD family member 5	[287]
ZIC3	Zic family member 3	[287]
ZNF652	Zinc finger protein 652	[287]
JARID2	Jumonji, AT rich interactive domain 2	[288]
TP53INP1	Tumour protein p53 induced nuclear protein 1	[296]
Protein receptors		
AT1R	Angiotensin II receptor, type 1	[297,298]
CSF1R	Colony stimulating factor 1 receptor	[288]
CTLA-4	Cytotoxic T-lymphocyte-associated protein	[299]
IL13Rα1	IL-13 receptor α1	[300]
S1PR1	Sphingosine-1-phosphate receptor 1	[299]
TLR3	Toll like receptor 3	[301]
Cytosolic proteins		
FADD	Fas (TNFRSF6)-associated via death domain protein	[302]
MyD88	Myeloid differentiation primary response gene 88	[154,303]
NKIRAS1	NFκB inhibitor-interacting Ras-like protein 1	[304]

Gene symbol	Gene name	References
PICALM	Phosphatidylinositol binding clathrin assembly protein	[288]
RHOA	Ras homologue gene family, member A	[305]
SLA	Scr-like-adaptor	[288]
SOCS1	Suppressor of cytokine signalling protein 1	[306,307]
Enzymes		
CASP3	Caspase-3	[308]
IKKε	Inhibitor of kappa light polypeptide gene enhancer in B cells, kinase ε	[302]
MAP3K7IP2 (TAB2)	Mitogen-activated protein kinase kinase kinase 7 interacting protein 2	[309,310]
RIPK1	Receptor (TNFRSF)-interacting serine/threonine kinase 1	[302]
SHIP1	SH2 domain containing inositol 5'-phosphatase 1	[311-313]

1.4.4.1. miR-155 functions

miR-155 is required for normal immune function in both adaptive and innate immunity, as evident in the miR-155 knock out mice [293]. These mice contain normal numbers of most myeloid and lymphoid cells, probably because miR-155 expression is generally low in homeostasis. However, protective immunity against *Salmonella enterica* serovar Typhimurium appears to be impaired, as vaccination with an attenuated form of the pathogen does not prevent these knockout mice from dying, unlike wild type mice. Specifically, these mice have impaired B cell (reduced production of IgM and switched antigen-specific antibodies) and T cell responses. *In vitro* assays using purified subsets of cells show that dendritic cells, although they mature normally in the absence of miR-155, fail to activate T cell efficiently, indicating a defect in antigen presentation. Additional studies have suggested that miR-155 has important roles in the development and functions of different T cell subsets, including Th1, Th2, Th17 and regulatory T cells (Tregs) [314].

miR-155 has been implicated as a positive regulator of inflammation. Bone marrow derived dendritic cells from miR-155 knockout mice show reduced production of pro-inflammatory cytokines such as IL-12 and IL-6 in response to LPS [315]. When miR-155-specific oligonucleotides are introduced in human monocyte-derived dendritic cells to reduce miR-155 inside the cells, production of IL-1β is decreased [316]. Similarly in macrophages, expression of miR-155 is strongly induced by ligands of TLR2, TLR3, TLR4, and TLR9, as well as pro-inflammatory cytokines TNFα, IFNβ and IFNγ [122]. This induction of miR-155 by TLR ligands is important for the production of pro-inflammatory cytokines. For instance, miR-155 can enhance TNFα potentially via mRNA stabilization [120,121]. Another target of miR-155 is SH2 containing inositol 5'-phosphatase 1 (SHIP1) [311]. SHIP1 is a negative regulator of the PI3K/AKT pathway, which has a role in TLR-mediated cytokine production [317]. Luciferase reporter assays show that miR-155 targets SHIP1 by direct interaction at the 3'-UTR of SHIP1 mRNA. Overexpression of miR-155 in the macrophage cell line RAW264.7 reduces SHIP1 protein level, and thereby increases AKT activation after LPS stimulation [311]. The strong link between SHIP1 and miR-155 is emphasized by the fact that knocking down SHIP1 or overexpressing miR-155 in the hematopoietic system in mice show strikingly similar histological features of myeloproliferative disorders [288].

The importance of miR-155 in inflammation is also seen in human disorders. Patients with RA have upregulated level of miR-155 in their synovial membrane and synovial fluid macrophages, and this upregulation is associated with lower SHIP1 level and higher TNFα production [318]. Similarly, peripheral blood samples of RA patients have upregulated TNFα and IL-1β levels [319]. *In vitro* studies have suggested that the

underlying mechanism might involve miR-155 repression of suppressor of cytokine signalling 1 (SOCS1) expression [319]. In mice, knocking out miR-155 prevents the development of collagen-induced arthritis [318]. However, miR-155 also has a negative role in inflammation. In macrophages, miR-155 suppresses LPS/TLR4 signalling by targeting IKKε, RIPK1, and FADD [120]. MyD88 is also a target of miR-155, and silencing miR-155 enhances inflammatory responses in the human macrophage-like cell line THP-1 [154]. These observations highlight that miR-155 has a fine-tuning role, rather than merely acts as an on/off switch for inflammation.

miR-155 may be oncogenic, because overexpressing miR-155 in the B cells of transgenic mice eventually leads to the development of B-cell lymphomas [320]. Furthermore, an elevated level of miR-155 was found in B cell lymphomas (e.g. diffuse large B-cell lymphoma (DLBCL) [281,321], Hodgkin lymphoma [322,323] and primary mediastinal B-cell lymphoma (PMBL) [323]), B-cell chronic lymphocytic leukemia (B-CLL) [324], B cell and T cell acute lymphoblastic leukemia [325], and acute myeloid leukemia (AML) [326]. In addition, miR-155 is overexpressed in solid tumors such as breast cancer, colon cancer, cervical cancer and lung cancer [327].

1.4.4.2. miR-155 regulation

Due to its wide-ranging effects on immune cell functions as well as its association with cancer, extensive efforts have been put into identifying the signalling pathways responsible for the expression of BIC/miR-155. Promoter analysis of the BIC gene revealed that it contains a classic TATA box, and binding sites for transcription factors including NFκB, AP-1, and E26 transformation specific (Ets) [328]. With the use of different synthetic pathway inhibitors as well as luciferase reporter assays, B cell

activation has been found to induce miR-155 upregulation via AP-1 and NFκB, but not Ets [328]. Both AP-1 and NFκB pathways are also utilized by Epstein-Barr virus to attenuate miR-155 expression in B cells [287].

Genome-wide studies in Tregs showed that miR-155 is a direct target of the Treg-specific transcription factor, forkhead box P3 (FOXP3) [329,330]. miR-155 deficiency results in impaired development of Tregs [330]. By targeting SOCS1 in Tregs, miR-155 is involved in the homeostasis and survival of Tregs [330]. Interestingly, SOCS1 is also necessary for Treg function partly by maintaining FOXP3 expression [331]. This is another example of how miR-155 fine-tunes cell functions.

In macrophages that are stimulated by TLR ligands, both MyD88-dependent and independent signalling pathways are involved in the induction of miR-155, and this induction is blocked by inhibition of the c-Jun N-terminal kinase (JNK), suggesting that AP-1 is involved in miR-155 expression [122]. TNFα, IFNα and IFNβ stimulations also induce miR-155 expression [122]. While upregulation by IFNβ and IFNγ are mediated through the autocrine production of TNFα, TNFα directly activates miR-155 expression, also via JNK/AP-1 signalling [122]. Consistent with this observation, TNFα induction of miR-155 in THP-1 cells is reversed by pretreatment with an anti-inflammatory compound (resveratrol) due to the induction of miR-633, which decreases AP-1 activity [332]. Luciferase reporter assays confirm that LPS-induced miR-155 expression is mediated via the AP-1 site, but not the Ets or the NFκB sites [333]. The same study also shows that the anti-inflammatory cytokine IL-10 suppresses miR-155 expression, and that it requires the Ets site in the promoter region of BIC gene. Although, the AP-1 mediated pathway is important in miR-155 upregulation, Tili *et al.* reports that LPS upregulates miR-155 in

RAW264.7 cells in an NFκB-dependent manner [120]. NFκB is required for vesicular stomatitis virus (VSV) infection and *Helicobactor pylori* infection to upregulate miR-155 expression in mouse bone-marrow derived macrophages (BMDM) [334,335]. Together, these studies showed that TLR agonists can stimulate the transcription of BIC/miR-155 through both AP-1 and NFκB-dependent mechanisms.

miR-155 is regulated by other transcription factors in non-immune cells. SMAD4 mediates miR-155 expression in epithelial cells after TGFβ stimulation [336]. Requirement for BRCA1 to suppress miR-155 expression was discovered in differentiating mouse embryonic stem cells and depends on the interaction between BRCA1 and HDAC2 complex, suggesting that the BIC/miR-155 promoter is regulated epigenetically [337].

Besides transcriptional regulation, post-transcriptional regulation is also important in the production of mature miR-155 in LPS-stimulated macrophages. Maturation of miR-155 is mediated by the RNA-binding protein, KH-type splicing regulatory protein (KSRP) [262]. KSRP binds to the terminal loop of pre-miR-155, which promotes the maturation of pre-miR-155 to functional miR-155. Deficiency of KSRP causes an accumulation of pri-miR-155 and pre-miR-155, and a reduction in mature miR-155 level. Besides miR-155, KSRP also binds to the terminal loop of let-7a-1, miR-21, miR-206, miR-1-1 and miR-1-2, and promotes their maturation at the Drosha-mediated processing, Dicer-mediated processing, or both [211].

1.4.4.3. miR-155 orthologue

To date, two viral-encoded miR-155 orthologues have been discovered. miR-K12-11, found in the Kaposis sarcoma-associated herpesvirus (KSHV), has an identical

seed region as mammalian miR-155 [338]. Moreover, this viral miRNA shows functional similarity to miR-155 such as repressing BACH1 [339], C/EBPβ [339] and SMAD5 [340]. miR-K12-11 also shows similar *in vivo* activity to miR-155 in a mouse model [341]. Overexpression of miR-K12-11 or miR-155 results in splenic B cell expansion by targeting C/EBPβ. The investigators suggested that it may be the underlying mechanism for the development of KSHV-associated lymphomagenesis. More recently, Marek's disease virus (MDV) was also found to encode a miR-155 orthologue, named mdv1-miR-M4-5p [342], which may play a role in the induction of Marek's disease lymphomas [342,343].

1.5.Interleukin-10 (IL-10)

IL-10 was first discovered as a Th2 cell secreted factor, and originally named cytokine synthesis inhibitory factor due to its ability to inhibit Th1 cell cytokine production [344]. Later, it was found that much of the inhibitory role of IL-10 on T cells is indirectly mediated by its effect on macrophages. IL-10 inhibits the production of pro-inflammatory cytokines (e.g. TNFα, IL-1β, IL-6, IL-8, IL-12 and IL-18) and chemokines (e.g. CXCL2, CXCL3 and IL-8), as well as the expression of MHC II and co-stimulating molecules that are important for macrophages to activate T cells [345-347].

IL-10 is produced by almost all immune cells, but its major producers are macrophages/monocytes, Th2 cells, mast cells and Tregs [348]. Expression of IL-10 can be induced by a wide range of stimuli including TLR agonists (e.g. LPS [345]), as well as TLR-independent stimuli (e.g. dectin-1 [349]). In macrophages, IL-10 induction by LPS is MyD88 and TRIF-dependent, and requires both MAPK and NFκB pathways [350-353]. IL-10 is transcriptionally regulated by numerous transcription factors including NFκB,

C/EBPβ, specific protein 1 (SP1), SP2, activating transcription factor 1 (ATF1) and cAMP-responsive-element binding protein (CREB). IL-10 expression is also mediated post-transcriptionally via its mRNA 3'-UTR [354], involving RNA-binding proteins (e.g. tristetraprolin [355]) and miRNAs (e.g. miR-106a [356], and miR-466I [357], miR-146b [354], and let-7 [358]).

IL-10 functions as a homodimer, and each monomer consists of 160 residues in human, and 157 residues in mouse, with 72% overall sequence identity. The two monomers associate with each other non-covalently. Structural studies show that each monomer consists of six α-helices, four of which from itself and the other two from the other monomer [359]. As a result, a homodimer with a V-shaped structure is formed.

1.5.1. IL-10 functions

IL-10 exerts effects on cells in both innate and adaptive immunity [348]. Macrophages are considered the major target of IL-10 due to its high expression level of the IL-10 receptor (IL-10R). Specifically, when IL-10R1 was deleted in specific immune cells in mice, only myeloid-specific knockout, but not T-cell or B-cell specific knockout, showed an increased sensitivity to LPS administration [360], suggesting that IL-10 signalling in myeloid cells (including monocytes, macrophages and neutrophils) is crucial in controlling LPS response. In the presence of inflammatory stimuli, macrophages become activated and execute an inflammatory response. IL-10 suppresses cell activation via multiple ways. Firstly, IL-10 can potently inhibit the production of cytokines (e.g. IL-1α, IL-1β, IL-6, IL-12, TNFα), chemokines (e.g. IL-8, CCL2, CCL3), and non-protein factors (e.g. nitric oxide, prostaglandin E2). IL-10 also changes the expression of surface proteins. IL-10 inhibits the expression of MCH II and co-

stimulatory molecule CD80 and CD86, which are necessary for antigen presentation and as a result, decreases macrophage's ability to activate T cells. In addition, IL-10 downregulates adhesion molecules such as intracellular adhesion molecule 1 (ICAM1) to inhibit macrophage interaction with epithelial cells, but upregulates the expression of CD16 and CD64, Fcγ-receptors (FcγR), to promote phagocytosis of inflammatory stimuli. Meanwhile, IL-10 induces the production of anti-inflammatory mediators such as IL-1 receptor agonist (IL1Ra) and soluble TNFα receptor, which sequester the respective cytokines to inhibit their subsequent actions on neighbouring immune cells. Furthermore, IL-10 modulates the expression of non-coding RNAs including miRNAs. Examples include inhibition of LPS-induced miR-155 [333], and upregulation of miR-187 that targets the NFκB pathway to suppress expression of TNFα, IL-6 and IL-12p40 [361].

1.5.2. IL-10 signalling

IL-10-mediated signalling starts with the engagement of IL-10 to the IL-10R [362]. The IL-10R is a tetramer composing of two copies each of two proteins: IL-10R1 [362] and IL-10R2 [363]. While IL-10R2 is shared by other cytokines in the IL-10 family, IL-10R1 is only utilized by IL-10 [364-366]. IL-10R1 is responsible for ligand association, and together with IL-10R2, transmits signals to downstream molecules [362,367]. Activation of the IL-10R causes the trans-phosphorylation and activation of receptor-bound tyrosine protein kinases, the Janus kinase 1 (Jak1) and tyrosine kinase 2 (Tyk2) [368]. These kinases in turn phosphorylate IL-10R1 at Y446 and Y496 in human (Y427 and Y477 in mouse), which then become the docking sites for signal transducer and activator of transcription 3 (STAT3) [369]. The interaction is mediated via the Src-

homology 2 (SH2) domain of STAT3 [369]. Upon recruitment, STAT3 is phosphorylated at Y705 and Y727, which promote its dimerization and its transactivational activity [368]. A recent study showed that the AMP-activated protein kinase (AMPK) is required for IL-10-induced phosphorylation of STAT3 [370]. The dimerized STAT3 then translocates to the nucleus, binds to STAT response elements, and regulates the expression of IL-10-response genes that execute the anti-inflammatory response. IL-10 also suppresses inflammation via post-transcriptional mechanisms, such as increasing mRNA stability of anti-inflammatory molecules (e.g. IL1Ra) while destabilizing certain cytokine mRNAs (e.g. IL-1 [46,371], and TNFα [46,56,371,372]).

Analysis of intracellular signalling pathways downstream of the IL-10R has led to the model that activation of the STAT3 and expression of STAT3-response genes are sufficient to mediate all the anti-inflammatory actions of IL-10 [55,373,374]. However, there are both *in vitro* and *in vivo* evidence showing that STAT3 is not the sole mediator of IL-10 signalling (see Section 1.6.2). Previous and ongoing studies in our laboratory found that the inositol 5'-phosphatase, SHIP1, could mediate IL-10 inhibition of activated macrophages [56,375,376]. Deficiency of SHIP1 results in reduced IL-10-mediated inhibition of LPS-induced TNFα both in a macrophage cell line and primary mouse macrophages [376]. IL-10 inhibits TNFα both transcriptionally, by reducing RNA polymerase II association with the TNFα promoter, and post-transcriptionally, by destabilizing TNFα mRNA. SHIP1 appears to be involved in both processes [56,376]. Furthermore, IL-10 inhibits the mRNA levels of an additional 17 LPS-induced genes, and SHIP1 deficiency abolishes this inhibition for the majority of them [376]. Administration of IL-10 to mice treated with LPS in an endotoxemia model shows that IL-10 inhibits

TNFα production in wild type but not SHIP1 knockout mice [376]. These data support a role of SHIP1 in IL-10 function.

1.5.3. IL-10 in human diseases

Due to its anti-inflammatory property, a defect in IL-10 signalling is associated with many autoimmune/inflammatory diseases [348,377]. The phenotype of IL-10 knockout mice clearly demonstrates the normal anti-inflammatory functions of IL-10. These mice spontaneously develop colitis, and they become hypersensitive to inflammatory stimuli [378-380]. Similarly, in human, deficiencies or mutations in IL-10 or IL-10R cause early onset of IBD [381]. Also, polymorphisms in IL-10 genes are associated with asthma, allergies, and RA [382-384]. Emerging studies have shown a link between inflammation and metabolic disorders such as T2D [385], and in support of this link, several studies have found that IL-10's anti-inflammatory action was compromised in T2D [10,386-388]. However, enhanced IL-10 activity is also not desirable. Many tumour cells and pathogens express or induce expression of IL-10 to escape from the host immune system and to enhance their survival [389,390].

In the search for treating inflammatory diseases, IL-10 administration has showed satisfactory efficacy in mouse colitis models [391,392]. However, similar approaches in human IBD patients were not successful [393,394]. That may be because systemic IL-10 administration is not sufficient to deliver IL-10 to the inflammatory site in these patients [393]. Moreover, systemic IL-10 stimulates the production of pro-inflammatory cytokines such as IFNγ [395]. Also, some IBD patients have polymorphisms in their IL-10R1 gene [381], and that may cause them to be unresponsive to IL-10 administration.

1.6.Signal transducer and activator of transcription 3 (STAT3)

STAT3 is a transcription factor that belongs to the STAT protein family, all of which have similar structures consisting of a N-terminal domain, a coiled coil region, a DNA-binding domain, a linker, a SH2 domain and a transactivating domain [396]. STAT3 proteins were discovered through their ability to transmit signals from IFN and IL-6 receptors [397-399]. Mutations or activation of STAT3 are associated with different diseases in human. Gain-of-function mutations in STAT3 have been reported to cause early-onset multisystem autoimmunity [400-402], whereas loss-of-function mutations in STAT3 are responsible for hyperimmunoglobulin E syndrome, characterized by recurrent infection, unusual skin rashes and severe lung infections [403]. These highlight the importance of STAT3 in regulation of immunity. Besides, STAT3 (and STAT5) have been associated with cancer progression and survival [404-406]. In particular, persistent activation of STAT3 in cancer suppresses anti-tumour immunity, and mediates tumour-promoting inflammation [407-411].

1.6.1. STAT3 functions in immune system

Knocking out STAT3 in mice lead to embryonic lethality, indicating the importance of STAT3 in early embryogenesis [412]. Thus, cell lines containing a dominant negative STAT3, as well as cell specific-knockout mice of STAT3 have been generated to assess the functions of STAT3 in different cell types in the immune system.

STAT3 plays a critical role in deactivation of macrophages and neutrophils. Mice lacking STAT3 specifically in macrophages and neutrophils are highly susceptible to LPS-induced endotoxin shock, and produce increased levels of TNFα, IL-1β and IFNγ, compared to wild type mice [413]. Macrophages isolated from these mice are

constitutively activated, and secrete augmented levels of inflammatory mediators in response to LPS [413]. Furthermore, IL-10 is unable to suppress the production of these inflammatory mediators, indicating that STAT3 is essential in IL-10's anti-inflammatory functions in macrophages [413].

STAT3 is also important in other immune cells. Studies using mouse pro-B cell line BAF-B03 in which dominant negative STAT3 proteins (Y705F or D434A/D435A) were overexpressed have shown that IL-6 mediated STAT3 activation is involved in preventing B cells from undergoing apoptosis [414]. Similarly, using T cell specific knockout of STAT3, Takeda *et al.* showed that STAT3 is required for IL-6 to prevent apoptosis of normal T cells, and that STAT3 deficiency severely impairs T cell proliferation [415]. These studies demonstrate the anti-apoptotic properties of STAT3.

1.6.2. STAT3's role in IL-10 signalling

Microarray analysis shows that IL-10 only inhibits about 24%, and further induces about 6%, of LPS-induced transcription [416]. STAT3's role is to stimulate the expression of specific gene products to mediate IL-10's anti-inflammatory response [45]. Many of these genes have implication in inhibiting TNFα expression. Bcl-3 inhibits TNFα transcription by interfering the binding of NFκB to the TNFα promoter [36]. ETV3, a transcription repressor, and SBNO2, a co-repressor, are also shown to inhibits NFκB transcription activity [417]. Furthermore, tristetraprolin (TTP), a RNA binding protein, binds to and destabilizes TNFα mRNA [46].

Recent genome-wide studies have revealed further details of STAT3's role in IL-10 signalling [45,418]. Many IL-10 induced genes have proximal STAT3 binding sites in their promoter regions, and the major effect of STAT3 is to activate the transcription of

specific gene products [45]. Since IL-10 inhibits LPS signalling by downregulating LPS-induced transcription, one of the possible ways STAT3 function is to stimulate the expression of transcription repressors that ultimately suppress the expression of pro-inflammatory genes [45]. Moreover, distinct sets of STAT3-binding events have been identified in different cell types [418]. A small set of 35 genes are found to be STAT3-regulated in all four cell types tested, and these genes are involved in the regulation of STAT3's own functions and cells growth [418]. The majority of STAT3-repsonse genes are cell-type specific, which can be explained by the different co-factors that STAT3 interacts with in each cell type [418]. In macrophages, IL-10 mediated STAT3 action is associated with the AP-1 transcription factor family, as well as the ETS family members [418].

While many of the studies aruge that STAT3 is sufficient for all IL-10 functions [55,373,374], other reports support a STAT3-independent mechanism. First of all, a dominant negative STAT3, which lacks the transactivation domain, blocks IL-10-mediated inhibition of cell proliferation, but IL-10 is still able to suppress LPS-induced expression of IL-1β and TNFα [419]. Secondly, human monocytes containing another dominant negative STAT3 (Y705F) behave like the STAT3 knockout cells [420]. In cells containing STAT3 Y705F, IL-10 cannot inhibit the expression of TNFα receptor, COX2 and MHC II, as well as LPS-induced TNFα and IL-6 expression [420]. However, TNFα mRNA is still suppressed in these cells at early time point, while reversal of this suppression is seen at later time points, suggesting that a STAT3-independent mechanism is utilized by IL-10 to suppress TNFα mRNA at early time point.

The presence of a STAT3-independent mechanism is also supported by *in vivo* studies when comparing the results of endotoxemia experiments done in IL-10 knockout mice [421] and myeloid-specific STAT3 knockout mice [413]. In wild type mice, LPS administration leads to increasing serum TNFα levels peaking at 1 hour, which then slowly declines to baseline level after 3 hours. In the IL-10 knockout mice, LPS-induced TNFα levels are sustained up to 6 hours [421]. In contrast, in the myeloid-specific STAT3 knockout mice, the high serum TNFα level induced by LPS gradually declines, which coincides with the production of endogenous IL-10 [413], suggesting that a STAT3-independent signalling pathway can mediate IL-10 function in these mice.

1.7.SH2-containing inositol-5´-phosphatse 1 (SHIP1)

SHIP1 is a negative regulator of the PI3K pathway by hydrolyzing $PI(3,4,5)P_3$, which in effect, stops recruitment of downstream signalling molecules. Two other phosphatases are also important in stopping PI3K activation; they are phosphatase and tensin homologue (PTEN) and SHIP2. PTEN converts $PI(3,4,5)P_3$ to $PI(4,5)P_2$, and is a well-known tumour suppressor, whose mutations or deletions are often found in human cancers [422]. PTEN-deficient cells show over-activation of AKT, a crucial mediator of PI3K signalling, preventing them from responding to normal apoptotic signals, and resulting in abnormal tissue growth [422]. While SHIP1 and SHIP2 share high sequence identity and both convert $PI(3,4,5)P_3$ to $PI(3,4)P_2$, they have dissimilar roles *in vivo* due to the differences in their tissue distribution [423,424] and the protein-protein interaction domains they each possess [425]. SHIP2 is ubiquitously expressed and is important in insulin signalling. SHIP1 has a more restricted expression profile. It is primarily expressed in the hematopoietic system, but it is also found in osteoblasts and

mesenchymal stem cells [423]. The biological functions of SHIP1 not only depend on its phosphatase activity, but also rely on its adaptor function via its multiple protein domains [425,426].

1.7.1. SHIP1 structure

SHIP1 is encoded by the INPP5D gene on chromosome 2 in human, and was first identified as a 145-kDa phosphorylated protein based on its ability to interact with adaptor proteins, Shc and Grb2, in immune cells after cytokine and growth factor stimulation [427]. SHIP1 was subsequently cloned and characterized as an inositol 5'-phosphatase [428]. Besides the phosphatase domain, SHIP1 contains an N-terminal SH2 domain, a PH-related (PH-R) domain [429], a C2 domain [430], and a C-terminal proline-rich region (PRR) that contains two NPXY motifs (**Figure 1.3**).

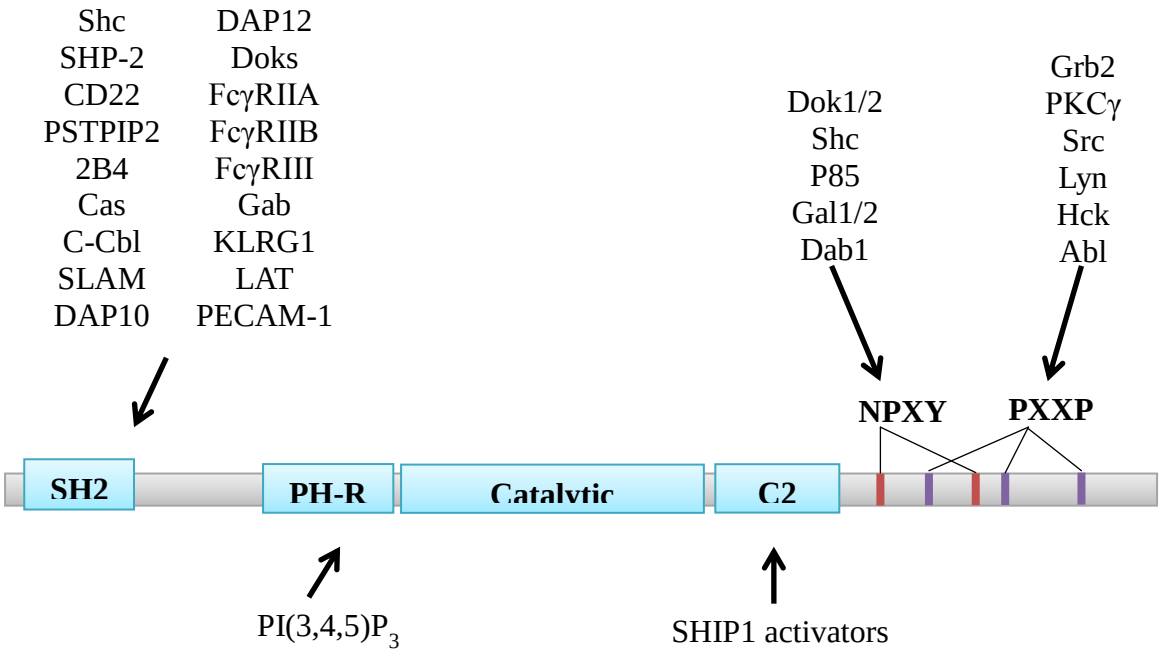

Figure 1.3 The structure of SHIP1 and its binding partners.
SHIP1 contains a N-terminal SH2 domain, a central catalytic domain that is flanked by a PH-R domain and a C2 domain, and a C-terminal region that contains two NPXY motifs and three

PXXP motifs. Proteins or small molecules that have been shown to interact with SHIP1 are indicated with the arrows.

SHIP1 has been demonstrated to hydrolyze inositol-1,3,4,5-tertrakisphosphatase (IP_4) *in vitro*, and PI(3,4,5)P_3 *in vitro* and in *vivo*. SHIP1 has been described by our laboratory as an allosterically regulated enzyme that can be activated by its product, PI(3,4)P_2, with the C2 domain being the binding site of PI(3,4)P_2 [430]. A SHIP1 mutant that lacks the C2 domain shows normal catalytic activity, but PI(3,4)P_2 can no longer enhance its activity [430].

Other domains on SHIP1 are important for its interaction with other proteins, as well as its recruitment to the plasma membrane, where its substrate is located [429,431-437]. The SH2 domain is characterized by a highly conserved sequence (DGSFLSV) that can mediate interaction with phosphorylated tyrosine (pTyr) of many proteins, including Shc, Grb2, Doks proteins, and with membrane receptors via their immune receptor tyrosine-based inhibition motif (ITIM) or immune receptor tyrosine-based activation motif (ITAM). Conversely, when one or both of the NPXY motifs in SHIP1 are phosphorylated, SHIP1 can interact with SH2-containing proteins such as Shc, Dok1/2, and Grb2. Moreover, the C-terminal PRR contains both Type I and Type II pro-rich motifs [438], which can mediate interaction with SH3-containing proteins like Grb2. These protein-protein interactions indirectly bring SHIP1 to the plasma membrane. Recently, our laboratory has identified the PH-R domain, a previously unknown domain of SHIP1, as a PI(3,4,5)P_3 binding site, and found that it is important for direct recruitment of SHIP1 to the plasma membrane during phagocytosis [429].

1.7.2. SHIP1 functions in immune cells

The importance of SHIP1 in immune homeostasis is demonstrated in SHIP1 knockout mice [439-442]. These mice are smaller in size, have shorten lifespan, and display abnormal pathologies such as progressive splenomegaly, osteoporosis, and massive myeloid infiltration of the lungs [439]. Their mast cells are hypersensitive, producing elevated levels of TNFα, IL-6 and IL-5, and causing chronic lung inflammation. Myeloid cells from SHIP1 knockout mice are also hypersensitive to cytokines, growth factors and chemokines, causing the overproductions of granulocytes, mast cells and macrophages. As a result, the SHIP1 knockout mice develop splenomegaly. In addition, the SHIP1 knockout mice exhibit higher level of myeloid-derived suppressor cells (MDSCs) [443] and Tregs [444,445], possibly as a counter response to the inflammatory environment created by overproduction and hypersensitivity of myeloid cells. Development of B cells and T cells are also altered in these mice, but studies using cell specific knockout mice show that these are indirect effects of SHIP1-deficient myeloid cells [446].

1.7.2.1. SHIP1 function in B cell activation

SHIP1 acts as a negative regulator in the activation of the B cell receptor (BCR) [426]. After BCR crosslinking with specific antigens, the ITAM region of BCR is phosphorylated and triggers downstream signalling events including the activation of PI3K pathway and MAPK pathway [447-449]. The generation of $PI(3,4,5)P_3$ recruits AKT, which promotes cell growth, survival and differentiation [450], as well as BTK, which activates the phosphatase PLCγ2 that generates soluble effector inositol triphosphate (IP_3) and diacylglycerol (DAG) [451]. These factors are important for

proper BCR activation. Negative regulation is achieved via the activation of the inhibitory Fc receptor, FcγRIIB, and the subsequent recruitment of SHIP1 to the receptor's phosphorylated ITIM [452]. There, SHIP1 dephosphorylates PI(3,4,5)P_3 to inhibit AKT and BTK activation [453]. Also, SHIP1 interacts with other adaptor proteins (such as Grb2, Dok1 and Dok3) to suppress MAPK activation [454].

1.7.2.2. SHIP1 function in T cell activation

SHIP1 is also implicated in the negative regulation of T cell activation. Engagement of the T cell receptor (TCR) results in the phosphorylation of the TCR and the recruitment of tyrosine kinases such as ZAP70 [455]. That leads to the activation of PI3K-induced AKT and PLCγ2 via the adaptor LAT [455]. TCR activation also causes phosphorylation of DOK1 and DOK2, which then recruits SHIP1 through SHIP1's SH2 domain [456]. At the same time, SHIP1 interacts with Grb2 via its PRR. The SHIP1-Doks-Grb2 complex is then recruited to LAT, and subsequently inhibits PI3K and PLCγ2 activation [456]. However, *in vivo* studies using T cell specific knockout mice show that deficiency of SHIP1 does not alter TCR signalling [444,446].

1.7.2.3. SHIP1 function in NK cells function

Natural killer cells, or NK cells, are cytotoxic cells that mediate rejection of virally infected and tumour cells. They express a wide range of receptors including FcγRIIIA that can recognize abnormalities on target cells in order to induce apoptosis [457]. NK cells can also produce inflammatory cytokines such as TNFα and IFNγ [458]. SHIP1 has been shown to negatively regulate FcγRIIIA-mediated cytotoxicity by its interaction with the receptor-associated adaptor Shc [459]. This interaction is mediated via the pTyr on Shc and SHIP1's SH2 domain [459].

1.7.2.4. SHIP1 function in mast cells

Mast cells have cytoplasmic granules that contain various mediators including cytokines, chemokines, proteolytic enzymes and vasoactive mediators. The best characterized stimulus for mast cells is IgE, which has important roles in allergic reaction [460]. Upon binding of IgE to its receptor, FcεRI, the ITAM of FcεRI is phosphorylated, and recruits and activates the Src kinase Syk, leading to the activation of PI3K and degranulation [461]. Activated mast cells also produce cytokines such as TNFα and IL-6 via the phosphorylation of LAT, recruitment of adaptor proteins, and the activation of Ras-dependent MAPK pathway [461]. SHIP1 has been shown to interact with FcεRI directly under supra-optimal IgE stimulation to downregulate PI3K-dependent signalling [462]. In addition, SHIP1 can suppress MAPK signalling through its interaction with Dok1, which recruits Ras GTPase-activating protein (RasGAP) to promote hydrolysis of GTP bound to Ras, resulting in the downregulation of Ras activation [463].

1.7.2.5. SHIP1 function in macrophages

Macrophages can adopt any activation state along an activation spectrum with one end having the previously named "M1" macrophages and the other end with "M2" macrophages [73]. Macrophages isolated from SHIP1 knockout mice demonstrate an M2 skewing phenotype [464], suggesting a suppressive role of SHIP1 in the development of this macrophage subtype. Indeed, it has been showed that SHIP1 degradation induced by IL-4 is crucial for M2 skewing [465]. Also, SHIP1 knockout macrophages are hypersensitive to immune stimuli such as LPS; they produce elevated levels of TNFα, IL-6, IFNβ, IL-1β and ROS. Therefore, SHIP1 is implicated in the development of endotoxin tolerance, a phenomenon of desensitization of certain immune cells to LPS by

prior exposure to a low dose of LPS. Tolerant cells produce less pro-inflammatory cytokines in response to second challenge of LPS. The development of endotoxin tolerance protects the host from hyperactivation of innate immune cells that can cause cell damage and eventually death. In fact, SHIP1 knockout mice cannot establish an endotoxin tolerant state [112]. These studies suggest a negative role for SHIP1 in TLR4 signalling. SHIP1 is upregulated by LPS via the production of TGFβ [466]. Upregulation of SHIP1 causes inhibition of the PI3K activation and thus decreases the production of TLR4-induced cytokines [112,317,466]. SHIP1 can also inhibit TLR4 signalling through a phosphatase-independent manner, perhaps by interference with the association of TLR4 and MyD88 [317]. Similarly, SHIP1 has a negative role in TLR3-induced IFNβ production possibly by destabilizing the interaction between TBK1 and the TRIF [467].

Moreover, SHIP1 has both positive and negative regulatory roles in the phagocytic activity of macrophages. While SHIP1 knockout cells have enhanced particle uptake, SHIP1 overexpressing cells have attenuated phagocytosis [468]. Imaging experiments showed that SHIP1 localized to the phagocytic cup and the generation of $PI(3,4)P_2$ by SHIP1 is essential for the proper formation and maturation of phagosome [469,470]. Our laboratory has shown recently that the PH-R domain is responsible for recruiting SHIP1 to the phagocytic cup [429].

1.7.3. SHIP1 regulation

Expression of SHIP1 protein can be regulated via both transcriptional and post-transcriptional controls. TGFβ induces SHIP1 expression through the SMAD transcription factors [466,471]. Additionally, SHIP1 mRNA is a target of miR-155 [311-

313,472]. Ubiquitination of SHIP1 and subsequent proteosomal degradation are also observed as a way to reduce SHIP1 protein level in cells [473].

The function of SHIP1 also depends on its cellular localization through different protein-protein interactions mediated by its NPXY motifs, PRR and SH2 domains, or direct interaction with the plasma membrane through PH-R domain, as summarized in Section 1.7.1. SHIP1 enzyme activities can be altered as well. For example, SHIP1 can be phosphorylated on Ser440 (mouse numbering) by cyclic AMP-dependent protein kinase (PKA), and this phosphorylation increases SHIP1's catalytic activity [474,475]. Furthermore, the C-terminal region of SHIP1 may have inhibitory effects on the enzyme since a truncated mutant (residues 1-822) shows activity 8-10 fold higher than full length SHIP1 [474]. A more recent study suggested that SHIP1's SH2 domain could interact with pTyr1020 in the SHIP1's C-terminus to regulate its interaction with ITAM of FcεRI [476].

SHIP1 enzymatic activity can also be modulated by small molecules. Our laboratory has discovered that SHIP1 phosphatase activity is allosterically activated by its product. The allosteric binding domain is defined to be a C2-like domain C-terminal to the phosphatase domain [430]. We screened for small molecules that can act as allosteric activators of SHIP1 and identified a naturally occurring meroterpenoid called pelorol found in a Papua New Guinea sea sponge, *Dactylospongia elegans*, as a SHIP1 agonist [477]. Structural derivatives of pelerol were tested for the SHIP1-activating ability and one called AQX-016A, was found to have more potent activation ability on SHIP1 than pelorol [430]. AQX-016A inhibits macrophage and mast cell activation, and this inhibition is abolished in SHIP1 knockout cells, showing that AQX-016A selectively

targets SHIP1 [430]. *In vitro* enzyme assays show that AQX-016A preferentially activates SHIP1 over its close homologue SHIP2 [430]. Moreover, AQX-016A inhibits LPS-induced TNFα, as effective as dexamethasone (a reference standard), in a mouse endotoxemia model [430]. Another pelorol-based SHIP1 activator, AQX-MN100 was also described in the same study, and found to have the same activity as AQX-016A both *in vitro* and *in vivo* [430]. AQX-MN100 directly interacts with the C2 domain of SHIP1, as shown by scintillation proximity assay [430]. Furthermore, competitive assay suggests that AQX-MN100 competes with SHIP1's natural activator (also its product), $PI(3,4)P_2$, for the same site in the C2 domain, indicating that AQX-MN100 acts as an allosteric activator [430]. When a SHIP1 mutant that lacks the C2 domain was tested in an *in vitro* enzyme assay, it was found that this mutant was as active as the wild type enzyme, but it could no longer be activated by either AQX-MN100 or $PI(3,4)P_2$, showing that the C2 domain is necessary for SHIP1's allosteric activation [430]. In a later study, AQX-MN100 was found to decrease cell viability and induce apoptosis in several multiple myeoloma cell lines [478]. Additional studies showed that AQX-MN100 could enhance the efficacy of drugs currently used to treat multiple myeloma patients [478], suggesting a potential for SHIP1 activator to use in synergy with existing drugs. Other SHIP1 agonists such as australin E [479] and turnagainolide B [480], as well as antagonists (3-α-aminocholestane, 3AC [481]), have also been described (review in [482]).

1.7.4. SHIP1 in diseases

Given SHIP1's negative effect on PI3K/AKT signalling, mutations or altered expression of SHIP1 are associated with a number of diseases including cancer and inflammatory diseases. For example, SHIP1 expression is often downregulated in cells

from AML patients. Moreover, 10 different missense mutations have been described in 3% of the patients, including mutations at the SH2 domain, the phosphatase domain and the C-terminal region of SHIP1 [483]. Interestingly, a high level of miR-155 has been found as a high-risk factor for AML [326], which may be due to miR-155 mediated reduction of SHIP1 levels. Mutations or total loss of SHIP1 expression are also observed in T acute lymphoblastic leukemia (T-ALL) [484]. In chronic myelogenous leukemia (CML), SHIP1 is phosphorylated by a mechanism depending on the oncogenic BCR/ABL protein-tyrosine kinase [473]. Phosphorylated SHIP1 is then targeted for polyubiqutination by the E3 ligase c-Cbl and subsequent proteosomal degradation [473]. These studies suggest that SHIP1 is a tumour suppressor. However, emerging data have pointed to a more complicated role of SHIP1 in cancer. In fact, both agonistic [478] and antagonistic [481] SHIP1 modulators have demonstrated abilities to kill multiple myeloma cells. That leads to the development of the "Two PIP Hypothesis" [436]. Unlike PTEN, which hydrolyzes $PI(3,4,5)P_3$ to regenerate the PI3K substrate $PI(4,5)P_2$, SHIP1 generates $PI(3,4)P_2$. This difference is crucial as it allows PTEN and SHIP1 to have very different effect on AKT signalling. In fact, the PH domain of AKT actually has higher affinity to $PI(3,4)P_2$ than to $PI(3,4,5)P_3$ [485]. There is also evidence showing that the presence of both $PI(3,4,5)P_3$ and $PI(3,4)P_2$ are necessary for full activation of AKT [486,487]. Therefore, elevated levels of $PI(3,4)P_2$ can potentially enhance AKT activation, and thus mediate cancer cell growth. Consistent with this hypothesis, some leukemia cells contain increased levels of $PI(3,4)P_2$ [488]. Moreover, mutations in, or reduced expression of, the INPP4B gene, which normally encodes a phosphatase that converts $PI(3,4)P_2$ to PI(3)P, are associated with increased transformation of human

mammary epithelial cells, as well as decreased patients survival in breast and ovarian cancers [489]. It must also be added that $PI(3,4)P_2$ can actually recruit a distinct set of proteins to the plasma membrane [469,490-498]. These results highlight the importance of *balancing* $PI(3,4,5)P_3$ and $PI(3,4)P_2$ levels in cells to avoid the development of malignancies.

Since SHIP1 is a negative regulator of inflammatory signalling events in the immune system, SHIP1 is also implicated in inflammatory diseases. SHIP1 knockout mice develop inflammation in their small intestine that closely resembles human IBD [499,500]. Consistent with that, single nucleotide polymorphisms (SNPs) that are enriched in patients with Crohn's disease, a form of IBD, have been found in the area where the SHIP1 gene is located in the human genome [501]. Recently, significant reduction in SHIP1 protein level was found in about 15% of IBD patients, despite having normal mRNA levels [502]. While the details of SHIP1 action in these diseases are still being discovered, there is a clear implication of targeting SHIP1 as a potential therapeutic.

Because of SHIP1's restricted expression in the immune system, drugs that specifically target SHIP1 will only affect the immune system with minimal side effects on other tissues. In fact, a specific SHIP1 agonist, AQX-1125, is currently being developed and is shown to have satisfactory efficacy in reducing the symptoms of inflammation in different human diseases in clinical trials [503-505].

1.8. Objectives and aims

The overall objective of this thesis is to define the roles of STAT3 and SHIP1 in mediating IL-10 inhibition of activated macrophages. Our laboratory has shown that both STAT3 and SHIP1 are required for IL-10 action, as SHIP1-deficient cells are

similarly resistant to IL-10 treatment, like STAT3-deficient cells. Work from previous members of our laboratory has implicated SHIP1 in the regulation of transcription and translation of a representative inflammatory mediator, TNFα. We hypothesized that IL-10 can also regulate non-coding RNAs such as miRNAs. During the course of the project, two miRNAs have been independently identified by two other research groups as IL-10 regulated [333], one of which was also identified by us. Furthermore, we expanded our search for other IL-10 regulated genes that depend on SHIP1, STAT3, or both proteins. Finally, we have previously described a small molecule that activates SHIP1 enzymatic activity, and executes anti-inflammatory action similar to IL-10. We characterized the ligand-SHIP1 interaction in hope of developing other (better) small molecular modulators of SHIP1.

The first aim of my thesis research was to determine the mechanism by which IL-10 inhibits miR-155 in LPS-stimulated macrophages. miR-155 is one of the highly expressed miRNAs in TLR-activated macrophages, and while its targets include molecules involved in both positive and negative regulatory action, it is overall considered as a pro-inflammatory mediator. McCoy *et al.* [333] has shown that IL-10 could inhibit LPS upregulation of miR-155 in a STAT3-dependent manner. We specifically asked if SHIP1 is also involved in IL-10 inhibition of miR-155. My second aim was to examine how STAT3 and SHIP1 work together downstream of IL-10. To do this, we explored the relative contribution of STAT3 and SHIP1 on IL-10 regulation in activated macrophages with the use of a continuous flow system and also through global gene expression profiling. Data from the first two aims reiterate the involvement of SHIP1 in IL-10 signalling, and highlight the use of SHIP1 activators to mimic IL-10

function to deactivate immune cells. Thus, my final aim focused on the characterization of the interaction between SHIP1 and SHIP1 activators. Specifically, we have characterized the SHIP1's phosphatase and C2 domains, the minimal regions necessary for the regulation by SHIP1 activators, through the use of x-ray crystallography and other biochemical approaches.

Chapter 2: Materials and Methods

2.1 Cells and reagents

RAW264.7 cells were obtained from American Type Culture Collection and cultured in Dulbecco's Modified Eagle Medium (DMEM) supplemented with 9% (v/v) fetal calf serum (FCS) (Thermo Fisher Scientific, Nepean, ON). The generation of the doxycycline (Dox) inducible Scrambled siRNA and SHIP1 knockdown cell lines is described previously [56]. To generate the AKT-ER stable cell line, RAW264.7 cells were transduced with an AKT-ER construct as described in the "Plasmids and Lentivirus" section below. AKT-ER expressing cells were selected by growth in 5 µg/ml blasticidin.

Primary peritoneal macrophages (perimacs) were isolated from mice by peritoneal lavage with 3 ml of sterile Phosphate Buffered Saline (PBS) (Thermo Fisher Scientific, Nepean, ON). Perimacs were collected and transferred to "Primary cell media" consisting of Iscove's Modified Dulbecco's Medium (IMDM) (Thermo Fisher Scientific, Nepean, ON) supplemented with 10% (v/v) FCS, 10 µM β-mercaptoethanol, 150 µM monothioglycolate and 1 mM L-glutamine. Bone marrow-derived macrophages (BMDMs) were generated by first collecting femurs and tibias from mice, and then flushing out the bone marrow through a 26-G needle. Extracted cells were plated in "Primary cell media" on a 10-cm tissue culture plate for 2 hours at 37°C. Non-adherent cells were collected and seeded at 9×10^6 cells per 10-cm tissue culture plate. Cells were then cultured in the presence of 5 ng/ml colony stimulating factor-1 (CSF-1) (Stem Cell Technologies, Vancouver, BC). Differentiated BMDMs were used after 7 to 8 days. All cells were maintained in a 37°C, 5% CO_2, 95% humidity incubator.

Antibodies used include anti-SHIP1 (P1C1) mouse antibody (Santa Cruz Biotechnology, Santa Barbara, CA), anti-STAT3 mouse antibody (BD Transduction

Laboratories, Mississauga, ON), anti-His mouse antibody (Sigma-Aldrich, St. Louis, MO), and Alexa Fluor® 660 anti-mouse IgG antibody (Invitrogen, Burlington, ON). LPS (*E. coli* Serotype 0111:B4) was purchased from Sigma-Aldrich (St. Louis, MO) and His_6-tagged IL-10 was made in-house by expression in the mammalian 293T cells and purified by column chromatography to homogeneity as assessed by Coomassie staining of SDS-PAGE gels. The STAT3 inhibitor STA-21 (Cedarlane Laboratories, Burlington, ON) was dissolved in dimethylsulphoxide (DMSO). AQX-MN100 (Aquinox Pharmaceuticals, Vancouver, BC) and AQX-151 (Dr. Raymond Andersen, University of British Columia, Vancouver, BC) were dissolved in ethanol. AQX-1125 (Aquinox Pharmaceuticals, Vancouver, BC) was dissolved in appropriate aqueous buffers depending on the experiments.

2.2 Mouse colonies

BALB/c mice wild type (WT) or SHIP1 knockout (SHIP1 KO) mice were provided by Dr. Gerald Krystal (BC Cancer Research Centre, Vancouver, BC). The generation of STAT3 KO mice started with crossing C57BL/6 $STAT3^{flox/flox}$ mice (Dr. Shizuo Akira, Hyogo College of Medicine, Nishinomiya, Japan) with C57BL/6 LysMcre mice (Jackson Laboratory) Their offspring were heterozygous on both alleles, which were then crossed with homozygous $STAT3^{flox/flox}$ mice to produce mice that had genotype of $STAT3^{flox/flox}$ /$LysMCre^{+/-}$. These mice were crossed with $STAT3^{flox/flox}$ mice to generate both $STAT3^{flox/flox}$ /$LysMCre^{+/-}$ mice (referred to be STAT3 KO mice) and $STAT3^{flox/flox}$ mice (STAT3 WT mice) in the same litters. All mice were maintained in accordance with the ethic protocols approved by the University of British Columbia Animal Care Committee.

2.3 Plasmids

2.3.1 Mammalian expression plasmids

Luciferase reporter plasmids containing the BIC promoter were obtained from Dr. Eric Flemington (Tulane University, New Orleans, LA). The mouse IkBζ promoter luciferase reporter was constructed into the pGL3-basic plasmid (Promega, Madison, WI) between the SacI and NheI sites, and contained the IkBζ promoter fragment (-400 to +1) generated by reverse transcription and PCR amplification from total mouse RNA. The c-fos promoter reporter was previously described [506].

A plasmid construct containing a modified form of human AKT was kindly provided by Dr. Megan Levings (University of British Columbia, Vancouver, BC). This AKT construct lacks the PH domain but has a src myristoylation signal sequence at the amino terminal end and the steroid binding domain of the estrogen receptor (ER) and a hemagglutinin tag at the carboxyl terminal end. The AKT-ER sequence was sub-cloned into the pENTR-1A vector (Invitrogen, Mississauga, ON) and recombined into a modified lentiviral vector, pTRIPZ.

The mammalian expression plasmids of SHIP1 and PPAC were generated previously by past members of our laboratory. Briefly, the coding region of full length SHIP1 or the PPAC fragment were amplified by PCR and cloned into the pENTR1A vector (Life Technologies) between the EcoRI and XhoI sites. To generate the SHIP1 Y190F mutant, standard site-directed mutagenesis method was employed. pENTR1A-His_6-SHIP1 WT plasmid was used as the template for site-directed mutagenesis. The primers used are in **Table A.2**. The presence of the mutation was confirmed by DNA sequencing. Subsequently, a LR reaction (Invitrogen, Burlington, ON) was performed

between pENTR1A construct and FUGWBW, which contains an ubiquitin promoter and a blasticidin-resistant gene to generate the desired expression plasmids. Success of the LR reaction was confirmed by restriction enzyme digest.

2.3.2 Bacterial expression plasmids

Ligase-independent cloning (LIC) methodology was used to make the bacterial expression plasmids. The LIC-HMT plasmid was obtained from Dr. Filip Van Petegem (University of British Columbia, Vancouver, BC). This plasmid contains a N-terminal tag composed of His_6 and maltose binding protein (MBP), followed by a TEV protease cleavage site (abbreviated as the HMT-tag). PCR was performed on pENTR1A-His_6-SHIP1 WT with primers listed in **Table A.3**. The PCR product was purified and treated with T4 DNA polymerase (LIC-quality) (Novagen, Madison, WI) in the presence of dCTP only. The LIC-HMT vector was digested with SspI and the linearized plasmid was treated with T4 DNA polymerase in the presence of dGTP only. Equal volumes of insert and vector were mixed and incubated at room temperature for 10 minutes, followed by transformation into chemical competent *E. coli DH5α* cells using the standard heat shock protocol, and selection on kanamycin-containing LB agar plates. To generate different PAC mutants, standard site-directed mutagenesis was employed. Primers used are listed in **Table A.2**. Identity of all plasmids were confirmed by DNA sequencing.

His_6-C2 (residues 725 to 861) expression plasmid was generated by a past member of our laboratory using standard cloning strategy; PCR fragment containing His_6-C2 coding sequence was cloned in the pET28c vector between EcoRI site and NdeI site. Residue numbering of mouse SHIP1 sequence is based on the RefSeq entry with accession number of NP_034696.

2.4 Lentivirus production and transduction

VSV-pseudotyped second-generation lentiviruses were produced by transient 3-plasmid co-transfection into HEK293T cells using either calcium phosphate method (AKT-ER reconstituted cells) or polyethylenimine (PEI) (Polysciences Inc., Warrington, PA) [507] as the transfection reagent (J2M KO reconstituted cells). Lentivirus supernatant was concentrated by ultracentrifugation (25000 rpm for 2.5 hours) to generate the AKT-ER reconstituted cells, while fresh lentrivirus supernatant was used on J2M KO cells directly without purification. FUGWBW lentivirus was also made as a control. Cells were transduced with these viruses in the presence of 8 μg/ml protamine sulphate. The successfully transduced cells were selected by growth in 5 μg/ml blasticidin (Invitrogen, Burlington, ON).

2.5 Cell stimulation

RAW264.7 cells were seeded at 1.5 x 10^6 cells per well on 6-well tissue culture plates or 3 x 10^5 cells per well on 24-well tissue culture plates 1 day prior to stimulation. The SHIP1 siRNA-transduced cell lines were left untreated or treated with 2 μg/ml Dox for 24 hours prior to cell seeding (a total of 48 hours treatment before stimulation) to induce knockdown of SHIP1. The AKT-ER transduced cells were pretreated with 150 nM 4-hydroxytamoxifin (4-HT) for 20 minutes prior to stimulation. For the STA-21 experiments, 30 μM STA-21 or DMSO control was added to the cells 1 hour prior to stimulation. Cells were stimulated with 1-10 ng/ml LPS with or without the indicated concentrations of IL-10. Perimacs were seeded at 3 x 10^6 cells per well in 6-well tissue culture plates and allowed to adhere overnight before stimulation. For mRNA microarray analysis, 2 x 10^6 perimacs were seeded per well in 6-well tissue culture plate and left to

adhere for 2 hours prior to stimulation with 10 ng/ml LPS +/- 100 ng/ml IL-10 for 30 minutes.

2.6 Luciferase reporter analysis

RAW264.7 cells were seeded at 2 x 10^5 cells per well on 24-well tissue culture plates 4 hours before transfection. Each promoter reporter plasmid was co-transfected with phRL-TK using the XtremeGene HP transfection reagent (Roche Diagnostics, Laval, QC) according to manufacturer's instruction. Cells were rested for 24 hours prior to stimulation with LPS +/- IL-10. Cells were then lysed in 200 µl of 1X Passive Lysis Buffer (Promega, Madison, WI) and luciferase activities were measured using the Dual-Luciferase Reporter Assay System (Promega, Madison, WI). The typical transfection efficiency in RAW264.7 macrophages was about 20%.

2.7 Fractionation of nuclear and cytoplasmic RNA

After stimulation, cells were rinsed with PBS and lysed in lysis buffer containing 10 mM Tris-HCl pH7.4, 150 mM NaCl, 1.5 mM $MgCl_2$ and 0.65% Nonidet P-40 (NP-40), supplemented with 100 unit/ml RNase inhibitor (Roche Diagnostics, Laval, QC) for 30 minutes at 4°C. Nuclei were pelleted by centrifugation and the supernatant (cytoplasmic fraction) was transferred to a new tube. Both cytoplasmic and nuclear fractions were then prepared in Trizol reagent (Invitrogen, Burlington, ON) for RNA extraction.

2.8 Immunoblot analysis

Cells were lysed with lysis buffer containing 50 mM HEPES, 2 mM EDTA, 1 mM $NaVO_4$, 100 mM NaF, 50 mM $NaPP_i$ and 1% NP-40, supplemented with Complete Protease Inhibitor Cocktail (Roche Diagnostics, Laval, QC). Lysates were incubated at

4°C for 30 minutes and clarified by centrifugation for 20 minutes at 12,000 g. Proteins were then separated on a 7.5% SDS-PAGE and transferred onto polyvinylidene fluoride (PVDF) membrane (Millipore, Etobicoke, ON). The membrane was blocked, probed with the indicated primary antibodies overnight, washed, developed with the Alexa Fluor® 660 anti-mouse IgG antibody and imaged using a LICOR Odyssey Imager. Band intensities were quantified using the Quantity One Software (BioRad, Mississauga, ON).

2.9 RNA extraction and real-time quantitative PCR

Total RNA was extracted using Trizol reagent (Invitrogen, Burlington, ON) according to manufacturer's instructions. About 2-5 μg of RNA were treated with DNAseI (Roche Diagnostics, Laval, QC) according to the product manual. For miRNA expression analysis, 20 ng of RNA were used as the starting material in miRNA TaqMan assays (Applied Biosystems, Burlington, ON) according to manufacturer's instructions. For mRNA expression analysis, 120 ng of RNA were used in the Transcriptor First Strand cDNA synthesis kit (Roche Diagnostics, Laval, QC), and 0.1 μl to 0.2 μl of cDNA generated were analyzed by SYBR Green-based real time PCR (real time-PCR) (Roche Diagnostics, Laval, QC) using 300 nM of gene-specific primers (**Table A.1**). Expression levels of miRNA and mRNA were measured with the 7300 RT-PCR system (Applied Biosystems, Burlington, ON), and the comparative Ct method was used to quantify miRNA or mRNA levels using snoRNA202 or GAPDH as the normalization control. In the CHX studies, 18S rRNA was used as normalization control instead of GAPDH.

2.10 RT-PCR of pri-miR-155 for DNA sequencing analysis

Total RNA was extracted from unstimulated or stimulated cells, as well as treated with DnaseI as described in the previous section. About 500 ng of RNA were used to

generate cDNA consisting the pre-miR-155 sequence using a gene-specific RT primer (5'- TCTGTCTAGAAGTGGACTATCCTAGTAACC-3'). The resultant cDNA was then amplified by PCR using the following primers: forward, 5'-TATGCTCGAGACCAGCTCATCTGAGAAAAC-3'; reverse primer was the gene-specific RT primer. RT-PCR products were purified from agarose gel with the Qiagen Gel Extraction Kit (QIAGEN, Mississauga ON, Canada), and the sequence was determined through sequencing.

2.11 Measurement of TNFα production level

J2M macrophages were seeded at 50000 cells per well in a 96-well tissue culture plate the day prior to experiment. Media was changed the next day about an hour prior to stimulation. Cells were stimulated with 1 ng/ml LPS +/- various concentrations of IL-10 for 1 hour. Supernatant was collected and secreted TNFα protein levels were measured using a BD OptEIA Mouse TNFα Enzyme-Linked Immunosorbent Assay (ELISA) kit (BD Biosciences, Mississauga, ON). Triplicates wells were used for each stimulation condition.

2.12 Continuous flow system

The continuous flow apparatus was constructed by a previous member of our laboratory [376]. BMDMs were seeded at $3x10^5$ cells per well in a 24-well tissue culture plate that had been coated with poly-L-lysine (Thermo Fisher Scientific, Nepean, ON) and rinsed with PBS. After overnight incubation, culture media was removed and Leibovitz's L-15 (L-15) media (Invitrogen, Burlington, ON) supplemented with 3% FCS, 10 μM β-mercaptoethanol and 150 μM monothioglycolate was added. Cells were allowed to equilibrate in L-15 media for 1 hour before being placed in the continuous

flow apparatus. Stimulation solution was made in the same media equilibrated at 37°C, and was passed through a modified inlet fitted to the well by a syringe pump (New Era Syringe Pumps Inc., Farmingdale, NY). A flow rate of 150 µl per minute was used. At the same time, cell supernatants were removed from the well at the same flow rate, and fractions were collected at 5-minute intervals over the course of 4 hours. These fractions were analyzed for secreted TNFα levels by ELISA.

2.13 *In vitro* pull down assay

Flag-STAT3 was expressed in HEK293T cells in a similar fashion as His_6-SHIP1, as described below. Cell lysate was prepared in the same lysis buffer but without TCEP, and then incubated with M2-affinity resins (Eastman Kodak Company, New Haven, CT) for 1 hour at 4°C on a nutator. Unbound proteins were washed by 3 x 10 column volumes (CV) of wash buffer (50 mM TrisHCl pH7.4, 150 mM NaCl, 0.02% Tween-20). (Semi-)purified His_6-SHIP1 protein was prepared in wash buffer, supplemented with 6 mM $MgCl_2$, 2 mM $CaCl_2$, and/or 20 µM AQX-151 before incubating with the Flag-STAT3 bound M2 affinity resins for 1 hour at 30C with agitation. Resins were then washed three times in wash buffer, and proteins bound were released with the addition of boiled 1X SDS sample buffer. Samples were then analyzed by immunoblotting with anti-SHIP1 antibody and anti-Flag antibody.

2.14 mRNA microarray

Total RNA was extracted using Trizol reagent according to manufacturer's instructions. The quality of the RNA was assessed with the Agilent 2100 Bioanalyzer (Agilent, Mississauga, ON), and only samples with a RNA integrity number (RIN) greater than or equal to 8.0 were used for microarray analysis. The suitable RNA

samples were then prepared following instruction of Agilent's One-Color Microarray-Based Gene Expression Analysis Low Input Quick Amp Labeling kit (v6.0). Briefly, 100 ng of total RNA were used to generate Cyanine-3 labeled cRNA and samples were hybridized on the Agilent Whole Mouse Genome Oligo Microarrays (Design ID 014868). Arrays were then scanned with the Agilent DNA Microarray Scanner. Data was processed with Agilent Feature Extraction 10.5.1 software and analyzed in Agilent GeneSpring 7.3.1 program.

2.15 Identification of SHIP1, STAT3 regulated genes

Data sets of 41174 probes were compared using Microsoft Excel (Microsoft, Redmond, WA). We first excluded genes that were scored absent in any of the samples. To identify differentially expressed genes, fold change was calculated as the "LPS+IL-10/LPS" ratio separately in SHIP1 WT and KO cells at 0.5 hour. Threshold ratio was set to be smaller than 0.5 or greater than 1.5 for the genes to be considered as IL-10 regulated. Genes that showed a 2-fold difference in "LPS+IL-10/LPS" ratios between SHIP1 WT and SHIP1 KO cells were considered as potential SHIP1-regulated genes. A total of 122 genes were identified.

To identify IL-10/STAT3-regulated genes, two publications were consulted: Lang *et al.* [480] and Hutchins *et al.* [45]. Genes that appeared in both the SHIP1-regulated list (described above) and in one or both of these two publications were considered as potential SHIP1-STAT3-regulated genes. The remaining STAT3-regulated genes that were not in our SHIP1-regulated gene subset were refereed as STAT3-regulated genes.

2.16 Protein expression and purification

2.16.1 HEK293T expression system

About 6 x 10^6 HEK293T cells per plate were seeded on 15 cm tissue culture plate the day prior to transfection. Using polyethylenimine (PEI) (Polysciences Inc., Warrington, PA) as the transfection reagent, 60 μg of the expression plasmid were introduced in the cells. Usually 3-6 plates of HEK293T were transfected at once. Transfection media was replaced by fresh media after 4 hours incubation at 37°C, and cells were left in the incubator for about 60-66 hours before cells were collected by centrifugation at 2000 rpm for 15 minutes at 4°C. Cell pellet was washed once with PBS, and lysed in lysis buffer containing 20 mM Tris-HCl pH 7.4, 150 mM NaCl, 10 mM tris(2-carboxyethyl)phosphine (TCEP) (Soltec Ventures, Beverly, MA), 5 mM imidazole, 0.5% NP-40, supplemented with 1X EDTA-free Protease Inhibitor Cocktail (Roche Diagnostics, Laval, QC) for 30 minutes at 4°C with nutation. Cell debris was removed by centrifugation at 18000 rpm for 30 minutes at 4°C, and cleared cell lysate was loaded directly onto a Talon Co^{2+}-affinity column (Clontech, Mountain View, CA). The column was washed with 5 CV of Buffer I (20 mM Tris-HCl pH 7.4, 150 mM NaCl, 1 mM TCEP, 5 mM imidazole, 0.5% NP-40), followed by 5 CV of Buffer II (20 mM Tris-HCl pH 7.4, 250 mM NaCl, 1 mM TCEP, 5 mM imidazole, 0.005%-0.05% Tween-20). Bound proteins were eluted with 6 CV of Buffer III (Buffer II + 50 mM imidazole). The purity of the protein was analyzed by SDS-PAGE.

2.16.2 Bacterial expression system

The procedure for the expression and purification of PAC1 and PAC2 is as follows. LIC-HMT expression vector was transformed into *E. coli Rosetta(DE3) placI*

cells. Overnight culture was inoculated with a 250-fold dilution to start the actual culture. The cells were grown at 37°C in LB medium (supplemented with 50 μg/ml of kanamycin and 34 μg/ml of chloramphenicol) with shaking at 225 rpm. When OD_{600} reached about 0.6, the culture was cooled down to room temperature before the addition of 0.4 mM isopropyl β-D-1-thiogalactopyranoside (IPTG) to induce the expression of recombinant protein. Culture was left in the shaker overnight (usually 16-18 hours) at 22°C, and then collected by centrifugation (5000 rpm for 10 minutes at 4°C). The cell pellet was subsequently resuspended in lysis buffer (20 mM Tris-HCl pH 7.4, 350 mM NaCl, 10 mM TCEP, 5 mM imidazole, supplemented with 1X EDTA-free Protease Inhibitor Cocktail (PIC) (Roche Diagnostics, Laval, QC) and 25 μg/ml lysozyme), and lysed via sonication (2 cycles of 2 minutes pulse) on ice. Cell debris was removed by two rounds of centrifugation, first at 5000 rpm for 15 minutes at 4°C followed by 18000 rpm for 30 minutes at 4°C. Supernatant was filtered with a 0.45 μm filter and loaded onto a Talon Co^{2+}-affinity column, previously equilibrated with Buffer A (20 mM Tris-HCl pH 7.4, 250 mM NaCl, 1 mM TCEP), and washed with 10 CV of Buffer B (Buffer A + 5 mM imidazole). Bound proteins were eluted with 6 CV of Buffer C (Buffer A + 50 mM imidazole). To remove the HMT tag, TEV protease (purified in house as a His_6-tagged protein) was added to the eluted protein, which was then dialyzed against Buffer D (20 mM Tris-HCl pH 7.4, 250 mM NaCl, 1 mM TCEP) overnight at 4°C with gentle stirring. The dialyzed sample was loaded onto the Amylose column (New England Biolabs, Whitby, ON), and the flow through, which contained the untagged protein, was loaded onto the Talon column to remove the His6-TEV protease. The flow through from the Talon column was dialyzed against Buffer E (20 mM Tris-HCl pH 7.4, 25 mM NaCl, 1

mM TCEP) overnight at 4°C with gentle stirring, and then loaded onto the ResourceQ column (6 ml column volume) (GE Healthcare, Mississauga, ON), followed by washes with 3 CV of Buffer E. To elute the protein, Buffer F (20 mM Tris-HCl pH 7.4, 1000 mM NaCl, 1 mM TCEP) was also used. A gradient from 25 mM NaCl (0% buffer G) to 200 mM NaCl (20% Buffer G) was used across 20 CV to separate the components in the protein sample. The fractions were analyzed by SDS-PAGE. PAC1/2 usually eluted from the ResourceQ column at ~130 mM NaCl. The purified protein was concentrated to about 5-10 mg/ml using Amicon concentrators with 30K MWCO (Millipore, Etobicoke, ON), and exchanged into the desired buffer. For protein crystallization, the desired buffer contained 50 mM Tris-HCl pH7.4, 25 mM NaCl and 0.5 mM TCEP. Protein was stored at 4°C and used within 2-3 weeks of time. We found that freezing and thawing the protein caused precipitation of the protein; thus, for long-term storage at -20°C, we included 50% glycerol in the protein solution to prevent freezing. Expression and purification of His_6-C2 were similar to those of HMT-tagged fusion protein, with the exclusion of TEV protease incubation, Amylose column and the second Talon column.

2.17 *In vitro* phosphatase assay

The concentration of enzyme used in the reaction was pre-determined as followed: (1) phosphatase assay was performed on a 3-fold dilution series of each batch of enzymes in the absence of any activator under standard assay condition (described below), (2) a titration curve was plotted as A650 vs enzyme concentration, and (3) the concentration of enzyme that gave half-maximal A650 value was chosen for experiments. Usually, 2 to 5 nM of enzyme were used.

The assay was performed in 96-well plates, and the standard volume per reaction

well was 25 ul. Assay buffer contained 20 mM Tris-HCl pH 7.4, 150 mM NaCl, 0.05% Tween-20 and 4-10 mM $MgCl_2$ +/- 2 mM $CaCl_2$. Enzyme was diluted in the assay buffer, and was incubated with or without test compounds (dissolved in ethanol) for 10 minutes at room temperature, before the addition of 50 μM of inositol-1,3,4,5-tetrakisphosphate (IP_4) (Echelon Bioscience Inc., Salt Lake City, Utah). The reaction was allowed to proceed for 10 minutes at 37C, and then stopped by the addition of malachite green reagent. The amount of inorganic phosphate released was assessed by absorbance measurement at 650 nm. Triplicate wells were done with each reaction.

For enzyme kinetics studies, different concentration of IP_4 was used and reactions were stopped at different time points. Initial velocities were calculated, and V_{max} and K_m were determined using the GraphPad 6 software.

2.18 Protein crystallization, data collection, phasing and refinement

Initial crystallization hits were obtained via sparse matrix screening. The sitting drop vapour diffusion method was performed in 96-well plates using commercially available crystallographic solutions (Qiagen, Toronto, ON). The protein mixture was allowed to equilibrate for at least 19 hours before scoring under the microscope. Several conditions gave crystals of PAC1 or PAC2, but none of these conditions gave diffraction quality crystals. Optimization of crystallization conditions were performed by varying the pH and/or precipitant concentrations from the original screen conditions, as well as changing the concentration of protein used, in 24-well plate format using the hanging drop vapour diffusion method. Diffraction-quality protein crystals were obtained at 4-7 mg/ml protein at room temperature: wild type PAC2 crystallized in 0.1 M Tris-HCl pH.5 and 20% PEG5000; PAC1cc crystallized in 0.1 M Tris-HCl pH7.7, 22% PEG1500 and 2

mM $MgCl_2$ (space group C121), or 0.1 M HEPES-NaOH pH6.7, 20% PEG1500 and 5 mM $MgCl_2$ (space group P 21 21 21). Unique fragments of crystal clusters of protein were soaked for 5 to 10 seconds in the crystallization solution containing 25% isopropanol, and flash-frozen under liquid nitrogen.

Diffraction data sets were collected at the Advance Proton Source (APS) beamline 23-ID-D-GM/CA and the Canadian Light Source (CLS) beamline 08ID-1, and processed with XDS [508]. The first model built was PAC1cc with space group C121. The data set was processed to 1.74Å. Matthews coefficient calculation predicted two molecules in the asymmetric unit (ASU) with a solvent content of 42%. A mixed model of the phosphatase-domain was created with the SCWRL server at the JCSG [509], built from SHIP2 phosphatase domain (PDB ID: 3NR8). Initial phases were then obtained using Phaser MR [510], which could place two molecules (two phosphatase domains). The result was analyzed in COOT [511] with obvious errors corrected and model in areas of weak density deleted. After a round of restrained refinement in Refmac5 [512], ARP/wARP Classic [513] was used for automated model building starting from existing model. ARP/wARP was able to build large parts of one C2 domain and fragments of the other. These models for C2 domain were merged with the previous phosphatase-domain model from Refmac5. After several rounds of manual model building, another round of ARP/wARP was utilized that built further pieces of the C2 domains as alanine backbone. After this step, it was feasible to assign several stretches of sequence in one C2 domain and to manually build additional pieces in the second C2 domain. The model was completed with subsequent rounds of manual model building in COOT and refinement in Refmac5. The utilized resolution was limited to 2.1Å during this stage. Automatically

generated local non-crystallographic symmetry (NCS) restraints were used in the refinement. Towards the completion of the model, one TLS group per domain was defined and used in Refmac5.

For the second PAC1cc structure, the Matthews coefficient calculation indicated one molecule per ASU with a solvent content of 38%. Chains A (phosphatase domain) and B (C2 domain) from the first PAC1cc model were used as a search model in Phaser. One solution was found with RFZ=6.3, TFZ=8.5, PAK=6, LLG=144, LLG=11942. The loop consisting of residues 436-444 was responsible for the clashes in the solution, and thus was removed in subsequent refinement. The final model was built and refined with COOT and Refmac5.

The Matthews Coefficient calculation of the wild type PAC2 data set predicted three, four or five molecules in the ASU. Probability for 4 molecules was 0.70 with a predicted solvent content of 47%. A search model was built from the second PAC1cc structure, with some areas deleted prior to the search. The used search model consisted of residues 403-438, 446-516, 522-659, 669-718, 733-741, 749-768, 784-827 and 834-856. Phaser MR was able to place four molecules with TFZ-scores between 21.8 and 89.3. Model was refined using local NCS restraints throughout and TLS refinement in the final stages.

2.19 Protein lipid overlay (PLO) assay

PLO assays were described previously [429] with minor modifications. Lyophilized PI(3,4)P_2-diC16 and PI(3,4,5)P_2-diC16 were reconstituted in methanol:water (2:1.8 ratio), and diluted in the same solution to desired concentration before spotting on PVDF membranes (Millipore, Etobicoke, ON). The membranes were dried, incubated in

blocking buffer (3% BSA in TBS) for 1 hour at room temperature, and then washed with TBST buffer (TBS and 0.05% Tween-20) until the membranes were wet. Purified proteins were diluted in TBS and incubated with the PIP-spotted membranes for 5 hours at room temperature with gentle agitation. Membranes were then washed with TBST thrice, incubated with anti-His antibody for 1 hour at room temperature, and washed again with TBST thrice before being incubated with the Alexa Fluor® 660 anti-mouse IgG antibody for 45 minutes at room temperature. After three final washes in TBST, the membranes were imaged using LI-COR Odyssey Imager, and intensities were quantified with the ImageStudio software (LI-COR, Lincoln, NE).

2.20 Saturation transfer difference nuclear magnetic resonance (STD-NMR)

Purified protein was concentrated and exchanged into D_2O buffer containing 20 mM Tris-HCl pH7.4, 150 mM NaCl, and 1 mM TCEP. Concentration of H_2O was kept below 1% in all cases. In some experiments, 6 mM $MgSO_4$ was included in the buffer. The STD ^{1}H NMR spectra were recorded on a Bruker AV-600 spectrometer with a 5-mm CPTCI cryoprobe utilizing a standard Bruker pulse sequence (Bruker Corporation, Milton, ON). In all experiments, 1.01 mM ligand and 10.1 μM of protein were used with a total volume of 600 μl D_2O/buffer. When AQX-151 was used, the total volume included 6 μl of DMSO-d6 containing 0.2 mg of ligand.

2.21 Isothermal titration calorimetry (ITC)

Purified recombinant protein was dialyzed against ITC buffer (50 mM HEPES-NaOH pH 7.4, 150 mM NaCl, 1 mM TCEP) overnight at 4C with gentle stirring. Protein was collected and any precipitation was removed by centrifugation at 13000 rpm for 15 minutes at 4C. Protein concentration was determined by first measuring absorbance at

280 nm (A280) and then performing the appropriate conversion using the theoretical extinction coefficient, according to Beer's Law. Protein was then diluted to 0.1 mM with ITC buffer. Lyophilized PI(3,4)P_2-diC8 or AQX-1125 were reconstituted in ITC buffer at 1 mM on the day of experiment. ITC experiments were performed in an ITC200 instrument (GE Healthcare, Mississauga, ON) at 25°C and a stirring speed of 300 rpm. Twenty injections of 2 μl ligands were titrated into protein at a 3-minute interval. Control experiment corresponded to ligand titration into ITC buffer. Data were processed using MicroCal Origin 7.0 SR4.

2.22 Statistical analysis

All statistical analysis was performed using GraphPad Prism 6 software.

Chapter 3: LPS and IL-10 Regulate miR-155 at the Maturation Step in Macrophages

3.1. Introduction

Since the discovery of the first miRNA (lin-4) in 1993 [514] and the term "microRNAs" was coined in 2001 [515], scientists have found that miRNAs are involved in essentially all biological processes. In particular, the critical roles of miRNAs in the development, maintenance and functions of immune cells have been extensively studied.

The first TLR-induced miRNA expression profiling study was done in human macrophages, and found that miR-146a, miR-132 and miR-155 are upregulated by LPS [123]. Subsequent studies reported that TLR activation upregulates the production of other miRNAs including miR-147 [516], miR-9 [517], miR-21 [49], miR-27b [518], miR-210 [519] and let-7e [520]. TLR activation also downregulates the expression of certain miRNAs such as miR-223 [521], miR-125b [120], and miR-98 [522]. The interplay of these miRNAs fine-tunes TLR signalling [115,116,523].

Our studies focus on miR-155, whose enhanced expression is associated with cancer [284,306,312] and inflammation-related diseases such as rheumatoid arthritis [318]. Thus, studying the regulation of miR-155 will be beneficial for development of useful therapeutics to treat the diseases. miR-155 was the first miRNA that has been knocked out in mice, which developed normally but had defective innate and adaptive immunity [293]. When miR-155 is ubiquitously expressed in the hematopoietic compartment, the mice develops a myeloproliferavtive disorder, characterized by granulocyte and monocyte expansion, and splenomegaly due to extramedullary hematopoiesis [288].

Besides LPS, miR-155 expression can be induced by a wide range of immune stimuli [122], and its expression is positively correlated with the production of pro-

inflammatory cytokines such as TNFα [120]. Interestingly, miR-155 effect on TNFα production appears to be direct [121,302], likely due to increased stability of TNFα mRNA in the presence of miR-155 [121]. Other miR-155 targets include SHIP1 [311] and SOCS1 [335], both of which have negative roles in macrophage activation [112,317,524-526]. Even though the overall effect of miR-155 is pro-inflammatory, miR-155 also fine-tunes inflammation by targeting signalling molecules important in TLR signalling, such as IKKε [120], RIPK1 [120], and MyD88 [154].

Since IL-10 is a negative regulator of inflammation and macrophage activation, we hypothesized the IL-10 might suppress miR-155 induction by TLR agonists. Indeed, as detailed in this chapter, IL-10 is able to inhibit miR-155 expression. During the course of the experiments described in this chapter, another research group has also found that IL-10 inhibits LPS-induced miR-155 expression [333]. These investigators have showed that LPS induces miR-155 expression via the activation of the JNK pathway, and requires the AP-1 motif in the BIC promoter. They have also demonstrated that IL-10 inhibits miR-155 expression in a STAT3-dependent manner via the Ets1 motif in the BIC promoter. In addition, Ruggiero *et al.* [262] have found that LPS induction of miR-155 is post-transcriptionally regulated by the RNA binding protein KSRP, which specifically facilitates the maturation of pre-miR-155 to matured miR-155.

Here, we show that IL-10 treatment does not affect the transcription of the miR-155 host gene nor the nuclear export of pre-miR-155, but rather destabilizes both pri-miR-155 and pre-miR-155 transcripts, as well as interferes with the final maturation of miR-155. This inhibitory effect of IL-10 on miR-155 expression involves both the transcription factor, STAT3, and the phosphoinositol phosphatase, SHIP1.

3.2. Results

3.2.1. IL-10 inhibits LPS-induced pri-miR-155 and miR-155 expression in macrophages

We first examined the kinetics of IL-10 inhibition of pri-miR155 and mature miR155. On one hand, as shown in **Figure 3.1A**, LPS-induced expression of pri-miR-155 was detected as early as 1 hour in the RAW264.7 macrophage cell line, peaked at 2 hours and declined after that. The level of mature miR-155, on the other hand, was barely detectable at 1 hour and continued to increase over the course of 4 hours. Addition of IL-10 inhibited expression of pri-miR-155, but inhibition was only observed after 1 hour and was statistically significant after 2 hours and later. IL-10 inhibition of miR-155 was also delayed, with inhibition being statistically significant only at 4 hours. Similar kinetics was observed in peritoneal macrophages freshly isolated from mice (**Figure 3.1B**). The inhibitory effect of IL-10 on pri-miR-155 and miR-155 levels are similar to that reported previously [333].

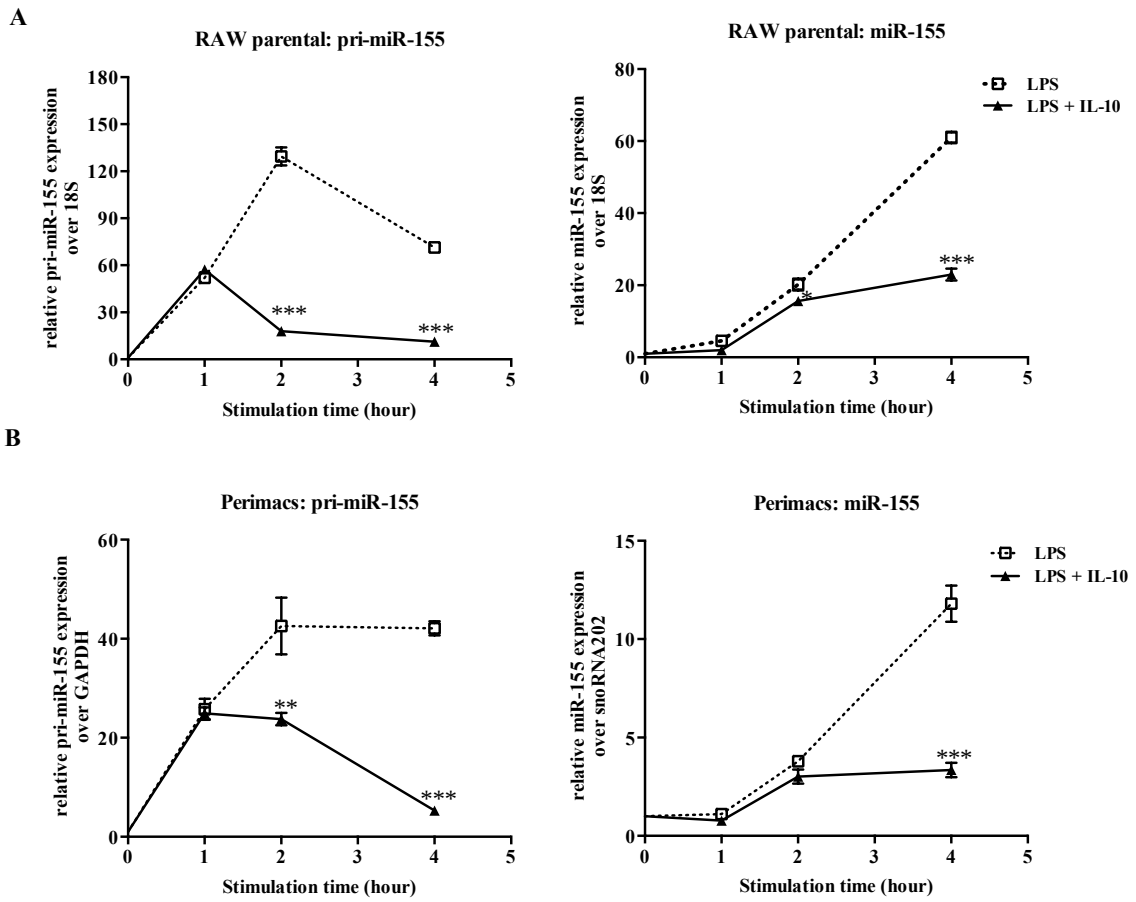

Figure 3.1 IL-10 inhibits LPS induction of pri-miR-155 and miR-155 expression in macrophages.

(A) RAW264.7 parental cells or (B) perimacs were stimulated with LPS +/- IL-10 for the indicated times prior to total RNA extraction. Expression levels of pri-miR-155 and miR-155 were determined by real time PCR and plotted relative to unstimulated samples. Statistical significance between LPS and LPS + IL-10 treatments was calculated by a two-way ANOVA test with a 95% confidence (* $p < 0.05$, ** $p < 0.01$, *** $p < 0.001$, **** $p < 0.0001$). Similar results were observed in at least three independent experiments. Representative data are shown.

3.2.2. LPS and IL-10 do not regulate miR-155 at the level of transcription

Several check points are in place to regulate the level of particular miRNAs in cells: transcription of pri-miRNA, Drosha-mediated generation of pre-miRNA, export of pre-miRNA and finally Dicer-mediated maturation of miRNA. The kinetics of miR-155 expression in response to LPS +/- IL-10 (**Figure 3.1A-B**) indicated that the regulation of pri-miR-155 and mature miR-155 differs. We first examined the potential effect of LPS

and IL-10 on the transcription of pri-miR-155 by using a luciferase reporter construct controlled by the BIC promoter (the host gene of miR-155). A reporter harbouring the promoter of IkBζ acted as the control for our reporter assays. IkBζ is a known LPS response gene. As shown by real time PCR, we found that IL-10 inhibited LPS-induced IkBζ mRNA expression in RAW264.7 cells (**Figure 3.2A**). The IkBζ promoter reporter showed similar LPS induction and IL-10 inhibition pattern (**Figure 3.2B**). In contrast, we found that LPS did not induce BIC promoter activity compared to the unstimulated control (**Figure 3.2B**). Similarly, addition of IL-10 did not affect the activity of the BIC promoter either. The data were surprising since pri-miR-155, the primary transcript from the BIC gene, increased with LPS stimulation and decreased with IL-10 treatment (**Figure 1A**). Also, the unresponsiveness of the BIC reporter to stimuli differs from McCoy *et al.*'s finding that LPS stimulated, while IL-10 inhibited, BIC reporter activity [333]. We assessed whether the difference between our and McCoy *et al.*'s BIC reporter results might be due to cell stimulation time, transfection reagent used, and/or transfection times; however, we consistently observed no change in the BIC reporter activity upon LPS and IL-10 treatment (**Figure A.1**).

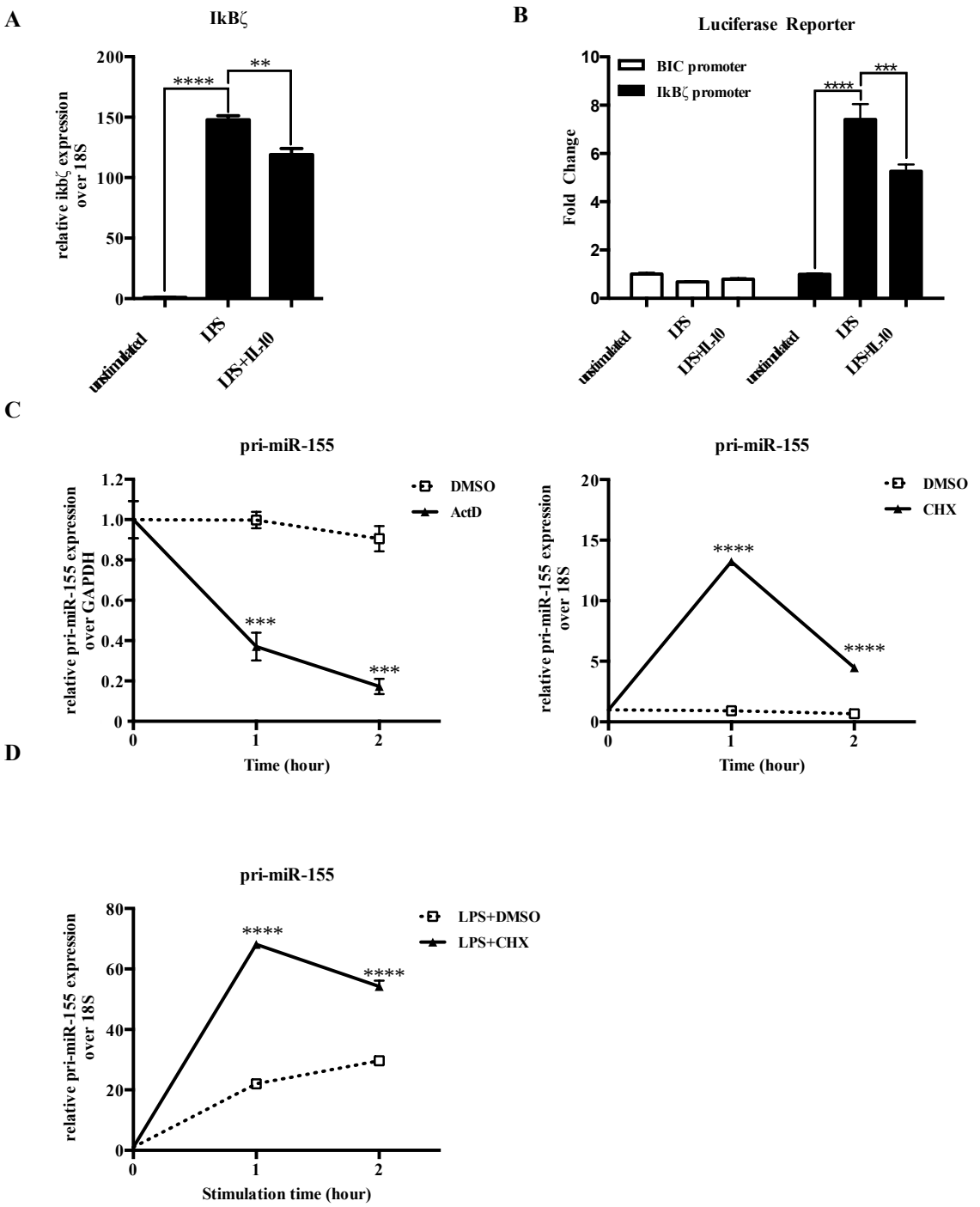

Figure 3.2 IL-10 does not regulate miR-155 expression at the transcription level.
(A) RAW264.7 parental cells were stimulated with LPS +/- IL-10 for 1 hour before total RNA was extracted. Expression levels of IkBζ were determined by real time PCR and plotted relative to unstimulated samples. Statistical significance between the treatments was calculated by an unpaired two-tailed student's *t*-test with a 95% confidence (** $p < 0.01$, **** $p < 0.0001$). (B) RAW264.7 cells were transfected with TK-Renilla and BIC promoter reporter or IkBζ promoter reporter. After 24 hours rest, cells were stimulated with LPS +/- IL-10 for 2 hours. Reporter

activity was normalized to the TK-Renilla and plotted as fold change relative to the unstimulated sample. (C – D) RAW264.7 cells were treated with (C) ActD, CHX or DMSO, or (D) LPS + DMSO or CHX for the indicated time prior to RNA extraction and determination of pri-miR-155 level by real time PCR. Statistical significance between DMSO treatment and drug treatment was calculated by a two-way ANOVA test with a 95% confidence (**** $p < 0.0001$). Similar results were observed in at least two independent experiments. Representative data are shown.

3.2.3. Pri-miR-155 is constitutively transcribed but maintained at low level via degradation mechanism.

The lack of responsiveness of the BIC reporter to LPS and IL-10 was unexpected, since LPS clearly increased the level of pri-miR-155 in cells (**Figure 3.1**). However, the steady state transcript level of a gene is not a sole result of increased transcription; it can also be due to decreased transcript degradation. To examine the possibility that the pri-miR-155 is constitutively transcribed and undergoes regulated degradation, we looked at the effect of the transcription inhibitor actinomycin D (ActD) or translation inhibitor cycloheximide (CHX) on pri-miR-155 levels. In the experiments using CHX, we used 18S rRNA as the normalization control, instead of GAPDH, because the GAPDH expression level was sensitive to CHX treatment while 18S rRNA expression level was not (**Figure B.2**).

We treated resting RAW264.7 with ActD and found that steady state pri-miR-155 level dropped more than 2-fold by 1 hour and was almost undetectable at 2 hours (**Figure 3.2C, left panel**). This indicated that pri-miR-155 is constitutively transcribed even in unstimulated RAW264.7 cells. By contrast, CHX treatment increased pri-miR-155 levels by 6-fold in 1 hour, which indicated that *de novo* translation of short-lived decay factors contributes to maintain pri-miR-155 level at a low level in unstimulated cells (**Figure 3.2C, right panel**). CHX treatment also enhanced LPS-induced pri-miR-155 expression (**Figure 3.2D**).

3.2.4. LPS and IL-10 do not cause editing of pre-miR-155

miRNAs can also be regulated by RNA editing, such as by adenosine deaminases (ADARs) [222,527,528]. These enzymes modify the RNA sequence by converting adenosine to inosine. Since inosine is being read as guanosine, the biological consequence is an A to G conversion. This can affect both Drosha- and Dicer-mediated cleavage, as well as the export of pre-miRNAs.

We addressed this possibility by sequencing two samples of cDNA obtained from cells left unstimulated, stimulated with LPS or LPS+IL-10. The sequencing analysis revealed that there is no nucleotide change in pre-miR-155 sequence upon LPS or LPS+IL-10 treatment (**Figure 3.3**).

Figure 3.3 LPS and IL-10 do not cause editing on the pre-miR-155 sequence.
DNA sequencing results of RT-PCR products were performed on pri-miR-155. The expected sequences of pre-miR-155 and mature miR-155 are included at the top. Two samples of each treatment (unstimulated, LPS, LPS+IL-10) were analyzed, and showed in blue.

3.2.5. LPS and IL-10 do not regulate nuclear export of pre-miR-155

Another miRNA regulation checkpoint occurs at the export of pre-miRNAs from the nucleus to the cytoplasm. The delayed expression of mature miR-155 relative to pri-miR-155 and pre-miR-155 might be due to delayed export of pre-miR-155 into the cytoplasm for processing by Dicer. To investigate the possible effect of LPS and IL-10

on the nuclear export of pre-miR-155, we stimulated RAW 264.7 cells with LPS +/- IL-10 and fractionated the cells into nuclear and cytoplasmic fractions. The levels of pre-miR-155 expression in the total cellular, nuclear, and cytoplasmic fractions were determined by real time PCR. The kinetics of pre-miR-155 expression in total cellular RNA (**Figure 3.4A**) mirrored that of pri-miR-155 (**Figure 3.1A**). Pre-miR-155 expression was induced quickly by LPS and peaked at 2 hours. IL-10 inhibition of pre-miR-155 was observed at 2 hours. The kinetic profiles of pre-miR-155 in nuclear and cytoplasmic RNA fractions were quite similar to that in total RNA, indicating that neither LPS nor IL-10 regulated or altered the nuclear export of pre-miR-155.

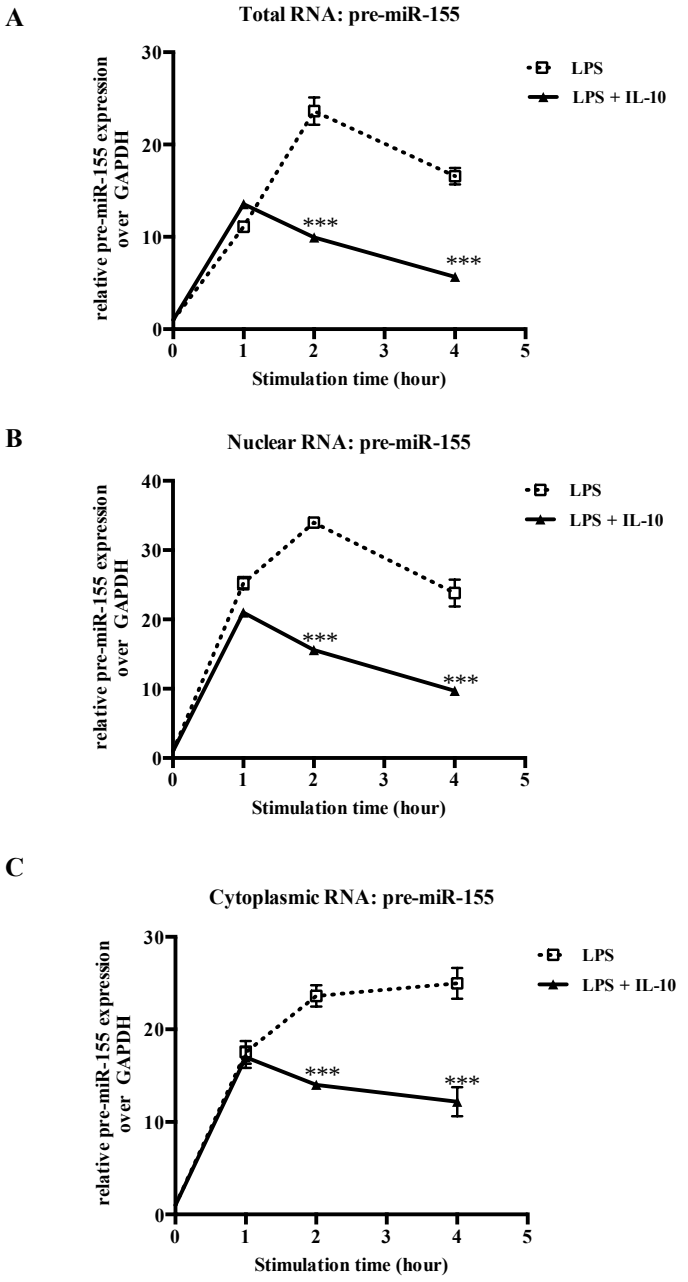

Figure 3.4 IL-10 does not affect the export of pre-miR-155 from the nucleus to the cytoplasm.

RAW264.7 cells were stimulated with LPS +/- IL-10 for the indicated times prior to fractionation of nuclei and cytoplasm. Levels of pre-miR-155 in (A) total, (B) nuclear and (C) cytoplasmic fractions were determined by real time PCR. Statistical significance between LPS and LPS + IL-10 treatment was calculated by a two-way ANOVA test with a 95% confidence (* $p < 0.05$, ** $p < 0.01$, *** $p < 0.001$). Similar results were observed in at least three independent experiments. Representative data are shown.

3.2.6. IL-10 inhibits LPS induction of miR-155 via SHIP1 and STAT3

McCoy *et al.* [333] found that IL-10 inhibition of miR-155 expression required the presence of STAT3 protein. The STAT3 pathway is the best-characterized pathway downstream of the IL-10R. However, we recently found that IL-10 also signals through the phosphatase SHIP1 [56], so we investigated the contribution of SHIP1 to IL-10 inhibition of pre-miR-155 and mature miR-155 levels. We tested the ability of IL-10 to inhibit miR-155 in peritoneal macrophages (perimacs) from wild type or SHIP1 knockout (SHIP1 KO) mice. As shown in **Figure 3.5A**, IL-10 could not inhibit miR-155 expression to the same extent in SHIP1 deficient cells as compared to wild type cells.

To confirm these findings, we generated RAW264.7 cell lines in which SHIP1 protein levels were reduced by RNA silencing. siRNA sequence targeting SHIP1 or a scrambled (SCRMB) sequence was cloned into the pTRIPZ lentiviral vector that contains miRNA-like processing elements to express the siRNA sequence under the control of a doxycycline (Dox) regulated promoter. The addition of Dox to the SHIP1 siRNA transduced cells reduced SHIP1 protein expression by 80% (**Figure 3.5B**). Similar to that observed in wild type perimacs, IL-10 inhibited pri-miR-155 and miR-155 in the SCRMB siRNA transduced cells (**Figure 3.5C**). Similar to SHIP KO perimacs, the SHIP1 siRNA transduced cells had reduced IL-10 inhibition of mature miR-155 (**Figure 3.5C**).

Our data suggested that SHIP1 negatively regulated LPS-induced miR-155 expression. To determine whether activation of SHIP1 alone could inhibit miR-155 expression, we made use of a small molecule SHIP1 activator, AQX-MN100, which binds to the allosteric activation site on SHIP1 and activates its phosphatase activity.

AQX-MN100 is specific for SHIP1 and does not activate even the closely related SHIP2 inositol phosphatase. We found AQX-MN100 inhibited miR-155 expression in LPS-stimulated macrophages (**Figure 3.5D**), indicating that SHIP1 activation alone can reduce miR-155 levels. Notably, SHIP1 activation alone does not reduce miR-155 levels to the same extent as IL-10 (**Figure 3.5C**), suggesting other IL-10 regulated signalling pathways also contribute to IL-10's effect.

Since SHIP1 is a negative regulator of the PI3K/AKT pathway, we reasoned that the PI3K/AKT pathway would have a positive role in miR-155 expression. We tested this hypothesis by expressing a conditionally active form of AKT in RAW264.7 cells. This AKT-Estrogen Receptor (ER) fusion protein is activated by the addition of 4-hydroxytamoxifen (4-HT), which displaces HSP90 and allows AKT-ER access to its substrates. Pretreating the cells with 150 nM 4-HT for 20 minutes was sufficient to activate AKT-ER, indicated by the increased phosphorylation of GSK3β, a substrate of AKT (**Figure A.3**). The untreated cells and the 4-HT treated cells produced similar miR-155 level in respond to LPS, but their responses to IL-10 differed (**Figure 3.5E**). IL-10 inhibition of miR-155 was impaired in 4-HT treated AKT-ER expressing cells (**Figure 3.5E**).

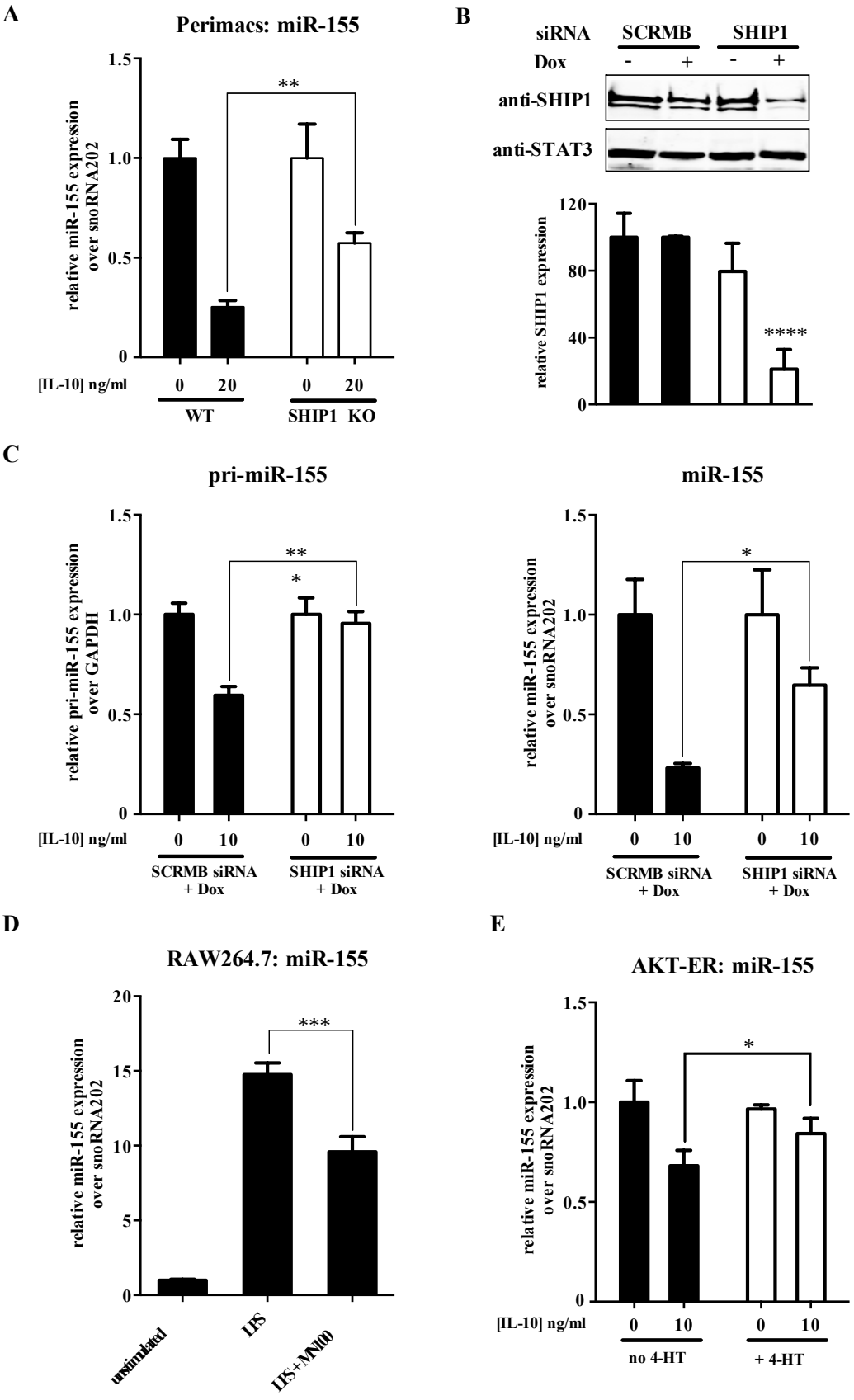
A
Perimacs: miR-155
relative miR-155 expression over snoRNA202
1.5
1.0
0.5
0
**
[IL-10] ng/ml
0
20
0
20
WT
SHIP1 KO
B
siRNA
SCRMB
SHIP1
Dox
-
+
-
+
anti-SHIP1
anti-STAT3
relative SHIP1 expression
120
80
40
0
****
C
pri-miR-155
relative pri-miR-155 expression over GAPDH
**
*
[IL-10] ng/ml
0
10
0
10
SCRMB siRNA + Dox
SHIP1 siRNA + Dox
miR-155
relative miR-155 expression over snoRNA202
*
D
RAW264.7: miR-155
relative miR-155 expression over snoRNA202
20
15
10
5
0
***
unstimulated
LPS
LPS+MM00
E
AKT-ER: miR-155
relative miR-155 expression over snoRNA202
*
[IL-10] ng/ml
0
10
0
10
no 4-HT
+ 4-HT

Figure 3.5 SHIP1 mediates IL-10 inhibition of miR-155.
(A) Perimacs were extracted from either WT or SHIP1 KO mice, and stimulated with 10 ng/ml LPS or LPS + 10 ng/ml IL-10. miR-155 expression levels were measured by real time PCR and plotted relative to the LPS alone sample in each cell type. (B) SCRMB and SHIP1 siRNA transduced cells were treated with 2 μg/ml Dox for 48 hours or left untreated prior to immunoblotting analysis for SHIP1 and STAT3 (loading control). Band intensities were quantified using the Quantity One Software. Statistical significance between treatments was calculated by a two-way ANOVA test with a 95% confidence (**** $p < 0.0001$). (C) SCRMB and SHIP1 siRNA transduced cells were treated with 2 μg/ml Dox for 48 hours and then stimulated with LPS +/- IL-10 for 2 or 4 hours. Expression levels of pri-miR-155 in the 2-hour samples and miR-155 in the 4-hour samples were measured by real time PCR and plotted relative to the LPS alone samples. (D) RAW264.7 cells were left untreated, treated with 10 μM AQX-MN100 or ethanol control for 30 minutes before being stimulated with LPS or LPS+AQX-MN100 for 4 hours. Expression level of miR-155 was measured by real time PCR and plotted relative to LPS samples. (E) AKT-ER transduced cells were treated with 150 nM 4-HT for 20 minutes or left untreated before being stimulated by LPS +/- IL-10 for 4 hours. Expression level of miR-155 was measured by real time PCR and plotted relative to the LPS alone samples. Statistical significance between stimulation conditions was calculated by a two-way ANOVA test with a 95% confidence (** $p < 0.01$, ***, $p < 0.001$, **** $p < 0.0001$). Similar results were observed in at least two independent experiments. Representative data are shown.

We then examined whether the contribution of STAT3 and SHIP1 to IL-10 inhibition of mature miR-155 were additive or redundant. To do this we made use of the synthetic STAT3 inhibitor, STA-21. We first tested the efficacy of STA-21 by testing its ability to inhibit IL-10 activation of the STAT3-responsive, c-fos promoter luciferase reporter. RAW264.7 cells were transiently co-transfected with the c-fos firefly luciferase and SV40 renilla luciferase control constructs. Cells were then treated with STA-21 or vehicle control, and stimulated with IL-10 or left unstimulated. As shown in **Figure 3.6A**, IL-10 induced the activity of the c-fos promoter, but pretreatment of 30 μM STA-21 reduced this induction. We then added STA-21 to SCRMB or SHIP1 siRNA transduced cells and measured the levels of pri-miR-155 and mature miR-155. As shown in **Figure 3.6B**, STA-21 impaired IL-10's ability to inhibit pri-miR-155 and mature miR-155 in both cells. In cells lacking SHIP1, the effect of STA-21 was more pronounced

than untreated cells. In fact, the expression of pri-miR-155 and miR-155 was enhanced, rather than inhibited by IL-10. These data suggest that SHIP1 and STAT3 play additive, non-redundant roles in IL-10 inhibition of miR-155.

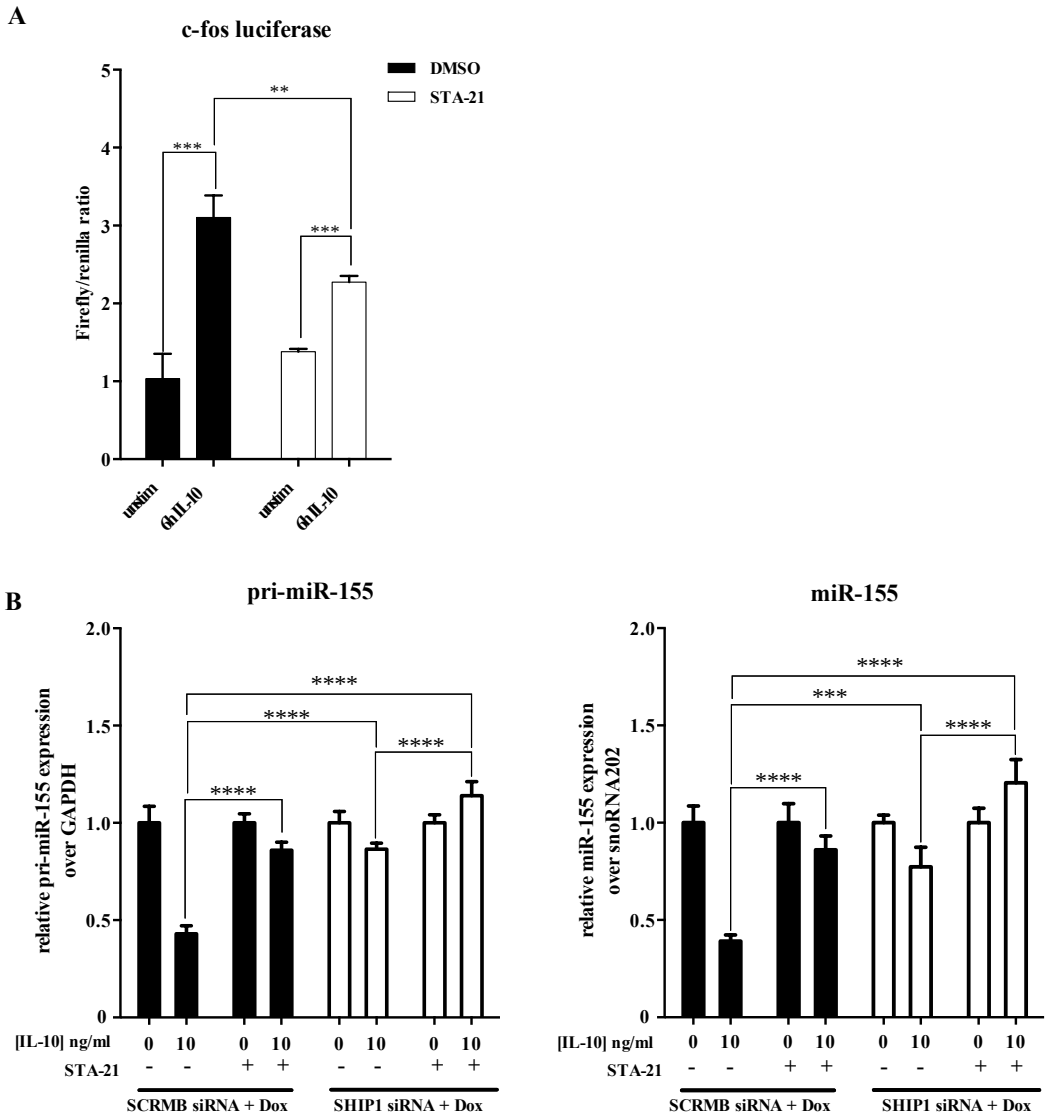

Figure 3.6 SHIP1 and STAT3 play additive roles in IL-10 inhibition of miR-155.
(A) RAW264.7 cells were transfected with the c-fos promoter reporter and TK-Renilla, and were pretreated with DMSO or 30 μM STA-21 for 1 hour prior to IL-10 stimulation for 6 hours. Luciferase activity was measured and plotted as firefly/renilla ratio. (B) SCRMB and SHIP1 siRNA transduced cells were treated as Figure 4C except the cells were pretreated with DMSO or 30 μM STA-21 for 1 hour prior to stimulation. Expression levels of pri-miR-155 at 2 hours and miR-155 at 4 hours were measured by real time PCR and plotted relative to the LPS alone samples. Statistical significance between stimulation conditions was calculated by a two-way

ANOVA test with a 95% confidence (** $p < 0.01$, *** $p < 0.001$, **** $p < 0.0001$). Similar results were observed in at least two independent experiments. Representative data are shown.

3.3. Discussion

miRNAs regulate both immune cell development and function [118,263,265]. In particular, miR-155 is extensively involved in different aspects of the immune system including haematopoiesis, T cell development, B cell differentiation, dendritic cell maturation, as well as mediating inflammation [122,288,293,294,309]. Enhanced miR-155 expression is associated with various human diseases such as rheumatoid arthritis [318] and cancers [284,306,323]. The multiple roles of miR-155 are mediated by its numerous targets that include transcription factors, protein receptors, kinases and other signalling molecules [314]. Because of miR-155's pro-inflammatory roles in macrophage activation, we examined whether IL-10 regulated miR-155 levels in our cells and if so, whether SHIP1 played a role. We found that IL-10 was able to inhibit the expression of miR-155 in activated macrophages (**Figure 1.1A-B**), which is consistent with a previous report. However, unlike McCoy *et al.* [333], we found that neither LPS nor IL-10 regulated miR-155 at the transcriptional level.

miRNAs can be regulated at multiple steps: transcription, nuclear export and maturation. We, Ruggiero *et al.* [262], and McCoy *et al.* [333] all observe upregulation of pri-miR-155 RNA. Although Ruggiero *et al.* [262] and we both concluded that pri-miR-155 levels are regulated primarily through post-transcriptional mechanisms [262], McCoy *et al.* [333] concluded that pri-miR-155 levels rise through increased transcription. Ruggiero *et al.* [262] used chromatin immunoprecipitation and sequencing to show that pri-miR-155 transcription rates do not change with LPS stimulation. We came to the same conclusion using BIC promoter luciferase reporter assays and cycloheximide

experiments. Our results with the BIC promoter reporter differed from McCoy *et al.*'s BIC promoter reporter assays in that they found LPS stimulated reporter activity while we did not. We do not know why our results differ, but we note that McCoy *et al.* [333] based their conclusion solely on luciferase reporter experiments, without using any other additional experimental approaches such as the ones Ruggiero *et al.* [262] and we used. Although neither LPS nor IL-10 altered BIC promoter activity, the level of pri-miR-155 transcript increased with LPS and decreased with IL-10 treatment. Steady state transcript levels are controlled not only by transcriptional activity, but also maintained through transcript stability. Therefore we used ActD and CHX treatments to examine whether pri-miR-155 transcript levels were being kept low in resting cells through degradation (**Figure 3.2C-D**). ActD reduced pri-miR-155 levels while CHX enhanced it, indicating that pri-miR-155 is constitutively transcribed and, at the same time, degraded in unstimulated cells.

Interestingly, although IL-10 significantly decreases the levels of pri-miR-155 by 2 hours after addition, significant decreases in mature miR-155 do not occur until 4 hours after stimulation. This discrepancy in kinetics suggests an additional layer of control past the regulation of pri-miR-155 levels. Thus, we examined whether IL-10 regulated the nuclear export of pre-miR-155 by fractioning total RNA into nuclear and cytoplasmic RNA. We found that the kinetics of pre-miR-155 expression in the nucleus and the cytoplasm were similar, which suggested that nuclear export of miR-155 was not regulated by IL-10. From these observations, we deduced that IL-10 likely regulated the processing of pre-miR-155 to functional, mature miR-155. Emerging evidence shows that miRNA biogenesis or processing can be regulated at the post-transcriptional steps by

different RNA-binding proteins that modulate Drosha or Dicer activities. In particular, the RNA binding protein KSRP was found to be required for miR-155 maturation in response to LPS stimulation in macrophages [262]. Furthermore, the ability of KSRP to support miRNA maturation was found to be stimulated by AKT-mediated phosphorylation [529]. Future studies in the laboratory are directed to examine whether IL-10 may modulate the function of KSRP to inhibit the production of mature miR-155.

IL-10 function is well known to be mediated by the transcription factor STAT3 [368,374,413,416,420] and STAT3 is involved in IL-10 inhibition of miR-155 [333]. We also found that the phosphatase SHIP1 is also involved in mediating IL-10 inhibition of LPS-induced TNFα production and AKT activation [56,376]. We now report that IL-10 inhibition of miR-155 expression was impaired in macrophages lacking SHIP1 but such inhibition could be achieved by the addition of the SHIP1 activator, AQX-MN100 (**Figure 3.5**). The addition of the STAT3 inhibitor STA-21 further reduced IL-10 inhibition (**Figure 3.6**). The additive effect of SHIP1 knockdown and STAT3 inhibition suggests that SHIP1 and STAT3 regulate miR-155 expression through independent mechanisms.

Consistent with the fact that SHIP1 is a negative regulator of the PI3K/AKT pathway, we found that 4-HT mediated activation of AKT-ER abolished IL-10 inhibition of miR-155 expression (**Figure 3.5C**), indicating a positive role of AKT in miR-155 expression. This finding appears to disagree with a previous study in which a myristylated, constitutively active AKT reduced LPS-induced miR-155 in macrophages [520]. The difference in conclusions between ours and the Androulidaki *et al.*'s [520] studies may be due to the use of the constitutively active AKT in their study. Persistent

activation of AKT may change the nature of the cells. In contrast, the AKT-ER fusion protein we used in our experiments was only active when we added 4-HT.

SHIP1 is a well-characterized miR-155 target. Thus, the involvement of SHIP1 in IL-10 inhibition of miR-155 expression constitutes an elegant regulatory circuit composed of SHIP1, AKT and miR-155: LPS-induced activation of AKT promotes the expression of miR-155, which suppresses SHIP1, to allow PI3K/AKT pro-inflammatory events. Conversely, IL-10 mediated activation of SHIP1 inhibits AKT signalling and reduces miR-155 expression. As a result, SHIP1 protein translation is resumed and further suppresses macrophage activation.

Together, our data supported a new mode of action for the anti-inflammatory cytokine IL-10 in which IL-10 controls the overall level of functional miR-155 by regulating the stability of pre-miR-155 and its maturation through SHIP1 and STAT3-dependent mechanisms.

Chapter 4: STAT3 and SHIP1 Work Together to Mediate IL-10 Functions

4.1. Introduction

Since the discovery of IL-10, a large number of genes have been identified as regulated by IL-10 in activated macrophages including cytokines, chemokines, adhesion molecules, receptor proteins and enzymes [348]. For a long time, the transcription factor STAT3 was thought to be the sole molecule responsible for all IL-10 functions by either inducing expression of anti-inflammatory mediators (such as IL-1RA [530]), or inducing expression of other factors that inhibit selective gene expression. Lang *et al.* [416] performed microarray analyses of LPS +/- IL-10 regulated genes in macrophages derived from IL-10 knockout mice. They have found that IL-10 represses about 24% of LPS-induced genes, including cytokines (e.g.TNFα, and IL-10 itself), transcription factors (e.g. B-ATP, BCL-6 and C/EBPβ), surface molecules (e.g. IL-4Rα), genes implicated in NFκB activation (e.g. metallothionein-2 [531] and BCL-3 [532]), and those involved in regulating the MAPK pathway (e.g. GADD45γ [533] and TPL-2 [534]). Some of these genes (TNFα, B-ATF and IL-4Rα.) have also been verified to be STAT3-dependent by RT-PCR based analyses of IL-10 induced genes in wild type and STAT3 KO macrophages. A more recent study combined the use of chromatin immunoprecipitation-sequencing (ChIP-seq) and RNA-sequencing (RNA-seq) to identify IL-10 regulated genes whose promoter regions are bound by STAT3 upon IL-10 treatment [45]. Many of the genes that are upregulated by IL-10 and possess STAT3-binding sites (within 20 kb of their transcription start site, as defined by the authors) are implicated in chromatin remodeling, suggesting major chromatin remodeling may be one mechanism IL-10 uses to mediate gene expression. The authors have also found that IL-10, through STAT3, upregulates a number of transcription repressors that might be the ultimate effectors of

IL-10 anti-inflammatory responses by inhibiting the expression of pro-inflammatory cytokines.

However, data from our laboratory and other laboratories have showed that IL-10 can still function in the absence of STAT3 activity. For example, STAT3 deficiency or STAT3 inactivation (for example, through the expression of a dominant negative mutant) cannot completely abolish IL-10's ability to inhibit LPS-induced TNFα [419,420,535]. Also, a comparison of IL-10 KO [421] and STAT3 KO [413] mice in endotoxin models shows that although STAT3 KO mice, similar to IL-10 KO mice, produce elevated serum TNFα level after LPS injection, their TNFα eventually declines, unlike in IL-10 KO mice, where TNFα level remains high throughout the course of the experiment. More importantly, the decline of TNFα level in STAT3 KO mice coincides with the production of endogenous IL-10 [413], suggesting that IL-10 can reduce TNFα via a STAT3-independent manner. Through chromatin immunoprecipitation experiments using RNA polymerase II antibodies, we have found that IL-10 inhibits the transcription of TNFα by interfering with the elongation signal of RNA polymerase II, and that such inhibition is impaired in SHIP1-deficient macrophages [376]. In addition, we have also showed that SHIP1 is involved in IL-10 inhibition of TNFα production by inhibiting its translation, and that a small molecule SHIP1 activator can mimic IL-10 action [56]. Moreover, as detailed in Chapter 3 [375], although knocking out SHIP1 or inhibiting STAT3 activity alone does impair IL-10's ability to inhibit miR-155 expression, complete impairment is only observed when both SHIP1 and STAT3 actions are blocked. We thus hypothesize that SHIP1 and STAT3 cooperate to mediate IL-10 function.

SHIP1 negatively regulates the PI3K pathway by hydrolyzing the second messenger, $PI(3,4,5)P_3$, and thus reducing the recruitment and activation of PH-domain containing proteins. Besides its catalytic domain, SHIP1 also functions by acting as an adaptor protein through its multiple protein domains [426]. These domains allow SHIP1 to be recruited to the plasma membrane, where it hydrolyzes its substrate, or to act as an adaptor protein such as in the case of suppressing B cell activation [426]. While SHIP1 enzymatic activity is needed to suppress the activated PI3K pathway, SHIP1 decreases Ras activation by interacting with another adaptor protein Shc, dissociating the Shc-containing complex necessary for Ras activation [454]. This suppression of Ras activation does not require the enzymatic property of SHIP1. Other SHIP1-interacting proteins include Grb2, Dok1 and Dok2, whose interaction is important for inhibiting T cell activation [456]. Moreover, while SHIP1 negatively regulates TLR4-signalling by inhibiting PI3K in activated macrophages, a phosphatase dead SHIP still partly suppresses TNFα production in LPS-activated macrophages [317], again supporting an adaptor role for SHIP independent of its phosphatase activity. Perhaps, in the context of IL-10 signalling, SHIP1 cooperates with STAT3 by acting as an adaptor to recruit STAT3 to the IL-10R or other signalling proteins necessary for IL-10 function.

This chapter describes experiments that determine whether SHIP1 and STAT3 interact with each other, as well as global gene expression data that show the regulatory range of each protein in IL-10 inhibition of macrophages.

4.2. Results

4.2.1 Both STAT3 and SHIP1 mediate IL-10 inhibition of LPS-induced TNFα production.

To understand the relative contribution of SHIP1 and STAT3 in IL-10 function, we constructed a continuous flow apparatus, in which cells are exposed to stimulation media under continuous flow. In the conditions of continuous flow, cells experience similar environment as they are inside an animal where the flow of blood and extracellular fluid are continually removing autocrine factors from the cells. BMDMs derived from STAT3 WT and STAT3 KO mice were stimulated with LPS+/- IL-10. Consistent with previous data, we found that LPS induced two waves of TNFα production (**Figure 4.1A**), which peaked at about 75 minutes and 160 minutes, respectively. Inclusion of IL-10 drastically reduced TNFα production at both peaks in STAT3 WT cells. As reported [413], STAT3 KO cells produced higher level of TNFα upon LPS stimulation. We found that these cells also displayed the biphasic TNFα production profile as STAT3 WT cells. However, IL-10 function was impaired in the inhibition of the first peak of TNFα production. Similarly, IL-10 was not able to inhibit the first peak of TNFα production in SHIP1 KO cells, compared to SHIP1 WT cells. By contrast, IL-10 was capable to inhibit the second peak of TNFα production in STAT3 KO and SHIP1 KO cells, suggesting that IL-10 uses more than just STAT3 or SHIP1 to mediate its effects.

Together with our finding that STAT3 and SHIP1 additively mediate IL-10 inhibition of miR-155 [375], we believe that STAT3 and SHIP1 work together.

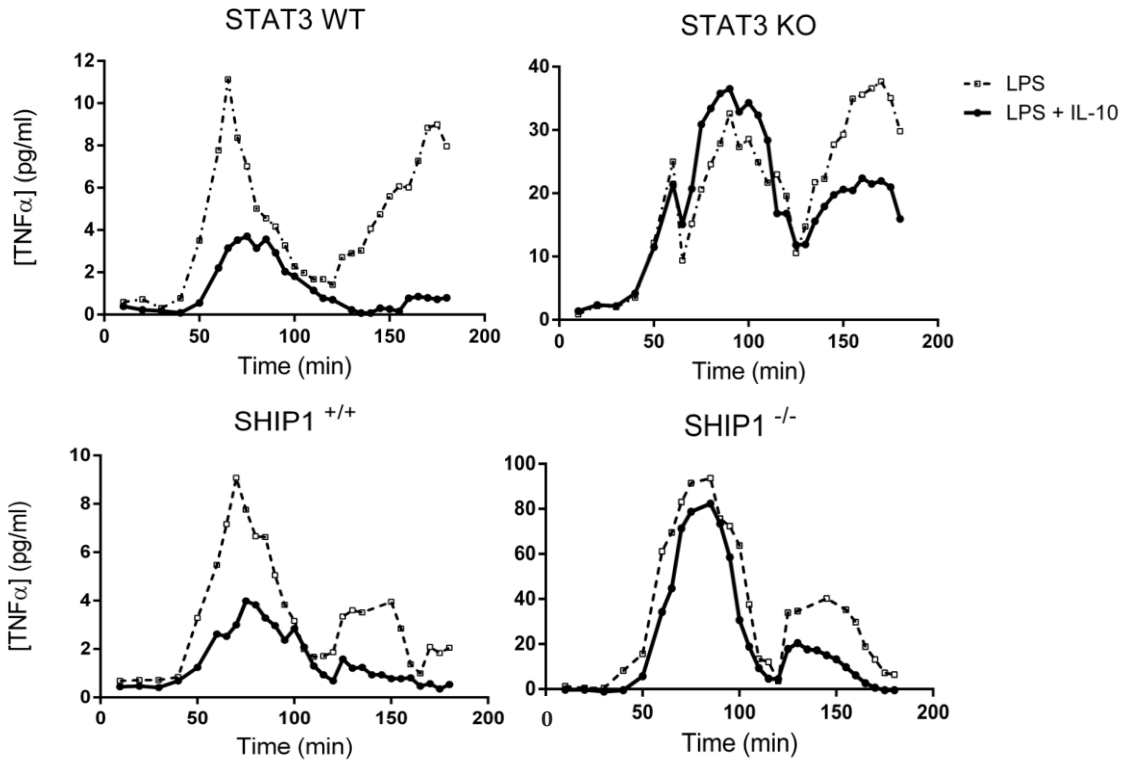

Figure 4.1 Deficiency in STAT3 or SHIP1 results in impaired IL-10 inhibition in the first peak of TNFα production, but not the second peak.

STAT3 WT, STAT3 KO, SHIP1 WT and SHIP1 KO BMDMs were stimulated with LPS (dotted line) or LPS+/- IL-10 (solid line) over the course of 200 minutes in the continuous-flow apparatus. Fractions were collected every 5 minutes, and were subjected to TNFα ELISA analysis. STAT3 WT and STAT3 KO cells were from mice with C57BL/6 background, whereas the SHIP1 WT and SHIP1 KO cells were from mice with BALB/c background. Data are representative of two independent experiments.

4.2.2 Physical interaction of SHIP1 and STAT3

Concurrent with functional assays to elucidate the relative contribution of SHIP1 and STAT3 in IL-10 function, data from our laboratory revealed that epitope-tagged SHIP1 was able to pull down endogenous STAT3 in IL-10 treated macrophages (data not shown). We thus want to explore the possibility that these proteins physically interact with each other to function. To do that, we first immobilized Flag-tagged STAT3 onto M2 affinity resins, and incubated these beads with purified His_6-tagged SHIP1. After washes, immunoblotting analysis was used to determine the amount of His_6-SHIP1

binding to Flag-STAT3. Different buffer conditions were also examined, including $MgCl_2$ that is necessary for SHIP1's enzymatic function, $CaCl_2$ that enhances SHIP1 activation by its activator (see Chapter 5), and AQX-151, a SHIP1 modulator that shows similar biological function as AQX-MN100 [430]. However, despite our efforts, we saw no evidence that Flag-STAT3 interacted with His_6-SHIP1 (**Figure 4.2**). One possible explanation is that one (or both) of these proteins needs to be phosphorylated for interaction to occur.

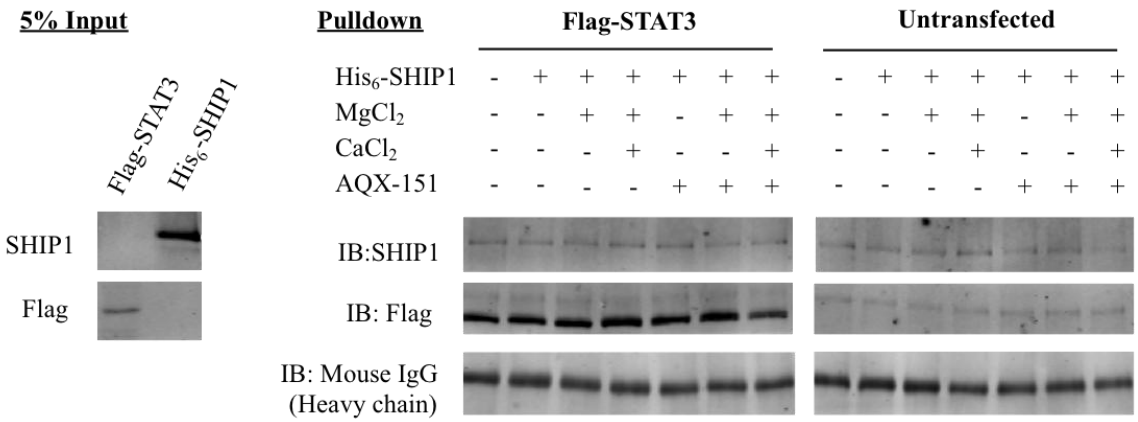

Figure 4.2 His_6-SHIP1 does not bind to Flag-STAT3 in an *in vitro* pulldown assay. Flag-STAT3 was expressed in HEK293T cells and immobilized on M2 affinity resins, and then incubated with purified His_6-SHIP1 in TBS+0.02% Tween-20 supplementaed with different reagents. The pulldown samples were then analyzed by immunoblotting with anti-SHIP1, anti-Flag and anti-mouse IgG antibodies.

4.2.3 Y190F mutation on SHIP1 abolishes IL-10's ability to inhibit TNF*α*

One regulatory mechanism of signalling proteins is the phosphorylation states on selected amino acid residues including tyrosine. Phosphorylated tyrosine (pTyr) is able to interact with the SH2 domain of another protein leading to subsequent signalling events. Since both SHIP1 and STAT3 can be phosphorylated at tyrosine residues, we wondered if any of the pTyr in one of these proteins could be recognized by the SH2 domain of the other protein. We decided to look at phosphorylation sites on SHIP1.

Using the online prediction tool NetPhos 2.0 [536], we identified 11 tyrosine residues that can be potentially phosphorylated. Comparing to the conventional STAT3's SH2 domain recognition sequences, we decided to focus our effects on four potential tyrosine residues (**Figure 4.3**). Three of the residues (Y657, Y659, Y799) locate within known structured domains (catalytic and C2 domains), while Y190 is in the region between SH2 and PH-R domains. FoldIndex program predicts whether a protein will fold based on its hydrophobicity [537], and using the SHIP1 primary sequence as the input, the program found that the area around Y190 might be folded.

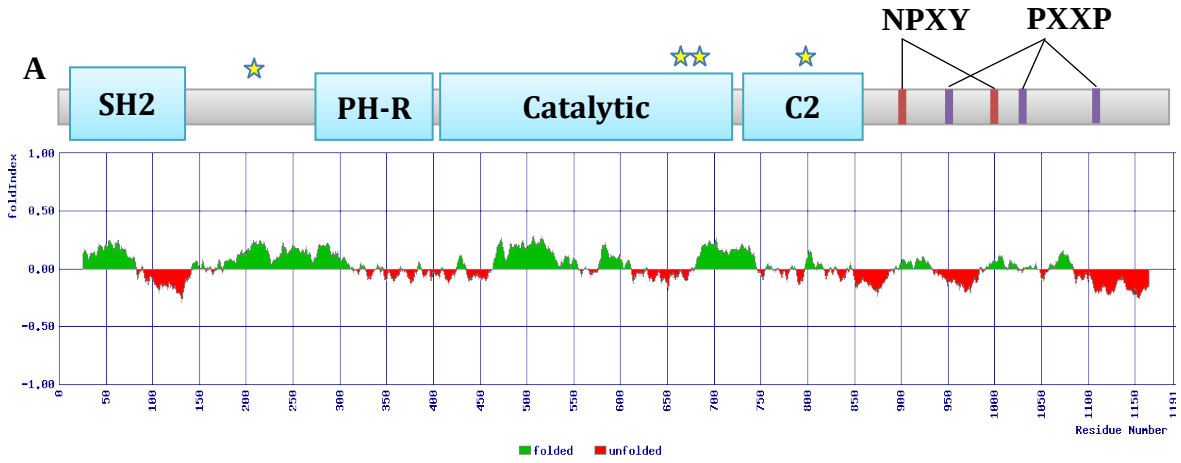

B

Residue	Location on SHIP1	Amino acid sequence
Y190	Between SH2 and PH-R domains	EEHLKAIQD**Y**LSTQLLLDSD
Y657	Within catalytic domain	RLTRDK**Y**AYTKQKATGMKYN
Y659	Within catalytic domain	RLTRDKYA**Y**TKQKATGMKYN
Y799	Within C2 domain	KPIISDPEYLLDQHILISIK

Figure 4.3 Location of the mutated tyrosine in SHIP1 sequence.
(A) The FoldIndex program [537] was used to predict the folded and unfolded regions of SHIP1. A schematic diagram of the SHIP1 structure is on top, and the stars show where the identified tyrosine residues are. (B) Summary of the residues mutated.

These residues were mutated individually to phenylalanine, and the SHIP1 mutants were introduced into the J2M SHIP1 KO macrophage cell line. As shown in **Figure 4.4**, J2M SHIP1 KO macrophages reconstituted with wild type SHIP1 (J2M

KO:SHIP1 WT) showed expected LPS and IL-10 responses. However, we found that J2M KO:SHIP1 Y190F cells became resistant to IL-10. Efforts are currently focused on determining if Y190 is indeed phosphorylated by IL-10, and if this phosphorylation is necessary for STAT3 interaction. All the other mutants showed similar IL-10 response as J2M KO:SHIP1 WT (data not shown).

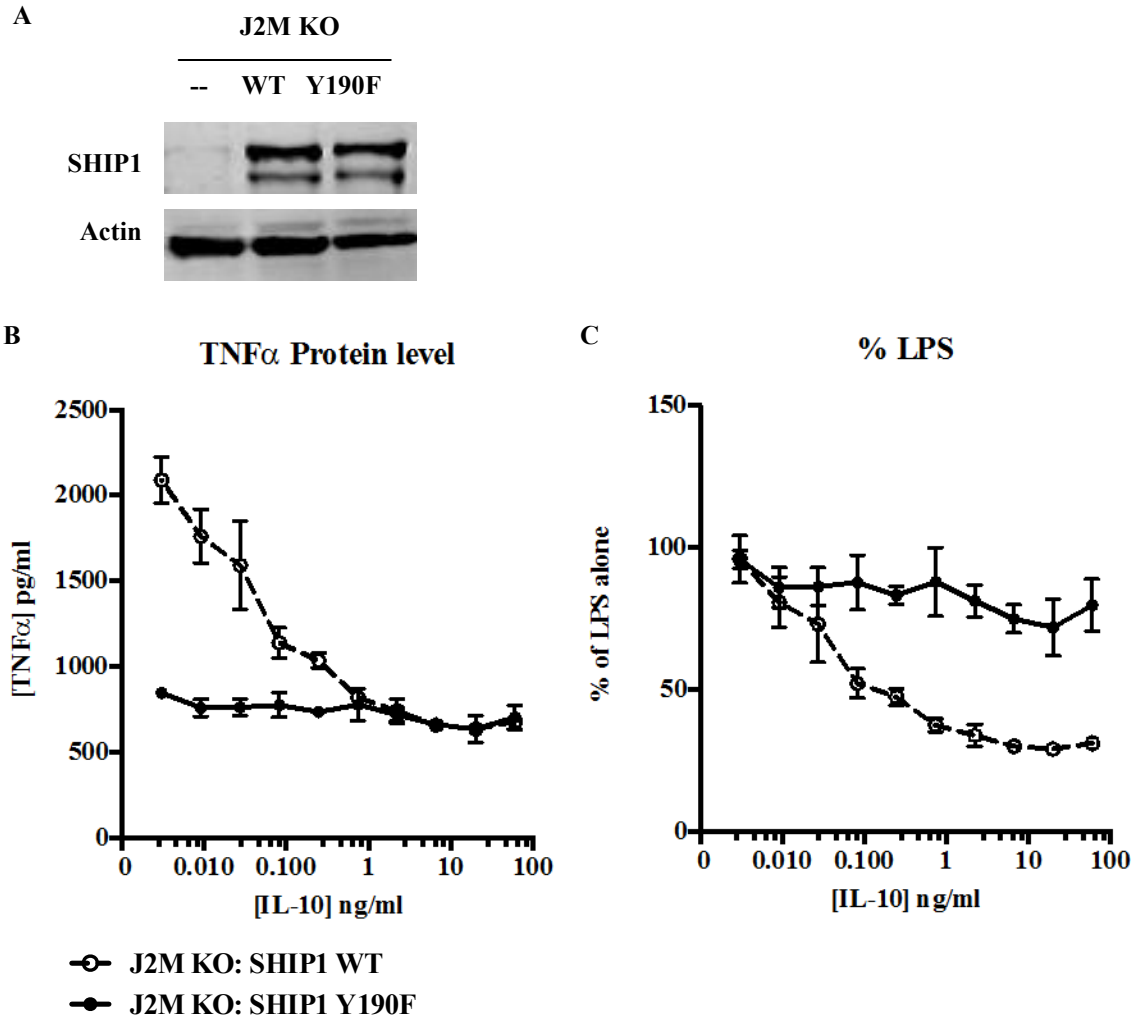

Figure 4.4 SHIP1 Y190F impairs IL-10 inhibition of TNFα in activated macrophages.

(A) Immunoblot analysis of J2M SHIP1 KO reconstituted with either SHIP1 WT or SHIP1 Y190F. Anti-SHIP1 antibody was used to detect the expression of the recombinant SHIIP1 proteins. Actin was the loading control. (B) These cells were stimulated with LPS +/- IL-10 for 1 hour. TNFα level in the supernatant was measured by ELISA. (C) The same data were replotted as a percentage of LPS alone treated samples.

4.2.4 SHIP1 and STAT3 co-regulate a number of IL-10 regulated genes.

To this point, we have only examined the roles STAT3 and SHIP1 play in IL-10 inhibition of specific molecules, miR-155 and TNFα, in activated macrophages. However, IL-10 is known to be a general negative regulator of macrophage activation, and it regulates a wide variety of molecules. We decided to perform a microarray analysis to measure the global effect of IL-10 in activated macrophages and to identify genes that are regulated by SHIP1 alone, STAT3 alone, or SHIP1/STAT3.

To identify SHIP1-regulated genes, we compared the gene expression profiles from SHIP1 WT and SHIP1 KO perimacs treated with LPS +/- IL-10 for 30 minutes. We are aware that the time point and the macrophage type chosen have a tremendous effect on gene expression profiling. We chose to look at a relatively short time point for two main reasons. First of all, with long treatment, cytokines produced by the cells could feedback to the cell in an autocrine cytokine manner; that can mask the direct effect of IL-10. Secondly, we found previously that LPS was able to induce TNFα mRNA expression as early as 30 minutes, and that IL-10 was able to suppress its production. We also decided to use perimacs as our choice of macrophages because these cells develop inside the mice without *ex vivo* manipulation (besides the stimulation) and likely give the most physiological relevant response, compared to macrophages differentiated and matured in a tissue culture dish (i.e. BMDMs). From our own experiences as well as from the literature [416], BMDMs produced a much higher level of endogenous IL-10 than perimacs upon LPS stimulation, and thus using BMDMs in our studies may blunt our ability to determine the complete range of IL-10 induced changes in cells.

Expression levels of 27,122 genes, 4,578 long non-coding RNAs were measured, and we found that over 100 genes were regulated by IL-10 in activated macrophages. A comparison of the gene expression profiles of wild type macrophages treated with LPS or LPS+IL-10, we found that 341 genes were regulated by IL-10 by at least 2-fold at 0.5 hour (194 induced, 147 repressed). One hour stimulation showed 654 genes whose expression were altered at least 2-fold by IL-10 (336 induced, 318 repressed). About 80 genes were regulated by IL-10 at both time points. Our microarray analysis confirmed a number of known IL-10 regulated genes [348] including TNFα, IL-1R antagonist, CSF3, SBNO2 and IL-10 itself. Since only 0.5-hour data were available in SHIP1 knockout cells, we decided to work with the set of 0.5-hour IL-10 regulated genes. In the SHIP1 knockout cells, 122 out of the 341 genes were differentially regulated by IL-10 showing at least a 2-fold difference from SHIP1 wild type cells. Among them, 70 were induced by IL-10 in SHIP1 WT cells, while 52 were repressed. We defined these genes as the SHIP1-regulated genes (**Table 4.1**). Surprisingly, TNFα is not in this gene subset even though we have other data supporting SHIP1's role in its regulation [56,376]. We examined the microarray data closely and found that there was a modest IL-10 resistance observed in SHIP1 KO cells (~11% less inhibited by IL-10) at 0.5 hour, lower than our selection criteria of 2-fold changes. Nevertheless, it is reassuring to confirm in our microarray that TNFα is regulated by IL-10 through SHIP1. We decided to add TNFα in our SHIP1-regulated gene subset.

Table 4.1: SHIP1-regulated genes identified after 0.5-hour stimulation of LPS and LPS+IL-10 in SHIP1 WT and SHIP1 KO macrophages

GenBank ID	Gene Symbol	SHIP1 WT	SHIP1 KO	Fold difference between WT and KO
		LPS+IL-10 over LPS	LPS+IL-10 over LPS	
IL-10 Upregulated Genes				
NM_001039392	Tmsb10	2.046	0.16	12.50
X71478	Cyp4a10	2.453	0.25	9.74
NM_022320	Gpr35	2.748	0.29	9.44
NM_080561	Rnf216	2.081	0.23	9.08
NM_008564	Mcm2	2.180	0.25	8.58
NM_001081281	Trim55	8.533	1.24	6.89
NM_133731	Prss22	2.399	0.37	6.43
AK009475	Zfp560	2.392	0.39	6.14
NM_008462	Klra2	3.250	0.54	6.02
NM_022028	Sav1	3.068	0.61	5.05
NM_025297	Mecr	2.732	0.56	4.84
NM_028276	Utp14a	2.073	0.44	4.71
NM_019928	Klk4	3.038	0.69	4.42
NM_025706	Tbc1d15	2.958	0.71	4.20
AK032013	Anxa7	2.264	0.56	4.08
NM_001039552	2210404J11Rik	2.641	0.68	3.87
BC038320	4930581F22Rik	2.318	0.60	3.87
NM_026615	Urm1	2.433	0.65	3.75
NM_010638	Klf9	2.224	0.60	3.72
NM_153820	Arhgap15	2.670	0.72	3.71
NM_029786	Pomgnt1	2.021	0.55	3.70
NM_028121	Adpgk	2.281	0.62	3.68
NM_027147	Enho	2.295	0.63	3.62
XM_980696	AI607873	2.300	0.64	3.59
NM_023884	Ralgps2	2.125	0.60	3.54
NM_007968	Ewsr1	2.052	0.58	3.53
XM_001001284	EG667795	2.362	0.69	3.41
NM_021893	Cd274	4.249	1.25	3.39
NM_172015	Iars	2.684	0.82	3.27
AK078885	AI842136	3.527	1.13	3.12
NM_178700	Grsf1	2.266	0.74	3.07
NM_153585	Cnot10	2.373	0.81	2.92
ENSMUST00000042610	AI607873	2.703	0.94	2.88
U63712	Tfam	2.179	0.76	2.85
NM_175013	Pgm5	2.684	0.95	2.83
NM_133238	Cd209a	4.125	1.46	2.82
NM_025837	Mpi	2.551	0.92	2.79

GenBank ID	Gene Symbol	SHIP1 WT LPS+IL-10 over LPS	SHIP1 KO LPS+IL-10 over LPS	Fold difference between WT and KO
NM_024172	Hspbp1	2.171	0.78	2.78
NM_013683	Tap1	2.345	0.85	2.76
NM_010072	Dpm1	4.202	1.53	2.75
NM_198602	Cux1	2.182	0.82	2.65
NM_177224	Chd9	2.422	0.92	2.63
NM_008684	Neo1	2.709	1.05	2.59
NM_172488	9030625A04Rik	2.132	0.84	2.54
NM_008965	Ptger4	3.682	1.50	2.46
AK045877	Atp6v0a1	2.888	1.19	2.43
NM_008039	Fpr2	2.476	1.05	2.36
NM_008950	Psmc5	2.369	1.01	2.34
AK017886	5830400J07Rik	5.801	2.48	2.34
NM_015741	Krtap9-1	2.517	1.09	2.30
NM_011274	C80913	2.072	0.90	2.30
AK020773	A430106F12Rik	2.575	5.87	2.28
NM_007969	Expi	3.453	1.52	2.28
NM_013785	Ip6k1	2.111	0.93	2.26
NM_024495	Car13	2.361	1.05	2.25
NM_008654	Myd116	2.028	0.90	2.24
NM_145431	Nle1	2.038	0.92	2.22
NM_172501	Nhlrc3	2.258	1.02	2.21
NM_016715	Crlf2	2.492	1.14	2.18
NM_029068	Snx16	2.335	1.08	2.17
AK148276	Slc11a2	2.127	0.99	2.15
AK009502	Tia1	2.316	1.08	2.14
AK035265	Aftph	2.545	1.19	2.14
AK036220	Rbm18	2.123	1.00	2.13
NM_008057	Fzd7	2.629	1.25	2.10
NM_007443	Ambp	4.522	2.16	2.10
NM_023892	Icam4	2.699	1.31	2.05
NM_139236	Nol6	2.041	1.00	2.04
NM_172911	D8Ertd82e	2.104	1.03	2.04
NM_028810	Rnd3	2.277	1.13	2.02
AK041830	Pcif1	2.318	1.15	2.01
IL-10 Downregulated Genes				
NM_027572	Slc22a16	0.150	1.33	8.88
NM_175294	Nucks1	0.233	1.60	6.88
NM_030253	Parp9	0.361	2.24	6.21
NM_001081216	Phip	0.476	2.94	6.17
NM_018745	Azin1	0.366	2.19	5.99

GenBank ID	Gene Symbol	SHIP1 WT	SHIP1 KO	Fold difference between WT and KO
		LPS+IL-10 over LPS	LPS+IL-10 over LPS	
NM_013742	Cars	0.449	2.16	4.82
NM_133871	Ifi44	0.369	1.70	4.61
NM_008320	Irf8	0.429	1.96	4.56
BY711602	Klf12	0.352	1.56	4.42
NM_144884	Tor1a	0.457	2.00	4.38
NM_019825	Ncoa6	0.405	1.70	4.21
NM_145564	Fbxo21	0.422	1.77	4.20
NM_025886	Rassf7	0.328	1.29	3.93
NM_008522	Ltf	0.197	0.77	3.92
NM_029083	Ddit4	0.321	1.24	3.85
NM_009114	S100a9	0.306	1.16	3.80
M89786	Gas2l1	0.322	1.21	3.74
NM_019972	Sort1	0.478	1.68	3.52
NM_015743	Nr4a3	0.453	1.58	3.48
BC061478	2010109K11Rik	0.433	1.49	3.44
AY149175	Zfp640	0.227	0.75	3.31
BC042572	H2-Q10	0.395	1.30	3.29
NM_026952	Crkrs	0.420	1.28	3.04
AK077833	Cpsf6	0.484	1.39	2.88
AK049901	Mthfd2l	0.499	1.41	2.82
NM_016812	Banp	0.463	1.30	2.81
NM_009058	Ralgds	0.452	1.25	2.77
NM_172503	Zswim4	0.359	0.99	2.76
AK020355	Zkscan1	0.452	1.24	2.74
NM_011075	Abcb1b	0.463	1.24	2.68
NM_145459	Zfp503	0.472	1.21	2.56
NM_026219	Uqcrb	0.487	1.23	2.53
NM_007684	Cetn3	0.496	1.21	2.44
AK077312	D7Ertd413e	0.319	0.78	2.43
NM_001033156	Fbxo33	0.423	1.02	2.41
NM_153063	Zfp472	0.340	0.82	2.40
NM_027044	Pfdn5	0.427	1.02	2.40
NM_173396	Tgif2	0.484	1.15	2.38
NM_025965	Ssr1	0.214	0.51	2.37
NM_020507	Tob2	0.487	1.15	2.36
NM_013613	Nr4a2	0.330	0.78	2.36
BC058175	Bcl2l11	0.362	0.84	2.33
NM_013650	S100a8	0.476	1.10	2.31
BC035255	Gpatch8	0.454	1.04	2.29
NM_138953	Ell2	0.460	1.04	2.26

GenBank ID	Gene Symbol	SHIP1 WT LPS+IL-10 over LPS	SHIP1 KO LPS+IL-10 over LPS	Fold difference between WT and KO
AK036755	Apbb1ip	0.312	0.70	2.25
AK014174	Chka	0.470	1.05	2.24
NM_001002927	Penk1	0.357	0.79	2.23
NM_029466	Arl5b	0.437	0.97	2.21
NM_020596	Egr4	0.437	0.89	2.05
NM_001025566	Chka	0.476	0.97	2.04
NM_026518	Rnf146	0.356	0.72	2.03
NM_009829	Ccnd2	0.497	0.99	2.00

Then we compared the SHIP1-regulated gene subset more closely with published data on IL-10 regulated genes, focusing on two studies that specifically looked at gene expression in IL-10 treated macrophages. Lang *et al.* [416] examined the gene expression profiles of IL-10 KO BMDMs treated with LPS +/- IL-10 for 3 hours and identified 112 genes that were regulated by IL-10 in LPS-activated macrophages. Three of these genes were on our SHIP1 subset (Ambp, Bcl2l11, Fzd7) (**Figure 4.5A**). These investigators also found STAT3-dependence in 13 of these IL-10 regulated genes using quantitative RT-PCR and Northern blot in STAT3 KO macrophages. AMBP is one of the STAT3-regulated genes. AMBP is a precursor of two proteins, α1-microglobulin (α1-m) and bikunin. α1-m (also called protein HC) belongs to the lipocain protein family, which acts as transporter of small hydrophobic molecules, and has been found to suppress immune response of lymphocytes and neutrophils [538]. Bikunin is a member of the Kunin family of serine protease inhibitors, and also has negative role in multiple immune processes including leukocyte migration and activation [539]. We and Lang *et al.* [416] both found that AMBP was upregulated upon IL-10 treatment, consistent with its immunosuppressive properties. BCL2L11, commonly known as BIM, is an apoptosis

facilitator [540,541]. FZD7 is a receptor for the Wnt signalling which is involved in modulating inflammatory response [542]. Other STAT3-regulated genes verified by Lang *et al.* [416] are either not detected on our microarray (e.g. Il12p40 and Ccl12), not upregulated by IL-10 by at least 2-fold in SHIP1 WT cells (e.g. Bcl3, Mt2 and protein C receptor), not regulated by SHIP1 (e.g. Nfil3) or only weakly affected by SHIP1 KO, i.e. < 2-fold difference between SHP1 WT and KO cells (e.g. Tnf and Map3k8) (Table 4.2).

Table 4.2: Comparison of expression profiles of Lang *et al.* identified IL-10/STAT3-regulated genes in SHIP1 WT and SHIP1 KO cells.

GenBank ID	Gene Symbol	Probe ID	SHIP WT	SHIP KO	Fold difference between WT and KO
			LPS+IL-10 over LPS	LPS+IL-10 over LPS	
NM_007443	Ambp	A_51_P145785	4.522	2.16	2.10
NM_001303244	Il12b	N/A	N/A	N/A	N/A
NM_011331	Ccl12	N/A	N/A	N/A	N/A
NM_001039701	Il1rn	A_51_P307166	1.441	0.23	6.18
		A_52_P431159	1.434	0.94	1.53
NM_016767	Batf	A_51_P114616	1.814	0.78	2.32
NM_011171	Procr	A_51_P382152	0.852	1.78	2.09
NM_010288	Gja1	A_52_P174915	1.533	0.80	1.92
NM_001008700	Il4ra	A_51_P464478	1.412	2.29	1.62
NM_008630	Mt2	A_51_P246317	0.970	1.23	1.27
NM_033601	Bcl3	A_51_P136542	1.219	1.39	1.14
NM_017373	Nfil3	A_51_P111492	1.797	1.67	1.08
		A_52_P500027	1.231	1.48	1.20
		A_51_P111492	1.797	1.67	1.08
		A_52_P500027	1.231	1.48	1.20
D13759	Map3k8	A_51_P115575	2.177	1.48	1.47
NM_013693	Tnf	A_51_P385099	0.377	0.49	1.31

Hutchins *et al.* [45] has recently identified over 354 genes that were upregulated by IL-10 and that have nearby STAT3 binding sites, constituting a global view of IL-10/STAT3 mediated anti-inflammatory response in mouse macrophages. A comparison with our subset of SHIP1-regulated genes showed that Cd274, Gpr35 and Crlf2 are

potentially upregulated by IL-10 in a SHIP1- and STAT3-dependent manner (**Figure 4.5B**). CD274, also known as B7-H1 or PD-L1, is a co-stimulating molecule that is involved in negative regulation of T cell activation and cytokine production by inducing the production of IL-10 in monocytes [543]. GPR35 mRNA was found to be repressed by LPS in both BMDMs (2 hours and 6 hours) and perimacs (1 hour and 7 hours), as determined in microarray analysis [544] and its polymorphism is associated with a form of IBD [545]. Our microarray data showed that GPR35 was repressed by LPS at 0.5 hour, but induced at 1 hour. CRLF2 can activate STAT3, STAT5 and JAK2, all of which have important role in immune cell function, and its overexpression is strongly linked to B-cell acute lymphoblastic leukemias (B-ALLs) [546]. Moreover, thymic stroma lymphopoietin (TSLP), the ligand of CRLF2, was shown to induce IL-10 expression in dendritic cells [547]. Whether these proteins contribute to IL-10 anti-inflammatory response will require further research.

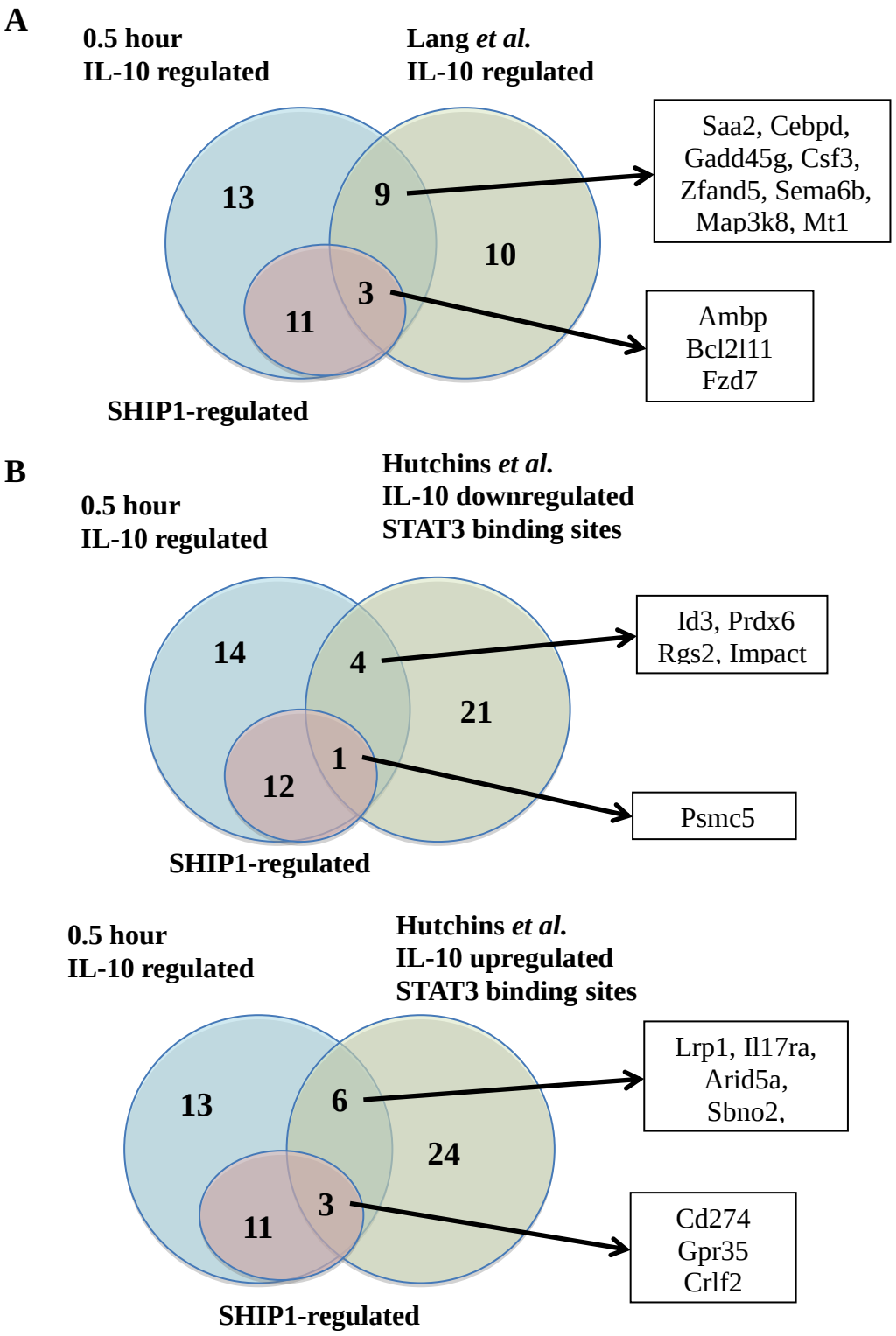

Figure 4.5 Identification of candidate SHIP1-STAT3 regulated genes.
Overlap of SHIP1-regulated gene subset with (A) IL-10 regulated gene subset from Lang *et al.* [416] or (B) IL-10 regulated genes that have STAT3 binding sites within 20 kb of transcription start site from Hutchins *et al.* [45] Identities of overlapping genes are listed.

We also examined if there is a particular biological network that SHIP1 may mediate its function. To do that, we used the NetworkAnalyst web-based tool that looks for enriched network using the user input gene list and genes (proteins) that directly interact with them [548]. The subset of SHIP1-regulated genes identified in our mircroarray (94 genes) was used as an input. As shown in **Figure 4.6**, 17 SHIP1-regulated genes are strongly connected with IRF8 in the centre of the largest sub-network. IRF8 is a transcription factor that can be upregulated by inflammatory stimuli including IFNγ and LPS [549], and downregulated by IL-10 [550]. Our microarray data also showed that IL-10 inhibited Irf8 in activated macrophages. The deficiency of SHIP1 actually caused IL-10 to increase IRF8 level, indicating a strong requirement for SHIP1 in IL-10 inhibition of IRF8. Out of the 17 genes mapped onto the network, 11 of them were downregulated by IL-10 at 0.5 hour in SHIP1 WT cells in our microarray, and SHIP1 deficiency either lessened the inhibition (e.g. BCL2L11 and TNFα), or actually reversed it to upregulation (e.g. IRF8). Given that IRF8 and related genes are represented in the SHIP1-regulated network, it is not surprising to see "Interferon signalling" as one of the enriched pathways, as determined by pathway analysis using the Reactome database. Other top hits include "Apoptosis" and "Cytokine signalling in immune system" (**Table 4.3**). Both STAT3 and SHIP1 have implication in apoptosis. STAT3 activation is likely to be anti-apoptotic since inhibition of STAT3 signalling causes cell death [551-554]. SHIP1, being a negative regulator of the survival-promoting PI3K, is usually considered as pro-apoptotic [555-558], but other reports showed that SHIP1 inhibits apoptosis [555,559,560]. Similarly, IL-10 has been shown to be apoptosis-inducing [561-563] and inhibiting [564-568], depending on the cell type, the state of

differentiation, and the type of stimuli. However, IL-10 appears to prevent apoptosis in activated macrophages [564-567].

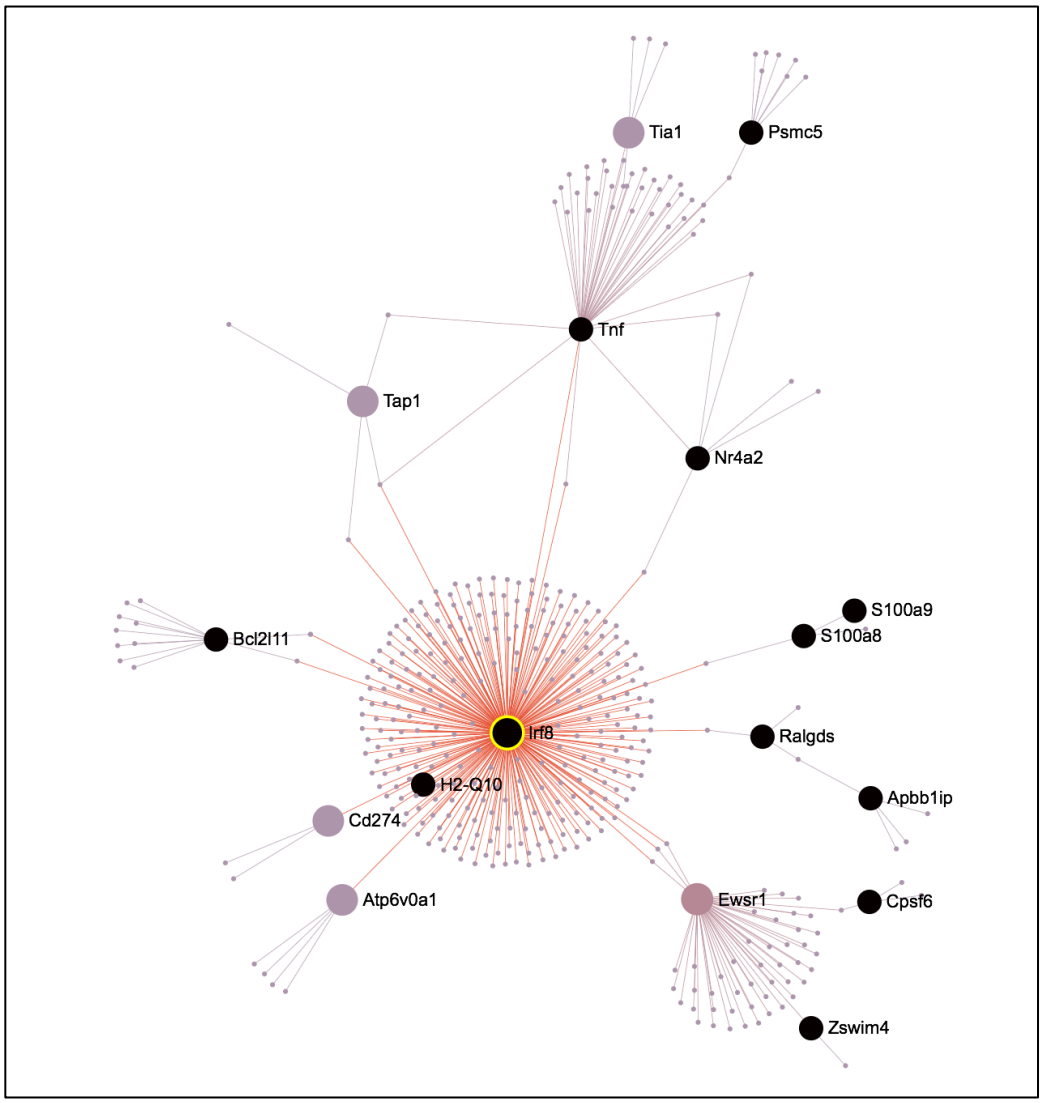

Figure 4.6 Interacting genes in the SHIP1-regulated gene subset.
The subset of SHIP1-regulated genes were analyzed in terms of network connectivity with NetworkAnalyst [548]. A total of 17 SHIP1-regulated genes are mapped into a network of 471 genes. Labeled genes/nodes are from the SHIP1-regulated gene subset, and non-labeled nodes are directly interacting proteins. Genes that are upregulated by IL-10 in SHIP1 WT cells are labeled in light purple, while downregulated genes are labeled black. The most highly connected node is further indicated by a yellow circle.

Table 4.3: Enriched pathways identified by NetworkAnalyst using Reactome database

Rank	Pathway	*P*-Value
1	Immune system	4.46E-17
2	Apoptosis	7.67E-09
3	Cytokine signalling in immune system	9.31E-09
4	Adaptive immune system	1.54E-08
5	Interferon signalling	4.87E-07
6	Innate immune system	6.06E-07
7	Antigen processing-cross presentation	1.27E-06
8	Class I MHC mediated antigen processing & presentation	1.69E-06
9	Activation of BH3-only proteins	3.21E-06
10	Intrinsic pathway for apoptosis	4.68E-06
11	Death receptor signalling	7.29E-06
12	Extrinsic pathway for apoptosis	7.29E-06
13	Interferon gamma signalling	7.80E-06
14	ER-phagosome pathway	1.04E-05
15	Antigen presentation: folding, assembly and peptide loading of class I MHC	1.64E-05
16	TNF signalling	2.12E-05
17	TRIF-mediated programmed cell death	4.15E-05
18	Phagosomal maturation (early endosomal stage)	6.97E-05
19	Latent infection of Homo sapiens with Mycobacterium tuberculosis	6.97E-05
20	BH3-only proteins associate with and inactivate anti-apoptotic BCL-2 members	7.30E-05
21	Activation of BIM and translocation to mitochondria	9.02E-05
22	Inflammasomes	0.000152
23	Toll-like receptors cascades	0.000176
24	TRIF-mediated TLR3/TLR4 signalling	0.000325
25	MyD88-independent cascade	0.000325
26	Toll-like receptor 3 (TLR3) Cascade	0.000325
27	Activated TLR4 signalling	0.000536
28	Signalling by the B cell receptor (BCR)	0.000541
29	RIG-I/MDA5 mediated induction of IFN-alpha/beta pathways	0.000657
30	Downstream signalling events of B cell receptor (BCR)	0.000667

Our ultimate goal was to categorize IL-10 regulated genes to be SHIP1-regulated, STAT3-regulated or SHIP1-STAT3-regulated subsets. The analysis described thus far

identified Ambp, Fzd7, Bcl2l11, Cd274, Gpr35, Crlf2 and Tnf to be SHIP1-STAT3 regulated. Comparing the ChIP-seq data from Hutchin *et al.* [45] with our SHIP1-regulated gene subset, we found 11 SHIP1-regulated genes to have STAT3 bound near their transcription start site. These are also grouped in the SHIP1-STAT3 subset. The other genes in our SHIP1-regulated gene subset are considered as solely SHIP1-dependent. Besides these genes, our laboratory has identified another 14 genes to be regulated by IL-10 in a SHIP1-dependent manner by real time-PCR [376]. None of these genes have passed our criteria for SHIP1-regulated genes in our microarray analysis. However, 12 of these genes showed modest dependence to SHIP1 (>10% difference between SHIP WT and SHIP KO cells) (**Table 4.4**). Genes described by Lang *et al.* [416] and Hutchins *et al.* [45] that did not show differential expression in SHIP1 WT and SHIP1 KO cells were considered STAT3-regulated.

Table 4.4: Microarray data of previously described SHIP1-regulated genes.

Genbank ID	Gene Symbol	Probe ID	SHIP1 WT	SHIP1 KO	Fold Change between WT and KO
			LPS+IL-10 over LPS	LPS+IL-10 over LPS	
NM_011333	Ccl2	A_51_P286737	1.99	1.51	1.32
NM_011337	Ccl3	A_51_P140710	1.77	1.39	1.28
NM_008176	Cxcl1	A_51_P363187	1.00	0.94	1.07
NM_009140	Cxcl2	A_51_P217463	1.04	1.09	1.05
NM_007913	Egr1	A_51_P367866	0.80	0.92	1.15
NM_010493	Icam1	A_52_P613241	1.78	0.94	1.89
BC008626	Icam1	A_51_P408506	1.12	0.79	1.42
NM_008416	Junb	A_51_P159194	0.83	1.14	1.38
NM_008416	Junb	A_51_P159201	0.85	1.12	1.31
NM_010807	Marcksl1	A_51_P257550	0.87	1.36	1.57
NM_010807	Marcksl1	A_52_P35801	1.18	0.85	1.39
NM_010907	Nfkbia	A_51_P295192	0.82	1.93	2.36
NM_030612	Nfkbiz	A_51_P387591	0.73	0.63	1.16
NM_010444	Nr4a1	A_51_P239654	0.72	0.69	1.05
NM_023324	Peli1	A_51_P232889	0.75	1.33	1.77
NM_023324	Peli1	A_52_P298093	1.22	1.03	1.19
AK047301	Pim1	A_52_P535619	1.82	1.56	1.17
NM_008842	Pim1	A_52_P530291	1.08	0.94	1.15
NM_013671	Sod2	A_51_P172573	0.82	1.37	1.67
NM_013693	Tnf	A_51_P385099	0.38	0.49	1.31
NM_009404	Tnfsf9	A_51_P460004	2.50	2.33	1.07

Expression of selected genes from these three categorizes were measured by real time-PCR analysis using RNA extracted from SHIP1 WT and KO perimacs, as well as STAT3 WT and KO perimacs, stimulated with LPS +/- IL-10. The SHIP1 KO cells and the STAT3 KO cells were obtained from mice with different genetic backgrounds (BALB/c and C57/BL6), and thus two different WT cells were used in the experiments (**Figure 4.7**). Out of the 42 genes tested, 10 genes were not regulated by IL-10 in both SHIP1 WT and STAT3 WT cells (**Figure 4.7E**), and a further 11 genes were only regulated by IL-10 in either SHIP1 WT or STAT3 WT cells but not both (**Figure 4.7F**). Among the 21 validated IL-10 regulated genes, 11 showed dependence to SHIP1 and

STAT3 (**Figure 4.7A**), 2 to SHIP1 alone (Impact and Ccl3) (**Figure 4.7B**), and 1 to STAT3 alone (Id3) (**Figure 4.7C**). IL-10 regulation of 3 genes (Bcl2l11, Irf8 and Nfil3) showed no impairment in SHIP1 KO and STAT3 KO cells (**Figure 4.7D**). The remaining 4 genes did not fall into any of the criteria above (**Figure 4.7G**). For example, Ambp was upregulated by IL-10 in both SHIP1 and STAT3 WT cells. While deficiency of SHIP1 reduced IL-10 induction, deficiency of STAT3 actually increased IL-10 induction, indicating opposite functions of SHIP1 and STAT3 in the regulation of Ambp.

A STAT3-SHIP1 regulated

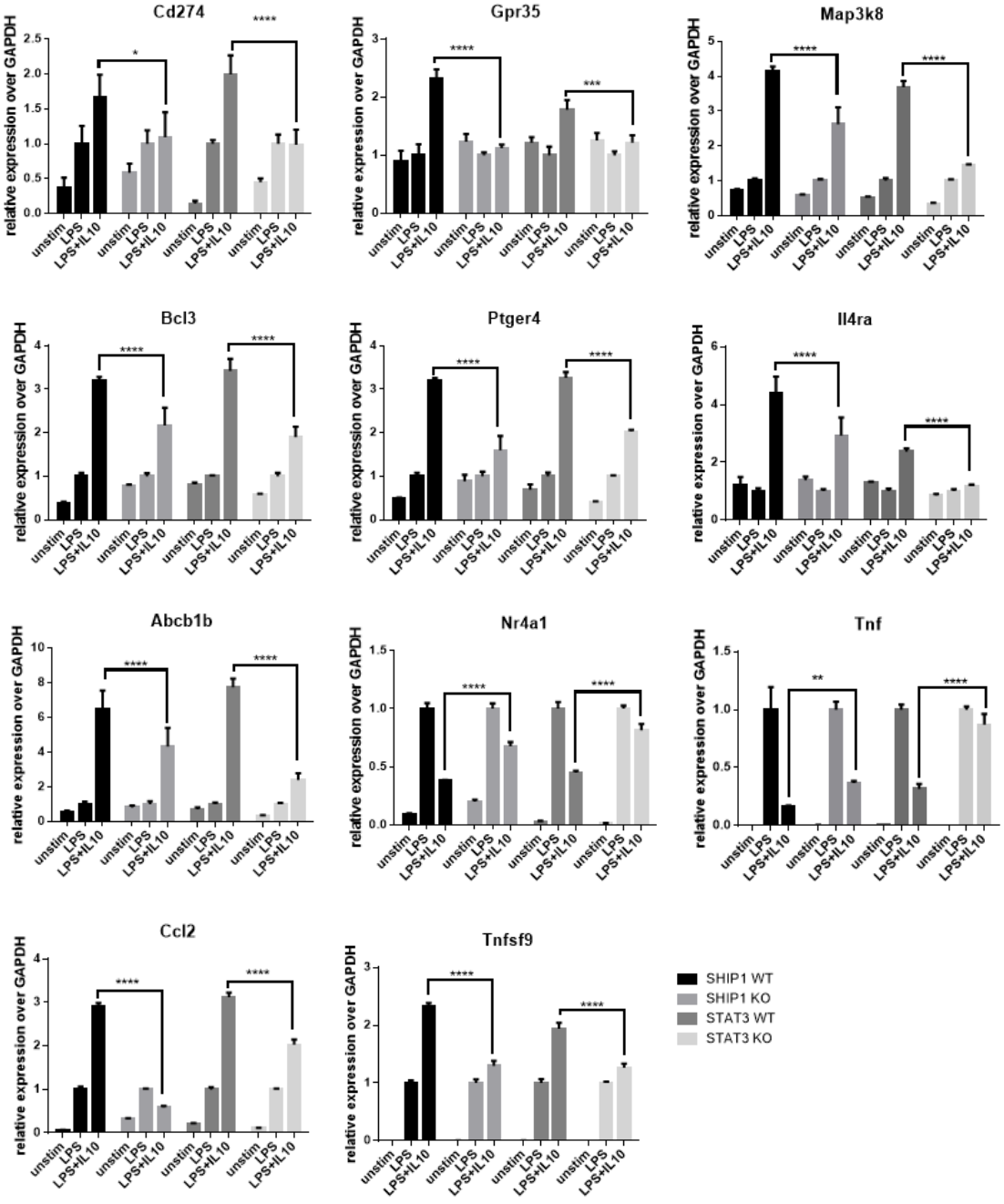

B SHIP1-regulated

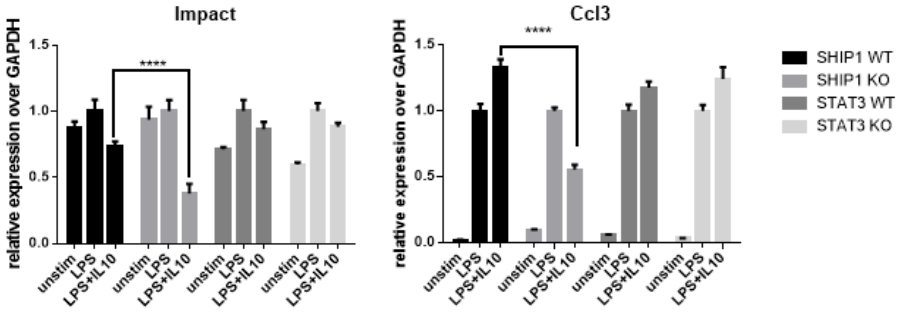

C STAT3-regulated

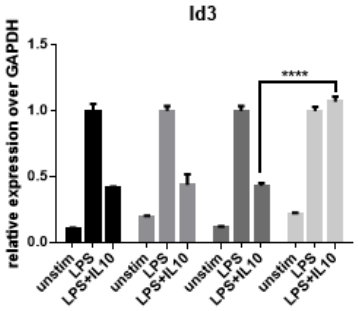

D Not SHIP1 nor STAT3 regulated

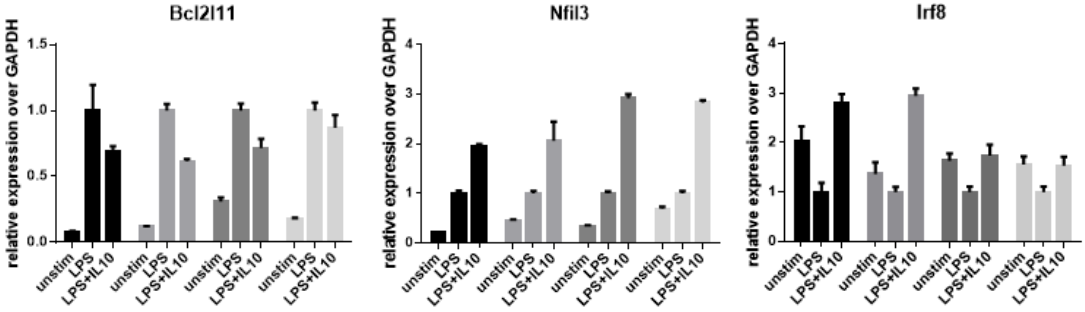

E Not regulated by IL-10 in both WT cells

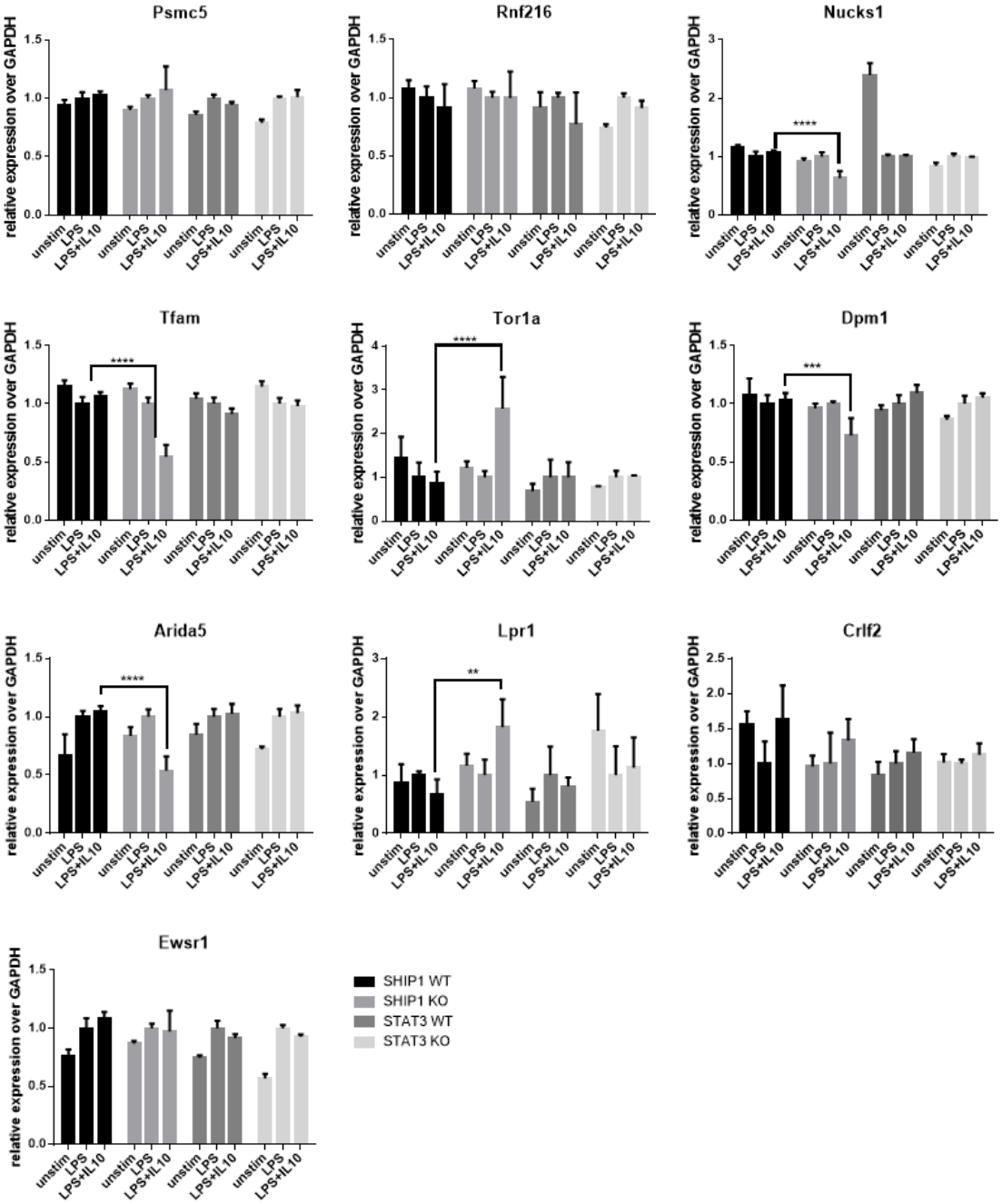

F Not regulated by IL-10 in one of the WT cells

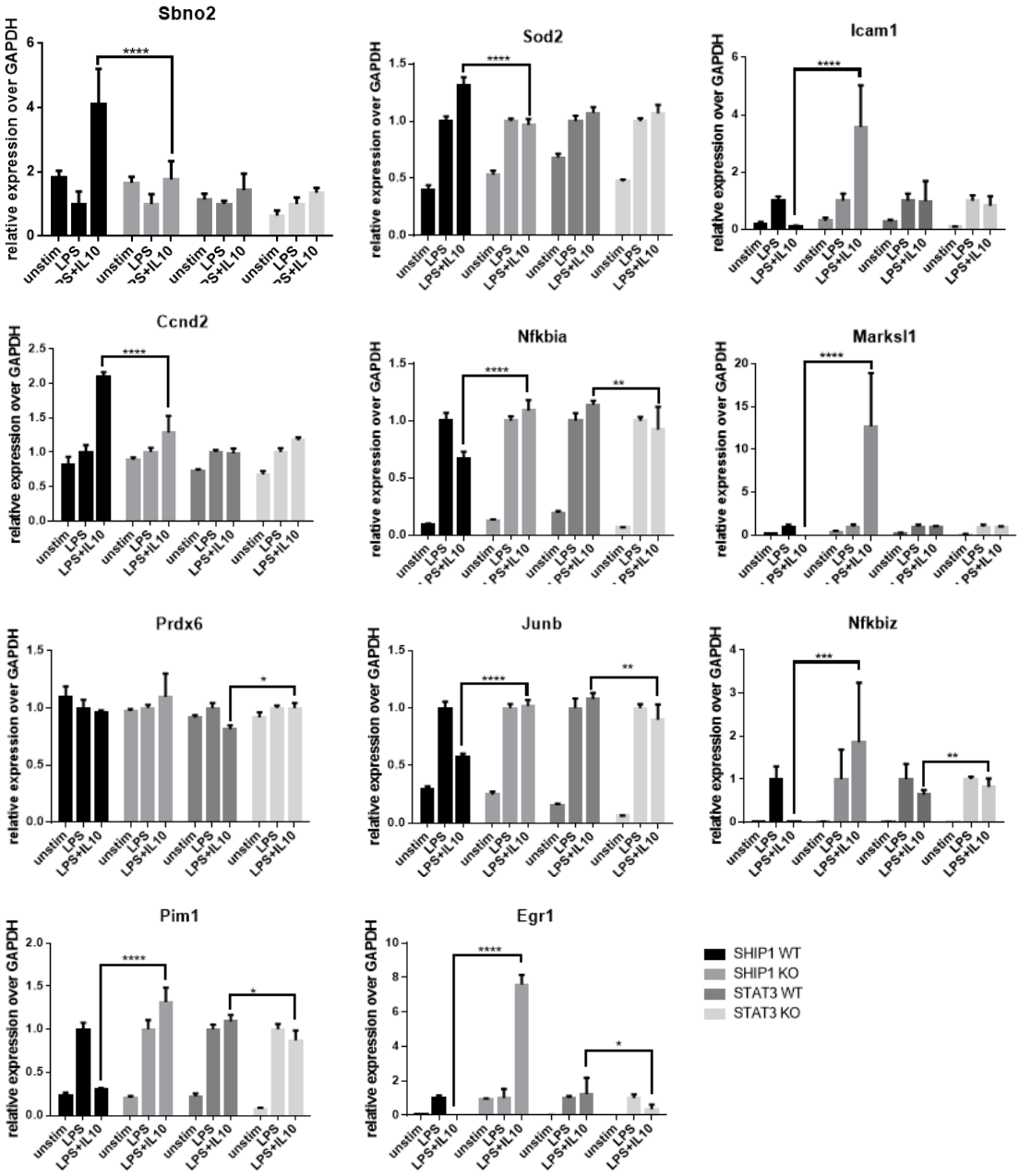

G Uncategorized

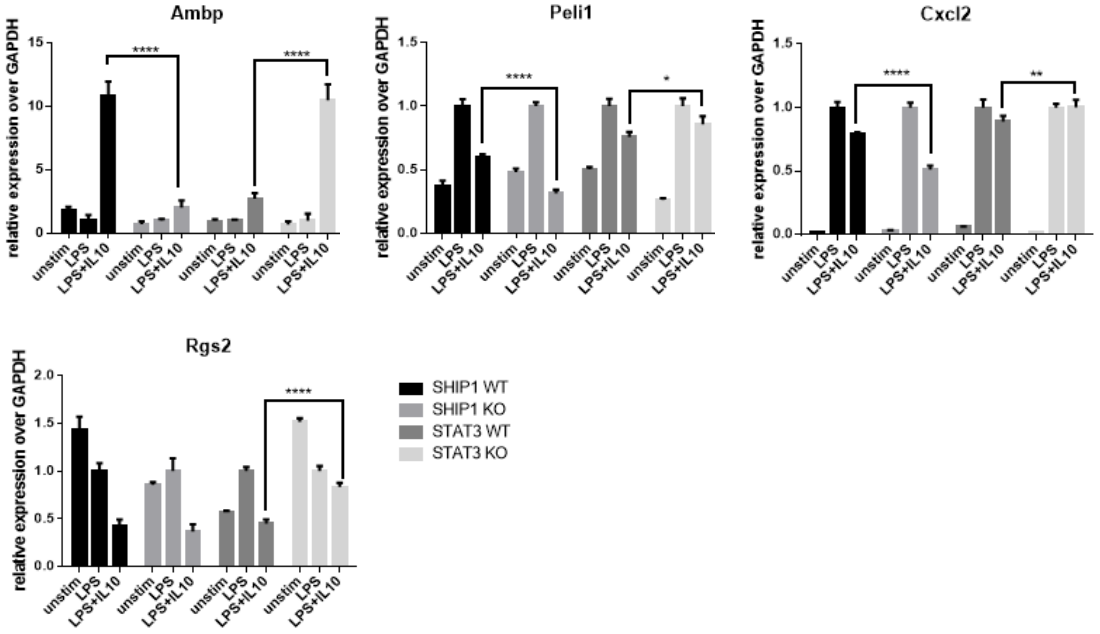

H

Group	Genes
SHIP1-STAT3 regulated	Cd274, Gpr35, Map3k8, Bcl3, Ptger4, Il4ra, Abcb1b, Nr4a1, Tnf, Ccl2, Tnfsf9
SHIP1-regulated	Impact, Ccl3
STAT3-regulated	Id3
Not SHIP1 nor STAT3 regulated	Bcl2l11, Nfil3, Irf8
Not IL-10 regulated in both WT cells	Psmc5, Rnf216, Nucks1, Tfam, Tor1a, Dpm1, Arida5, Lpr1, Crlf2, Ewsr1
Not IL-10 regulated in one of the WT cells	Sbno2, Sod2, Icam1, Ccnd2, Nfkbia, Marksl1, Prdx6, Junb, Nfkbiz, Pim1, Egr1
Uncategorized	Ambp, Peli1, Cxcl2, Rgs2

Figure 4.7 Real time PCR revealed that many of the IL-10 regulated genes require SHIP1 and STAT3.

Perimacs extracted from BALB/c mice (SHIP1 WT and SHIP1 KO), or C57BL/6 mice (STAT3 WT and STAT3 KO) were stimulated with LPS +/- IL-10 for 1 hour prior to total RNA extraction. Expression levels of different genes were determined by real time PCR and plotted relative to LPS alone samples. Statistical significance between WT and KO was calculated by a two-way ANOVA test with a 95% confidence (* $p < 0.05$, ** $p < 0.01$, *** $p < 0.001$, **** $p < 0.0001$). (A) IL-10 regulated genes that required both SHIP1 and STAT3, (B) SHIP1 alone, (C) STAT3 alone, (D) or neither SHIP1 nor STAT3. (E) Genes that were not regulated by IL-10 in both SHIP1 WT and STAT3 WT cells. (F) Genes that were not regulated by IL-10 either in SHIP1 WT

or STAT3 WT. (G) Genes that do not belong to any of the groups above. (H) Table summarizing the gene expression data.

Among the SHIP1-STAT3 subset, we found that the expression levels of Ambp, Fzd7 and Crlf2 were relatively low in perimacs; Fzd7 expression was even below detection limit. Crlf2 expression was not affected by IL-10 treatment. Similar to the microarray analysis, real time-PCR analysis showed that Bcl2l11 was downregulated by IL-10, while Ambp, Cd274 and Gpr35 were upregulated by IL-10. However, unlike the microarray analysis, deficiency of SHIP1 or STAT3 did not affect IL-10 regulation of Bcl2l11 (**Figure 4.7F).** By contrast, IL-10's ability to upregulate Cd274 and Gpr35 was impaired in both SHIP1 KO and STAT3 KO cells, indicating these genes were regulated by IL-10 in a SHIP1-STAT3 dependent manner (**Figure 4.7C**). We have also examined the expression levels of selected validated STAT3-regulated genes and genes in our SHIP1-regulated gene subset. Consistent to the observations Lang *et al.* [416] had, Map3k8, Bcl3 and Il4ra were found to be IL-10/STAT3 regulated genes as STAT3 KO cells showed resistance to IL-10 treatment as compared to STAT3 WT cells **(Figure 4.7C)**. Additionally, we found that the absence of SHIP1 reduced IL-10 induction of these genes, showing SHIP1 involvement in IL-10 regulation of these genes. Correspondingly, a few genes in the SHIP1-regulated subset were also found to be regulated by STAT3; these included Ccl2, Nr4a1, Tnfsf9, Abcb1b and Ptger4 (**Figure 4.7C**). Unexpectedly, real time PCR showed that Irf8 was downregulated by LPS and upregulated by IL-10 (**Figure 4.7GF**), opposite to our microarray data and previous reports [549,550]. Also, SHIP1 deficiency did not impair IL-10 regulation of Irf8, unlike the observation shown by microarray.

Combining the microarray data and the real-time PCR data, we have generated new subsets of SHIP1-regulated, STAT3-regulated and SHIP1-STAT3 regulated genes; there are 113, 1089, and 22 genes in each gene subset respectively. To determine the transcription factors responsible for the differential gene regulation, enrichment analysis was done with Enrichr [569]. The ChIP-x Enrichment Analysis (ChEA) database contains gene lists extracted from reported experiments of profiling of transcription factors binding to DNA from mammalian cells, and was used to identify transcription factors that were enriched for our gene subsets. Expectedly, STAT3 is ranked 1st for both the STAT3 subset and STAT3-SHIP1 subset. In the SHIP1 subset, STAT3 is ranked 44th. The most enriched transcription factor is E2F transcription factor 1 (E2F1), which plays a crucial role in cell cycle control. In addition, E2F1 has been shown to suppress NFκB activity [570-573], and may exert anti-inflammatory properties. However, others have reported that E2F1 can bind to the p65 subunit of NFκB and act as a transcriptional activator for NFκB target genes [574]. Interestingly, p65 is the 3rd ranked transcription factor enriched in the SHIP1 subset, when we used another enrichment analysis tool, position weight matrices (PWMs) from TRANSFAC and JASPAR, also offered by Enrichr, which scan for transcription factor binding sites in the gene region composing -2000 to +500 from the transcription start site. However, p65 is ranked 46th and 52th, respectively, for the STAT3 and SHIP1-STAT3 subsets. These observations indicate that maybe SHIP1 predominately regulates NFκB target genes via regulation on E2F1. Besides transcription factors enriched in our gene subsets, we also examined the possibility of differential miRNA-mediated regulation using the TargetScan database. **Table 4.5** lists the first 10 miRNAs enriched in each gene subset. In the 1st ranked

miRNA family enriched in the SHIP1 subset, miR-93 was reported to reduce LPS-induced NFκB cytokine production by targeting IRAK4 in mouse macrophages [575]. This miRNA family is ranked 45th and 63th in the STAT3 and SHIP1-STAT3 subsets respectively, suggesting that it may be involving in the SHIP1-only regulation. For the STAT3 subset, the second ranked miRNA, miR-181, has been shown to regulate inflammatory response by decreasing the production of pro-inflammatory cytokines such as IL-1α and IL-6 [576,577] and increasing the production of IL-10 [578]. miR-181 is ranked 58th and 25th in the SHIP1 and SHIP1-STAT3 subsets respectively. The most enriched miRNA in the SHIP1-STAT3 subset is miR-448, which was found to form an autoregulatory loop with NFκB in breast cancer cells [579], and associated with interferon-mediated antiviral response [580]. miR-448 is ranked 78th in the SHIP1 subset, and 88th in the STAT3 subset. The non-overlapping miRNA enrichment analysis suggests that the three gene subsets may be regulated differentially at the post-transcriptional level.

Table 4.5: TargetScan analysis of SHIP1, STAT3, SHIP1-STAT3 gene subsets

Index	Name	P-value	Adjusted p-value	Z-score	Combined score
SHIP1-regulated genes					
1	AGCACTT,MIR-93,MIR-302A,MIR-302B,MIR-302C,MIR-302D,MIR-372,MIR-373,MIR-520E,MIR-520A,MIR-526B,MIR-520B,MIR-520C,MIR-520D	0.0011	0.1225	-1.9	3.99
2	TATTATA,MIR-374	0.0018	0.1225	-1.88	3.95
3	TGTGTGA,MIR-377	0.0078	0.2711	-1.74	2.27
4	ACATTCC,MIR-1,MIR-206	0.0102	0.2845	-1.75	2.2
5	CACTGCC,MIR-34A,MIR-34C,MIR-449	0.0075	0.2711	-1.64	2.15
6	AAGCACT,MIR-520F	0.0158	0.2914	-1.72	2.12
7	GTCTTCC,MIR-7	0.0210	0.2914	-1.59	1.96
8	ACCATTT,MIR-522	0.0183	0.2914	-1.55	1.91
9	TGTTTAC,MIR-30A-5P,MIR-30C,MIR-30D,MIR-30B,MIR-30E-5P	0.0245	0.3098	-1.62	1.9
10	TTCCGTT,MIR-191	0.0151	0.2914	-1.47	1.81
STAT3-regulated genes					
1	GTGTTGA,MIR-505	0.0001	0.0148	-1.89	7.97
2	TGAATGT,MIR-181A,MIR-181B,MIR-181C,MIR-181D	0.0001	0.0148	-1.86	7.85
3	TTGCACT,MIR-130A,MIR-301,MIR-130B	0.0008	0.0438	-1.91	5.96
4	TTTGCAC,MIR-19A,MIR-19B	0.0008	0.0438	-1.89	5.9
5	ATGTACA,MIR-493	0.0024	0.0998	-1.77	4.08
6	CATTTCA,MIR-203	0.0040	0.1195	-1.73	3.67
7	ACTTTAT,MIR-142-5P	0.0038	0.1195	-1.68	3.57
8	GTGCAAT,MIR-25,MIR-32,MIR-92,MIR-363,MIR-367	0.0058	0.1529	-1.64	3.08
9	TGCTTTG,MIR-330	0.0092	0.1759	-1.63	2.84
10	GCTTGAA,MIR-498	0.0082	0.1759	-1.63	2.83
SHIP1-STAT3 regulated genes					
1	ATATGCA,MIR-448	0.0042	0.2936	-1.82	2.23
2	ACTGTGA,MIR-27A,MIR-27B	0.0368	0.3803	-1.89	1.83
3	CACTTTG,MIR-520G,MIR-520H	0.0547	0.3803	-1.76	1.7
4	CAGCTTT,MIR-320	0.0622	0.3803	-1.72	1.67
5	GTGACTT,MIR-224	0.0258	0.3803	-1.69	1.63
6	ATGTTAA,MIR-302C	0.0563	0.3803	-1.68	1.63
7	ACATTCC,MIR-1,MIR-206	0.0819	0.3803	-1.64	1.58
8	TGCACTG,MIR-148A,MIR-152,MIR-148B	0.0847	0.3803	-1.62	1.56
9	GTAAACC,MIR-299-5P	0.0815	0.3803	-1.62	1.56
10	TTGCACT,MIR-130A,MIR-301,MIR-130B	0.1350	0.3803	-1.53	1.48

4.3. Discussion

IL-10 and IL-6 both induce STAT3 activation, but these cytokines have opposite effects on macrophage functions: IL-6 stimulation induces a pro-inflammatory phenotype while IL-10 is considered anti-inflammatory. One mechanism underlying the divergent effect of STAT3 activated by IL-6 and IL-10 is the action of the protein SOCS3 [581]. Both IL-6 and IL-10 are able to induce the expression of SOCS3 mRNA and protein in a STAT3-dependent manner [582], with IL-10 induction being stronger. However, SOCS3 only inhibits IL-6 signalling but not IL-10 signalling because the gp130 subunit of the IL-6 receptor contains a binding site for SOCS3, while IL-10 receptor does not [581]. In macrophages lacking SOCS3 or carrying a mutation in the SOCS3-binding site of IL-6 receptor, IL-6 actually becomes anti-inflammatory and inhibits LPS-induced TNFα production. However, we must be cautious in making the conclusion that SOCS3 is the only essential molecule distinguishing IL-6 signalling and IL-10 signalling. Thus, it is necessary to determine other mediators downstream of STAT3-activation that are differentially induced by these cytokines.

The majority of the studies have suggested that STAT3 is responsible for all IL-10's anti-inflammatory functions by activating the expression of specific gene products that inhibit pro-inflammatory signalling [55,333,373,374,416,583]. But now, we know that although STAT3 is required for IL-10 function, it is not sufficient [419,420,535]. In particular, SHIP1 is also necessary for IL-10 function, and that SHIP1 appears to interact with STAT3 to mediate IL-10 function. This chapter has described studies that examined the SHIP1-STAT3 model.

Consistent with data obtained from standard stimulation procedure, our data from using the continuous flow cell apparatus also showed that SHIP1 and STAT3 were required to mediate IL-10 inhibition of LPS-induced TNFα production, and deficiency of one but not the other showed incomplete inhibition (**Figure 4.1**). We speculated that SHIP1 and STAT3 form a signalling complex for IL-10 function; indeed, we found that upon IL-10 or SHIP1 activator treatment, SHIP1 becomes associated with STAT3 in macrophages (data not shown). However, our efforts to show the physical interaction of SHIP1 and STAT3 and to map out the interacting domain using purified His_6-SHIP1 and Flag-STAT3 have been fruitless (**Figure 4.2**). Certain interaction features must be missing in our system, for example, phosphorylation events commonly required on signalling molecules. It is also possible that another protein is either acting as a bridge between SHIP1 and STAT3, or necessary for stabilizing the SHIP1-STAT3 complex. A candidate protein is AMPK, which phosphorylates and activates STAT3 after IL-10 stimulation [370]. Moreover, AMPK deficiency leads to the loss of STAT3 activation and insufficient inhibition of pro-inflammatory cytokine production in activated macrophages [370]. Consistent with its role in IL-10 function, our unpublished data showed that AMPK was actually pulled down by SHIP1 in IL-10 treated macrophages, strengthening the hypothesis that AMPK may be part of the SHIP1-STAT3 complex (S. Shakibakho, unpublished).

To address the possibility that phosphorylation may be required for SHIP1-STAT3 function, we mutated 4 different tyrosine residues in SHIP1 and examined if any of these mutants behaved differently from wild type SHIP1. By measuring IL-10 inhibition of TNFα production in LPS-stimulated macrophages, we found that cells

containing Y190F SHIP1 were no longer inhibited by IL-10 (**Figure 4.3**), suggesting that Y190 may be important to interact with STAT3 (and potentially other proteins) to form the necessary signalling complex. Also, the integrity of the SHIP1 protein structure could be disrupted with the Y190F mutation, causing misfolding of the protein and thus eliminating its biological functions. These can be examined by determining if this SHIP1 mutant could still pull down STAT3 in IL-10 treated macrophages in a pull down assay. An *in vitro* phosphatase assay performed with SHIP1 Y190F protein would be informative on its structure as well; misfolded protein should have reduced or even no enzymatic activity. However, it is worth noting that the catalytic activity of SHIP1 may not be essential for its anti-inflammatory role; a triple-point mutation in the active site of SHIP1, which causes the enzyme to be inactive, was still able to inhibit TNFα production in activated macrophages (to a lesser extent) [317].

IL-10 inhibition of macrophages is not limited to TNFα production alone, and several studies have looked at IL-10 regulating global gene expression profiling [45,416,584,585] and identified previously unknown IL-10 regulated genes in macrophages. We decided to focus on two studies, one using microarray analysis [416], and the other using a combination of ChIP-seq and RNA-seq [45]. The first observation we had is the small number of overlapping genes identified in their studies and our presented data. That can be due to the differences in cell types (BMDMs vs perimacs), the stimulation condition (with or without LPS and the concentration of IL-10), the time points (0.5 hour vs 3 or 4 hours), as well as the differential gene sets detectable in each methodology. Also, SHIP1 KO macrophages were found to be skewed towards an alternatively activated phenotype [464], which may affect expression of certain genes.

Nevertheless, we have identified a few IL-10 induced genes that may be regulated by both SHIP1 and STAT3 when we compared our SHIP1-regulated gene subset to each of the two studies (**Figure 4.6 and 4.7**).

Ambp, Bcl2l11, Fzd7, Cd274, Gpr35 and Crlf2 are all upregulated by IL-10 in our microarray analysis. Expression of Ambp was verified to be STAT3-dependent by RT-PCR [416], and Cd274, Gpr35 and Crlf2 have STAT3 bound near their promoters after IL-10 treatment [45]. Among these, we are particularly interested in GPR35, a G-protein coupled receptor that has anti-inflammatory properties [586]. Genome wide studies have associated polymerophism of the GPR35 gene with inflammatory diseases such as IBD [587], type 2 diabetes [588], and atherosclerosis [589]. Also, a number of GRP35 agonists and antagonists have been described ([590-592], reviewed in [593]). In macrophages, binding of GPR35 by kynurenic acid has been shown to attenuate LPS-induced TNFα [591], suggesting an inhibitory role in macrophage activation. It is consistent with IL-10's ability to upregulate GPR35. Our real time-PCR analysis confirmed IL-10 induction of GPR35 mRNA, and also showed that both SHIP1 and STAT3 were required for this upregulation. Future experiments should focus on whether the GPR35 protein level is altered by IL-10, as well as the biological relevance of this regulation.

Through network analysis, apoptosis is one of the highest ranked pathways that may also be regulated via SHIP1. Lang *et al.* [416] and we both found that Bcl2l11 (also known as Bim), an apoptosis facilitator, was regulated by IL-10. Lang *et al.* [416] showed that IL-10 enhanced the LPS-induced Bcl2l11 by 1.3-fold at 3 hours, but we found that IL-10 actually downregulated Bcl2l11 as detected by both microarray and real

time-PCR analysis. The discrepancy may be due to the cell types used or the time points tested. Bcl2l11 is upregulated by TLR signalling through MAPK activation [564,594] At the same time, TLR signalling results in the phosphorylation of Bcl2l11 that leads to degradation of the protein [595]. Previous studies show that IL-10 induces apoptosis in the development and differentiation of different myeloid cells in order to maintain immune hemostasis [561-563] but IL-10 usually inhibits apoptosis in activated cells [564,565]. The downregulation of Bcl2l11 by IL-10 in LPS-stimulated macrophages is consistent with these reports. However, we did not observe SHIP1 and STAT3 involvement in IL-10 regulation of Bcl2l11 by real time-PCR. More replicates and experimental conditions will be required to draw definitive conclusion. The literatures supported an anti-apoptosis function mediated by STAT3 [551-554]. While studies using overexpression of SHIP1 in cells or SHIP1 KO cells showed that SHIP1 promoted apoptosis [555-557], inhibition of SHIP1 may actually be anti-apoptotic [481,558-560]. The actual role of SHIP1 in IL-10 mediated apoptosis will require further experimentation.

The last part of the study focuses on a wider view on IL-10 regulation on gene expression via SHIP1 and STAT3 by categorizing genes into SHIP1-regulated, STAT3-regulated, and SHIP1-STAT3 regulated subsets. Preliminary efforts to identify differential regulatory mechanism with bioinformatics tools have shown that the transcription factor E2F1 may be important for SHIP1-regulated genes. E2F1 is known to regulate NFκB activity, but both positive and negative regulations have been reported. [570-574]. While E2F1 is not identified as highly enriched in our STAT3 subset (rank 19th) and SHIP1-STAT3 gene subset (rank 166th), a genome-wide study has shown that

STAT3 is recruited to E2F1 pre-bound DNA in four different cell types including macrophages [418]. The specific mechanism E2F1 uses may be cell type, stimulation, and time dependent. Additionally, we found that the three gene subsets may be regulated differentially via post-transcriptional mechanism because each subset is enriched for seed sequences of different miRNAs. One of the caveats of our analysis is that the STAT3 subset is quite substantial with 1089 genes, compared to only 113 and 22 genes in the SHIP1 and SHIP1-STAT3 subsets. Nevertheless, with our real time PCR data, we found that a large percentage of IL-10 regulated genes require both SHIP1 and STAT3, suggesting that SHIP1 and STAT3 may cooperate to mediate IL-10 regulation and it may be a more common mechanism than SHIP1 and STAT3 work independently downstream of IL-10.

In summary, we have provided evidence that SHIP1 and STAT3 cooperate to mediate IL-10's anti-inflammatory function in macrophages, perhaps due to the formation of a signalling complex consisting of SHIP1, STAT3 and other unconfirmed proteins, and the subsequent signalling events triggered by such a complex. Our microarray analysis supports a model in which SHIP1 and STAT3 differentially mediate IL-10's regulation of gene expression, although further delineation will be needed. This new mechanism opens up the possibility to regulate specific clusters of genes using a SHIP1 modulator or a STAT3 modulator in conditions where global inhibition of IL-10 function is not desired.

Chapter 5: Crystal Structure of SHIP1 Fragment Reveals Insight into SHIP1 Activator Binding

5.1 Introduction

Class I PI-3 kinases (PI3K) have critical roles in regulating cell proliferation, survival, differentiation and metabolism in all cell types. In immune cells, ligand engagement of nearly all receptors can activate PI3K. Once activated, PI3K phosphorylates $PI(4,5)P_2$ to generate $PI(3,4,5)P_3$ in the plasma membrane. $PI(3,4,5)P_3$ then triggers a cascade of downstream signalling events via the recruitment of PH-domain containing proteins such as AKT. Deregulation of the PI3K pathway has been implicated in cancer and inflammatory disorders [596], and therefore intensive research has been put into the development of therapeutics targeting PI3K and its downstream signalling molecules. However, because PI3K is involved in so many cellular processes, PI3K inhibitors can easily show off-target effects and lead to undesired complications [597-600]. Also, emerging studies show that the different isoforms of PI3K can have different roles, and even opposite roles, in certain processes [601-604]. Drugs that inhibit individual PI3K isoforms are wanted in this case. Thus, isoform specific inhibitors have been developed, but that leads to the question of whether other isoforms may compensate for the functions of the inhibited isoforms. Because kinases and phosphatases orchestrate the phosphorylation changes necessary for proper cell functions, an attractive alternative is to develop drugs that can activate phosphoinositol phosphatases to reduce $PI(3,4,5)P_3$ level. SHIP1 is an especially unique target in treating immune-related disorders, because its expression is restricted to cells in the hematopoietic lineages, and any therapeutics targeting SHIP1 should limit its effect to these cells and minimalize any side-effects.

SHIP1 contains a 300-residues catalytic domain common to all 5'-phosphatases as predicted by primary sequence alignments; this domain has a similar fold to the

apurineic/apyrimidinic repair endonucleases [605]. SHIP1 also contains additional protein domains that facilitate its functions (**Figure 5.1A**), as described in Chapter 1. The regulation of SHIP1 was previously thought to be solely dependent on its location in the cells, which is mediated mainly by its SH2 domain and its C-terminal regions. However, this view has been challenged in recent years. We showed by kinetic studies that SHIP is allosterically activated by its end product $PI(3,4)P_2$, as well as a small molecule AQX-MN100 [430]. This allosteric regulation requires PH-R and C2 domains that flank the phosphatase catalytic domain; deletion of either domain abolishes the impact of AQX-MN100 on SHIP1 enzyme activity ([430] and data not shown). We have also identified the site of AQX-MN100 binding to be the C2 domain [430], while the PH-R domain is the PIP_3 binding site [429].

The objective of this chapter is to characterize the molecular basis of the association of SHIP1 activators to SHIP1. We first identified the minimal region of SHIP1 that can be allosterically activated by SHIP1 activators. We then solved the structure of this region via x-ray crystallography, which, together with various biochemical approaches, provides valuable information on the interaction of the SHIP1 activators and the SHIP1 enzyme.

5.2 Results

5.2.1 The minimal enzymatic region of SHIP1 contains the phosphatase and C2 domains.

To gain more understanding of the interaction between SHIP1 and its activators, we aimed to obtain a crystal structure of the protein-ligand complex. However, crystallizing the full-length protein would be challenging because (1) SHIP1 is a relatively large protein (about 145 kDa with 1911 amino acids in mouse SHIP1) and thus contains multiple flexible loops that likely hinder crystallization, (2) full-length SHIP1 is quite unstable and has the tendency to degrade during purification. Hence, a truncated SHIP1 construct containing the PH-R, phosphatase and C2 domains (PPAC) was generated (**Figure 5.1A**). PH-R and C2 domains were included, because they were shown to be required for allosteric regulation [430].

To verify the integrity of the enzyme, we first expressed and purified SHIP1 and PPAC from HEK293T cells and compared their enzymatic properties in an *in vitro* phosphatase assay using IP_4 as the substrate (**Figure 5.1B**). PPAC had a similar K_{cat} value as SHIP1 but had a higher affinity to the substrate (lower K_m but statistically insignificant), suggesting that the domains that were deleted did not appear to affect the catalytic activity of enzyme. We also tested whether the synthetic SHIP1 activator, AQX-MN100, could still enhance activity of PPAC, and found that PPAC was activated by AQX-MN100 to similar level as full length SHIP1 (**Figure 5.2**).

HEK293T expression systems are impractical for producing enough protein for crystallization screening so we attempted to express PPAC in bacteria, as well as in Sf9, an insect cell line. Unfortunately, recombinant PPAC was mostly insoluble when

expressed in bacteria, even when it was expressed as a fusion protein with maltose binding protein (MBP), a well-known solubility enhancer [606]. The small amount of soluble PPAC protein purified from bacteria was found to have similar enzymatic properties as PPAC expressed in HEK293T cells (**Figure 5.1B**). While we obtained reasonable amounts of active PPAC from Sf9 cells for crystallization, this protein did not yield any crystal in all the conditions tested. We also systematically screened for different PPAC constructs by shortening the C-terminus. The N-terminus was not altered because the structure of the PH-R domain was previously modeled based on NMR studies [429]. However, none of these constructs crystallized.

Previous data showed that SHIP1 activators directly interact with C2 domain but not PH-R domain [430]. We thus decided to generate a second set of truncated constructs that only contain the phosphatase and the C2 domains (PAC). Two different C-termini were chosen, and these proteins were named PAC1 (residues 402-861) and PAC2 (residues 402-857) respectively. Satisfyingly, we were able to produce a large quantity of both PAC1 and PAC2 proteins from bacteria as MBP-fusion proteins. The proteins were soluble and stayed as monomers after tag removal. Similar to PPAC, PAC2 has a lower K_m value than SHIP1 and a comparable K_{cat} as SHIP1 (**Figure 5.1B**). Surprisingly, AQX-MN100 was still able to enhance activity of PAC2 to the same extend as SHIP1 (**Figure 5.2**), even though PAC2 lacks the PH-R domain.

A

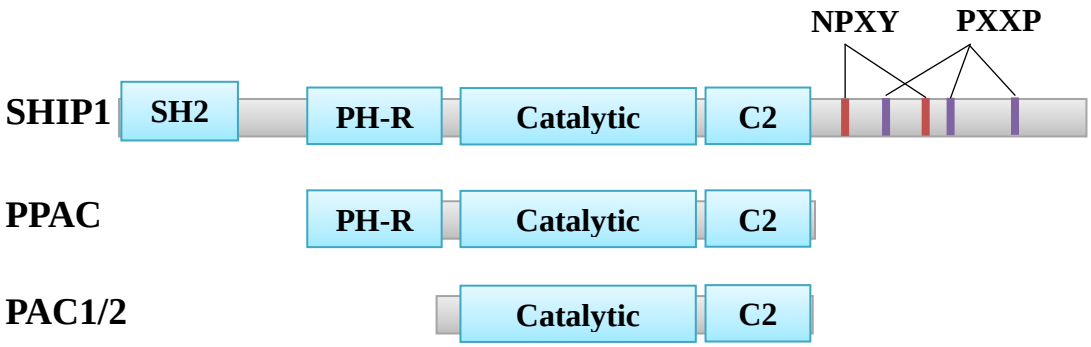

B

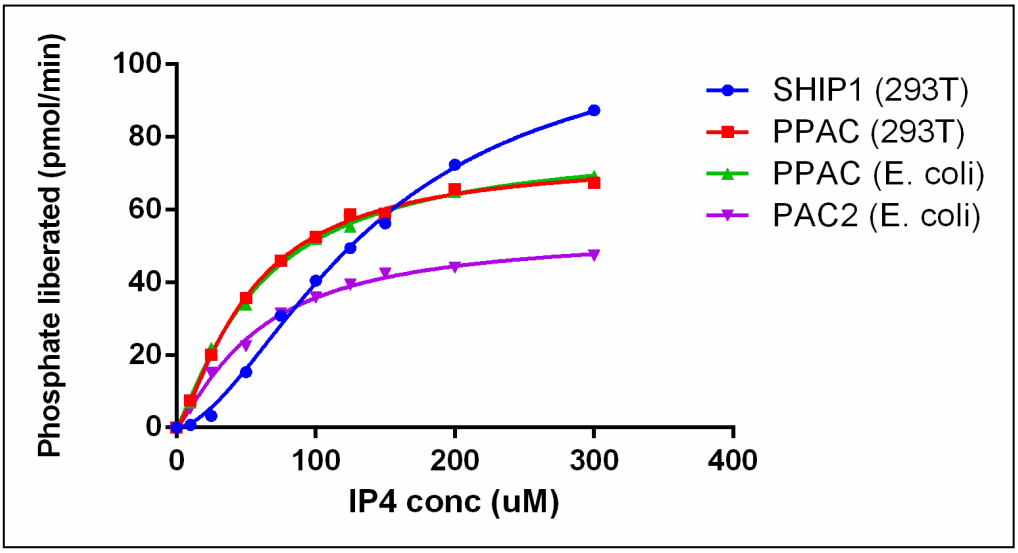

Enzyme	K_{cat} (min $^{-1}$)	K_m (µM)	K_{cat}/K_m (pmol PO_4/min /pmol enzyme /µM substrate)
SHIP1 (293T)	1290 +/- 420	148+/-9	**8.7 +/-3.3**
PPAC (293T)	1032 +/-413	67 +/-34	**16.0 +/-1.7**
PPAC (*E. coli*)	1020 +/-203	65 +/-8	**15.5 +/-1.3**
PAC2 (*E. coli*)	708 +/-355	66 +/-22	**10.3 +/-3.1**

Figure 5.1 PPAC and PAC have similar enzymatic activity as full length SHIP1.
(A) Schematic diagram of the different SHIP1 truncation constructs. (B) Initial velocities were determined at the indicated concentrations of IP_5. K_{cat} and K_m values were calculated using GraphPad software.

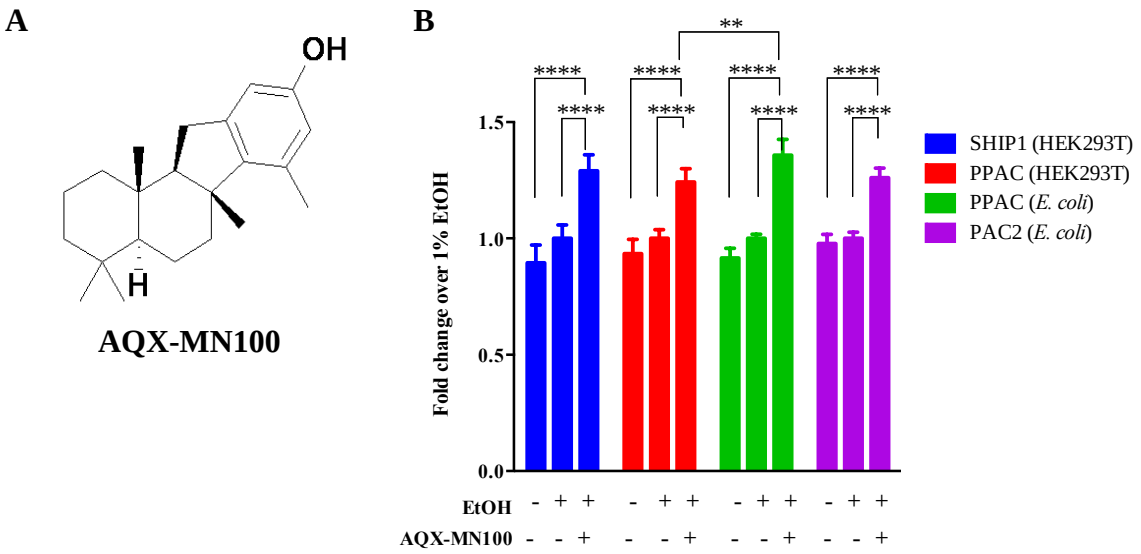

Figure 5.2 AQX-MN100 is able to enhance the enzymatic activity of PPAC and PAC. (A) The structure of AQX-MN100. (B) Recombinant proteins were preincubated with 0.2 mM AQX-MN100 or ethanol (solvent control) for 10 minutes at 23°C before incubating with 50 uM IP4 for 10 minutes at 37°C. The reaction was stopped by the addition of Malachite Green reagent. Data are presented as fold activation compared to the ethanol treatment. Statistical significance between treatments was calculated by a two-way ANOVA test with a 95% confidence (** $p <$ 0.01, **** $p < 0.0001$). Similar results were observed in at least two independent experiments.

To more definitively determine the role of C2 domain in regulating SHIP1 phosphatase activity, we made a construct containing only the phosphatase domain (residues 402 to 718). However, this isolated phosphatase domain was found to be highly insoluble in bacteria and we were not able to determine the complete enzyme kinetic parameters of this domain alone. This observation agrees with a recent study showing that the phosphatase domain of SHIP2, a close homologue of SHIP1, is only marginally active compared to other 5'-phosphatases [607]. The authors pointed out the possibility that SHIP2's phosphatase domain might require other domains to reach optimal activity. Also, our definition of minimal enzymatic region (PAC) is consistent with previous report [608] that defines the minimal enzyme as having the boundaries between residues

400 and 866 in mouse SHIP1. We thus conclude that PAC is the minimal catalytic region of SHIP1 that can be regulated allosterically, and used both PAC1 and PAC2 in our crystallization screens.

We have also explored the possibility that the enzyme might be regulated by calcium because it contains a C2 domain, a known calcium-binding domain. As shown in **Figure 5.3A**, the addition of $CaCl_2$ decreased the basal activity of SHIP1 and PAC1, but did not inhibit enzyme activation by AQX-MN100. To our surprise, calcium actually enhanced the activation ability of AQX-MN100, as demonstrated by comparison to untreated sample (**Figure 5.3B**). We thus included $CaCl_2$ in some of our crystallization conditions.

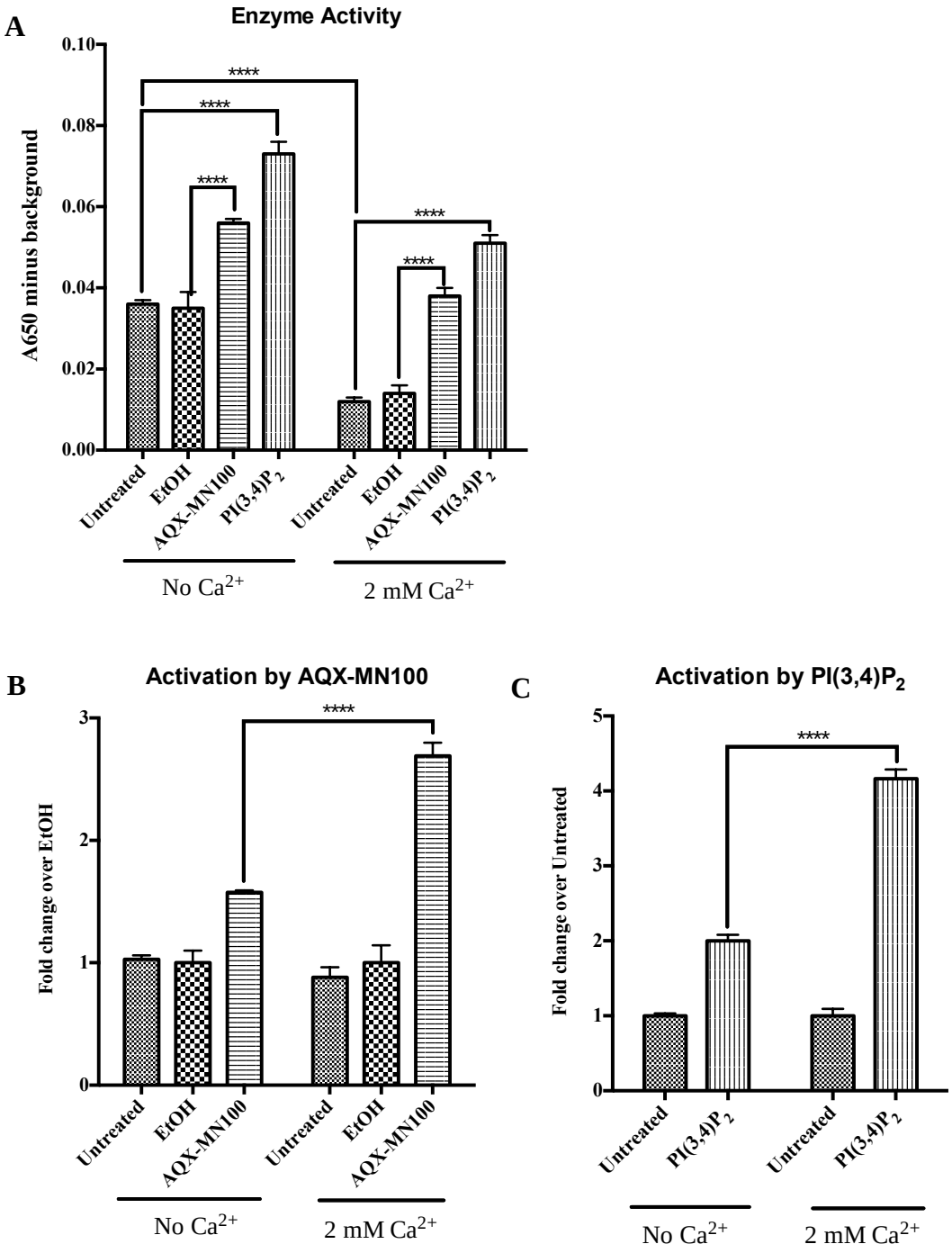

Figure 5.3 Calcium reduces basal enzyme activity but enhances activation by SHIP1 activators.

PAC1 enzyme was preincubated with, 0.2 mM AQX-MN100, ethanol (solvent control), or 80 μM of $PI(3,4)P_2$-diC8 for 10 minutes at 23°C before incubating with 50 μM IP_4 for 10 minutes at 37°C. The reaction was stopped by the addition of Malachite Green reagent. Data are presented as either (A) background-corrected A650 values, (B) fold change compared to the ethanol treatment for AQX-MN100 or (C) fold change compared to untreated sample for $PI(3,4)P_2$. Statistical significance between treatments was calculated by a two-way ANOVA test with a 95%

confidence (**** $p < 0.0001$). Similar results were observed in at least two independent experiments. Representative data are shown.

5.2.2 Crystal structure of PAC

The first crystal obtained was of wild type PAC2 and it diffracted at resolution of 2.56Å. SHIP2's phosphatase domain (PDB: 3NR8) was used in molecular replacement to determine the structure of PAC2 phosphatase domain. However, we exhausted our means in solving the C2 domain and were still unsuccessful; there were too many regions with discontinued electron density, suggesting that the C2 domain might be quite flexible in nature. We approached this problem by mutating residues in those flexible regions. Residues with flexible side chains on the protein surface can impede the ability of the protein to form intermolecular contacts necessary for crystal formation. The Surface Entropy Reduction (SER) approach, as described by Derewenda [609], replaces large and flexible hydrophilic residues chains, such as Lys and Glu, to smaller side chains, usually Ala, on the surface of the protein. Using the SERp server [610], we identified three regions in the PAC2 protein that are enriched with either Lys or Glu; we labeled them as Cluster A to Cluster C (**Table A.4**); only Cluster C is located in the C2 domain. These mutations were introduced in both PAC1 and PAC2. We obtained diffraction-quality crystals of PAC1 with mutation at Cluster C (E770A E772A E773A); this mutant is termed as PAC1cc. Crystals of PAC1cc diffracted at a higher resolution than those of wild type PAC2. We were able to determine its structure and then used it to solve structure of wild type PAC2 using molecular replacement. PAC1cc were found to crystallize in two different space groups (**Table 5.1**).

Table 5.1: Data collection and refinement statistics

	PAC1cc	wild type PAC2	PAC1cc
X-ray source	CLS-08ID-1	APS-IDD	APS-IDD
Wavelength	1.03317	1.03317	1.03319
Detector	CCD	CCD	CCD
Space group	C121	P 1 21 1	P 21 21 21
Unit cell parameters (Å)	a=128.21, b=45.1, c=162.56	a=140.07, b=45.53, c=155.17	a=45.10, b=73.20, c=125.21
Unit cell angles (°)	α=90.0, β= 107.7, γ= 90.0	α=90.0, β= 91.44, γ= 90.0	α=90.0, β= 90.0 γ= 90.0
Angle increment (°)	0.5	1	0.5
Number of images	360?	180	267
Biological assembly per ASU	2	4	1
Solvent content (%)	42	47	38
Resolution range (Å) [a]	47.12-2.10 (2.15-2.10)	48.64-2.34 (2.48-2.34)	47.36-1.50 (1.59-1.50)
Completeness (%) [a]	99.7 (99.8)	97.8 (91.9)	98.9 (98.6)
R_{meas} **(%)** [a]	8.6 (106.0)	11.9 (112)	5.9 (78.7)
CC (1/2)	99.8 (68.6)	99.6 (60.6)	99.9 (68.2)
Unique reflections [a]	51106 (3678)	80146 (11997)	66070 (10528)
Observed reflections [a]	191535 (13756)	295158 (41343)	217029 (34822)
Average redundancy [a]	3.7 (3.7)	3.68 (3.44)	3.28 (3.31)
Average $I/\sigma(I)$ [a]	12.0 (1.49)	11.14 (1.33)	13.79 (1.85)
Wilson B **factor (Å^2)**	39.73	50.94	25.38
Refinement statistics	REFMAC 5.8.0071	REFMAC 5.8.0071	REFMAC 5.8.0071
R_{work} / R_{free} / R_{total}	19.06/23.67/19.29	22.12/25.56/22.29	18.27/20.72/18.35
R.m.s.d. bond length (Å)/bond angle (°)	0.015/1.726	0.020/1.930	0.019/1.965
Ramachandran plot (% of residues in core/ additional allowed/ disallowed regions)	97/2.53/0.47	95.8/3.77/0.43	97.28/2.18/0.54
Average B **values (Å^2) all atoms/protein main chain/ protein side chains/solvent atoms/isopropanol atoms**	53.339/51.811/ 55.839/42.741/ 49.340	50.101/48.663/ 51.573/29.663/ none	23.299/21.183/ 25.219/25.037/ 25.762
Number of protein atoms	6871	13234	3591
Number of solvent atoms	114	46	175
Number of ligand atoms	4	0	4

[a] Numbers in parenthesis indicate data in the last resolution shell.

5.2.1.1 Overall structure

The PAC structures contained the phosphatase and the C2 domains (**Figure 5.4A**). The phosphatase domain has a similar fold as found in other phosphoinositide 5'-phosphatases including INPP5B, OCRL and SHIP2 [607]. The structure of SHIP1 C2 domain is similar to other C2 domains despite low sequence identity (**Figure 5.9**). The C2 domain interacts with the phosphatase domain extensively across an interface that is away from the active site. The C2 domain may be more mobile than the phosphatase domain, indicated by an overall higher B factor (**Figure 5.4B-D**). The B-factor describes how spread-out the electron density is for each atom, and gives the uncertainty for the position of each atom. A number of factors can contribute to a high B factor, including high mobility of individual atoms and side chains. In all three solved structures, the linker between the two domains (about 20 residues long) gave no electron density and thus is not modeled.

There are four, two, and one molecules in the asymmetrical units for the three crystals respectively, and their overall structures and domain orientations are similar to each other with slight shift in the positions in the loops and some β-strands. We focused on the structure of wild type PAC2 for majority of analyses, but the differences in these three structures will be discussed when appropriate.

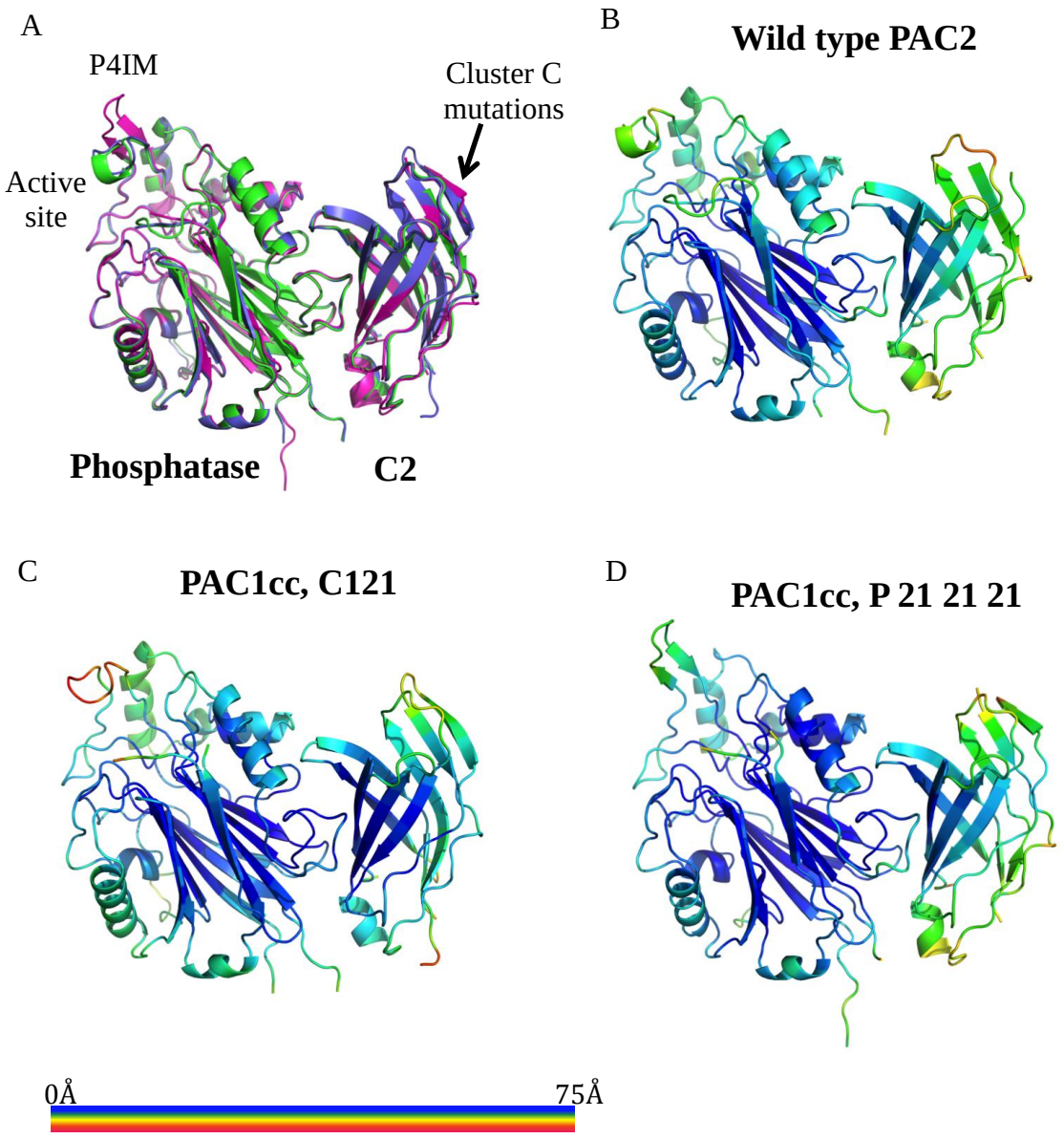

Figure 5.4 Structures of wild type PAC2 and PAC1cc.
(A) Superposition of the three structure: wild type PAC2 (Green), PAC1cc (Space group C121, Purple) and PAC1cc (Space group P 21 21 21, Magenta). (B-D) The structures are coloured based on B-factor. Red represents high dynamic regions while blue represents low dynamic regions.

5.2.1.2 Phosphatase domain

The phosphatase domain has an overall fold of a β-sandwich containing eleven β-strands that are surrounded by a few α-helices at the periphery. Sequence alignments

show that SHIP1 contains all the conserved residues in the active sites as other 5'phosphatases (**Figure 5.5**). A structure of the INPP5B phosphatase domain with PI(3,4)P_2 has been solved recently (PBD:4CML) and detailed interaction between the active site and PI(3,4)P_2 have been documented [607]. In the same study, the authors had also determined the structure of the OCRL phosphatase domain bound by a phosphate ion that mimics the position of the 5-phosphate in the substrate. These two structures give us crucial information of the interaction between the active site and the enzyme substrate PI(3,4,5)P_3, such as the conversed residues important for substrate binding, the atomic basis of substrate specificity, and potential membrane interaction interface.

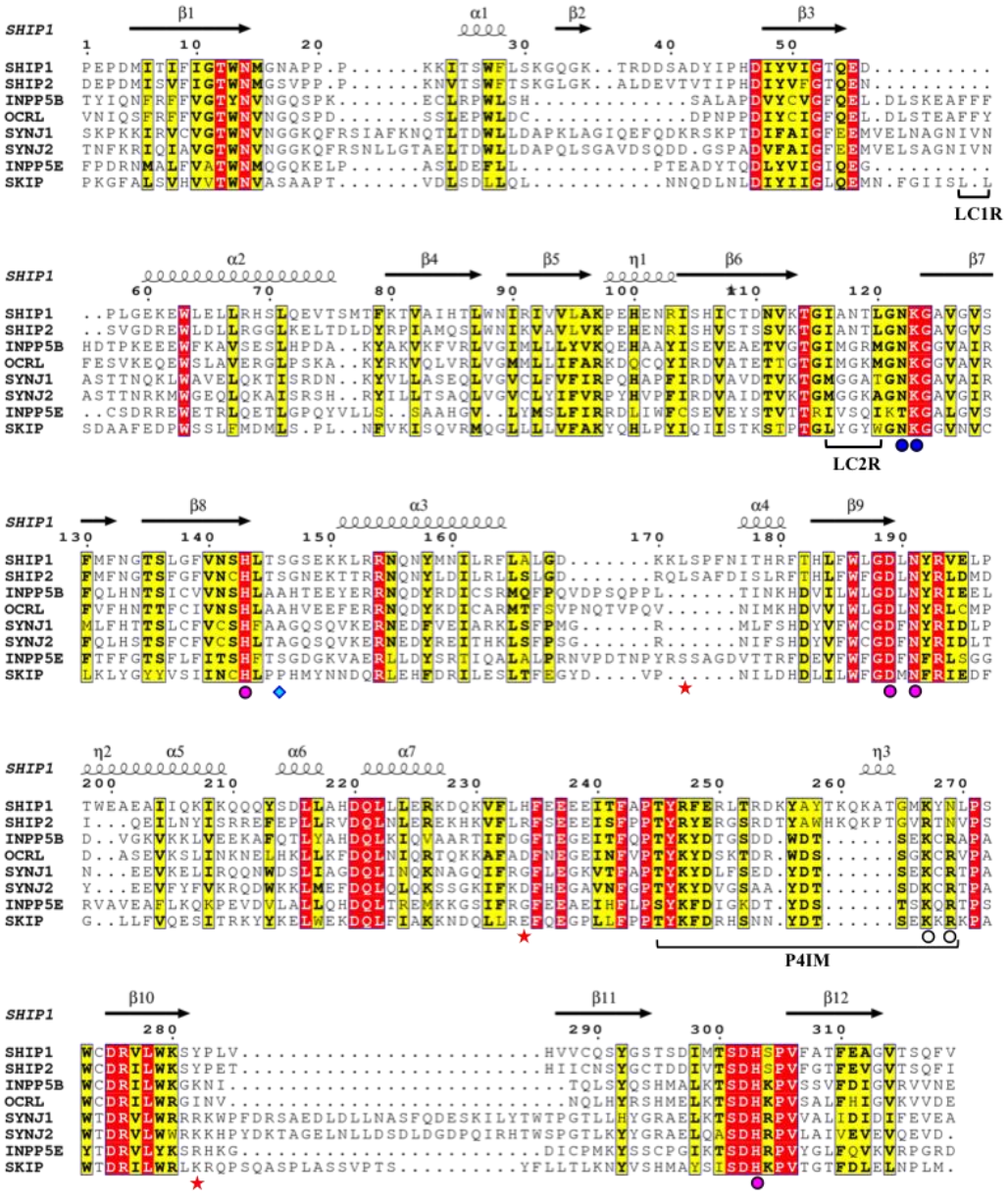

Figure 5.5 Sequence alignments of mouse phosphoinositol-5'-phosphatases.
The sequence alignments of the phosphatase domains of a few mouse phosphoinositol-5-phosphatases were performed by Clustal Omega [611]. The secondary structure, according to the SHIP1 structure, is showed at the top of the sequences. Residues that are identically conserved are written in white with red background. Residues that are 70-100% functionally conserved are written in bold with yellow background. The inositol-ring interacting residue is indicated by a cyan diamond. Residues interacting with 1-phosphatase, 3/4-phosphates and 5-phosphates are indicated with blue circles, white circles and magenta circles respectively. The P4 interacting motif, the lipid chain 1 recognition and the lipid chain 2 recognition motifs, as defined in the INPP5B by Tresaugues *et al.* [607], are labeled as P4IM, LC1R and LC2R. Residues that were selected for Ala mutations are indicated with red stars.

Figure 5.6 shows a superposition of the structures of SHIP1, SHIP2 and PI(3,4)P_2-bound-INPP5B phosphates domains. Comparison of the SHIP1 phosphatase domain to the structure of SHIP2 phosphatase domain shows a root-mean squared deviation (rmsd) of 0.437 Å for 233 superimposed Cα atoms out of 317 Cα atoms (SHIP1 structure). The similarity lies within the core of the domain while the periphery is more dissimilar. The rmsd value from PI(3,4)P_2-bound-INPP5B is 0.524 Å (183 Cα atoms), with highly similar folds in the core of the domains. Most of the residues interacting with 1-P and 5-P units of substrate are conserved and are positioned similarly in SHIP1 phosphatase domain with minor differences. In the INPP5B structure, the 1-P moiety of the substrate forms hydrogen bond with the side chain of Asn379 (Asn523 in SHIP1) and Lys380 (Lys524), but in the SHIP1 structure, Asn523 points to a different direction (**Figure 5.6B**). This shift of the side chain could be due to the lack of ligand in the SHIP1 phosphatase domain. Ala403 in INPP5B lines the inositol ring, and this residue is replaced by Ser547 in SHIP1 (and SHIP2), which should be small enough to accommodate the inositol ring. The 5-P moiety locates in a highly conserved pocket in 5-phosphatases containing six conserved residues (Asn523, Lys524, His544, Asp590, Asn592, His704 in SHIP1) (**Figure 5.6C**); the positions of these residues in SHIP1 structure are almost identical to those in other 5-phosphatases, with minor shifts in the side chains of Asn523 and Lys525.

Most 5-phosphatases prefer to hydrolyze the 5-P from either PI(4,5)P_2 or PI(3,4,5)P_3 [612,613], suggesting the enzymatic selectivity towards the 4-phosphate. SHIP1 and SHIP2 have an additional requirement for 3'-position to be phosphorylated [614,615]. INPP5B extensively interacts with the 4-P moiety through a conserved loop

called the P4-interacting motif (P4IM), which contains Tyr502, Lys503, Arg518 and Lys516. These residues stabilize 4-P through a combination of hydrogen bonds and electrostatic interactions. The P4IM loop is seven residues longer in SHIP1 (and SHIP2), making it quite different than that in INPP5B (**Figure 5.5**). A molecular dynamics study using the structure of SHIP2 in complex with a competitive inhibitor (PDB:4A9C) indicates that the longer P4IM loop could fold over and provide additional interaction [616]. Arg682 and Asn684 in SHIP2 are well positioned to interact with 3-P and 4-P. The corresponding residues in SHIP1 are Lys668 and Asn670, both of which should still be able to interact with 3-P and 4-P (**Figure 5.6D**). Worthy of note is that the P4IM loop is not modeled in majority of molecules in the asymmetrical unit, pointing out the flexibility of the loop. We also found that the P4IM loop in our wild type PAC2 structure adopts an "opened" conformation, while one of the PAC1cc structures shows a "closed" conformation (**Figure 5.6E**). While the conformation adopted in different crystals is likely a result of the different crystal environments (e.g. in the "open" conformation, the loop interacts with the neighbouring molecule in the crystal lattice), the flexibility of this loop cannot be ignored – it may shift its position depending on ligand binding. Tresaugues *et al.* [607] suggested that the driving force for this conformation change would likely be caused by the interaction of 3-P of the substrate and Arg682 in SHIP2 (Lys668 in SHIP1). The additional interactions form after closing of the P4IM could explain why SHIP1 and SHIP2 strongly prefer substrates that contain a phosphate at the 3'-position on the inositol ring even thought both only hydrolyze the 5'-phosphate [615,617].

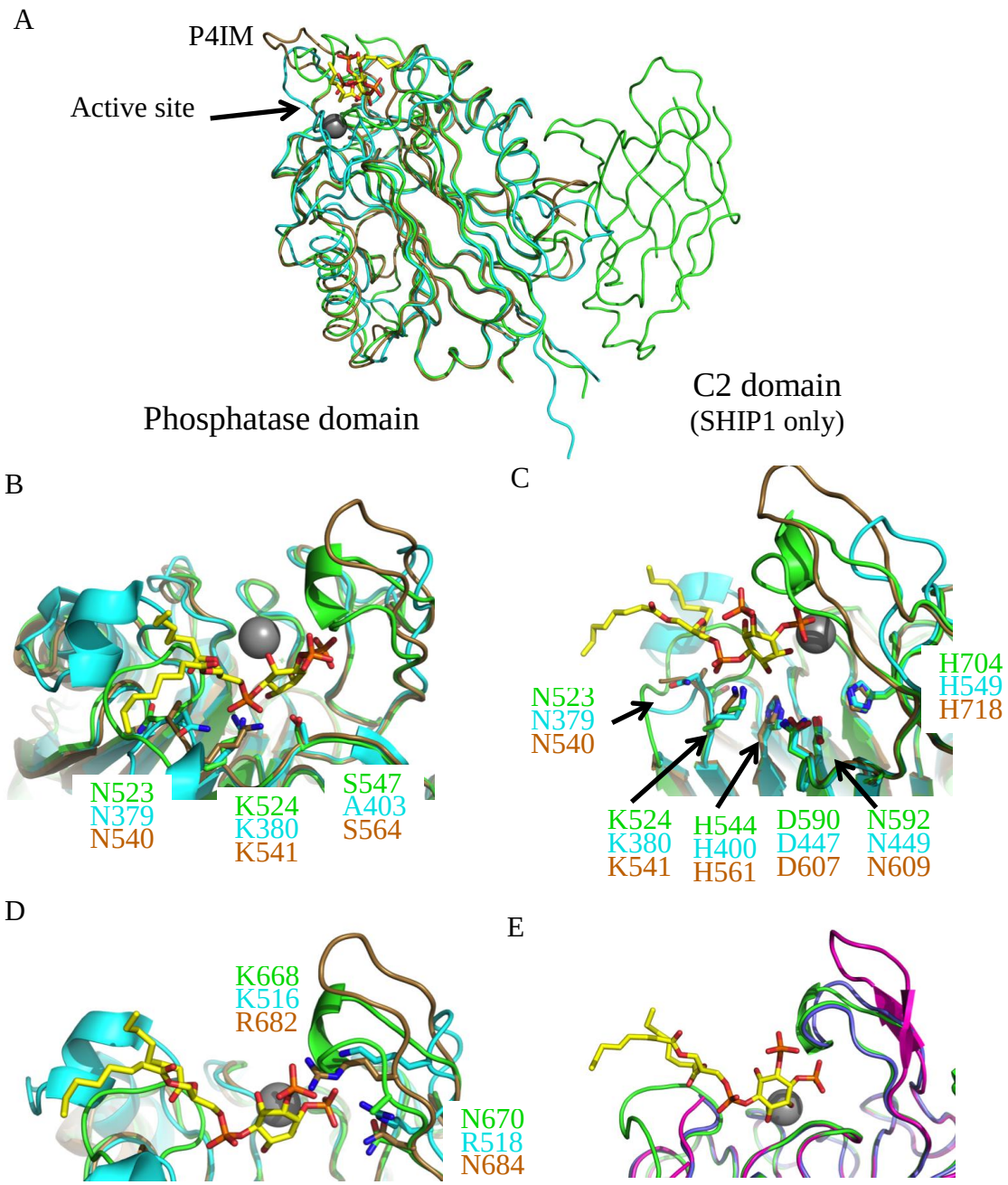

Figure 5.6 Superposition of mouse SHIP1, human INPP5B and human SHIP2 phosphatase domains.

(A) Ribbon diagrams of mouse SHIP1 (green), human INPP5B (PDB:4CML, cyan) and human SHIP2 (PDB:3NR8, brown). PI(3,4)P_2 from the INPP5B structure is depicted as stick representation in yellow, and Mg^{2+} ion is shown as a grey sphere. (B) Residues interacting with 1-phosphate and inositol ring of PI(3,4)P_2. (C) Residues interacting with 5-phosphate of PI(3,4)P_2. (D) Comparison of the P4IM loops. (E) Comparison of the P4IM loops in wild type PAC2 (Green), PAC1cc (Space group C121, Purple) and PAC1cc (Space group P 21 21 21, Magenta).

INPP5B contains two loops that provide interaction to the aliphatic regions of PI(3,4)P_2. These loops are called lipid chain 1 recognition motif (LC1R-motif) and lipid chain 2 recognition motif (LC2R-motif), and they serve as the membrane-interacting regions for the phosphatase to penetrate into the membrane. SHIP1 and SHIP2 lack the first motif, and they do not have the equivalent lipid-interacting residues in the second motif as shown by sequence alignment (**Figure 5.5**). Since the phosphatase domain would need to interact with the membrane, where the substrate locates, for catalysis to occur, we have examined closely at the area to determine potential lipid-interacting residues (**Figure 5.7**). The LC2R loop is not modeled in the SHIP2 structure due to its apparent flexibility. We found this loop to be flexible in SHIP1 as we were only able to model this loop in the wild type PAC2 structure, but not in PAC1cc structures. Overlaying the PI(3,4)P_2-bound INPP5B structure to our structure, we saw that the two LC2R loops do not correlate well in position. The LC2R motif in SHIP1 shifts so it also occupies where the LC1R motif would be, with Ile517 and Leu521 as the potential lipid-interacting residues.

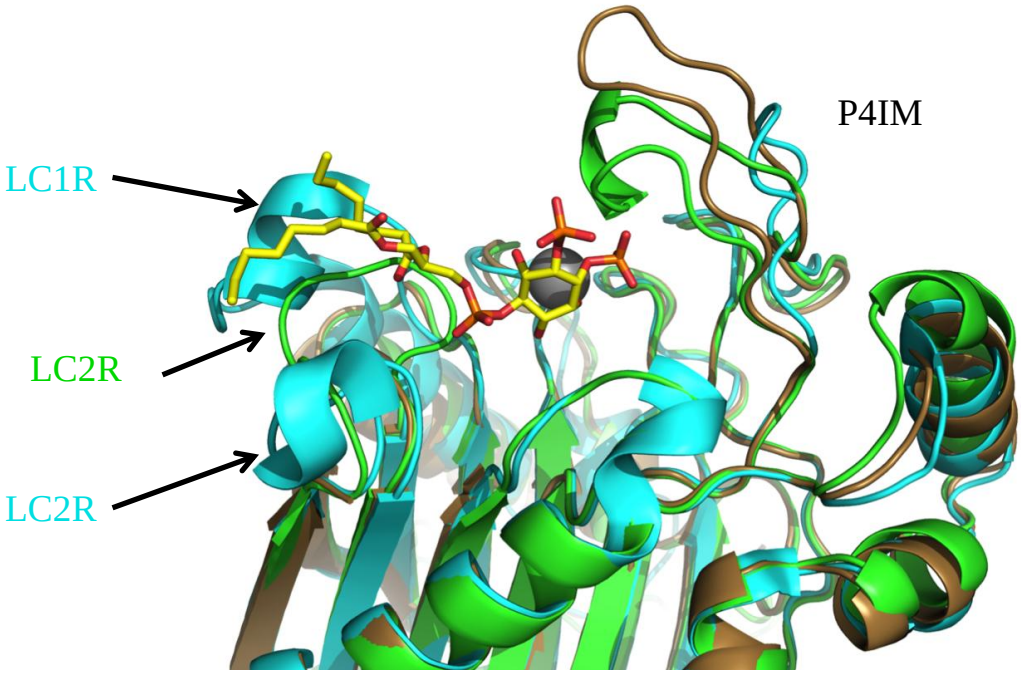

Figure 5.7 Position of LC1R and LC2R in mouse SHIP1 or INPP5B phosphatase domains.

Structures of SHIP1 (green) and INPP5B (cyan) phosphatase domains are superposed. LC1R and LC2R are indicated with arrows. PI(3,4)P_2 is depicted in orange and Mg^{2+} ion is represented as a grey sphere.

5.2.1.3 C2 domain

The C2 domain forms a β-sandwich core that contains two sheets of 4 antiparallel β-strands, with 1 α-helix at the peripheral, and it interacts with the phosphatase domain on the surface away from the active site. The mutations in PAC1cc locate after β2-strand, and appear to stabilize the structure around that region (**Figure 5.4**). The wild type PAC2 structure is actually missing (part of) β3-strand due to the disordered nature of this region. Structure-based sequence alignment (VAST-MMDB) [618] using wild type PAC2 as input found that the SHIP1 C2 domain is most similar to the C2B domain of the extended synaptotagmin 2 (E-Syt2) (PDB: 4NPJ) [619] with a VAST score of 13.6 (**Figure 5.8**). Similar to E-Syt2 C2B, SHIP1 C2 adopts a Type II topology (as described

in Rizo *et al.* [620]), with both N- and C-termini located at the bottom of the domain, opposite to the (potential) calcium-binding regions (CBRs). There are four loops at the top (the loop between β3and β4 is not modeled) and three loops at the bottom of the domain, one of which forms a short α-helix.

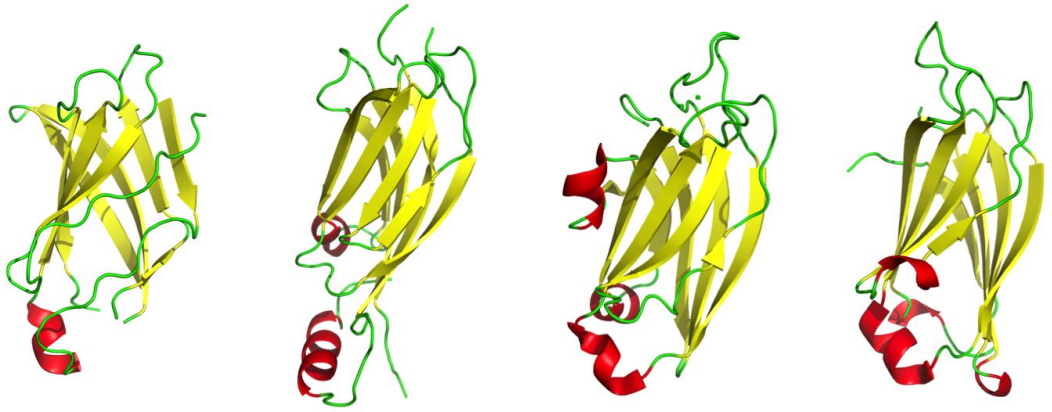

Figure 5.8 Structures of C2 domains.
The structures of SHIP1 C2, E-Syt2 C2B (PDB: 4NPJ), PKCα C2 (PDB: 3GPE) and rabphilin C2A (PDB: 4NS0) are shown in cartoon representation. Coils are coloured in green, α-helices are coloured in red and β-strands are coloured in yellow.

C2 domains were discovered as a calcium-binding domain, and numerous structural studies reported five conserved Asp residues critical for Ca^{2+} binding. We found that SHIP1 C2 lacks all but one of these Asp residues (Asp813 in CBR3 loop), and likely does not bind Ca^{2+} ions. However, our *in vitro* phosphatase results showed that Ca^{2+} ions reduced the basal enzymatic activity of SHIP1 and PAC1. It is possible that the Ca^{2+} ions may be interacting with the protein in the phosphatase domain. Unfortunately, we were unable to produce a co-crystal structure of PAC1/2 and Ca^{2+} ions.

Another feature of C2 domains is the ability to interact with phospholipids (such as phosphoserine) at near the CBRs by a combination of hydrophobic interaction and

electrostatic interaction (review in [621]). Ca^{2+} binding changes the electrostatic potential needed for the protein to associate with the negatively charged phosphate head group of phospholipid. At the same time, phospholipid binding also enhances the affinities of Ca^{2+} ions, because its phosphate head groups fill the coordination shell of the ions. Some C2 domains show phospholipid binding in a Ca^{2+}-independent manner [622-625]; one example is the C2 domain of PTEN. PTEN C2 only contains one Asp residues in the CBR loops and does not bind Ca^{2+}; however, it was able to bind to vesicles consisting of anionic phospholipid [626]. The authors used full length PTEN, which has a much higher affinity to phospholipid vesicles than isolated C2 domain, to compare protein binding to phosphoserine and phosphoglycerol, and found no significant difference indicating that the binding was likely due to non-specific electrostatic interactions. The positively charged CBR3 loop (+5 net charge) may play a role. By contrast, SHIP1 C2 does not contain a loop enriched with basic residues that could serve as interacting partners for anionic phospholipids. This observation does not rule out the possibility that SHIP1 C2 may bind to neutral phospholipids such as phosphatidylchloline in the case of cPLA2.

C2 domains are also capable of associating with phosphoinositides involved in signal transduction and membrane traffic [621,627,628]. The X-ray structure of PKCα C2 in complex with Ca^{2+}, phosphoserine and $PI(4,5)P_2$ showed that $PI(4,5)P_2$ bound at the concave surface formed by β3and β4 strands (PDB: 3GPE) [629]. This cluster was named lysine-rich cluster, polybasic cluster, or β -groove. The authors identified six key residues involved in $PI(4,5)P_2$ binding [629]. In a review, Corbalan-Garcia and Gomez-Fernandez [630] compared sequences of different C2 domains and proposed a consensus

PI(4,5)P_2-binding sequence (Y-X-K-Xn-K-X-K-Xn-W-Y/L/C-Xn-N). A few of those C2 domains used in their report also showed up in our VAST search, and using their sequence alignment as a guide, we found that the corresponding PIP_2-binding sequence in SHIP1 C2 does not follow the consensus sequence (**Figure 5.9A**). Also, electrostatic potential calculation shows that SHIP1 C2 has a relatively neutral surface, as compared to the C2 domain PKCα and the C2A domain of rabphilin 3A (**Figure 5.9C**). This observation shows that it is unlikely for PIP_2 to binds to SHIP1 C2 at the nonbasic "β-groove". It is surprising to us, because we have shown that the C2 domain is important for SHIP1's allosteric activation by PI(3,4)P_2 and that it directly interacts with PI(3,4)P_2 [430]. Where PI(3,4)P_2 exactly binds SHIP1 C2 domain remains to be determined.

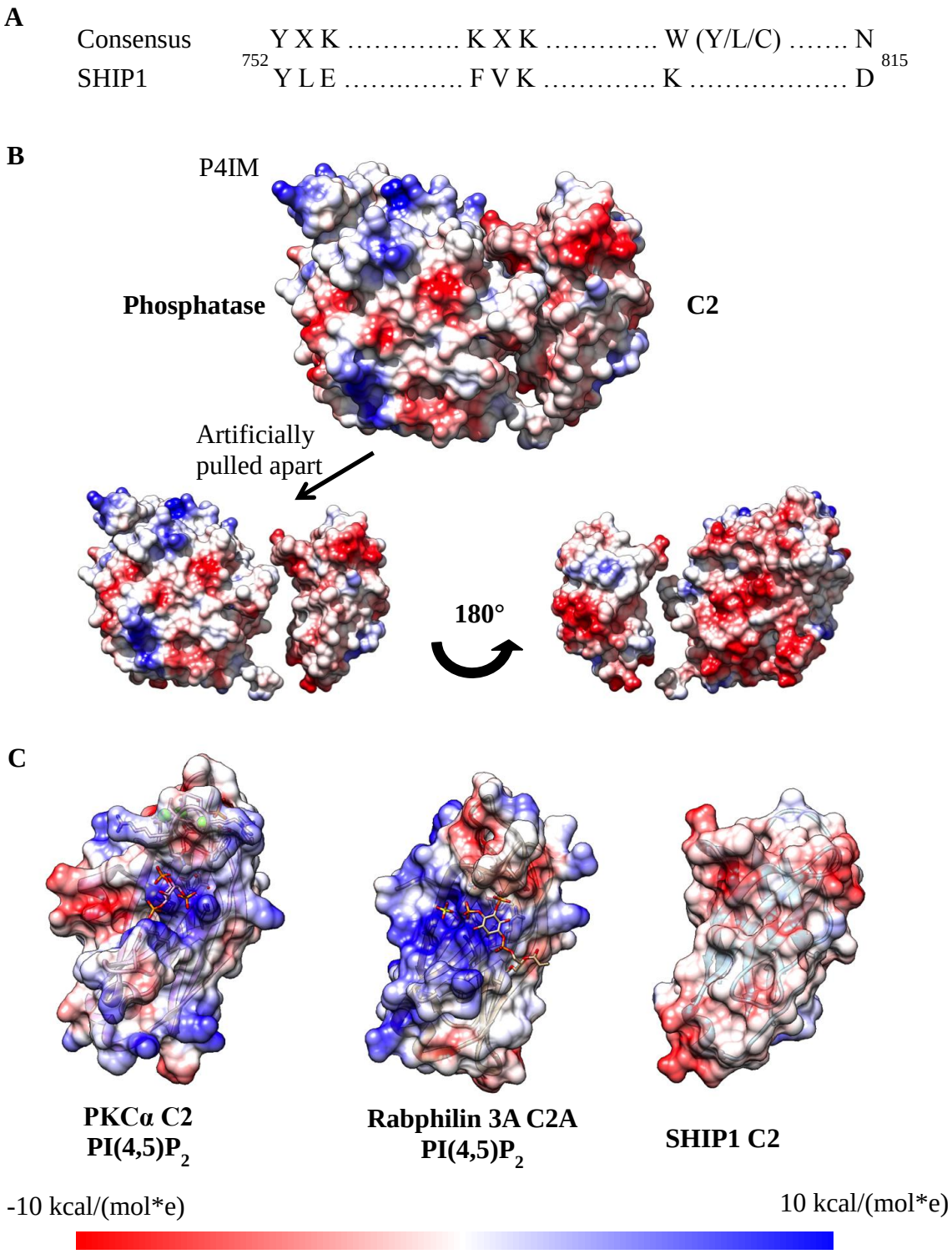

Figure 5.9 SHIP1 C2 domain does not contain the polybasic cluster as other C2 domains.

(A) Comparison of $PI(4,5)P_2$ binding sequences and SHIP1 C2 sequence. (B) The surface of wild type PAC2 structure is coloured according to Coulombic electrostatic potential as calculated by

Chimera. The two domains are artificially pulled apart in the bottom panel. (C) Electrostatic potential of different C2 domains. PKCα C2 structure (PBD:3GPE), rabphilin 3A C2A (PBD:4NS0) and SHIP1 C2, as coloured by Coulombic electrostatic potential calculation by Chimera. Both PKCa C2 and rabphilin 3A C2A are in complex with $PI(4,5)P_2$, as showed as stick representation in the polybasic cluster.

5.2.1.4 Phosphatase-C2 interface

Interface analysis using the PISA server [631] suggests that about 25 residues from each domain participate in domain-domain interaction, burying a surface area of about 900$Å^2$ (**Figure 5.10**). The interface has a hydrophobic core formed between the flexible loops of phosphatase domain (mainly α4-β8 and β9-β10 loops) and β-strands of the C2 domains (β4 and β5). In particular, the α4-β8 loop protrudes out of the phosphates domain and fits quite well into a shallow cavity on the C2 domain (**Figure 5.10B**). In addition, the carboxyl oxygen of Pro684 and Leu685 forms hydrogen bond interactions with the side chain of His804 and Arg826 respectively (**Figure 5.10C**).

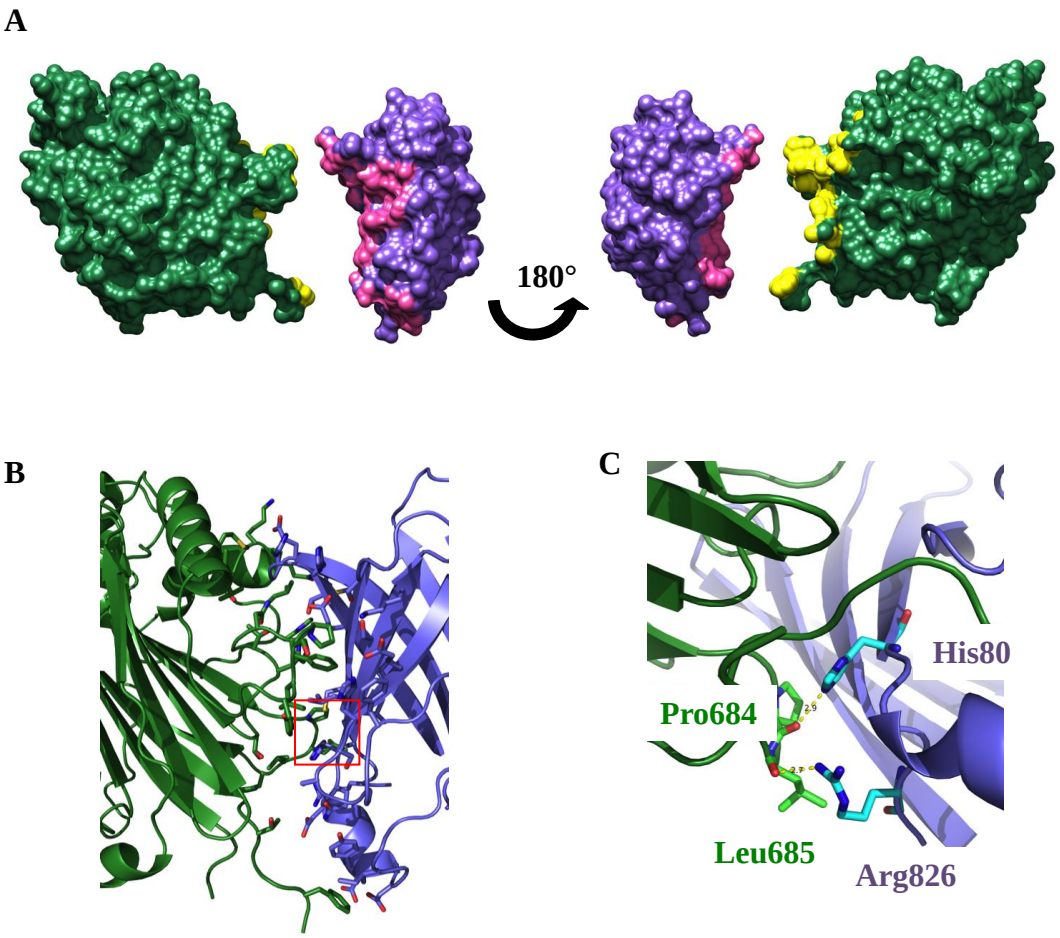

Figure 5.10 The interface between phosphatase domain and C2 domain.
(A) The two domains in wild type PAC2 structure is artificially pulled apart, with phosphatase domain in green and the C2 domain in purple. Interfacing surfaces are colored in yellow or magenta. (B) The residues involved in the interface. Phosphatase domain and C2 domain are shown in green and purple respectively. Interacting residues as predicted by PISA analysis are represented as sticks. The red box shows where the hydrogen bond interactions occur. (C) Hydrogen bond interactions at the interface.

Besides $PI(3,4)P_2$, SHIP1 C2 also contains the binding site for the synthetic SHIP1 activator, AQX-MN100 [430]. Furthermore, AQX-MN100 was found to bind to the same site as $PI(3,4)P_2$, as the addition of AQX-MN100 interfered with C2's ability to bind to $PI(3,4)P_2$ in a protein lipid overlay (PLO) assay [430]. Using the first PAC1cc structure as a docking template, we have predicted two potential AQX-MN100 binding

sites in the structure (**Figure 5.11A-D**), both of which are located at the phosphatase-C2 interface; they are designated as Pocket 1 and Pocket 2 [632]. A number of single mutations have been made in these pockets, and *in vitro* phosphatase assays were performed to assess their ability to be activated by AQX-MN100 (**Figure 5.11E**). Purification of all mutants as an MBP-fusion, except H635A, gave similar yield as wild type protein, indicating that the mutations mostly did not affect the integrity of the protein. These proteins were then tested for their ability to be activated by AQX-MN100 in *in vitro* phosphatase assay as MBP-fusion proteins. A titration of enzyme was first performed to determine the amount of enzymes needed to give half-max activity, as described in Materials and Methods. **Figure 5.11F** shows an immunoblot of the amount of each mutants used in the assays. As shown in **Figure 5.11E**, none of the mutants lost their response to AQX-MN100. Mutant Y683A may be slightly defective in response to AQX-MN100, compared to other mutants, but it was still significantly activated by the ligand. Two possibilities could explain this observation: AQX-MN100 does not bind either of the two sites, or the single mutations are not enough to abolish binding of AQX-MN100. Further experiments with PAC1 mutants containing more than one mutation will be needed to determine which is true.

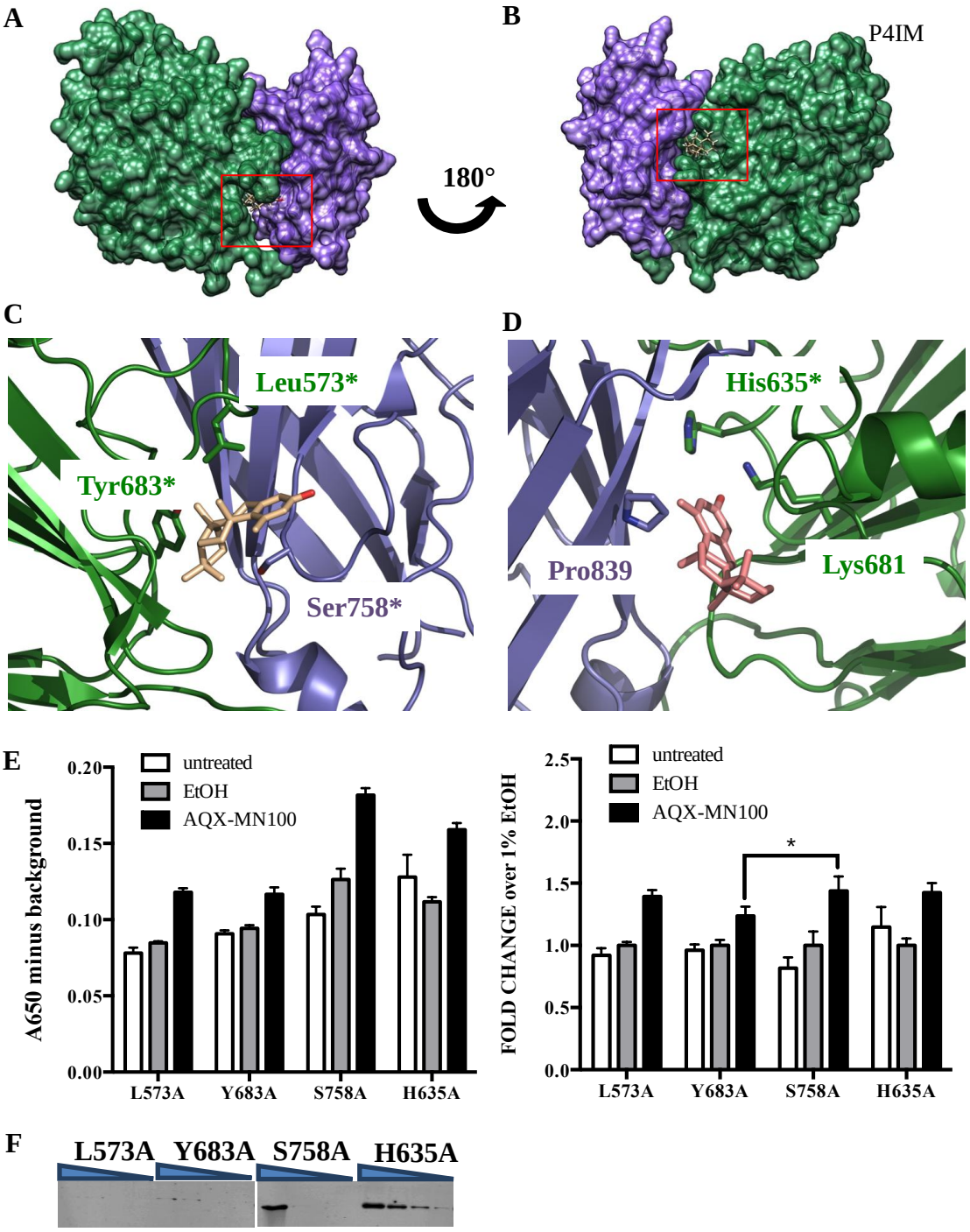

Figure 5.11 Potential AQX-MN100 binding sites in PAC.

(A-B) The locations of AQX-MN100 binding sites are predicted by docking. (C-D) Close-up of Pocket 1 and Pocket 2. Several interacting residues are depicted in stick. Residues indicated with an asterisk are selected for alanine scanning mutagenesis analysis. (E) Recombinant MBP-tagged PAC1 mutants were incubated with 0.2 mM AQX-MN100 or ethanol (solvent control) for 10 minutes at 23°C before incubating with 50 μM IP_4 for 10 minutes at 37°C. The reaction was

stopped by the addition of Malachite Green reagent. Data are presented as background-corrected A650 values (left) or fold change compared to the ethanol treatment (right). Statistical significance of AQX-MN100 response in different mutants was calculated by a two-way ANOVA test with a 95% confidence (*$p < 0.05$). Results were observed in one independent experiment. (F) The amounts of mutant proteins used in the *in vitro* phosphatase assay were detected by immunoblotting with anti-His antibody.

5.2.3 Binding of SHIP1 activators to SHIP1

To characterize the binding of lipid to SHIP1, we employed the protein lipid overlay (PLO) assay [633]. Recombinant His_6-SHIP1 was expressed in HEK293T cells and purified before incubating with PVDF membranes that had been spotted with either PI(3,4)P_2-diC16 or PI(3,4,5)P_3-diC16. Bound protein was then detected by anti-His antibody. As shown in **Figure 5.12A**, His_6-SHIP1 was able to bind to its substrate, PI(3,4,5)P_3. Binding to its product PI(3,4)P_2 is also detected, consistent with previous observation that PI(3,4)P_2 acts as an allosteric activator (**Figure 5.2**) [430]. About five times more PI(3,4)P_2 amounts than PI(3,4,5)P_3 were needed to generate similar protein binding intensity, suggesting that SHIP1 binds to PI(3,4,5)P_3 at a higher affinity than to PI(3,4)P_2. Recombinant His_6-C2 was similarly tested in PLO assay, and we reproduced previous results showing that C2 indeed bound to PI(3,4)P_2 (**Figure 5.12B**) [430]. C2 also bound PI(3,4,5)P_3 seemingly with a higher affinity. The presence of Ca^{2+} ions increased both PI(3,4)P_2 and PI(3,4,5)P_3 binding. PLO assays using PAC were not performed, because His_6-PAC did not express in HEK293T cells, and it was mostly insoluble when expressed in bacteria making it unfeasible to produce enough protein in bacteria.

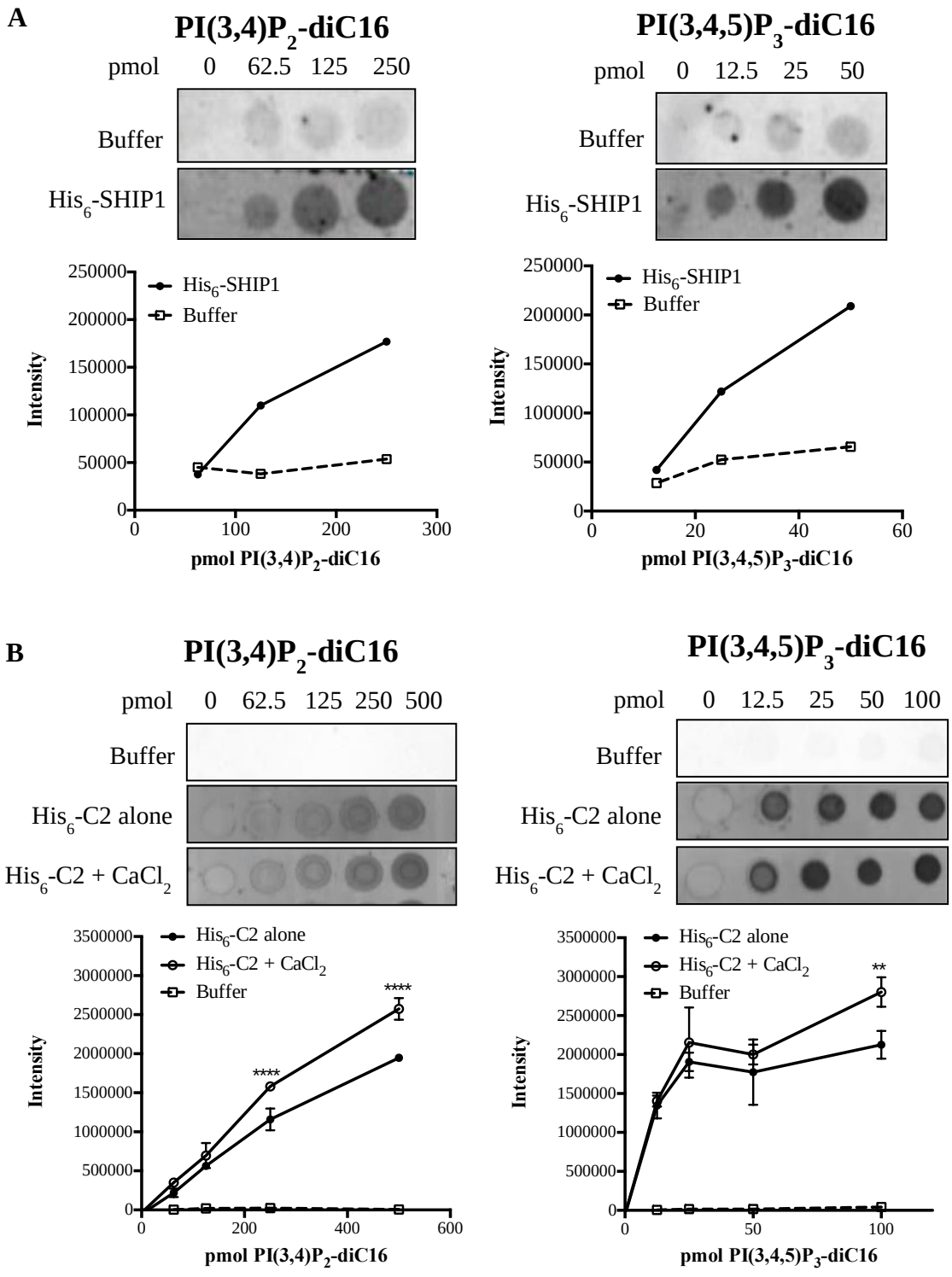

Figure 5.12 SHIP1 binds to both PI(3,4)P_2 and PI(3,4,5)P_3 through its C2 domain. (A) Recombinant His_6-SHIP1 was incubated with PVDF membrane spotted with different amounts of PI(3,4)P_2-diC16 and PI(3,4,5)P_3-diC16 for 5 hours at room temperature. Bound protein was detected by anti-His antibody. The membranes were

scanned with the Odyssey instrument, and the intensities of the spots were quantified using the ImageStudio software. Similar results were observed in at least two independent experiments. (B) Recombinant His_6-C2 was tested in PLO assay in identical condition as (A) except the addition of 2 mM $CaCl_2$ in one of the conditions. Statistical significance between His_6-C2 +/- $CaCl_2$ at individual amount of lipid was calculated by a two-way ANOVA test with a 95% confidence (** $p < 0.01$, **** $p < 0.0001$). Similar results were observed in at least two independent experiments.

We also tested the binding of pelorol-based small molecule SHIP1 activators to SHIP1. However, AQX-MN100 is quite insoluble in aqueous solution and that hinders our ability to measure its binding to SHIP1. We thus used the derivative AQX-151, which is more water-soluble than AQX-MN100, in saturation transfer difference nuclear magnetic resonance (STD-NMR) experiments. The methodology detects protein-ligand interaction by measuring the transfer of magnetization from the protein to the ligand. Only ligands that bind to the protein will give an STD signal. We found that AQX-151 bound to isolated C2 domain, as well as PAC1 (**Figure 5.13A-B**). The transfer was quite strong in the aromatic signals, with weaker transfer in the methyl groups. $PI(3,4)P_2$ also associated with the C2 domain but with weaker signal; all the transfer went into the acryl chains from the terminal methyl groups and along the chain (**Figure 5.13C**). Unfortunately, the experimental set-up does not allow us to detect binding between the head group and the protein. However, given that the STD signal for $PI(3,4)P_2$ was quite weak, it is possible that the major interaction may be mediated by the phosphates in the head group. Controls including $PI(3,4,5)P_3$ and other PIP_2 (that do not activate SHIP1) will be needed to determine if the specific head group dictates the interaction.

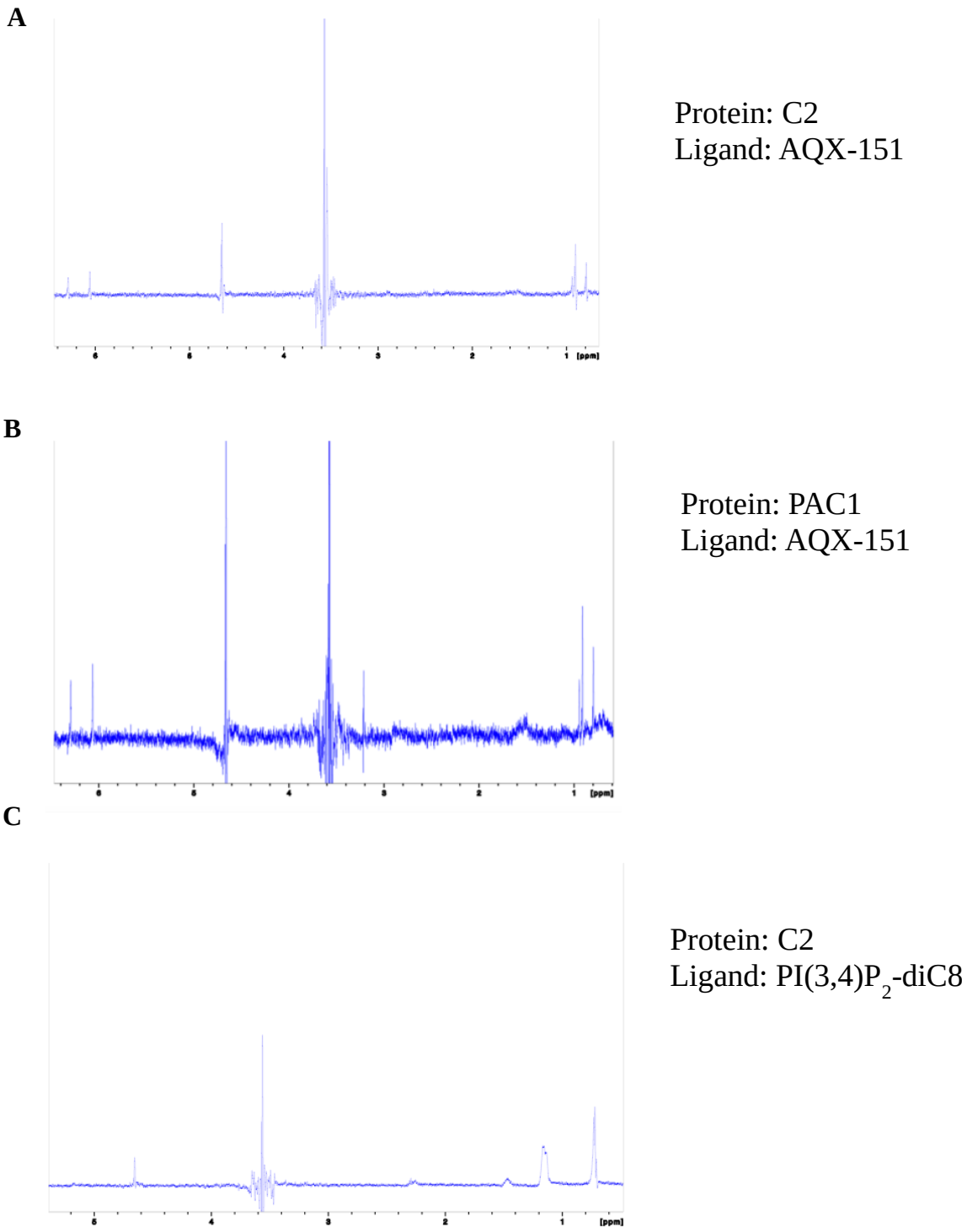

Figure 5.13 Binding of AQX-151 and PI(3,4)P_2 to C2 domain by STD-NMR.
STD-NMR spectra of (A) AQX-151 and isolated C2 domain, (B) AQX-151 and PAC1 in buffer supplemented with 6 mM $MgSO_4$ and (C) PI(3,4)P_2-diC8 and isolated C2 domain.

To obtain quantitative measurement of the protein-ligand interaction, isothermal titration calorimetry (ITC) was used. Both AQX-MN100 and AQX-151 require ethanol or DMSO to dissolve, and thus become unsuitable in ITC experiments. We hence obtained AQX-1125, a completely water-soluble derivative of AQX-MN100. High concentration of AQX-1125 was titrated into either buffer or PAC1, and the measured heat changes were then used to determine the thermodynamic parameters of the protein-ligand interaction. ITC analysis showed no binding of AQX-1125 to PAC1 (**Figure 5.14**); the heat changes generated were identical to AQX-1125 titration into buffer. Similarly, no binding was observed when the natural ligand PI(3,4)P_2-diC8 was titrated into PAC1. This result was unexpected, since PLO assays and STD-NMR clearly showed ligand binding to the protein (either to C2 alone or PAC1). A possibility is that the ligand binding was too weak to be detected by ITC. PIP_2 binding to other proteins have been investigated by ITC, and the K_d values are of the low micromolar range [623,634,635]. These studies all used PIP_2-containing vesicles (with phosphatidylchloline) as the interacting partners, while we purposely used soluble, short chained PI(3,4)P_2 in our ITC experiment. There are caveats in using the different forms of phosphoinositides in *in vitro* binding assays, as discussed by Narayan and Lemmon, and they pointed out that vesicles provide a more representative system of the cellular situation and less prone to artefacts [636]. Also, it has been observed that membrane curvature, in additional to membrane charge, could have an effect in protein membrane, as shown with acyl-CoA binding protein (ACBP) that preferentially interacted with small unilameter vesicles (i.e. highly curved) rather than large unilameter vesicles (i.e. less as curved) [637]. Perhaps the formation of vesicles provide additional (and necessary)

features for protein interaction, and using soluble $PI(3,4)P_2$ in our study may have contributed to our inability to detect $PI(3,4)P_2$ binding to the protein.

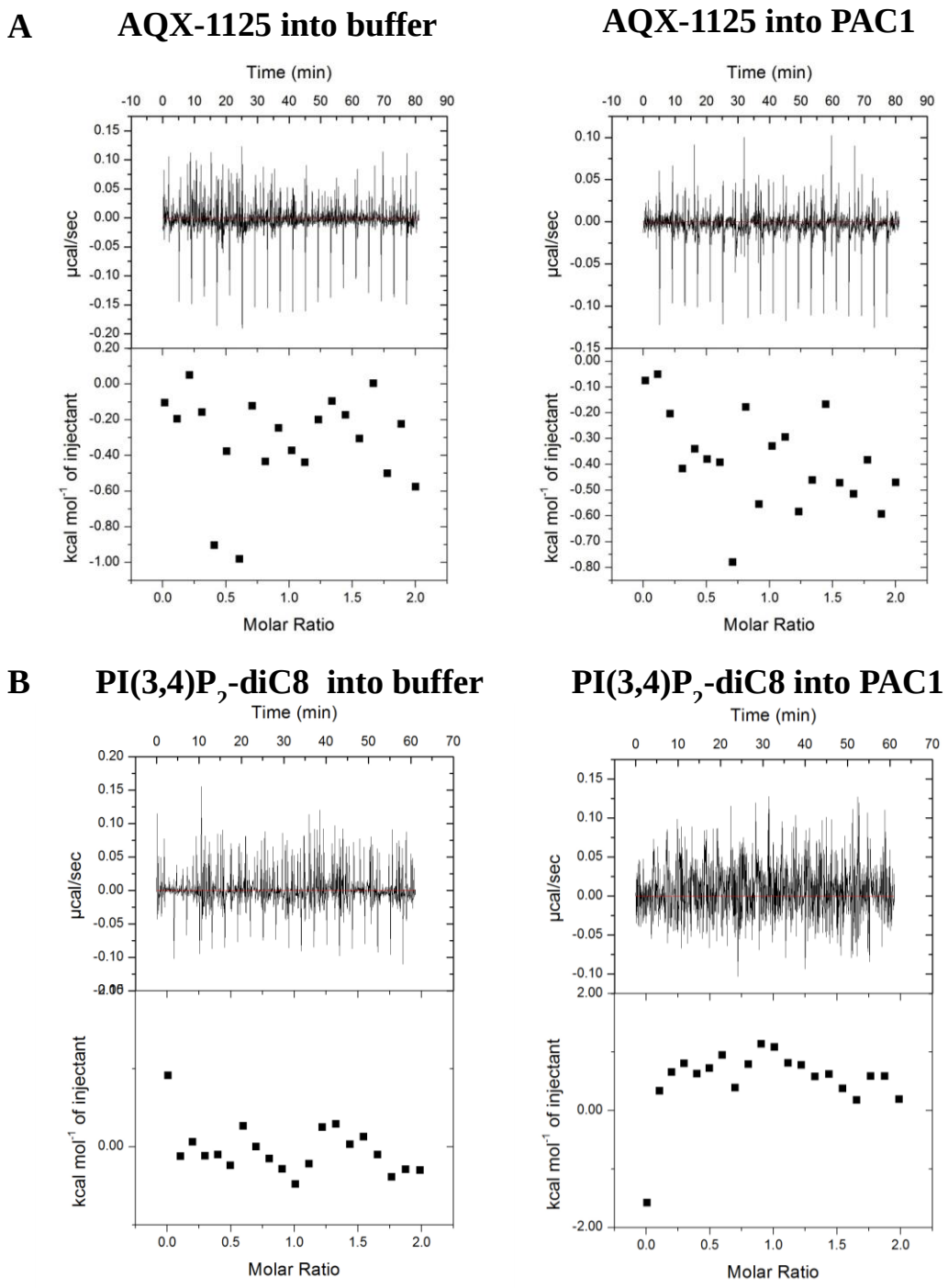

Figure 5.14 No binding of AQX-1125 or $PI(3,4)P_2$-diC8 to PAC1 is detected by ITC. (A) 1 mM of AQX-1125 or (B) 1 mM of $PI(3,4)P_2$-diC8 was titrated into ITC buffer or 0.1 mM PAC1 over the course of 20 injections of 2 µl at 180-second interval at room temperature. Shown are plots of heat produced of each titration.

5.3 Discussion

Phosphoinositides are important in many cellular signalling events. The reversible phosphorylation of the inositol ring is tightly controlled by the activity of inositol kinases and phosphatases. While a large number of drugs have been developed to target inositol kinases such as PI3K, recent studies also focus on the search for drugs that modulate the activity of inositol phosphatases. One example is the development of SHIP2 inhibitors in treating Type 2 diabetes, characterized by insulin resistance and glucose intolerance. SHIP2 is a negative regulator of insulin signalling, which activates the PI3K pathways. Treating diabetic mice with a SHIP2-specific inhibitor (AS1949490) restored insulin signalling and caused significant improvement in glucose tolerance [638]. Thus, drugs targeting inositol phosphatases can be used as an alternative to modulate the PI3K pathway.

SHIP1 is a particularly attractive target in treating hematopoietic malignance, and inflammatory and autoimmune diseases due to its restricted expression in hematopoietic cells. Previous work from our laboratory has found that SHIP1 can be allosterically regulated by its product $PI(3,4)P_2$, and also identified AQX-MN100 as a specific SHIP1 allosteric activator [430]. Domain deletion analysis shows that the PH-R and the C2 domains are required for the allosteric activation. While $PI(3,4)P_2$ can bind to both the PH-R and C2 domains, AQX-MN100 only interacts with the C2 domain [429].

Here, we performed more in-depth studies in the regulation of SHIP1 by its activators. We showed by *in vitro* phosphatase assay that SHIP1 fragment containing only the phosphatase and C2 domains (aka PAC), but not the PH-R domain, corresponds to the minimal enzyme (**Figure 5.1**). PAC was activated by $PI(3,4)P_2$ or AQX-MN100

equally well compared to full length SHIP1, which tends to discount a role of PH-R domain in SHIP1 allosteric activation. This observation seemed surprising at first, because SHIP1 enzyme lacking PH-R domain (SHIP1 ΔPH-R) showed inability to be activated by both activators, even though SHIP1 ΔPH-R retains enzymatic activity. However, deleting an entire domain may potentially alter the folding of the protein outside of the phosphatase domain. In fact, when comparing the enzyme kinetic parameters of PAC to PPAC, which contains the PH-R domain, PAC showed a lower V_{max} value but similar K_m value (**Figure 5.1**). The lack of PH-R domain showed a similar effect on enzyme activity as a noncompetitive inhibitor would, suggesting that the conformation of the enzyme may have changed in the absence of PH-R domain. Worthy of note is that PH-R domain has a high affinity to PI(3,4,5)P_3 (and a lesser affinity to PI(3,4)P_2), and recruits SHIP1 to the plasma membrane [429]. Point mutations in the PH-R domain (K370A/K397A) reduced both PI(3,4,5)P_3 and PI(3,4)P_2 binding, but full length SHIP1 containing these mutations has indistinguishable allosteric activation profile as wild type SHIP1 [429]. It is consistent with present data showing only the C2 domain is needed for allosteric activation. Yet, even though PI(3,4)P_2 was shown to bind to C2 domain by PLO assay (**Figure 5.12**) and STD-NMR (**Figure 5.14**), we were unable to measure the affinity of PI(3,4)P_2 to PAC by ITC or obtain a co-crystal structure of PI(3,4)P_2-PAC, suggesting that PI(3,4)P_2 affinity to PAC is very weak, with K_d value likely above high micromolar range. That leads to the hypothesis that PH-R domain may facilitate PI(3,4)P_2 binding to the enzyme even though it does not participate in allosteric regulation.

Structures of SHIP1 phosphatase and C2 domains reveal a few differences from other 5'-phosphatases at the enzyme active site. The first difference is a longer P4IM loop in SHIP1 (and SHIP2) that may explain the strong preference of 3-P in the enzyme substrate. Arg668 and Asn670, especially Arg668, could potentially be the driving force for this preference. The second difference lies in the region that binds to the aliphatic region of the substrate, LC1R and LC2R loops. SHIP1 lacks the LC1R loop that contains multiple hydrophobic residues necessary for substrate interaction. SHIP1 maintains a LC2R that could interact with the lipid. Additional tryptophan residues (Trp489 and Trp600) may also facilitate membrane interaction. It is also likely that SHIP1 phosphatase domain does not interact with the membrane as extensively as the other 5-phosphatases. SHIP1 is a multi-domain protein, and other domains in SHIP1 might have a bigger role in membrane binding. For example, the SH2 domain in the N-terminal end or the NPXY motifs at the C-terminal end mediate membrane recruitment indirectly via transmembrane receptor proteins, or adaptor proteins such as Shc and Dok [426]. The PH-R domain directly interacts with the $PI(3,4,5)P_3$ and is necessary for SHIP1 recruitment to the phagocytic cup [429].

PTEN is another phosphatase that contains a C2 domain, adjacent to its phosphatase domain, that is necessary for its membrane interaction and its biological functions [639]. The PTEN C2 domain resides right next to the active site, and contains two basic regions, one at the CBR3 and one at the α-helix next to the CBRs, that target PTEN to the membrane and position the active site to its substrate within the membrane. However, our structure showed that the SHIP1 C2 domain lacks both of these basic regions and it also interacts with the phosphatase domain away from the active site.

Since the SHIP1 C2 domain has a relatively neutral surface, it likely does not interact with the positively charged head group of PIPs, but we cannot exclude the possibility that the C2 domain may interact with lipids via hydrophobic interaction instead of electrostatic interactions. Whether the SHIP1 C2 domain could serve as the membrane interacting domain of SHIP1 inside the cells remains to be elucidated. Regardless, the C2 domain is certainly important in the catalytic activity of the enzyme (in addition to its role in binding allosteric activators) by facilitating lipid binding, providing structural integrity, or both. The isolated phosphatase domain has surprisingly low activity (data not shown), while the PAC construct is fully functional, compared to the full-length protein (**Figure 5.1**).

Our structure showed that the SHIP1 C2 domain, unlike other C2 domains, lacks the binding site for Ca^{2+}, but PLO assays showed that Ca^{2+} enhances binding of $PI(3,4)P_2$ to the C2 domain. However, we need to interpret these results carefully. The isolated C2 domain, although soluble, exists as a higher order oligomer (likely a dimer) in solution according to its size exclusion profile. The lack of other domains could potentially expose hidden hydrophobic surfaces that is now accessible to interact with each other, or with other molecules such as lipids. Electrostatic potential representation of the C2 domain shows that it is highly hydrophobic (**Figure 5.9**). Moreover, the addition of Ca^{2+} in the assay increases the ionic strength of the PLO buffer, potentially driving the interaction between hydrophobic surface of the C2 domain and the hydrophobic lipid chain of $PI(3,4)P_2$. Nevertheless, Ca^{2+} appears to associate with SHIP1/PAC and inhibit its enzymatic activity (**Figure 5.2**). This inhibitory effect of Ca^{2+} is also seen in SPsynaptojanin, an archetypal inositol 5'-phosphatase [615]. In this case, Ca^{2+} acts as a

competitive inhibitor of Mg^{2+} that is required for 5'-phosphatase activity. The crystal structure of SPsynanptojanin shows that a Ca^{2+} ion actually occupies the active site [640]. Our data also support the association of Ca^{2+} ion(s) to the SHIP1 phosphatase domain. The physiological basal concentration of Ca^{2+} is very low compared to the level used in the *in vitro* phosphatase assay (<100 nM in the cytoplasm of resting cells vs 2 mM). A titration of $CaCl_2$ showed that SHIP1 enzyme activity was not affected at concentration lower than 2 mM $CaCl_2$ (data not shown), showing that the low resting concentration of Ca^{2+} inside the cells likely would have no effect on SHIP1 activity. Upon specific extracellular signals, intracellular Ca^{2+} level may rise up to 0.5 to 1 mM [641], and some proteins such as PI3K require elevated Ca^{2+} for activity [642,643]. Whether SHIP1 is regulated similarly by Ca^{2+} level inside the cell remains to be determined.

In summary, we have described the structure of the SHIP1 phosphatase domain and C2 domain for the first time. The SHIP1 C2 domain, although structurally similar to other C2 domains, contains unique features that may exert different functional roles from other C2 domains. Being an allosterically activated enzyme with the C2 domain as the binding site of allosteric modulators, this structure of SHIP1 will certainly aid in the development of drugs (either activators or inhibitors) in treating different immune disorders. For example, we have determined possible sites for AQX-MN100 binding by ligand-docking approach (Pocket 1: L573, Y683, S758, and Pocket 2: H635, K681, P839). While we still need further experiments to fully determine the ligand-interacting residues and the binding mechanism, we are confident that it can be done. A protein structure can be used *in silico* to screen for potential enzyme modulators [644,645]. Unfortunately, this kind of screening can only be performed once we have determined the

binding site of at least one ligand, either by structural analysis or site-directed mutagenesis approach. Usually, the *in silico* identified modulators interact with the active site to prevent access of the substrate or interfere with catalysis [646]. By comparing structures of related proteins (e.g. SHIP2 structure in complex with its inhibitor [616]) and identifying the differences, specific drugs that only affect selected proteins can be designed. However, functionally related enzymes usually have similar active sites, and thus the specificity of these active site modulators can be compromised. Thus, once we determine the allosteric regulator binding site in SHIP1/PAC, we will be able to screen for other potential allosteric regulators [647].

Chapter 6: Conclusions

6.1. Conclusions

This thesis investigated the role of STAT3 and SHIP1 in IL-10 regulation of activated macrophages. The importance of STAT3, SHIP1 and IL-10 in immune function has been shown biologically with knockout models, and through observed deficiencies in these proteins in human inflammatory diseases [382-384,403,502,648,649]. Thus, understanding how the mechanisms by which STAT3 and SHIP1 mediate IL-10 action will be beneficial in developing therapeutics to treat inflammatory diseases.

Since the discovery of IL-10 about two decades ago, a large number of studies have been published that support a model in which STAT3 is the dominant downstream molecule in IL-10 signalling and that STAT3 inhibits inflammation by inducing the expression of specific gene products. Some investigators even believed that STAT3 was the sole mediator of IL-10 signalling [374]. However, work from previous members from our laboratory has shown that while STAT3 is essential for IL-10's inhibition of immune cell activation, the 5'- phosphatase SHIP1 is also required, and that SHIP1 can regulate gene expression through transcriptional and post-transcriptional controls [56,376]. Our work favours a revised model in which both SHIP1 and STAT3 mediates the anti-inflammatory response of IL-10.

The findings presented in this thesis expand our understanding of IL-10 signalling and regulation. In Chapter 3, we examined IL-10 regulation of a particular miRNA, miR-155, in activated macrophages. miRNAs are indispensable in the development and function of the immune system as indicated by the fact that knocking out Dicer in mice causes embryonic lethality [258]. A growing number of miRNAs have been implicated

in different human diseases. We chose to focus on miR-155 due to its high expression in immune cells and its multiple roles in immune cell function. Kinetics studies show that LPS treatment induces pri-miR-155 transcription followed by maturation into functional miR-155, and that IL-10 inhibited pri-miR-155 expression at 1 hour and mature miR-155 expression at 4 hours. Interestingly, pri-miR-155 is transcribed constitutively in resting cells, but its expression level is greatly enhanced in the presence of LPS. Luciferase reporter assays show that both LPS and IL-10 does not affect pri-miR-155 transcription during the course of our experiments. These results prompted us to speculate that pri-miR-155 is being made at all times with its level kept low through some kind of degradation mechanism, but in the presence of an immune stimulus such as LPS, the degradation mechanism is removed and maturation into miR-155 begins. However, IL-10 switches on the degradation mechanism again to remove pri-miR-155, as well as interferes with the maturation process to prevent the generation of mature miR-155. We also found that the regulatory step exists between pre-miR-155 and mature miR-155. These observations open up a few questions that warrant further investigation. What factors are involved in maintaining the resting state of pri-miR-155 level and how do they function? Which of these factors do LPS and IL-10 regulate to convert pre-miR-155 to mature miR-155? To identify the factors that regulate pri-/pre-miR-155 RNA stability and the maturation step, RNA pulldown using pre-miR-155 oligo in combination with mass spectrometry analysis will reveal RNA binding proteins that bind to pre-miR-155. By comparing the differential binding pattern in unstimulated, LPS stimulated, and LPS+IL-10 stimulated cells, the proteins that regulate miR-155 maturation can be

identified. Validation experiments will include overexpression and knockdown of the candidate proteins, and measuring miR-155 level upon LPS and LPS+IL-10 treatment.

We also found that miR-155 expression is regulated by both SHIP1 and STAT3. Their contributions appear additive, but we unexpectedly found that the SHIP1 activator, AQX-MN100 is by itself sufficient to mimic the inhibitory effect of IL10 on miR-155 expression. That may seem surprising at first, because STAT3 is not activated (defined by the absence of phosphorylation at Y705) by treatment of cells with AQX-MN100. It is possible that activated SHIP1 (either by IL-10 or AQX-MN100) may modulate STAT3 activity independent of STAT3 phosphorylation, or that unphosphorylated STAT3 is still active in gene regulation (see discussion below). Lastly, miR-155 is only one of the many miRNAs involved in macrophage activation. Expanding our research to other miRNAs, for example through microarray analysis or other high-throughput approaches, will complement our current understanding of IL-10 regulation of miRNAs.

Having observed SHIP1 and STAT3 cooperativity in mediating IL-10 suppression of TNFα [376] and miR-155 (Chapter 3) [375], in Chapter 4, we investigated the role of SHIP1 and STAT3 on IL-10 regulation in gene expression globally. Using microarray analysis, we compared the gene expression profiles from either SHIP1 WT or SHIP1 KO macrophages stimulated with LPS or LPS+IL-10, and then identified a subset of genes that were regulated by IL-10 in a SHIP1-dependent manner. Both upregulated and downregulated genes were observed. Preliminary real time PCR experiments of selected genes show that many of the SHIP1-regulated genes are also regulated by STAT3, but we also identified a few genes that only required SHIP1 or STAT3 to be regulated by IL-10.

Thus, future experiments will include validating more candidate genes identified in our microarray studies. Besides determining mRNA levels of these genes from WT, SHIP1 KO and STAT3 KO macrophages that are stimulated by LPS +/- IL-10, it is also important to determine protein levels through immunoblot analyses. A time-course experiment will provide evidence on the kinetics of the regulation. Once validation is completed, the next question is whether the regulation of the validated genes is at the transcriptional level or post-transcriptional level. These can be examined via the use of luciferase reporters harbouring either the promoter region or the 3'-UTR. Also, we previously show that SHIP1 mediated IL-10 inhibition of TNFα translation without affecting its transcription [56]. SHIP1 may regulate the newly validated genes through similar mechanism, and that can be examined by determining the level of actively translated mRNA in SHIP1 WT and SHIP1 KO cells after IL-10 treatment. Similar experiments should be performed in STAT3 WT and STAT3 KO to elucidate the role of STAT3 in the regulation of these genes. STAT3 is a well-established transcription factor, and activates gene expression at the transcription level. However, a non-transcriptional role has been described for STAT3 in different cancer cells, including regulating DNA methyltransferase 1 (DNMT1) binding to gene promoters to induce promoter methylation, which causes repression of gene expression [650,651]. This activity of STAT3 requires acetylation at Lys685 but not phosphorylation [650,651]. Whether IL-10 induces STAT3 acetylation, and whether this acetylation is important for IL-10 function will require further investigation.

The results in our studies thus far support a model in which SHIP1 and STAT3 work together to mediate IL-10 function, and we have examined the possibility that

SHIP1 and STAT3 form a signalling complex. While we were not able to observe physical interaction between SHIP1 and STAT3, we cannot exclude that they may interact through a third protein. In addition, the SHIP1 activator, AQX-MN100 has been shown to inhibit TNFα [376] and miR-155 (Chapter 3) [375] even in the absence of STAT3 activation (STAT3 phosphorylated at Y705). Previous reports have shown that unphosphorylated STAT3 could also regulate gene expression upon cytokine stimulation [652,653]. These unphosphorylated STAT3 molecules can form dimers or remain as monomer to activate gene expression [654], or interact with the NFκB p65 homodimer and interfere with gene expression [655]. It is possible that SHIP1 works with unphosphorylated STAT3 to modulate gene expression. In support of this idea, we found that AQX-MN100 was able to cause nuclear translocation of STAT3 within 20 minutes (data not shown). If this hypothesis is correct, a STAT3 Y705 mutant will still be able to regulate gene expression in the presence of AQX-MN100. Furthermore, SHIP1 can act as an enzyme as well as a scaffold protein, and the use of an inactive enzyme in our cell-based assays will distinguish whether the activity of SHIP1 is due to its catalytic activity or the proteins that it recruits.

As described in Chapters 3 and 4, I have studied IL-10 regulation of miRNAs and mRNAs separately. The next step would be to generate an IL-10 regulated miRNA-mRNA interaction network to gain insight into how miRNAs and mRNAs interact to mediate IL-10 function [656]. Analysis of SHIP1 WT and SHIP1 KO or STAT3 WT and STAT3 KO macrophages stimulated with LPS +/- IL-10 may reveal the specific IL-10 regulated miRNA-mRNA network mediated by SHIP1, STAT3, or SHIP1 and STAT3.

Given the importance of SHIP1 in IL-10 signalling, and that SHIP1 activation by small molecule agonist, AQX-MN100, can mimic IL-10 biological function both *in vitro* [56,375] and *in vivo* [376], we investigated the structural basis of the interaction between SHIP1 and its activators in Chapter 5. We described a minimal enzyme composing only the phosphatase domain and the C2 domain, namely PAC. The PAC enzyme has similar enzymatic properties to full length SHIP1, as assessed by *in vitro* phosphatase assay. Our laboratory has previously identified the C2 domain as the binding site of SHIP1 agonists including AQX-MN100, and the SHIP1 product $PI(3,4)P_2$ [430]. Besides its role in allosteric regulation, we found that C2 domain may also provide additional support to the phosphatase domain for catalysis, since an isolated phosphatase domain has very low enzymatic activity. From the crystal structure of PAC, we found that the phosphatase domain and the C2 domain interact via a large interface, and that the C2 domain is located away from the active site. The phosphatase domain resembles previously described structures of other inositol 5'-phosphatases, especially that of SHIP2. Differences at the active site may explain the substrate preference of the different phosphatases, as well as requirement of the other domains in the proteins. Comparison to other C2 domains reveal that SHIP1 C2 domain lacks the basic loops at the top of the domain for Ca^{2+} binding and phospholipid binding, as well as the polybasic groove made up by two β-strands at the side of the structure for PIP binding. Surprisingly, while we observed $PI(3,4)P_2$ binding to isolated C2 domains via PLO and STD-NMR, we did not find potential binding pockets in the structure of the C2 domain. Similarly, STD-NMR studies showed that AQX-151, a derivative of AQX-MN100, is able to interact with C2 and PAC but we have not been able to obtain crystals of PAC containing either PIP2 or

AQX-151. We have attempted to obtain a ligand-PAC crystal structure either by soaking apo-PAC crystals in ligand-containing solution or by screening for new crystallization conditions. However, our efforts have been fruitless. Perhaps the binding of ligand has drastically changed the conformation of PAC and thus none of the conditions screened was the right condition to crystallize the complex, or the ligand-bound protein is too flexible for crystallization. It is also possible that the binding affinity of the ligands is too weak or too unstable for crystallization. Alternatively, NMR can be employed. Our initial STD-NMR experiments showed that $PI(3,4)P_2$ and AQX-151 interacted with both the isolated C2 domain and the PAC protein. Further experiments will validate this finding and also identify the interacting determinants on the ligands. It may give us more insight on the type of interactions, and thus the type of amino acid residues, involved. Using a site-directed mutagenesis approach, we can screen for the exact amino acid residues that interact with the lipid. Other types of NMR (e.g. ^{13}C-^{15}N-NMR) may also be used for identification of ligand-interacting residues on the protein. However, due to the size limitation on NMR, only the isolated C2 domain can be tested in this type of experiment. Since these ligands are allosteric regulators, they likely regulate enzyme activity by inducing conformational changes. In this case, small-angle x-ray scattering (SAXS) may be useful to detect these large structural changes by comparing the apo-PAC and the ligand-bound PAC. While this method will not directly identify the ligand-interacting residues, it may reveal the approximate binding location of ligands on the protein. Combining this information into our crystal structure may aid in pinpointing candidate residues important in ligand binding.

In summary, the data presented in this thesis has provided more insight into SHIP1's participation in IL-10 signalling and functions. This STAT3-independent pathway opens up a new field of research into treating inflammatory diseases, especially with the development of small molecule SHIP1 activators. The crystal structure of PAC (composing the minimal allosteric regulated region of SHIP1) reveals the unique features of the two domains for the first time. Once the details of ligand association are delineated, this structure will aid in the development of SHIP1 modulators that have clinical application, and serves as research tools in understand the molecular basis of regulation in SHIP1 and related proteins.

References

[1] Majno, G. (1975) The healing hand : man and wound in the ancient world, Harvard University Press. Cambridge, Mass.

[2] Rather, L.J. (1971). Disturbance of function (functio laesa): the legendary fifth cardinal sign of inflammation, added by Galen to the four cardinal signs of Celsus. Bull N Y Acad Med 47, 303-22.

[3] Sakamoto, N. *et al.* (2005). Dietary risk factors for inflammatory bowel disease: a multicenter case-control study in Japan. Inflamm Bowel Dis 11, 154-63.

[4] Burisch, J. *et al.* (2014). Environmental factors in a population-based inception cohort of inflammatory bowel disease patients in Europe--an ECCO-EpiCom study. J Crohns Colitis 8, 607-16.

[5] Ananthakrishnan, A.N. *et al.* (2014). Long-term intake of dietary fat and risk of ulcerative colitis and Crohn's disease. Gut 63, 776-84.

[6] Lee, W.R. (2000). The changing demography of diabetes mellitus in Singapore. Diabetes Res Clin Pract 50 Suppl 2, S35-9.

[7] Matsuoka, K. (2000). Genetic and environmental interaction in Japanese type 2 diabetics. Diabetes Res Clin Pract 50 Suppl 2, S17-22.

[8] Pickup, J.C. (2004). Inflammation and activated innate immunity in the pathogenesis of type 2 diabetes. Diabetes Care 27, 813-23.

[9] Gregor, M.F. and Hotamisligil, G.S. (2011). Inflammatory mechanisms in obesity. Annu Rev Immunol 29, 415-45.

[10] Barry, J.C., Shakibakho, S., Durrer, C., Simtchouk, S., Jawanda, K.K., Cheung, S.T., Mui, A.L. and Little, J.P. (2016). Hyporesponsiveness to the anti-inflammatory action of interleukin-10 in type 2 diabetes. Sci Rep 6, 21244.

[11] Medzhitov, R. (2010). Inflammation 2010: new adventures of an old flame. Cell 140, 771-776.

[12] Medzhitov, R. and Janeway, C. (2000). Innate immunity. N Engl J Med 343, 338-44.

[13] Medzhitov, R. and Janeway, C.A. (1998). Innate immune recognition and control of adaptive immune responses. Semin Immunol 10, 351-3.

[14] Leavy, O. (2015). Innate immunity: New PAMP discovered. Nat Rev Immunol 15, 402-3.

[15] Gallucci, S. and Matzinger, P. (2001). Danger signals: SOS to the immune system. Curr Opin Immunol 13, 114-9.

[16] Bianchi, M.E. (2007). DAMPs, PAMPs and alarmins: all we need to know about danger. J Leukoc Biol 81, 1-5.

[17] Kono, H. and Rock, K.L. (2008). How dying cells alert the immune system to danger. Nat Rev Immunol 8, 279-89.

[18] McEver, R.P. and Zhu, C. (2010). Rolling cell adhesion. Annu Rev Cell Dev Biol 26, 363-96.

[19] Wong, C.H., Heit, B. and Kubes, P. (2010). Molecular regulators of leucocyte chemotaxis during inflammation. Cardiovasc Res 86, 183-91.

[20] Imhof, B.A. and Aurrand-Lions, M. (2004). Adhesion mechanisms regulating the migration of monocytes. Nat Rev Immunol 4, 432-44.

[21] Headland, S.E. and Norling, L.V. (2015). The resolution of inflammation: Principles and challenges. Semin Immunol 27, 149-60.

[22] Serhan, C.N. and Savill, J. (2005). Resolution of inflammation: the beginning programs the end. Nat Immunol 6, 1191-7.

[23] Marshall, J.C. (2001). Inflammation, coagulopathy, and the pathogenesis of multiple organ dysfunction syndrome. Crit Care Med 29, S99-106.

[24] Bosmann, M. and Ward, P.A. (2013). The inflammatory response in sepsis. Trends Immunol 34, 129-36.

[25] Neurath, M.F. (2014). Cytokines in inflammatory bowel disease. Nat Rev Immunol 14, 329-42.
[26] McInnes, I.B. and Schett, G. (2007). Cytokines in the pathogenesis of rheumatoid arthritis. Nat Rev Immunol 7, 429-42.
[27] Tedgui, A. and Mallat, Z. (2006). Cytokines in atherosclerosis: pathogenic and regulatory pathways. Physiol Rev 86, 515-81.
[28] Ramji, D.P. and Davies, T.S. (2015). Cytokines in atherosclerosis: Key players in all stages of disease and promising therapeutic targets. Cytokine Growth Factor Rev 26, 673-85.
[29] Iwami, K.I., Matsuguchi, T., Masuda, A., Kikuchi, T., Musikacharoen, T. and Yoshikai, Y. (2000). Cutting edge: naturally occurring soluble form of mouse Toll-like receptor 4 inhibits lipopolysaccharide signaling. J Immunol 165, 6682-6.
[30] Kitchens, R.L., Thompson, P.A., Viriyakosol, S., O'Keefe, G.E. and Munford, R.S. (2001). Plasma CD14 decreases monocyte responses to LPS by transferring cell-bound LPS to plasma lipoproteins. J Clin Invest 108, 485-93.
[31] Raby, A.C. *et al.* (2009). Soluble TLR2 reduces inflammation without compromising bacterial clearance by disrupting TLR2 triggering. J Immunol 183, 506-17.
[32] Turer, E.E. *et al.* (2008). Homeostatic MyD88-dependent signals cause lethal inflamMation in the absence of A20. J Exp Med 205, 451-64.
[33] Kobayashi, K., Hernandez, L.D., Galán, J.E., Janeway, C.A., Medzhitov, R. and Flavell, R.A. (2002). IRAK-M is a negative regulator of Toll-like receptor signaling. Cell 110, 191-202.
[34] Ajibade, A.A. *et al.* (2012). TAK1 negatively regulates NF-κB and p38 MAP kinase activation in Gr-1+CD11b+ neutrophils. Immunity 36, 43-54.
[35] Kuwata, H., Matsumoto, M., Atarashi, K., Morishita, H., Hirotani, T., Koga, R. and Takeda, K. (2006). IkappaBNS inhibits induction of a subset of Toll-like receptor-dependent genes and limits inflammation. Immunity 24, 41-51.
[36] Kuwata, H., Watanabe, Y., Miyoshi, H., Yamamoto, M., Kaisho, T., Takeda, K. and Akira, S. (2003). IL-10-inducible Bcl-3 negatively regulates LPS-induced TNF-alpha production in macrophages. Blood 102, 4123-9.
[37] Oganesyan, G., Saha, S.K., Guo, B., He, J.Q., Shahangian, A., Zarnegar, B., Perry, A. and Cheng, G. (2006). Critical role of TRAF3 in the Toll-like receptor-dependent and -independent antiviral response. Nature 439, 208-11.
[38] Xiao, N., Li, H., Luo, J., Wang, R., Chen, H., Chen, J. and Wang, P. (2012). Ubiquitin-specific protease 4 (USP4) targets TRAF2 and TRAF6 for deubiquitination and inhibits TNFα-induced cancer cell migration. Biochem J 441, 979-86.
[39] Phillips, K., Kedersha, N., Shen, L., Blackshear, P.J. and Anderson, P. (2004). Arthritis suppressor genes TIA-1 and TTP dampen the expression of tumor necrosis factor alpha, cyclooxygenase 2, and inflammatory arthritis. Proc Natl Acad Sci U S A 101, 2011-6.
[40] Saijo, K., Winner, B., Carson, C.T., Collier, J.G., Boyer, L., Rosenfeld, M.G., Gage, F.H. and Glass, C.K. (2009). A Nurr1/CoREST pathway in microglia and astrocytes protects dopaminergic neurons from inflammation-induced death. Cell 137, 47-59.
[41] Honma, K. *et al.* (2005). Interferon regulatory factor 4 negatively regulates the production of proinflammatory cytokines by macrophages in response to LPS. Proc Natl Acad Sci U S A 102, 16001-6.
[42] Esser, C., Rannug, A. and Stockinger, B. (2009). The aryl hydrocarbon receptor in immunity. Trends Immunol 30, 447-54.
[43] Carrick, D.M., Lai, W.S. and Blackshear, P.J. (2004). The tandem CCCH zinc finger protein tristetraprolin and its relevance to cytokine mRNA turnover and arthritis. Arthritis Res Ther 6, 248-64.

[44] Whitmore, M.M., Iparraguirre, A., Kubelka, L., Weninger, W., Hai, T. and Williams, B.R. (2007). Negative regulation of TLR-signaling pathways by activating transcription factor-3. J Immunol 179, 3622-30.
[45] Hutchins, A.P., Poulain, S. and Miranda-Saavedra, D. (2012). Genome-wide analysis of STAT3 binding in vivo predicts effectors of the anti-inflammatory response in macrophages. Blood 119, e110-9.
[46] Schaljo, B. *et al.* (2009). Tristetraprolin is required for full anti-inflammatory response of murine macrophages to IL-10. J Immunol 183, 1197-206.
[47] Katsanou, V., Papadaki, O., Milatos, S., Blackshear, P.J., Anderson, P., Kollias, G. and Kontoyiannis, D.L. (2005). HuR as a negative posttranscriptional modulator in inflammation. Mol Cell 19, 777-89.
[48] Curtale, G., Mirolo, M., Renzi, T.A., Rossato, M., Bazzoni, F. and Locati, M. (2013). Negative regulation of Toll-like receptor 4 signaling by IL-10-dependent microRNA-146b. Proc Natl Acad Sci U S A 110, 11499-504.
[49] Sheedy, F.J. *et al.* (2010). Negative regulation of TLR4 via targeting of the proinflammatory tumor suppressor PDCD4 by the microRNA miR-21. Nat Immunol 11, 141-7.
[50] Sharma, A.R., Sharma, G., Lee, S.-S. and Chakraborty, C. (2016). miRNA-Regulated Key Components of Cytokine Signaling Pathways and Inflammation in Rheumatoid Arthritis. Medicinal Research Reviews, n/a-n/a.
[51] Colotta, F., Saccani, S., Giri, J.G., Dower, S.K., Sims, J.E., Introna, M. and Mantovani, A. (1996). Regulated expression and release of the IL-1 decoy receptor in human mononuclear phagocytes. J Immunol 156, 2534-41.
[52] Wilson, M.S. *et al.* (2007). IL-13Ralpha2 and IL-10 coordinately suppress airway inflammation, airway-hyperreactivity, and fibrosis in mice. J Clin Invest 117, 2941-51.
[53] Perrier, S., Darakhshan, F. and Hajduch, E. (2006). IL-1 receptor antagonist in metabolic diseases: Dr Jekyll or Mr Hyde? FEBS Lett 580, 6289-94.
[54] Schottelius, A.J., Mayo, M.W., Sartor, R.B. and Baldwin, A.S. (1999). Interleukin-10 signaling blocks inhibitor of kappaB kinase activity and nuclear factor kappaB DNA binding. J Biol Chem 274, 31868-74.
[55] Murray, P.J. (2005). The primary mechanism of the IL-10-regulated antiinflammatory response is to selectively inhibit transcription. Proc Natl Acad Sci U S A 102, 8686-91.
[56] Chan, C.S., Ming-Lum, A., Golds, G.B., Lee, S.J., Anderson, R.J. and Mui, A.L.F. (2012). Interleukin-10 inhibits lipopolysaccharide-induced tumor necrosis factor-α translation through a SHIP1-dependent pathway. The Journal of biological chemistry 287, 38020-38027.
[57] Cassatella, M.A., Meda, L., Gasperini, S., Calzetti, F. and Bonora, S. (1994). Interleukin 10 (IL-10) upregulates IL-1 receptor antagonist production from lipopolysaccharide-stimulated human polymorphonuclear leukocytes by delaying mRNA degradation. J Exp Med 179, 1695-9.
[58] Jenkins, J.K., Malyak, M. and Arend, W.P. (1994). The effects of interleukin-10 on interleukin-1 receptor antagonist and interleukin-1 beta production in human monocytes and neutrophils. Lymphokine Cytokine Res 13, 47-54.
[59] Ovchinnikov, D.A. (2008). Macrophages in the embryo and beyond: much more than just giant phagocytes. Genesis 46, 447-62.
[60] Murray, P.J. and Wynn, T.A. (2011). Protective and pathogenic functions of macrophage subsets. Nature Reviews Immunology 11, 723-737.
[61] Fujiwara, N. and Kobayashi, K. (2005). Macrophages in inflammation. Curr Drug Targets Inflamm Allergy 4, 281-6.
[62] Lavin, Y., Mortha, A., Rahman, A. and Merad, M. (2015). Regulation of macrophage development and function in peripheral tissues. Nat Rev Immunol 15, 731-44.

[63] Gordon, S. (2007). The macrophage: past, present and future. Eur J Immunol 37 Suppl 1, S9-17.
[64] Taylor, P.R., Martinez-Pomares, L., Stacey, M., Lin, H.H., Brown, G.D. and Gordon, S. (2005). Macrophage receptors and immune recognition. Annu Rev Immunol 23, 901-44.
[65] Mosser, D.M. and Edwards, J.P. (2008). Exploring the full spectrum of macrophage activation. Nat Rev Immunol 8, 958-69.
[66] Gordon, S. and Taylor, P.R. (2005). Monocyte and macrophage heterogeneity. Nat Rev Immunol 5, 953-64.
[67] Martinez, F.O. and Gordon, S. (2014). The M1 and M2 paradigm of macrophage activation: time for reassessment. F1000Prime Rep 6, 13.
[68] Murray, P.J. *et al.* (2014). Macrophage activation and polarization: nomenclature and experimental guidelines. Immunity 41, 14-20.
[69] Mills, C.D., Kincaid, K., Alt, J.M., Heilman, M.J. and Hill, A.M. (2000). M-1/M-2 macrophages and the Th1/Th2 paradigm. J Immunol 164, 6166-73.
[70] Stein, M., Keshav, S., Harris, N. and Gordon, S. (1992). Interleukin 4 potently enhances murine macrophage mannose receptor activity: a marker of alternative immunologic macrophage activation. J Exp Med 176, 287-92.
[71] Gordon, S. (2003). Alternative activation of macrophages. Nat Rev Immunol 3, 23-35.
[72] Mantovani, A., Biswas, S.K., Galdiero, M.R., Sica, A. and Locati, M. (2013). Macrophage plasticity and polarization in tissue repair and remodelling. J Pathol 229, 176-85.
[73] Xue, J. *et al.* (2014). Transcriptome-based network analysis reveals a spectrum model of human macrophage activation. Immunity 40, 274-88.
[74] Guilliams, M. and van de Laar, L. (2015). A Hitchhiker's Guide to Myeloid Cell Subsets: Practical Implementation of a Novel Mononuclear Phagocyte Classification System. Front Immunol 6, 406.
[75] Vu Manh, T.P., Bertho, N., Hosmalin, A., Schwartz-Cornil, I. and Dalod, M. (2015). Investigating Evolutionary Conservation of Dendritic Cell Subset Identity and Functions. Front Immunol 6, 260.
[76] Akira, S., Uematsu, S. and Takeuchi, O. (2006). Pathogen recognition and innate immunity. Cell 124, 783-801.
[77] Uematsu, S. and Akira, S. (2008). Toll-Like receptors (TLRs) and their ligands. Handb Exp Pharmacol, 1-20.
[78] Bowie, A. and O'Neill, L.A. (2000). The interleukin-1 receptor/Toll-like receptor superfamily: signal generators for pro-inflammatory interleukins and microbial products. J Leukoc Biol 67, 508-14.
[79] Akira, S. and Takeda, K. (2004). Toll-like receptor signalling. Nat Rev Immunol 4, 499-511.
[80] Kawai, T., Adachi, O., Ogawa, T., Takeda, K. and Akira, S. (1999). Unresponsiveness of MyD88-deficient mice to endotoxin. Immunity 11, 115-22.
[81] Hoshino, K., Takeuchi, O., Kawai, T., Sanjo, H., Ogawa, T., Takeda, Y., Takeda, K. and Akira, S. (1999). Cutting edge: Toll-like receptor 4 (TLR4)-deficient mice are hyporesponsive to lipopolysaccharide: evidence for TLR4 as the Lps gene product. J Immunol 162, 3749-52.
[82] Gallego, C., Golenbock, D., Gomez, M.A. and Saravia, N.G. (2011). Toll-like receptors participate in macrophage activation and intracellular control of Leishmania (Viannia) panamensis. Infect Immun 79, 2871-9.
[83] Takeuchi, O., Hoshino, K. and Akira, S. (2000). Cutting edge: TLR2-deficient and MyD88-deficient mice are highly susceptible to Staphylococcus aureus infection. J Immunol 165, 5392-6.

[84] Rietschel, E.T. *et al.* (1994). Bacterial endotoxin: molecular relationships of structure to activity and function. FASEB journal : official publication of the Federation of American Societies for Experimental Biology 8, 217-225.
[85] Poltorak, A. *et al.* (1998). Defective LPS signaling in C3H/HeJ and C57BL/10ScCr mice: mutations in Tlr4 gene. Science 282, 2085-8.
[86] Wright, S.D., Tobias, P.S., Ulevitch, R.J. and Ramos, R.A. (1989). Lipopolysaccharide (LPS) binding protein opsonizes LPS-bearing particles for recognition by a novel receptor on macrophages. J Exp Med 170, 1231-41.
[87] Wright, S.D., Ramos, R.A., Tobias, P.S., Ulevitch, R.J. and Mathison, J.C. (1990). CD14, a receptor for complexes of lipopolysaccharide (LPS) and LPS binding protein. Science 249, 1431-3.
[88] Shimazu, R., Akashi, S., Ogata, H., Nagai, Y., Fukudome, K., Miyake, K. and Kimoto, M. (1999). MD-2, a molecule that confers lipopolysaccharide responsiveness on Toll-like receptor 4. J Exp Med 189, 1777-82.
[89] Kawai, T. and Akira, S. (2010). The role of pattern-recognition receptors in innate immunity: update on Toll-like receptors. Nat Immunol 11, 373-84.
[90] Lu, Y.C., Yeh, W.C. and Ohashi, P.S. (2008). LPS/TLR4 signal transduction pathway. Cytokine 42, 145-51.
[91] Peri, F., Piazza, M., Calabrese, V., Damore, G. and Cighetti, R. (2010). Exploring the LPS/TLR4 signal pathway with small molecules. Biochem Soc Trans 38, 1390-5.
[92] Suzuki, N. *et al.* (2002). Severe impairment of interleukin-1 and Toll-like receptor signalling in mice lacking IRAK-4. Nature 416, 750-6.
[93] Lye, E., Mirtsos, C., Suzuki, N., Suzuki, S. and Yeh, W.C. (2004). The role of interleukin 1 receptor-associated kinase-4 (IRAK-4) kinase activity in IRAK-4-mediated signaling. J Biol Chem 279, 40653-8.
[94] Keating, S.E., Maloney, G.M., Moran, E.M. and Bowie, A.G. (2007). IRAK-2 participates in multiple toll-like receptor signaling pathways to NFkappaB via activation of TRAF6 ubiquitination. J Biol Chem 282, 33435-43.
[95] Gohda, J., Matsumura, T. and Inoue, J. (2004). Cutting edge: TNFR-associated factor (TRAF) 6 is essential for MyD88-dependent pathway but not toll/IL-1 receptor domain-containing adaptor-inducing IFN-beta (TRIF)-dependent pathway in TLR signaling. J Immunol 173, 2913-7.
[96] Sato, S. *et al.* (2005). Essential function for the kinase TAK1 in innate and adaptive immune responses. Nat Immunol 6, 1087-95.
[97] Kanarek, N., London, N., Schueler-Furman, O. and Ben-Neriah, Y. (2010). Ubiquitination and degradation of the inhibitors of NF-kappaB. Cold Spring Harb Perspect Biol 2, a000166.
[98] Chang, L. and Karin, M. (2001). Mammalian MAP kinase signalling cascades. Nature 410, 37-40.
[99] Yamamoto, M. *et al.* (2003). TRAM is specifically involved in the Toll-like receptor 4-mediated MyD88-independent signaling pathway. Nat Immunol 4, 1144-50.
[100] Yamamoto, M. *et al.* (2003). Role of adaptor TRIF in the MyD88-independent toll-like receptor signaling pathway. Science 301, 640-3.
[101] Guo, B. and Cheng, G. (2007). Modulation of the interferon antiviral response by the TBK1/IKKi adaptor protein TANK. J Biol Chem 282, 11817-26.
[102] Cusson-Hermance, N., Khurana, S., Lee, T.H., Fitzgerald, K.A. and Kelliher, M.A. (2005). Rip1 mediates the Trif-dependent toll-like receptor 3- and 4-induced NF-{kappa}B activation but does not contribute to interferon regulatory factor 3 activation. J Biol Chem 280, 36560-6.
[103] Sato, S., Sugiyama, M., Yamamoto, M., Watanabe, Y., Kawai, T., Takeda, K. and Akira, S. (2003). Toll/IL-1 receptor domain-containing adaptor inducing IFN-beta (TRIF)

associates with TNF receptor-associated factor 6 and TANK-binding kinase 1, and activates two distinct transcription factors, NF-kappa B and IFN-regulatory factor-3, in the Toll-like receptor signaling. The Journal of Immunology 171, 4304-4310.
[104] Ojaniemi, M., Glumoff, V., Harju, K., Liljeroos, M., Vuori, K. and Hallman, M. (2003). Phosphatidylinositol 3-kinase is involved in Toll-like receptor 4-mediated cytokine expression in mouse macrophages. Eur J Immunol 33, 597-605.
[105] Aksoy, E., Vanden Berghe, W., Detienne, S., Amraoui, Z., Fitzgerald, K.A., Haegeman, G., Goldman, M. and Willems, F. (2005). Inhibition of phosphoinositide 3-kinase enhances TRIF-dependent NF-kappa B activation and IFN-beta synthesis downstream of Toll-like receptor 3 and 4. Eur J Immunol 35, 2200-9.
[106] Dil, N. and Marshall, A.J. (2009). Role of phosphoinositide 3-kinase p110 delta in TLR4- and TLR9-mediated B cell cytokine production and differentiation. Mol Immunol 46, 1970-8.
[107] Horwood, N.J., Mahon, T., McDaid, J.P., Campbell, J., Mano, H., Brennan, F.M., Webster, D. and Foxwell, B.M. (2003). Bruton's tyrosine kinase is required for lipopolysaccharide-induced tumor necrosis factor alpha production. J Exp Med 197, 1603-11.
[108] Delcommenne, M., Tan, C., Gray, V., Rue, L., Woodgett, J. and Dedhar, S. (1998). Phosphoinositide-3-OH kinase-dependent regulation of glycogen synthase kinase 3 and protein kinase B/AKT by the integrin-linked kinase. Proc Natl Acad Sci U S A 95, 11211-6.
[109] Jhun, B.S. *et al.* (2004). 5-Aminoimidazole-4-carboxamide riboside suppresses lipopolysaccharide-induced TNF-alpha production through inhibition of phosphatidylinositol 3-kinase/Akt activation in RAW 264.7 murine macrophages. Biochem Biophys Res Commun 318, 372-80.
[110] Koide, N., Sugiyama, T., Mori, I., Mu, M.M., Yoshida, T. and Yokochi, T. (2003). C2-ceramide inhibits LPS-induced nitric oxide production in RAW 264.7 macrophage cells through down-regulating the activation of Akt. J Endotoxin Res 9, 85-90.
[111] Pengal, R.A., Ganesan, L.P., Wei, G., Fang, H., Ostrowski, M.C. and Tridandapani, S. (2006). Lipopolysaccharide-induced production of interleukin-10 is promoted by the serine/threonine kinase Akt. Mol Immunol 43, 1557-64.
[112] Sly, L.M., Rauh, M.J., Kalesnikoff, J., Song, C.H. and Krystal, G. (2004). LPS-induced upregulation of SHIP is essential for endotoxin tolerance. Immunity 21, 227-39.
[113] Troutman, T.D., Bazan, J.F. and Pasare, C. (2012). Toll-like receptors, signaling adapters and regulation of the pro-inflammatory response by PI3K. Cell Cycle 11, 3559-67.
[114] Gais, P., Tiedje, C., Altmayr, F., Gaestel, M., Weighardt, H. and Holzmann, B. (2010). TRIF signaling stimulates translation of TNF-alpha mRNA via prolonged activation of MK2. J Immunol 184, 5842-8.
[115] He, X., Jing, Z. and Cheng, G. (2014). MicroRNAs: new regulators of Toll-like receptor signalling pathways. Biomed Res Int 2014, 945169.
[116] O'Neill, L.A., Sheedy, F.J. and McCoy, C.E. (2011). MicroRNAs: the fine-tuners of Toll-like receptor signalling. Nat Rev Immunol 11, 163-75.
[117] Nahid, M.A., Satoh, M. and Chan, E.K. (2011). MicroRNA in TLR signaling and endotoxin tolerance. Cell Mol Immunol 8, 388-403.
[118] Olivieri, F., Rippo, M.R., Prattichizzo, F., Babini, L., Graciotti, L., Recchioni, R. and Procopio, A.D. (2013). Toll like receptor signaling in "inflammaging": microRNA as new players. Immun Ageing 10, 11.
[119] Krol, J., Loedige, I. and Filipowicz, W. (2010). The widespread regulation of microRNA biogenesis, function and decay. Nat Rev Genet 11, 597-610.

[120] Tili, E. *et al.* (2007). Modulation of miR-155 and miR-125b levels following lipopolysaccharide/TNF-alpha stimulation and their possible roles in regulating the response to endotoxin shock. The Journal of Immunology 179, 5082-5089.
[121] Bala, S., Marcos, M., Kodys, K., Csak, T., Catalano, D., Mandrekar, P. and Szabo, G. (2011). Up-regulation of microRNA-155 in macrophages contributes to increased tumor necrosis factor {alpha} (TNF{alpha}) production via increased mRNA half-life in alcoholic liver disease. J Biol Chem 286, 1436-44.
[122] O'Connell, R.M., Taganov, K.D., Boldin, M.P., Cheng, G. and Baltimore, D. (2007). MicroRNA-155 is induced during the macrophage inflammatory response. Proc Natl Acad Sci U S A 104, 1604-9.
[123] Taganov, K.D., Boldin, M.P., Chang, K.J. and Baltimore, D. (2006). NF-kappaB-dependent induction of microRNA miR-146, an inhibitor targeted to signaling proteins of innate immune responses. Proc Natl Acad Sci U S A 103, 12481-6.
[124] Kondo, T., Kawai, T. and Akira, S. (2012). Dissecting negative regulation of Toll-like receptor signaling. Trends Immunol 33, 449-58.
[125] Shi, M. *et al.* (2008). TRIM30 alpha negatively regulates TLR-mediated NF-kappa B activation by targeting TAB2 and TAB3 for degradation. Nat Immunol 9, 369-77.
[126] Rossato, M. *et al.* (2012). IL-10-induced microRNA-187 negatively regulates TNF-α, IL-6, and IL-12p40 production in TLR4-stimulated monocytes. Proc Natl Acad Sci U S A 109, E3101-10.
[127] Siednienko, J., Halle, A., Nagpal, K., Golenbock, D.T. and Miggin, S.M. (2010). TLR3-mediated IFN-β gene induction is negatively regulated by the TLR adaptor MyD88 adaptor-like. Eur J Immunol 40, 3150-60.
[128] Seregin, S.S., Aldhamen, Y.A., Appledorn, D.M., Aylsworth, C.F., Godbehere, S., Liu, C.J., Quiroga, D. and Amalfitano, A. (2011). TRIF is a critical negative regulator of TLR agonist mediated activation of dendritic cells in vivo. PLoS One 6, e22064.
[129] Choi, Y.J., Im, E., Pothoulakis, C. and Rhee, S.H. (2010). TRIF modulates TLR5-dependent responses by inducing proteolytic degradation of TLR5. J Biol Chem 285, 21382-90.
[130] Ahmed, S., Maratha, A., Butt, A.Q., Shevlin, E. and Miggin, S.M. (2013). TRIF-mediated TLR3 and TLR4 signaling is negatively regulated by ADAM15. J Immunol 190, 2217-28.
[131] Saitoh, T. *et al.* (2008). Loss of the autophagy protein Atg16L1 enhances endotoxin-induced IL-1beta production. Nature 456, 264-8.
[132] Saitoh, T. *et al.* (2006). Negative regulation of interferon-regulatory factor 3-dependent innate antiviral response by the prolyl isomerase Pin1. Nat Immunol 7, 598-605.
[133] Yu, Y. and Hayward, G.S. (2010). The ubiquitin E3 ligase RAUL negatively regulates type i interferon through ubiquitination of the transcription factors IRF7 and IRF3. Immunity 33, 863-77.
[134] Palsson-McDermott, E.M. *et al.* (2009). TAG, a splice variant of the adaptor TRAM, negatively regulates the adaptor MyD88-independent TLR4 pathway. Nat Immunol 10, 579-86.
[135] Zhao, W., Wang, L., Zhang, M., Yuan, C. and Gao, C. (2012). E3 ubiquitin ligase tripartite motif 38 negatively regulates TLR-mediated immune responses by proteasomal degradation of TNF receptor-associated factor 6 in macrophages. J Immunol 188, 2567-74.
[136] Troutman, T.D., Hu, W., Fulenchek, S., Yamazaki, T., Kurosaki, T., Bazan, J.F. and Pasare, C. (2012). Role for B-cell adapter for PI3K (BCAP) as a signaling adapter linking Toll-like receptors (TLRs) to serine/threonine kinases PI3K/Akt. Proc Natl Acad Sci U S A 109, 273-8.

[137] Ishida, A., Akita, K., Mori, Y., Tanida, S., Toda, M., Inoue, M. and Nakada, H. (2014). Negative regulation of Toll-like receptor-4 signaling through the binding of glycosylphosphatidylinositol-anchored glycoprotein, CD14, with the sialic acid-binding lectin, CD33. J Biol Chem 289, 25341-50.
[138] Yoshida, H., Jono, H., Kai, H. and Li, J.D. (2005). The tumor suppressor cylindromatosis (CYLD) acts as a negative regulator for toll-like receptor 2 signaling via negative cross-talk with TRAF6 AND TRAF7. J Biol Chem 280, 41111-21.
[139] Kayagaki, N. *et al.* (2007). DUBA: a deubiquitinase that regulates type I interferon production. Science 318, 1628-32.
[140] Wang, T. *et al.* (2006). Flightless I homolog negatively modulates the TLR pathway. J Immunol 176, 1355-62.
[141] Schneider, M. *et al.* (2012). The innate immune sensor NLRC3 attenuates Toll-like receptor signaling via modification of the signaling adaptor TRAF6 and transcription factor NF-κB. Nat Immunol 13, 823-31.
[142] Risco, A. *et al.* (2012). p38γ and p38δ kinases regulate the Toll-like receptor 4 (TLR4)-induced cytokine production by controlling ERK1/2 protein kinase pathway activation. Proc Natl Acad Sci U S A 109, 11200-5.
[143] Divanovic, S. *et al.* (2005). Negative regulation of Toll-like receptor 4 signaling by the Toll-like receptor homolog RP105. Nat Immunol 6, 571-8.
[144] Peng, J. *et al.* (2010). SARM inhibits both TRIF- and MyD88-mediated AP-1 activation. Eur J Immunol 40, 1738-47.
[145] Liu, X., Chen, W., Wang, Q., Li, L. and Wang, C. (2013). Negative regulation of TLR inflammatory signaling by the SUMO-deconjugating enzyme SENP6. PLoS Pathog 9, e1003480.
[146] Yuk, J.M. *et al.* (2011). The orphan nuclear receptor SHP acts as a negative regulator in inflammatory signaling triggered by Toll-like receptors. Nat Immunol 12, 742-51.
[147] An, H. *et al.* (2006). SHP-2 phosphatase negatively regulates the TRIF adaptor protein-dependent type I interferon and proinflammatory cytokine production. Immunity 25, 919-28.
[148] Kawagoe, T., Takeuchi, O., Takabatake, Y., Kato, H., Isaka, Y., Tsujimura, T. and Akira, S. (2009). TANK is a negative regulator of Toll-like receptor signaling and is critical for the prevention of autoimmune nephritis. Nat Immunol 10, 965-72.
[149] Ito, H. and Hamerman, J.A. (2012). TREM-2, triggering receptor expressed on myeloid cell-2, negatively regulates TLR responses in dendritic cells. Eur J Immunol 42, 176-85.
[150] Li, X.M., Su, J.R., Yan, S.P., Cheng, Z.L., Yang, T.T. and Zhu, Q. (2014). A novel inflammatory regulator TIPE2 inhibits TLR4-mediated development of colon cancer via caspase-8. Cancer Biomark 14, 233-40.
[151] Liang, J., Saad, Y., Lei, T., Wang, J., Qi, D., Yang, Q., Kolattukudy, P.E. and Fu, M. (2010). MCP-induced protein 1 deubiquitinates TRAF proteins and negatively regulates JNK and NF-kappaB signaling. J Exp Med 207, 2959-73.
[152] Carmody, R.J., Ruan, Q., Palmer, S., Hilliard, B. and Chen, Y.H. (2007). Negative regulation of toll-like receptor signaling by NF-kappaB p50 ubiquitination blockade. Science 317, 675-8.
[153] Ananieva, O. *et al.* (2008). The kinases MSK1 and MSK2 act as negative regulators of Toll-like receptor signaling. Nat Immunol 9, 1028-36.
[154] Huang, R.S., Hu, G.Q., Lin, B., Lin, Z.Y. and Sun, C.C. (2010). MicroRNA-155 silencing enhances inflammatory response and lipid uptake in oxidized low-density lipoprotein-stimulated human THP-1 macrophages. J Investig Med 58, 961-7.
[155] Matsushita, K. *et al.* (2009). Zc3h12a is an RNase essential for controlling immune responses by regulating mRNA decay. Nature 458, 1185-90.

[156] Gantier, M.P. (2010). New perspectives in MicroRNA regulation of innate immunity. J Interferon Cytokine Res 30, 283-9.
[157] Roberts, T.C. (2014). The MicroRNA Biology of the Mammalian Nucleus. Molecular therapy. Nucleic acids 3, e188.
[158] Lee, Y., Kim, M., Han, J., Yeom, K.H., Lee, S., Baek, S.H. and Kim, V.N. (2004). MicroRNA genes are transcribed by RNA polymerase II. EMBO J 23, 4051-60.
[159] Borchert, G.M., Lanier, W. and Davidson, B.L. (2006). RNA polymerase III transcribes human microRNAs. Nat Struct Mol Biol 13, 1097-101.
[160] Rodriguez, A., Griffiths-Jones, S., Ashurst, J.L. and Bradley, A. (2004). Identification of mammalian microRNA host genes and transcription units. Genome Res 14, 1902-10.
[161] Lee, Y. *et al.* (2003). The nuclear RNase III Drosha initiates microRNA processing. Nature 425, 415-9.
[162] Berezikov, E., Chung, W.J., Willis, J., Cuppen, E. and Lai, E.C. (2007). Mammalian mirtron genes. Mol Cell 28, 328-36.
[163] Yi, R., Qin, Y., Macara, I.G. and Cullen, B.R. (2003). Exportin-5 mediates the nuclear export of pre-microRNAs and short hairpin RNAs. Genes Dev 17, 3011-6.
[164] Zeng, Y. and Cullen, B.R. (2004). Structural requirements for pre-microRNA binding and nuclear export by Exportin 5. Nucleic Acids Res 32, 4776-85.
[165] Lund, E. and Dahlberg, J.E. (2006). Substrate selectivity of exportin 5 and Dicer in the biogenesis of microRNAs. Cold Spring Harb Symp Quant Biol 71, 59-66.
[166] Chendrimada, T.P., Gregory, R.I., Kumaraswamy, E., Norman, J., Cooch, N., Nishikura, K. and Shiekhattar, R. (2005). TRBP recruits the Dicer complex to Ago2 for microRNA processing and gene silencing. Nature 436, 740-4.
[167] Höck, J. and Meister, G. (2008). The Argonaute protein family. Genome Biol 9, 210.
[168] Dueck, A., Ziegler, C., Eichner, A., Berezikov, E. and Meister, G. (2012). microRNAs associated with the different human Argonaute proteins. Nucleic Acids Res 40, 9850-62.
[169] Siomi, M.C. and Siomi, H. (2008). Characterization of endogenous human Argonautes and their miRNA partners in RNA silencing. Nucleic Acids Symp Ser (Oxf), 59-60.
[170] Su, H., Trombly, M.I., Chen, J. and Wang, X. (2009). Essential and overlapping functions for mammalian Argonautes in microRNA silencing. Genes Dev 23, 304-17.
[171] Friedman, R.C., Farh, K.K., Burge, C.B. and Bartel, D.P. (2009). Most mammalian mRNAs are conserved targets of microRNAs. Genome Res 19, 92-105.
[172] Ardekani, A.M. and Naeini, M.M. (2010). The Role of MicroRNAs in Human Diseases. Avicenna J Med Biotechnol 2, 161-79.
[173] Tüfekci, K.U., Oner, M.G., Meuwissen, R.L. and Genç, S. (2014). The role of microRNAs in human diseases. Methods Mol Biol 1107, 33-50.
[174] Davis-Dusenbery, B.N. and Hata, A. (2010). Mechanisms of control of microRNA biogenesis. J Biochem 148, 381-92.
[175] Zhou, D. *et al.* (2015). DNMT1 mediates chemosensitivity by reducing methylation of miRNA-20a promoter in glioma cells. Exp Mol Med 47, e182.
[176] Kim, V.N., Han, J. and Siomi, M.C. (2009). Biogenesis of small RNAs in animals. Nat Rev Mol Cell Biol 10, 126-39.
[177] Kumar, P., Luo, Y., Tudela, C., Alexander, J.M. and Mendelson, C.R. (2013). The c-Myc-regulated microRNA-17~92 (miR-17~92) and miR-106a~363 clusters target hCYP19A1 and hGCM1 to inhibit human trophoblast differentiation. Mol Cell Biol 33, 1782-96.
[178] Wang, X., Zhao, X., Gao, P. and Wu, M. (2013). c-Myc modulates microRNA processing via the transcriptional regulation of Drosha. Sci Rep 3, 1942.
[179] Sun, Y., Ge, Y., Drnevich, J., Zhao, Y., Band, M. and Chen, J. (2010). Mammalian target of rapamycin regulates miRNA-1 and follistatin in skeletal myogenesis. J Cell Biol 189, 1157-69.

[180] Conaco, C., Otto, S., Han, J.J. and Mandel, G. (2006). Reciprocal actions of REST and a microRNA promote neuronal identity. Proc Natl Acad Sci U S A 103, 2422-7.
[181] Bracken, C.P., Gregory, P.A., Kolesnikoff, N., Bert, A.G., Wang, J., Shannon, M.F. and Goodall, G.J. (2008). A double-negative feedback loop between ZEB1-SIP1 and the microRNA-200 family regulates epithelial-mesenchymal transition. Cancer Res 68, 7846-54.
[182] Triboulet, R., Chang, H.M., Lapierre, R.J. and Gregory, R.I. (2009). Post-transcriptional control of DGCR8 expression by the Microprocessor. RNA 15, 1005-11.
[183] Kadener, S., Rodriguez, J., Abruzzi, K.C., Khodor, Y.L., Sugino, K., Marr, M.T., Nelson, S. and Rosbash, M. (2009). Genome-wide identification of targets of the drosha-pasha/DGCR8 complex. RNA 15, 537-45.
[184] Herbert, K.M., Pimienta, G., DeGregorio, S.J., Alexandrov, A. and Steitz, J.A. (2013). Phosphorylation of DGCR8 increases its intracellular stability and induces a progrowth miRNA profile. Cell Rep 5, 1070-81.
[185] Tang, X., Zhang, Y., Tucker, L. and Ramratnam, B. (2010). Phosphorylation of the RNase III enzyme Drosha at Serine300 or Serine302 is required for its nuclear localization. Nucleic Acids Res 38, 6610-9.
[186] Tang, X., Li, M., Tucker, L. and Ramratnam, B. (2011). Glycogen synthase kinase 3 beta (GSK3β) phosphorylates the RNAase III enzyme Drosha at S300 and S302. PLoS One 6, e20391.
[187] Wada, T., Kikuchi, J. and Furukawa, Y. (2012). Histone deacetylase 1 enhances microRNA processing via deacetylation of DGCR8. EMBO Rep 13, 142-9.
[188] Cheng, T.L., Wang, Z., Liao, Q., Zhu, Y., Zhou, W.H., Xu, W. and Qiu, Z. (2014). MeCP2 suppresses nuclear microRNA processing and dendritic growth by regulating the DGCR8/Drosha complex. Dev Cell 28, 547-60.
[189] Sabin, L.R. *et al.* (2009). Ars2 regulates both miRNA- and siRNA- dependent silencing and suppresses RNA virus infection in Drosophila. Cell 138, 340-51.
[190] Gurung, B., Katona, B.W. and Hua, X. (2014). Menin-mediated regulation of miRNA biogenesis uncovers the IRS2 pathway as a target for regulating pancreatic beta cells. Oncoscience 1, 562-6.
[191] Guil, S. and Cáceres, J.F. (2007). The multifunctional RNA-binding protein hnRNP A1 is required for processing of miR-18a. Nat Struct Mol Biol 14, 591-6.
[192] Michlewski, G. and Cáceres, J.F. (2010). Antagonistic role of hnRNP A1 and KSRP in the regulation of let-7a biogenesis. Nat Struct Mol Biol 17, 1011-8.
[193] Viswanathan, S.R., Daley, G.Q. and Gregory, R.I. (2008). Selective blockade of microRNA processing by Lin28. Science 320, 97-100.
[194] Ali, P.S., Ghoshdastider, U., Hoffmann, J., Brutschy, B. and Filipek, S. (2012). Recognition of the let-7g miRNA precursor by human Lin28B. FEBS Lett 586, 3986-90.
[195] Heo, I., Joo, C., Cho, J., Ha, M., Han, J. and Kim, V.N. (2008). Lin28 mediates the terminal uridylation of let-7 precursor MicroRNA. Mol Cell 32, 276-84.
[196] Bourguignon, L.Y., Spevak, C.C., Wong, G., Xia, W. and Gilad, E. (2009). Hyaluronan-CD44 interaction with protein kinase C(epsilon) promotes oncogenic signaling by the stem cell marker Nanog and the Production of microRNA-21, leading to down-regulation of the tumor suppressor protein PDCD4, anti-apoptosis, and chemotherapy resistance in breast tumor cells. J Biol Chem 284, 26533-46.
[197] Sakamoto, S. *et al.* (2009). The NF90-NF45 complex functions as a negative regulator in the microRNA processing pathway. Mol Cell Biol 29, 3754-69.
[198] Fukuda, T. *et al.* (2007). DEAD-box RNA helicase subunits of the Drosha complex are required for processing of rRNA and a subset of microRNAs. Nat Cell Biol 9, 604-11.
[199] Suzuki, H.I., Yamagata, K., Sugimoto, K., Iwamoto, T., Kato, S. and Miyazono, K. (2009). Modulation of microRNA processing by p53. Nature 460, 529-33.

[200] Davis, B.N., Hilyard, A.C., Lagna, G. and Hata, A. (2008). SMAD proteins control DROSHA-mediated microRNA maturation. Nature 454, 56-61.
[201] Davis, B.N., Hilyard, A.C., Nguyen, P.H., Lagna, G. and Hata, A. (2010). Smad proteins bind a conserved RNA sequence to promote microRNA maturation by Drosha. Mol Cell 39, 373-84.
[202] Wu, H., Sun, S., Tu, K., Gao, Y., Xie, B., Krainer, A.R. and Zhu, J. (2010). A splicing-independent function of SF2/ASF in microRNA processing. Mol Cell 38, 67-77.
[203] Yu, B. *et al.* (2008). The FHA domain proteins DAWDLE in Arabidopsis and SNIP1 in humans act in small RNA biogenesis. Proc Natl Acad Sci U S A 105, 10073-8.
[204] Auyeung, V.C., Ulitsky, I., McGeary, S.E. and Bartel, D.P. (2013). Beyond secondary structure: primary-sequence determinants license pri-miRNA hairpins for processing. Cell 152, 844-58.
[205] Di Carlo, V., Grossi, E., Laneve, P., Morlando, M., Dini Modigliani, S., Ballarino, M., Bozzoni, I. and Caffarelli, E. (2013). TDP-43 regulates the microprocessor complex activity during in vitro neuronal differentiation. Mol Neurobiol 48, 952-63.
[206] Kawahara, Y. and Mieda-Sato, A. (2012). TDP-43 promotes microRNA biogenesis as a component of the Drosha and Dicer complexes. Proc Natl Acad Sci U S A 109, 3347-52.
[207] Xhemalce, B., Robson, S.C. and Kouzarides, T. (2012). Human RNA methyltransferase BCDIN3D regulates microRNA processing. Cell 151, 278-88.
[208] Paroo, Z., Ye, X., Chen, S. and Liu, Q. (2009). Phosphorylation of the human microRNA-generating complex mediates MAPK/Erk signaling. Cell 139, 112-22.
[209] Edbauer, D. *et al.* (2010). Regulation of synaptic structure and function by FMRP-associated microRNAs miR-125b and miR-132. Neuron 65, 373-84.
[210] Upton, J.P. *et al.* (2012). IRE1α cleaves select microRNAs during ER stress to derepress translation of proapoptotic Caspase-2. Science 338, 818-22.
[211] Trabucchi, M., Briata, P., Garcia-Mayoral, M., Haase, A.D., Filipowicz, W., Ramos, A., Gherzi, R. and Rosenfeld, M.G. (2009). The RNA-binding protein KSRP promotes the biogenesis of a subset of microRNAs. Nature 459, 1010-4.
[212] Tokumaru, S., Suzuki, M., Yamada, H., Nagino, M. and Takahashi, T. (2008). let-7 regulates Dicer expression and constitutes a negative feedback loop. Carcinogenesis 29, 2073-7.
[213] Forman, J.J., Legesse-Miller, A. and Coller, H.A. (2008). A search for conserved sequences in coding regions reveals that the let-7 microRNA targets Dicer within its coding sequence. Proc Natl Acad Sci U S A 105, 14879-84.
[214] Suzuki, H.I., Arase, M., Matsuyama, H., Choi, Y.L., Ueno, T., Mano, H., Sugimoto, K. and Miyazono, K. (2011). MCPIP1 ribonuclease antagonizes dicer and terminates microRNA biogenesis through precursor microRNA degradation. Mol Cell 44, 424-36.
[215] Horman, S.R. *et al.* (2013). Akt-mediated phosphorylation of argonaute 2 downregulates cleavage and upregulates translational repression of MicroRNA targets. Mol Cell 50, 356-67.
[216] Qi, H.H., Ongusaha, P.P., Myllyharju, J., Cheng, D., Pakkanen, O., Shi, Y., Lee, S.W. and Peng, J. (2008). Prolyl 4-hydroxylation regulates Argonaute 2 stability. Nature 455, 421-4.
[217] Wu, C., So, J., Davis-Dusenbery, B.N., Qi, H.H., Bloch, D.B., Shi, Y., Lagna, G. and Hata, A. (2011). Hypoxia potentiates microRNA-mediated gene silencing through posttranslational modification of Argonaute2. Mol Cell Biol 31, 4760-74.
[218] Shen, J. *et al.* (2013). EGFR modulates microRNA maturation in response to hypoxia through phosphorylation of AGO2. Nature 497, 383-7.
[219] Rybak, A. *et al.* (2009). The let-7 target gene mouse lin-41 is a stem cell specific E3 ubiquitin ligase for the miRNA pathway protein Ago2. Nat Cell Biol 11, 1411-20.

[220] Zeng, Y., Sankala, H., Zhang, X. and Graves, P.R. (2008). Phosphorylation of Argonaute 2 at serine-387 facilitates its localization to processing bodies. Biochem J 413, 429-36.
[221] Leung, A.K., Vyas, S., Rood, J.E., Bhutkar, A., Sharp, P.A. and Chang, P. (2011). Poly(ADP-ribose) regulates stress responses and microRNA activity in the cytoplasm. Mol Cell 42, 489-99.
[222] Yang, W., Chendrimada, T.P., Wang, Q., Higuchi, M., Seeburg, P.H., Shiekhattar, R. and Nishikura, K. (2006). Modulation of microRNA processing and expression through RNA editing by ADAR deaminases. Nat Struct Mol Biol 13, 13-21.
[223] Kawahara, Y., Zinshteyn, B., Chendrimada, T.P., Shiekhattar, R. and Nishikura, K. (2007). RNA editing of the microRNA-151 precursor blocks cleavage by the Dicer-TRBP complex. EMBO Rep 8, 763-9.
[224] Chang, H.M., Triboulet, R., Thornton, J.E. and Gregory, R.I. (2013). A role for the Perlman syndrome exonuclease Dis3l2 in the Lin28-let-7 pathway. Nature 497, 244-8.
[225] Ustianenko, D. *et al.* (2013). Mammalian DIS3L2 exoribonuclease targets the uridylated precursors of let-7 miRNAs. RNA 19, 1632-8.
[226] Yang, Z., Ebright, Y.W., Yu, B. and Chen, X. (2006). HEN1 recognizes 21-24 nt small RNA duplexes and deposits a methyl group onto the 2' OH of the 3' terminal nucleotide. Nucleic Acids Res 34, 667-75.
[227] Katoh, T., Sakaguchi, Y., Miyauchi, K., Suzuki, T., Kashiwabara, S. and Baba, T. (2009). Selective stabilization of mammalian microRNAs by 3' adenylation mediated by the cytoplasmic poly(A) polymerase GLD-2. Genes Dev 23, 433-8.
[228] Das, S.K., Sokhi, U.K., Bhutia, S.K., Azab, B., Su, Z.Z., Sarkar, D. and Fisher, P.B. (2010). Human polynucleotide phosphorylase selectively and preferentially degrades microRNA-221 in human melanoma cells. Proc Natl Acad Sci U S A 107, 11948-53.
[229] Zhao, X., Duan, Z., Liu, X., Wang, B., Wang, X., He, J., Yao, Z. and Yang, J. (2013). MicroRNA-127 is downregulated by Tudor-SN protein and contributes to metastasis and proliferation in breast cancer cell line MDA-MB-231. Anat Rec (Hoboken) 296, 1842-9.
[230] Chatterjee, S., Fasler, M., Büssing, I. and Grosshans, H. (2011). Target-mediated protection of endogenous microRNAs in C. elegans. Dev Cell 20, 388-96.
[231] Lim, J., Ha, M., Chang, H., Kwon, S.C., Simanshu, D.K., Patel, D.J. and Kim, V.N. (2014). Uridylation by TUT4 and TUT7 marks mRNA for degradation. Cell 159, 1365-76.
[232] Rhoades, M.W., Reinhart, B.J., Lim, L.P., Burge, C.B., Bartel, B. and Bartel, D.P. (2002). Prediction of plant microRNA targets. Cell 110, 513-20.
[233] Bartel, D.P. (2009). MicroRNAs: target recognition and regulatory functions. Cell 136, 215-33.
[234] Loeb, G.B., Khan, A.A., Canner, D., Hiatt, J.B., Shendure, J., Darnell, R.B., Leslie, C.S. and Rudensky, A.Y. (2012). Transcriptome-wide miR-155 binding map reveals widespread noncanonical microRNA targeting. Molecular cell 48, 760-770.
[235] Vella, M.C., Choi, E.Y., Lin, S.Y., Reinert, K. and Slack, F.J. (2004). The C. elegans microRNA let-7 binds to imperfect let-7 complementary sites from the lin-41 3'UTR. Genes Dev 18, 132-7.
[236] Shin, C., Nam, J.W., Farh, K.K., Chiang, H.R., Shkumatava, A. and Bartel, D.P. (2010). Expanding the microRNA targeting code: functional sites with centered pairing. Mol Cell 38, 789-802.
[237] Lee, I. *et al.* (2009). New class of microRNA targets containing simultaneous 5'-UTR and 3'-UTR interaction sites. Genome Res 19, 1175-83.
[238] Ørom, U.A., Nielsen, F.C. and Lund, A.H. (2008). MicroRNA-10a binds the 5'UTR of ribosomal protein mRNAs and enhances their translation. Mol Cell 30, 460-71.

[239] Jakymiw, A. *et al.* (2010). Overexpression of dicer as a result of reduced let-7 MicroRNA levels contributes to increased cell proliferation of oral cancer cells. Genes Chromosomes Cancer 49, 549-59.
[240] Grimson, A., Farh, K.K., Johnston, W.K., Garrett-Engele, P., Lim, L.P. and Bartel, D.P. (2007). MicroRNA targeting specificity in mammals: determinants beyond seed pairing. Mol Cell 27, 91-105.
[241] Eulalio, A., Huntzinger, E. and Izaurralde, E. (2008). GW182 interaction with Argonaute is essential for miRNA-mediated translational repression and mRNA decay. Nat Struct Mol Biol 15, 346-53.
[242] Behm-Ansmant, I., Rehwinkel, J., Doerks, T., Stark, A., Bork, P. and Izaurralde, E. (2006). mRNA degradation by miRNAs and GW182 requires both CCR4:NOT deadenylase and DCP1:DCP2 decapping complexes. Genes Dev 20, 1885-98.
[243] Mathonnet, G. *et al.* (2007). MicroRNA inhibition of translation initiation in vitro by targeting the cap-binding complex eIF4F. Science 317, 1764-7.
[244] Djuranovic, S., Nahvi, A. and Green, R. (2012). miRNA-mediated gene silencing by translational repression followed by mRNA deadenylation and decay. Science 336, 237-40.
[245] Béthune, J., Artus-Revel, C.G. and Filipowicz, W. (2012). Kinetic analysis reveals successive steps leading to miRNA-mediated silencing in mammalian cells. EMBO Rep 13, 716-23.
[246] Bazzini, A.A., Lee, M.T. and Giraldez, A.J. (2012). Ribosome profiling shows that miR-430 reduces translation before causing mRNA decay in zebrafish. Science 336, 233-7.
[247] Meijer, H.A. *et al.* (2013). Translational repression and eIF4A2 activity are critical for microRNA-mediated gene regulation. Science 340, 82-5.
[248] Jackson, R.J., Hellen, C.U. and Pestova, T.V. (2010). The mechanism of eukaryotic translation initiation and principles of its regulation. Nat Rev Mol Cell Biol 11, 113-27.
[249] Komar, A.A. and Hatzoglou, M. (2011). Cellular IRES-mediated translation: the war of ITAFs in pathophysiological states. Cell Cycle 10, 229-40.
[250] Chekulaeva, M., Mathys, H., Zipprich, J.T., Attig, J., Colic, M., Parker, R. and Filipowicz, W. (2011). miRNA repression involves GW182-mediated recruitment of CCR4-NOT through conserved W-containing motifs. Nat Struct Mol Biol 18, 1218-26.
[251] Braun, J.E., Huntzinger, E., Fauser, M. and Izaurralde, E. (2011). GW182 proteins directly recruit cytoplasmic deadenylase complexes to miRNA targets. Mol Cell 44, 120-33.
[252] Jonas, S. and Izaurralde, E. (2015). Towards a molecular understanding of microRNA-mediated gene silencing. Nat Rev Genet 16, 421-33.
[253] Zekri, L., Kuzuoğlu-Öztürk, D. and Izaurralde, E. (2013). GW182 proteins cause PABP dissociation from silenced miRNA targets in the absence of deadenylation. EMBO J 32, 1052-65.
[254] Ricci, E.P., Limousin, T., Soto-Rifo, R., Allison, R., Pöyry, T., Decimo, D., Jackson, R.J. and Ohlmann, T. (2011). Activation of a microRNA response in trans reveals a new role for poly(A) in translational repression. Nucleic Acids Res 39, 5215-31.
[255] Norbury, C.J. (2013). Cytoplasmic RNA: a case of the tail wagging the dog. Nat Rev Mol Cell Biol 14, 643-53.
[256] Rehwinkel, J., Behm-Ansmant, I., Gatfield, D. and Izaurralde, E. (2005). A crucial role for GW182 and the DCP1:DCP2 decapping complex in miRNA-mediated gene silencing. RNA 11, 1640-7.
[257] Vasudevan, S., Tong, Y. and Steitz, J.A. (2007). Switching from repression to activation: microRNAs can up-regulate translation. Science 318, 1931-4.

[258] Kanellopoulou, C., Muljo, S.A., Kung, A.L., Ganesan, S., Drapkin, R., Jenuwein, T., Livingston, D.M. and Rajewsky, K. (2005). Dicer-deficient mouse embryonic stem cells are defective in differentiation and centromeric silencing. Genes Dev 19, 489-501.
[259] Muljo, S.A., Ansel, K.M., Kanellopoulou, C., Livingston, D.M., Rao, A. and Rajewsky, K. (2005). Aberrant T cell differentiation in the absence of Dicer. J Exp Med 202, 261-9.
[260] Koralov, S.B. *et al.* (2008). Dicer ablation affects antibody diversity and cell survival in the B lymphocyte lineage. Cell 132, 860-74.
[261] Kuipers, H., Schnorfeil, F.M., Fehling, H.J., Bartels, H. and Brocker, T. (2010). Dicer-dependent microRNAs control maturation, function, and maintenance of Langerhans cells in vivo. J Immunol 185, 400-9.
[262] Ruggiero, T. *et al.* (2009). LPS induces KH-type splicing regulatory protein-dependent processing of microRNA-155 precursors in macrophages. The FASEB Journal 23, 2898-2908.
[263] O'Connell, R.M., Rao, D.S., Chaudhuri, A.A. and Baltimore, D. (2010). Physiological and pathological roles for microRNAs in the immune system. Nat Rev Immunol 10, 111-22.
[264] O'Connell, R.M., Rao, D.S. and Baltimore, D. (2012). microRNA regulation of inflammatory responses. Annual Review of Immunology 30, 295-312.
[265] Stachurska, A., Zorro, M.M., van der Sijde, M.R. and Withoff, S. (2014). Small and Long Regulatory RNAs in the Immune System and Immune Diseases. Frontiers in Immunology 5, 843-18.
[266] Landgraf, P. *et al.* (2007). A mammalian microRNA expression atlas based on small RNA library sequencing. Cell 129, 1401-14.
[267] Jr, O.e.F., Moore, C.S., Kennedy, T.E., Antel, J.P., Bar-Or, A. and Dhaunchak, A.S. (2012). MicroRNA dysregulation in multiple sclerosis. Front Genet 3, 311.
[268] Ceribelli, A., Nahid, M.A., Satoh, M. and Chan, E.K. (2011). MicroRNAs in rheumatoid arthritis. FEBS Lett 585, 3667-74.
[269] Salehi, E., Eftekhari, R., Oraei, M., Gharib, A. and Bidad, K. (2015). MicroRNAs in rheumatoid arthritis. Clin Rheumatol 34, 615-28.
[270] Amarilyo, G. and La Cava, A. (2012). miRNA in systemic lupus erythematosus. Clin Immunol 144, 26-31.
[271] Carlsen, A.L. *et al.* (2013). Circulating microRNA expression profiles associated with systemic lupus erythematosus. Arthritis Rheum 65, 1324-34.
[272] Ventriglia, G., Nigi, L., Sebastiani, G. and Dotta, F. (2015). MicroRNAs: Novel Players in the Dialogue between Pancreatic Islets and Immune System in Autoimmune Diabetes. Biomed Res Int 2015, 749734.
[273] Ferland-McCollough, D., Ozanne, S.E., Siddle, K., Willis, A.E. and Bushell, M. (2010). The involvement of microRNAs in Type 2 diabetes. Biochem Soc Trans 38, 1565-70.
[274] Sonkoly, E. *et al.* (2010). MiR-155 is overexpressed in patients with atopic dermatitis and modulates T-cell proliferative responses by targeting cytotoxic T lymphocyte-associated antigen 4. J Allergy Clin Immunol 126, 581-9.e1-20.
[275] Rebane, A. *et al.* (2014). MicroRNA-146a alleviates chronic skin inflammation in atopic dermatitis through suppression of innate immune responses in keratinocytes. J Allergy Clin Immunol 134, 836-847.e11.
[276] Szeto, C.C. and Li, P.K. (2014). MicroRNAs in IgA nephropathy. Nat Rev Nephrol 10, 249-56.
[277] Chapman, C.G. and Pekow, J. (2015). The emerging role of miRNAs in inflammatory bowel disease: a review. Therap Adv Gastroenterol 8, 4-22.
[278] Magni, S. *et al.* (2014). miRNAs affect the expression of innate and adaptive immunity proteins in celiac disease. Am J Gastroenterol 109, 1662-74.

[279] Tam, W., Ben-Yehuda, D. and Hayward, W.S. (1997). bic, a novel gene activated by proviral insertions in avian leukosis virus-induced lymphomas, is likely to function through its noncoding RNA. Mol Cell Biol 17, 1490-502.
[280] Tam, W. (2001). Identification and characterization of human BIC, a gene on chromosome 21 that encodes a noncoding RNA. Gene 274, 157-67.
[281] Eis, P.S., Tam, W., Sun, L., Chadburn, A., Li, Z., Gomez, M.F., Lund, E. and Dahlberg, J.E. (2005). Accumulation of miR-155 and BIC RNA in human B cell lymphomas. Proc Natl Acad Sci U S A 102, 3627-32.
[282] Martin, M.M., Lee, E.J., Buckenberger, J.A., Schmittgen, T.D. and Elton, T.S. (2006). MicroRNA-155 regulates human angiotensin II type 1 receptor expression in fibroblasts. J Biol Chem 281, 18277-84.
[283] Agarwal, V., Bell, G.W., Nam, J.W. and Bartel, D.P. (2015). Predicting effective microRNA target sites in mammalian mRNAs. Elife 4
[284] Tili, E., Croce, C.M. and Michaille, J.J. (2009). miR-155: on the crosstalk between inflammation and cancer. Int Rev Immunol 28, 264-84.
[285] Teng, G., Hakimpour, P., Landgraf, P., Rice, A., Tuschl, T., Casellas, R. and Papavasiliou, F.N. (2008). MicroRNA-155 is a negative regulator of activation-induced cytidine deaminase. Immunity 28, 621-9.
[286] Dorsett, Y. *et al.* (2008). MicroRNA-155 suppresses activation-induced cytidine deaminase-mediated Myc-Igh translocation. Immunity 28, 630-8.
[287] Yin, Q., McBride, J., Fewell, C., Lacey, M., Wang, X., Lin, Z., Cameron, J. and Flemington, E.K. (2008). MicroRNA-155 is an Epstein-Barr virus-induced gene that modulates Epstein-Barr virus-regulated gene expression pathways. Journal of virology 82, 5295-5306.
[288] O'Connell, R.M., Rao, D.S., Chaudhuri, A.A., Boldin, M.P., Taganov, K.D., Nicoll, J., Paquette, R.L. and Baltimore, D. (2008). Sustained expression of microRNA-155 in hematopoietic stem cells causes a myeloproliferative disorder. J Exp Med 205, 585-94.
[289] Nazari-Jahantigh, M. *et al.* (2012). MicroRNA-155 promotes atherosclerosis by repressing Bcl6 in macrophages. The Journal of clinical investigation 122, 4190-4202.
[290] Hu, R., Huffaker, T.B., Kagele, D.A., Runtsch, M.C., Bake, E., Chaudhuri, A.A., Round, J.L. and O'Connell, R.M. (2013). MicroRNA-155 confers encephalogenic potential to Th17 cells by promoting effector gene expression. Journal of immunology (Baltimore, Md. : 1950) 190, 5972-5980.
[291] Romania, P., Lulli, V., Pelosi, E., Biffoni, M., Peschle, C. and Marziali, G. (2008). MicroRNA 155 modulates megakaryopoiesis at progenitor and precursor level by targeting Ets-1 and Meis1 transcription factors. British journal of haematology 143, 570-580.
[292] Sandhu, S.K. *et al.* (2012). miR-155 targets histone deacetylase 4 (HDAC4) and impairs transcriptional activity of B-cell lymphoma 6 (BCL6) in the Eμ-miR-155 transgenic mouse model. Proc Natl Acad Sci U S A 109, 20047-52.
[293] Rodriguez, A. *et al.* (2007). Requirement of bic/microRNA-155 for normal immune function. Science (New York, N.Y.) 316, 608-611.
[294] Vigorito, E. *et al.* (2007). microRNA-155 regulates the generation of immunoglobulin class-switched plasma cells. Immunity 27, 847-859.
[295] Louafi, F., Martinez-Nunez, R.T. and Sanchez-Elsner, T. (2010). MicroRNA-155 targets SMAD2 and modulates the response of macrophages to transforming growth factor-{beta}. The Journal of biological chemistry 285, 41328-41336.
[296] Gironella, M. *et al.* (2007). Tumor protein 53-induced nuclear protein 1 expression is repressed by miR-155, and its restoration inhibits pancreatic tumor development. Proc Natl Acad Sci U S A 104, 16170-5.

[297] Martin, M.M. *et al.* (2007). The human angiotensin II type 1 receptor +1166 A/C polymorphism attenuates microRNA-155 binding. J Biol Chem 282, 24262-9.
[298] Sethupathy, P., Borel, C., Gagnebin, M., Grant, G.R., Deutsch, S., Elton, T.S., Hatzigeorgiou, A.G. and Antonarakis, S.E. (2007). Human microRNA-155 on chromosome 21 differentially interacts with its polymorphic target in the AGTR1 3' untranslated region: a mechanism for functional single-nucleotide polymorphisms related to phenotypes. Am J Hum Genet 81, 405-13.
[299] Okoye, I.S. *et al.* (2014). Transcriptomics identified a critical role for Th2 cell-intrinsic miR-155 in mediating allergy and antihelminth immunity. Proc Natl Acad Sci U S A 111, E3081-90.
[300] Martinez-Nunez, R.T., Louafi, F. and Sanchez-Elsner, T. (2011). The interleukin 13 (IL-13) pathway in human macrophages is modulated by microRNA-155 via direct targeting of interleukin 13 receptor alpha1 (IL13Ralpha1). J Biol Chem 286, 1786-94.
[301] Hu, X., Ye, J., Qin, A., Zou, H., Shao, H. and Qian, K. (2015). Both MicroRNA-155 and Virus-Encoded MiR-155 Ortholog Regulate TLR3 Expression. PLoS One 10, e0126012.
[302] Tili, E. *et al.* (2007). Modulation of miR-155 and miR-125b levels following lipopolysaccharide/TNF-alpha stimulation and their possible roles in regulating the response to endotoxin shock. J Immunol 179, 5082-9.
[303] Tang, B. *et al.* (2010). Identification of MyD88 as a novel target of miR-155, involved in negative regulation of Helicobacter pylori-induced inflammation. FEBS Lett 584, 1481-6.
[304] Wang, L. *et al.* (2014). Notch-dependent repression of miR-155 in the bone marrow niche regulates hematopoiesis in an NF-κB-dependent manner. Cell stem cell 15, 51-65.
[305] Kong, W., Yang, H., He, L., Zhao, J.J., Coppola, D., Dalton, W.S. and Cheng, J.Q. (2008). MicroRNA-155 is regulated by the transforming growth factor beta/Smad pathway and contributes to epithelial cell plasticity by targeting RhoA. Mol Cell Biol 28, 6773-84.
[306] Jiang, S., Zhang, H.-W., Lu, M.-H., He, X.-H., Li, Y., Gu, H., Liu, M.-F. and Wang, E.-D. (2010). MicroRNA-155 functions as an OncomiR in breast cancer by targeting the suppressor of cytokine signaling 1 gene. Cancer research 70, 3119-3127.
[307] Zhang, J., Zhao, H., Chen, J., Xia, B., Jin, Y., Wei, W., Shen, J. and Huang, Y. (2012). Interferon-β-induced miR-155 inhibits osteoclast differentiation by targeting SOCS1 and MITF. FEBS Letters 586, 3255-3262.
[308] De Santis, R. *et al.* (2016). miR-155 targets Caspase-3 mRNA in activated macrophages. RNA biology 13, 43-58.
[309] Ceppi, M., Pereira, P.M., Dunand-Sauthier, I., Barras, E., Reith, W., Santos, M.A. and Pierre, P. (2009). MicroRNA-155 modulates the interleukin-1 signaling pathway in activated human monocyte-derived dendritic cells. Proc Natl Acad Sci U S A 106, 2735-40.
[310] Zhou, H., Huang, X., Cui, H., Luo, X., Tang, Y., Chen, S., Wu, L. and Shen, N. (2010). miR-155 and its star-form partner miR-155* cooperatively regulate type I interferon production by human plasmacytoid dendritic cells. Blood 116, 5885-94.
[311] O'Connell, R.M., Chaudhuri, A.A., Rao, D.S. and Baltimore, D. (2009). Inositol phosphatase SHIP1 is a primary target of miR-155. Proceedings of the National Academy of Sciences of the United States of America 106, 7113-7118.
[312] Pedersen, I.M. *et al.* (2009). Onco-miR-155 targets SHIP1 to promote TNFalpha-dependent growth of B cell lymphomas. EMBO molecular medicine 1, 288-295.
[313] Xue, H., Hua, L.M., Guo, M. and Luo, J.M. (2014). SHIP1 is targeted by miR-155 in acute myeloid leukemia. Oncol Rep 32, 2253-9.
[314] Mashima, R. (2015). Physiological roles of miR-155. Immunology 145, 323-33.

[315] Murugaiyan, G., Beynon, V., Mittal, A., Joller, N. and Weiner, H.L. (2011). Silencing microRNA-155 ameliorates experimental autoimmune encephalomyelitis. J Immunol 187, 2213-21.
[316] Ceppi, M., Pereira, P.M., Dunand-Sauthier, I., Barras, E., Reith, W., Santos, M.A. and Pierre, P. (2009). MicroRNA-155 modulates the interleukin-1 signaling pathway in activated human monocyte-derived dendritic cells. Proceedings of the National Academy of Sciences of the United States of America 106, 2735-2740.
[317] An, H., Xu, H., Zhang, M., Zhou, J., Feng, T., Qian, C., Qi, R. and Cao, X. (2005). Src homology 2 domain-containing inositol-5-phosphatase 1 (SHIP1) negatively regulates TLR4-mediated LPS response primarily through a phosphatase activity- and PI-3K-independent mechanism. Blood 105, 4685-4692.
[318] Kurowska-Stolarska, M. *et al.* (2011). MicroRNA-155 as a proinflammatory regulator in clinical and experimental arthritis. Proc Natl Acad Sci U S A 108, 11193-8.
[319] Li, X., Tian, F. and Wang, F. (2013). Rheumatoid arthritis-associated microRNA-155 targets SOCS1 and upregulates TNF-α and IL-1β in PBMCs. Int J Mol Sci 14, 23910-21.
[320] Costinean, S., Zanesi, N., Pekarsky, Y., Tili, E., Volinia, S., Heerema, N. and Croce, C.M. (2006). Pre-B cell proliferation and lymphoblastic leukemia/high-grade lymphoma in E(mu)-miR155 transgenic mice. Proc Natl Acad Sci U S A 103, 7024-9.
[321] Zhong, H., Xu, L., Zhong, J.H., Xiao, F., Liu, Q., Huang, H.H. and Chen, F.Y. (2012). Clinical and prognostic significance of miR-155 and miR-146a expression levels in formalin-fixed/paraffin-embedded tissue of patients with diffuse large B-cell lymphoma. Exp Ther Med 3, 763-770.
[322] van den Berg, A. *et al.* (2003). High expression of B-cell receptor inducible gene BIC in all subtypes of Hodgkin lymphoma. Genes Chromosomes Cancer 37, 20-8.
[323] Kluiver, J., Poppema, S., de Jong, D., Blokzijl, T., Harms, G., Jacobs, S., Kroesen, B.J. and van den Berg, A. (2005). BIC and miR-155 are highly expressed in Hodgkin, primary mediastinal and diffuse large B cell lymphomas. J Pathol 207, 243-9.
[324] Cui, B. *et al.* (2014). MicroRNA-155 influences B-cell receptor signaling and associates with aggressive disease in chronic lymphocytic leukemia. Blood 124, 546-54.
[325] Ferrajoli, A. *et al.* (2013). Prognostic value of miR-155 in individuals with monoclonal B-cell lymphocytosis and patients with B chronic lymphocytic leukemia. Blood 122, 1891-9.
[326] Marcucci, G. *et al.* (2013). Clinical role of microRNAs in cytogenetically normal acute myeloid leukemia: miR-155 upregulation independently identifies high-risk patients. J Clin Oncol 31, 2086-93.
[327] Volinia, S. *et al.* (2006). A microRNA expression signature of human solid tumors defines cancer gene targets. Proc Natl Acad Sci U S A 103, 2257-61.
[328] Yin, Q., Wang, X., McBride, J., Fewell, C. and Flemington, E. (2008). B-cell receptor activation induces BIC/miR-155 expression through a conserved AP-1 element. J Biol Chem 283, 2654-62.
[329] Zheng, Y., Josefowicz, S.Z., Kas, A., Chu, T.T., Gavin, M.A. and Rudensky, A.Y. (2007). Genome-wide analysis of Foxp3 target genes in developing and mature regulatory T cells. Nature 445, 936-40.
[330] Kohlhaas, S., Garden, O.A., Scudamore, C., Turner, M., Okkenhaug, K. and Vigorito, E. (2009). Cutting edge: the Foxp3 target miR-155 contributes to the development of regulatory T cells. J Immunol 182, 2578-82.
[331] Takahashi, R. *et al.* (2011). SOCS1 is essential for regulatory T cell functions by preventing loss of Foxp3 expression as well as IFN-{gamma} and IL-17A production. J Exp Med 208, 2055-67.
[332] Tili, E. *et al.* (2010). Resveratrol decreases the levels of miR-155 by upregulating miR-663, a microRNA targeting JunB and JunD. Carcinogenesis 31, 1561-6.

[333] McCoy, C.E., Sheedy, F.J., Qualls, J.E., Doyle, S.L., Quinn, S.R., Murray, P.J. and O'Neill, L.A.J. (2010). IL-10 inhibits miR-155 induction by toll-like receptors. The Journal of biological chemistry 285, 20492-20498.
[334] Koch, M., Mollenkopf, H.J., Klemm, U. and Meyer, T.F. (2012). Induction of microRNA-155 is TLR- and type IV secretion system-dependent in macrophages and inhibits DNA-damage induced apoptosis. Proc Natl Acad Sci U S A 109, E1153-62.
[335] Wang, P. *et al.* (2010). Inducible microRNA-155 feedback promotes type I IFN signaling in antiviral innate immunity by targeting suppressor of cytokine signaling 1. J Immunol 185, 6226-33.
[336] Kong, W., Yang, H., He, L., Zhao, J.-j., Coppola, D., Dalton, W.S. and Cheng, J.Q. (2008). MicroRNA-155 is regulated by the transforming growth factor beta/Smad pathway and contributes to epithelial cell plasticity by targeting RhoA. Molecular and cellular biology 28, 6773-6784.
[337] Chang, S. *et al.* (2011). Tumor suppressor BRCA1 epigenetically controls oncogenic microRNA-155. Nat Med 17, 1275-82.
[338] Gottwein, E. *et al.* (2007). A viral microRNA functions as an orthologue of cellular miR-155. Nature 450, 1096-9.
[339] Skalsky, R.L., Samols, M.A., Plaisance, K.B., Boss, I.W., Riva, A., Lopez, M.C., Baker, H.V. and Renne, R. (2007). Kaposi's sarcoma-associated herpesvirus encodes an ortholog of miR-155. J Virol 81, 12836-45.
[340] Liu, Y., Sun, R., Lin, X., Liang, D., Deng, Q. and Lan, K. (2012). Kaposi's sarcoma-associated herpesvirus-encoded microRNA miR-K12-11 attenuates transforming growth factor beta signaling through suppression of SMAD5. J Virol 86, 1372-81.
[341] Boss, I.W., Nadeau, P.E., Abbott, J.R., Yang, Y., Mergia, A. and Renne, R. (2011). A Kaposi's sarcoma-associated herpesvirus-encoded ortholog of microRNA miR-155 induces human splenic B-cell expansion in NOD/LtSz-scid IL2Rγnull mice. J Virol 85, 9877-86.
[342] Yu, Z.H. *et al.* (2014). Virus-encoded miR-155 ortholog is an important potential regulator but not essential for the development of lymphomas induced by very virulent Marek's disease virus. Virology 448, 55-64.
[343] Zhao, Y. *et al.* (2011). Critical role of the virus-encoded microRNA-155 ortholog in the induction of Marek's disease lymphomas. PLoS Pathog 7, e1001305.
[344] Fiorentino, D.F., Bond, M.W. and Mosmann, T.R. (1989). Two types of mouse T helper cell. IV. Th2 clones secrete a factor that inhibits cytokine production by Th1 clones. J Exp Med 170, 2081-95.
[345] de Waal Malefyt, R., Abrams, J., Bennett, B., Figdor, C.G. and de Vries, J.E. (1991). Interleukin 10(IL-10) inhibits cytokine synthesis by human monocytes: an autoregulatory role of IL-10 produced by monocytes. J Exp Med 174, 1209-20.
[346] Bogdan, C., Vodovotz, Y. and Nathan, C. (1991). Macrophage deactivation by interleukin 10. J Exp Med 174, 1549-55.
[347] Oswald, I.P., Wynn, T.A., Sher, A. and James, S.L. (1992). Interleukin 10 inhibits macrophage microbicidal activity by blocking the endogenous production of tumor necrosis factor alpha required as a costimulatory factor for interferon gamma-induced activation. Proc Natl Acad Sci U S A 89, 8676-80.
[348] Moore, K.W., de Waal Malefyt, R., Coffman, R.L. and O'Garra, A. (2001). Interleukin-10 and the interleukin-10 receptor. Annual Review of Immunology 19, 683-765.
[349] Saraiva, M. and O'Garra, A. (2010). The regulation of IL-10 production by immune cells. Nature Reviews Immunology 10, 170-181.
[350] Foey, A.D., Parry, S.L., Williams, L.M., Feldmann, M., Foxwell, B.M. and Brennan, F.M. (1998). Regulation of monocyte IL-10 synthesis by endogenous IL-1 and TNF-alpha: role of the p38 and p42/44 mitogen-activated protein kinases. J Immunol 160, 920-8.

[351] Saraiva, M. and O'Garra, A. (2010). The regulation of IL-10 production by immune cells. Nat Rev Immunol 10, 170-81.
[352] Banerjee, A., Gugasyan, R., McMahon, M. and Gerondakis, S. (2006). Diverse Toll-like receptors utilize Tpl2 to activate extracellular signal-regulated kinase (ERK) in hemopoietic cells. Proc Natl Acad Sci U S A 103, 3274-9.
[353] Kanters, E. *et al.* (2003). Inhibition of NF-kappaB activation in macrophages increases atherosclerosis in LDL receptor-deficient mice. J Clin Invest 112, 1176-85.
[354] Powell, M.J., Thompson, S.A., Tone, Y., Waldmann, H. and Tone, M. (2000). Posttranscriptional regulation of IL-10 gene expression through sequences in the 3'-untranslated region. J Immunol 165, 292-6.
[355] Stoecklin, G., Tenenbaum, S.A., Mayo, T., Chittur, S.V., George, A.D., Baroni, T.E., Blackshear, P.J. and Anderson, P. (2008). Genome-wide analysis identifies interleukin-10 mRNA as target of tristetraprolin. J Biol Chem 283, 11689-99.
[356] Sharma, A., Kumar, M., Aich, J., Hariharan, M., Brahmachari, S.K., Agrawal, A. and Ghosh, B. (2009). Posttranscriptional regulation of interleukin-10 expression by hsa-miR-106a. Proc Natl Acad Sci U S A 106, 5761-6.
[357] Ma, F., Liu, X., Li, D., Wang, P., Li, N., Lu, L. and Cao, X. (2010). MicroRNA-466l upregulates IL-10 expression in TLR-triggered macrophages by antagonizing RNA-binding protein tristetraprolin-mediated IL-10 mRNA degradation. J Immunol 184, 6053-9.
[358] Swaminathan, S. *et al.* (2012). Differential regulation of the Let-7 family of microRNAs in CD4+ T cells alters IL-10 expression. J Immunol 188, 6238-46.
[359] Zdanov, A., Schalk-Hihi, C., Gustchina, A., Tsang, M., Weatherbee, J. and Wlodawer, A. (1995). Crystal structure of interleukin-10 reveals the functional dimer with an unexpected topological similarity to interferon gamma. Structure/Folding and Design 3, 591-601.
[360] Pils, M.C. *et al.* (2010). Monocytes/macrophages and/or neutrophils are the target of IL-10 in the LPS endotoxemia model. Eur J Immunol 40, 443-8.
[361] Rossato, M. *et al.* (2012). IL-10-induced microRNA-187 negatively regulates TNF-α, IL-6, and IL-12p40 production in TLR4-stimulated monocytes. Proceedings of the National Academy of Sciences of the United States of America 109, E3101-10.
[362] Ho, A.S., Liu, Y., Khan, T.A., Hsu, D.H., Bazan, J.F. and Moore, K.W. (1993). A receptor for interleukin 10 is related to interferon receptors. Proc Natl Acad Sci U S A 90, 11267-71.
[363] Kotenko, S.V., Krause, C.D., Izotova, L.S., Pollack, B.P., Wu, W. and Pestka, S. (1997). Identification and functional characterization of a second chain of the interleukin-10 receptor complex. EMBO J 16, 5894-903.
[364] Sheppard, P. *et al.* (2003). IL-28, IL-29 and their class II cytokine receptor IL-28R. Nat Immunol 4, 63-8.
[365] Donnelly, R.P., Sheikh, F., Kotenko, S.V. and Dickensheets, H. (2004). The expanded family of class II cytokines that share the IL-10 receptor-2 (IL-10R2) chain. J Leukoc Biol 76, 314-21.
[366] Sheikh, F. *et al.* (2004). Cutting edge: IL-26 signals through a novel receptor complex composed of IL-20 receptor 1 and IL-10 receptor 2. J Immunol 172, 2006-10.
[367] Ding, Y., Qin, L., Zamarin, D., Kotenko, S.V., Pestka, S., Moore, K.W. and Bromberg, J.S. (2001). Differential IL-10R1 expression plays a critical role in IL-10-mediated immune regulation. J Immunol 167, 6884-92.
[368] Finbloom, D.S. and Winestock, K.D. (1995). IL-10 induces the tyrosine phosphorylation of tyk2 and Jak1 and the differential assembly of STAT1 alpha and STAT3 complexes in human T cells and monocytes. J Immunol 155, 1079-90.

[369] Weber-Nordt, R.M., Riley, J.K., Greenlund, A.C., Moore, K.W., Darnell, J.E. and Schreiber, R.D. (1996). Stat3 recruitment by two distinct ligand-induced, tyrosine-phosphorylated docking sites in the interleukin-10 receptor intracellular domain. J Biol Chem 271, 27954-61.
[370] Zhu, Y.P., Brown, J.R., Sag, D., Zhang, L. and Suttles, J. (2015). Adenosine 5'-monophosphate-activated protein kinase regulates IL-10-mediated anti-inflammatory signaling pathways in macrophages. Journal of immunology (Baltimore, Md. : 1950) 194, 584-594.
[371] Kishore, R., Tebo, J.M., Kolosov, M. and Hamilton, T.A. (1999). Cutting edge: clustered AU-rich elements are the target of IL-10-mediated mRNA destabilization in mouse macrophages. J Immunol 162, 2457-61.
[372] Rajasingh, J. *et al.* (2006). IL-10-induced TNF-alpha mRNA destabilization is mediated via IL-10 suppression of p38 MAP kinase activation and inhibition of HuR expression. FASEB J 20, 2112-4.
[373] El Kasmi, K.C. *et al.* (2006). General nature of the STAT3-activated anti-inflammatory response. J Immunol 177, 7880-8.
[374] Murray, P.J. (2006). STAT3-mediated anti-inflammatory signalling. Biochem Soc Trans 34, 1028-31.
[375] Cheung, S.T., So, E.Y., Chang, D., Ming-Lum, A. and Mui, A.L.F. (2013). Interleukin-10 Inhibits Lipopolysaccharide Induced miR-155 Precursor Stability and Maturation. PLoS One 8, e71336.
[376] Ming-Lum, A.N. (2012) The role of SH2-domain inositol 5' phosphatase in the inhibition of macrophage activation (Doctoral Dissertation)ed.^eds). University of British Columbia
[377] Ouyang, W., Rutz, S., Crellin, N.K., Valdez, P.A. and Hymowitz, S.G. (2011). Regulation and Functions of the IL-10 Family of Cytokines in Inflammation and Disease. Annual Review of Immunology 29, 71-109.
[378] Kuhn, R., Lohler, J., Rennick, D., Rajewsky, K. and Muller, W. (1993). Interleukin-10-deficient mice develop chronic enterocolitis. Cell 75, 263-74.
[379] Howard, M., Muchamuel, T., Andrade, S. and Menon, S. (1993). Interleukin 10 protects mice from lethal endotoxemia. J Exp Med 177, 1205-8.
[380] Rennick, D.M., Fort, M.M. and Davidson, N.J. (1997). Studies with IL-10-/- mice: an overview. J Leukoc Biol 61, 389-96.
[381] Moran, C.J. *et al.* (2013). IL-10R polymorphisms are associated with very-early-onset ulcerative colitis. Inflamm Bowel Dis 19, 115-23.
[382] Lyon, H. *et al.* (2004). IL10 gene polymorphisms are associated with asthma phenotypes in children. Genet Epidemiol 26, 155-65.
[383] Gaddam, S.L., Priya, V.H., Babu, B.M., Joshi, L., Venkatasubramanian, S. and Valluri, V. (2012). Association of interleukin-10 gene promoter polymorphism in allergic patients. Genet Test Mol Biomarkers 16, 632-5.
[384] Ying, B., Shi, Y., Pan, X., Song, X., Huang, Z., Niu, Q., Cai, B. and Wang, L. (2011). Association of polymorphisms in the human IL-10 and IL-18 genes with rheumatoid arthritis. Mol Biol Rep 38, 379-85.
[385] Esser, N., Legrand-Poels, S., Piette, J., Scheen, A.J. and Paquot, N. (2014). Inflammation as a link between obesity, metabolic syndrome and type 2 diabetes. Diabetes Res Clin Pract 105, 141-50.
[386] van Exel, E., Gussekloo, J., de Craen, A.J., Frölich, M., Bootsma-Van Der Wiel, A., Westendorp, R.G. and Study, L.P. (2002). Low production capacity of interleukin-10 associates with the metabolic syndrome and type 2 diabetes : the Leiden 85-Plus Study. Diabetes 51, 1088-92.
[387] Hong, E.G. *et al.* (2009). Interleukin-10 prevents diet-induced insulin resistance by attenuating macrophage and cytokine response in skeletal muscle. Diabetes 58, 2525-35.

[388] Gao, M., Zhang, C., Ma, Y., Bu, L., Yan, L. and Liu, D. (2013). Hydrodynamic Delivery of mIL10 Gene Protects Mice From High-fat Diet-induced Obesity and Glucose Intolerance. Mol Ther 21, 1852-61.
[389] Moore, K.W., Vieira, P., Fiorentino, D.F., Trounstine, M.L., Khan, T.A. and Mosmann, T.R. (1990). Homology of cytokine synthesis inhibitory factor (IL-10) to the Epstein-Barr virus gene BCRFI. Science 248, 1230-4.
[390] O'Garra, A. and Murphy, K.M. (2009). From IL-10 to IL-12: how pathogens and their products stimulate APCs to induce T(H)1 development. Nat Immunol 10, 929-32.
[391] Tomoyose, M., Mitsuyama, K., Ishida, H., Toyonaga, A. and Tanikawa, K. (1998). Role of interleukin-10 in a murine model of dextran sulfate sodium-induced colitis. Scand J Gastroenterol 33, 435-40.
[392] Duchmann, R., Schmitt, E., Knolle, P., Meyer zum Büschenfelde, K.H. and Neurath, M. (1996). Tolerance towards resident intestinal flora in mice is abrogated in experimental colitis and restored by treatment with interleukin-10 or antibodies to interleukin-12. Eur J Immunol 26, 934-8.
[393] Braat, H., Peppelenbosch, M.P. and Hommes, D.W. (2003). Interleukin-10-based therapy for inflammatory bowel disease. Expert Opin Biol Ther 3, 725-31.
[394] Marlow, G.J., van Gent, D. and Ferguson, L.R. (2013). Why interleukin-10 supplementation does not work in Crohn's disease patients. World J Gastroenterol 19, 3931-41.
[395] Tilg, H. *et al.* (2002). Treatment of Crohn's disease with recombinant human interleukin 10 induces the proinflammatory cytokine interferon gamma. Gut 50, 191-5.
[396] Lim, C.P. and Cao, X. (2006). Structure, function, and regulation of STAT proteins. Mol Biosyst 2, 536-50.
[397] Zhong, Z., Wen, Z. and Darnell, J.E. (1994). Stat3: a STAT family member activated by tyrosine phosphorylation in response to epidermal growth factor and interleukin-6. Science 264, 95-8.
[398] Darnell, J.E., Kerr, I.M. and Stark, G.R. (1994). Jak-STAT pathways and transcriptional activation in response to IFNs and other extracellular signaling proteins. Science 264, 1415-21.
[399] Darnell, J.E. (1998). Studies of IFN-induced transcriptional activation uncover the Jak-Stat pathway. J Interferon Cytokine Res 18, 549-54.
[400] Milner, J.D. *et al.* (2015). Early-onset lymphoproliferation and autoimmunity caused by germline STAT3 gain-of-function mutations. Blood 125, 591-9.
[401] Haapaniemi, E.M. *et al.* (2015). Autoimmunity, hypogammaglobulinemia, lymphoproliferation, and mycobacterial disease in patients with activating mutations in STAT3. Blood 125, 639-48.
[402] Flanagan, S.E. *et al.* (2014). Activating germline mutations in STAT3 cause early-onset multi-organ autoimmune disease. Nat Genet 46, 812-4.
[403] Levy, D.E. and Loomis, C.A. (2007). STAT3 signaling and the hyper-IgE syndrome. N Engl J Med 357, 1655-8.
[404] Buettner, R., Mora, L.B. and Jove, R. (2002). Activated STAT signaling in human tumors provides novel molecular targets for therapeutic intervention. Clin Cancer Res 8, 945-54.
[405] Yu, H. and Jove, R. (2004). The STATs of cancer--new molecular targets come of age. Nat Rev Cancer 4, 97-105.
[406] Haura, E.B., Turkson, J. and Jove, R. (2005). Mechanisms of disease: Insights into the emerging role of signal transducers and activators of transcription in cancer. Nat Clin Pract Oncol 2, 315-24.
[407] Yu, H., Pardoll, D. and Jove, R. (2009). STATs in cancer inflammation and immunity: a leading role for STAT3. Nat Rev Cancer 9, 798-809.

[408] Herrmann, A. *et al.* (2010). Targeting Stat3 in the myeloid compartment drastically improves the in vivo antitumor functions of adoptively transferred T cells. Cancer Res 70, 7455-64.
[409] Kortylewski, M. and Yu, H. (2008). Role of Stat3 in suppressing anti-tumor immunity. Curr Opin Immunol 20, 228-33.
[410] Kujawski, M., Kortylewski, M., Lee, H., Herrmann, A., Kay, H. and Yu, H. (2008). Stat3 mediates myeloid cell-dependent tumor angiogenesis in mice. J Clin Invest 118, 3367-77.
[411] Wang, L., Yi, T., Kortylewski, M., Pardoll, D.M., Zeng, D. and Yu, H. (2009). IL-17 can promote tumor growth through an IL-6-Stat3 signaling pathway. J Exp Med 206, 1457-64.
[412] Takeda, K., Noguchi, K., Shi, W., Tanaka, T., Matsumoto, M., Yoshida, N., Kishimoto, T. and Akira, S. (1997). Targeted disruption of the mouse Stat3 gene leads to early embryonic lethality. Proceedings of the National Academy of Sciences of the United States of America 94, 3801-3804.
[413] Takeda, K., Clausen, B.E., Kaisho, T., Tsujimura, T., Terada, N., Förster, I. and Akira, S. (1999). Enhanced Th1 activity and development of chronic enterocolitis in mice devoid of Stat3 in macrophages and neutrophils. Immunity 10, 39-49.
[414] Fukada, T., Hibi, M., Yamanaka, Y., Takahashi-Tezuka, M., Fujitani, Y., Yamaguchi, T., Nakajima, K. and Hirano, T. (1996). Two signals are necessary for cell proliferation induced by a cytokine receptor gp130: involvement of STAT3 in anti-apoptosis. Immunity 5, 449-60.
[415] Takeda, K., Kaisho, T., Yoshida, N., Takeda, J., Kishimoto, T. and Akira, S. (1998). Stat3 activation is responsible for IL-6-dependent T cell proliferation through preventing apoptosis: generation and characterization of T cell-specific Stat3-deficient mice. The Journal of Immunology 161, 4652-4660.
[416] Lang, R., Patel, D., Morris, J.J., Rutschman, R.L. and Murray, P.J. (2002). Shaping gene expression in activated and resting primary macrophages by IL-10. The Journal of Immunology 169, 2253-2263.
[417] El Kasmi, K.C. *et al.* (2007). Cutting edge: A transcriptional repressor and corepressor induced by the STAT3-regulated anti-inflammatory signaling pathway. The Journal of Immunology 179, 7215-7219.
[418] Hutchins, A.P., Diez, D., Takahashi, Y., Ahmad, S., Jauch, R., Tremblay, M.L. and Miranda-Saavedra, D. (2013). Distinct transcriptional regulatory modules underlie STAT3's cell type-independent and cell type-specific functions. Nucleic Acids Res 41, 2155-70.
[419] O'Farrell, A.M., Liu, Y., Moore, K.W. and Mui, A.L. (1998). IL-10 inhibits macrophage activation and proliferation by distinct signaling mechanisms: evidence for Stat3-dependent and -independent pathways. EMBO J 17, 1006-18.
[420] Williams, L., Bradley, L., Smith, A. and Foxwell, B. (2004). Signal transducer and activator of transcription 3 is the dominant mediator of the anti-inflammatory effects of IL-10 in human macrophages. The Journal of Immunology 172, 567-576.
[421] Berg, D.J., Kühn, R., Rajewsky, K., Müller, W., Menon, S., Davidson, N., Grünig, G. and Rennick, D. (1995). Interleukin-10 is a central regulator of the response to LPS in murine models of endotoxic shock and the Shwartzman reaction but not endotoxin tolerance. J Clin Invest 96, 2339-47.
[422] Chalhoub, N. and Baker, S.J. (2009). PTEN and the PI3-kinase pathway in cancer. Annual review of pathology 4, 127-150.
[423] Hazen, A.L., Smith, M.J., Desponts, C., Winter, O., Moser, K. and Kerr, W.G. (2009). SHIP is required for a functional hematopoietic stem cell niche. Blood 113, 2924-33.
[424] Pesesse, X., Deleu, S., De Smedt, F., Drayer, L. and Erneux, C. (1997). Identification of a second SH2-domain-containing protein closely related to the phosphatidylinositol polyphosphate 5-phosphatase SHIP. Biochem Biophys Res Commun 239, 697-700.

[425] Xie, J., Erneux, C. and Pirson, I. (2013). How does SHIP1/2 balance PtdIns(3,4)P 2and does it signal independently of its phosphatase activity? BioEssays : news and reviews in molecular, cellular and developmental biology 35, 733-743.
[426] CondÃ, C., Gloire, G. and Piette, J. (2011). Enzymatic and non-enzymatic activities of SHIP-1 in signal transduction and cancer. Biochemical Pharmacology 82, 1320-1334.
[427] Liu, L., Damen, J.E., Cutler, R.L. and Krystal, G. (1994). Multiple cytokines stimulate the binding of a common 145-kilodalton protein to Shc at the Grb2 recognition site of Shc. Mol Cell Biol 14, 6926-35.
[428] Damen, J.E., Liu, L., Rosten, P., Humphries, R.K., Jefferson, A.B., Majerus, P.W. and Krystal, G. (1996). The 145-kDa protein induced to associate with Shc by multiple cytokines is an inositol tetraphosphate and phosphatidylinositol 3,4,5-triphosphate 5-phosphatase. Proceedings of the National Academy of Sciences of the United States of America 93, 1689-1693.
[429] Ming-Lum, A. *et al.* (2012). A pleckstrin homology-related domain in SHIP1 mediates membrane localization during Fcγ receptor-induced phagocytosis. FASEB J 26, 3163-77.
[430] Ong, C.J. *et al.* (2007). Small-molecule agonists of SHIP1 inhibit the phosphoinositide 3-kinase pathway in hematopoietic cells. Blood 110, 1942-1949.
[431] Lamkin, T.D., Walk, S.F., Liu, L., Damen, J.E., Krystal, G. and Ravichandran, K.S. (1997). Shc interaction with Src homology 2 domain containing inositol phosphatase (SHIP) in vivo requires the Shc-phosphotyrosine binding domain and two specific phosphotyrosines on SHIP. J Biol Chem 272, 10396-401.
[432] Mason, J.M., Beattie, B.K., Liu, Q., Dumont, D.J. and Barber, D.L. (2000). The SH2 inositol 5-phosphatase Ship1 is recruited in an SH2-dependent manner to the erythropoietin receptor. J Biol Chem 275, 4398-406.
[433] Lemay, S., Davidson, D., Latour, S. and Veillette, A. (2000). Dok-3, a novel adapter molecule involved in the negative regulation of immunoreceptor signaling. Mol Cell Biol 20, 2743-54.
[434] Tu, Z. *et al.* (2001). Embryonic and hematopoietic stem cells express a novel SH2-containing inositol 5'-phosphatase isoform that partners with the Grb2 adapter protein. Blood 98, 2028-38.
[435] Sattler, M., Verma, S., Pride, Y.B., Salgia, R., Rohrschneider, L.R. and Griffin, J.D. (2001). SHIP1, an SH2 domain containing polyinositol-5-phosphatase, regulates migration through two critical tyrosine residues and forms a novel signaling complex with DOK1 and CRKL. J Biol Chem 276, 2451-8.
[436] Kerr, W.G. (2011). Inhibitor and activator: dual functions for SHIP in immunity and cancer. Ann N Y Acad Sci 1217, 1-17.
[437] Tridandapani, S., Kelley, T., Pradhan, M., Cooney, D., Justement, L.B. and Coggeshall, K.M. (1997). Recruitment and phosphorylation of SH2-containing inositol phosphatase and Shc to the B-cell Fc gamma immunoreceptor tyrosine-based inhibition motif peptide motif. Mol Cell Biol 17, 4305-11.
[438] Williamson, M.P. (1994). The structure and function of proline-rich regions in proteins. Biochem J 297 (Pt 2), 249-60.
[439] Helgason, C.D. *et al.* (1998). Targeted disruption of SHIP leads to hemopoietic perturbations, lung pathology, and a shortened life span. Genes Dev 12, 1610-20.
[440] Takeshita, S. *et al.* (2002). SHIP-deficient mice are severely osteoporotic due to increased numbers of hyper-resorptive osteoclasts. Nat Med 8, 943-9.
[441] Helgason, C.D., Antonchuk, J., Bodner, C. and Humphries, R.K. (2003). Homeostasis and regeneration of the hematopoietic stem cell pool are altered in SHIP-deficient mice. Blood 102, 3541-7.

[442] Locke, N.R., Patterson, S.J., Hamilton, M.J., Sly, L.M., Krystal, G. and Levings, M.K. (2009). SHIP regulates the reciprocal development of T regulatory and Th17 cells. J Immunol 183, 975-83.
[443] Ghansah, T. *et al.* (2004). Expansion of myeloid suppressor cells in SHIP-deficient mice represses allogeneic T cell responses. J Immunol 173, 7324-30.
[444] Kashiwada, M. *et al.* (2006). Downstream of tyrosine kinases-1 and Src homology 2-containing inositol 5'-phosphatase are required for regulation of CD4+CD25+ T cell development. J Immunol 176, 3958-65.
[445] Collazo, M.M. *et al.* (2009). SHIP limits immunoregulatory capacity in the T-cell compartment. Blood 113, 2934-44.
[446] Tarasenko, T., Kole, H.K., Chi, A.W., Mentink-Kane, M.M., Wynn, T.A. and Bolland, S. (2007). T cell-specific deletion of the inositol phosphatase SHIP reveals its role in regulating Th1/Th2 and cytotoxic responses. Proc Natl Acad Sci U S A 104, 11382-7.
[447] Buhl, A.M., Pleiman, C.M., Rickert, R.C. and Cambier, J.C. (1997). Qualitative regulation of B cell antigen receptor signaling by CD19: selective requirement for PI3-kinase activation, inositol-1,4,5-trisphosphate production and Ca2+ mobilization. J Exp Med 186, 1897-910.
[448] Hippen, K.L., Buhl, A.M., D'Ambrosio, D., Nakamura, K., Persin, C. and Cambier, J.C. (1997). Fc gammaRIIB1 inhibition of BCR-mediated phosphoinositide hydrolysis and Ca2+ mobilization is integrated by CD19 dephosphorylation. Immunity 7, 49-58.
[449] Brauweiler, A.M., Tamir, I. and Cambier, J.C. (2000). Bilevel control of B-cell activation by the inositol 5-phosphatase SHIP. Immunol Rev 176, 69-74.
[450] Gold, M.R., Scheid, M.P., Santos, L., Dang-Lawson, M., Roth, R.A., Matsuuchi, L., Duronio, V. and Krebs, D.L. (1999). The B cell antigen receptor activates the Akt (protein kinase B)/glycogen synthase kinase-3 signaling pathway via phosphatidylinositol 3-kinase. J Immunol 163, 1894-905.
[451] Fluckiger, A.C. *et al.* (1998). Btk/Tec kinases regulate sustained increases in intracellular Ca2+ following B-cell receptor activation. EMBO J 17, 1973-85.
[452] Isnardi, I., Bruhns, P., Bismuth, G., Fridman, W.H. and Daëron, M. (2006). The SH2 domain-containing inositol 5-phosphatase SHIP1 is recruited to the intracytoplasmic domain of human FcgammaRIIB and is mandatory for negative regulation of B cell activation. Immunol Lett 104, 156-65.
[453] Bolland, S., Pearse, R.N., Kurosaki, T. and Ravetch, J.V. (1998). SHIP modulates immune receptor responses by regulating membrane association of Btk. Immunity 8, 509-16.
[454] Tridandapani, S., Phee, H., Shivakumar, L., Kelley, T.W. and Coggeshall, K.M. (1998). Role of SHIP in FcgammaRIIb-mediated inhibition of Ras activation in B cells. Mol Immunol 35, 1135-46.
[455] Okkenhaug, K. and Vanhaesebroeck, B. (2003). PI3K in lymphocyte development, differentiation and activation. Nat Rev Immunol 3, 317-30.
[456] Dong, S., Corre, B., Foulon, E., Dufour, E., Veillette, A., Acuto, O. and Michel, F. (2006). T cell receptor for antigen induces linker for activation of T cell-dependent activation of a negative signaling complex involving Dok-2, SHIP-1, and Grb-2. J Exp Med 203, 2509-18.
[457] Pegram, H.J., Andrews, D.M., Smyth, M.J., Darcy, P.K. and Kershaw, M.H. (2011). Activating and inhibitory receptors of natural killer cells. Immunol Cell Biol 89, 216-24.
[458] Fauriat, C., Long, E.O., Ljunggren, H.G. and Bryceson, Y.T. (2010). Regulation of human NK-cell cytokine and chemokine production by target cell recognition. Blood 115, 2167-76.

[459] Galandrini, R., Tassi, I., Morrone, S., Lanfrancone, L., Pelicci, P., Piccoli, M., Frati, L. and Santoni, A. (2001). The adaptor protein shc is involved in the negative regulation of NK cell-mediated cytotoxicity. Eur J Immunol 31, 2016-25.
[460] Galli, S.J. and Tsai, M. (2012). IgE and mast cells in allergic disease. Nat Med 18, 693-704.
[461] Rivera, J., Fierro, N.A., Olivera, A. and Suzuki, R. (2008). New insights on mast cell activation via the high affinity receptor for IgE. Adv Immunol 98, 85-120.
[462] Gimborn, K., Lessmann, E., Kuppig, S., Krystal, G. and Huber, M. (2005). SHIP down-regulates FcepsilonR1-induced degranulation at supraoptimal IgE or antigen levels. J Immunol 174, 507-16.
[463] Ott, V.L., Tamir, I., Niki, M., Pandolfi, P.P. and Cambier, J.C. (2002). Downstream of kinase, p62(dok), is a mediator of Fc gamma IIB inhibition of Fc epsilon RI signaling. J Immunol 168, 4430-9.
[464] Rauh, M.J., Sly, L.M., Kalesnikoff, J., Hughes, M.R., Cao, L.P., Lam, V. and Krystal, G. (2004). The role of SHIP1 in macrophage programming and activation. Biochem Soc Trans 32, 785-8.
[465] Weisser, S.B., McLarren, K.W., Voglmaier, N., van Netten-Thomas, C.J., Antov, A., Flavell, R.A. and Sly, L.M. (2011). Alternative activation of macrophages by IL-4 requires SHIP degradation. Eur J Immunol 41, 1742-53.
[466] Pan, H., Ding, E., Hu, M., Lagoo, A.S., Datto, M.B. and Lagoo-Deenadayalan, S.A. (2010). SMAD4 is required for development of maximal endotoxin tolerance. J Immunol 184, 5502-9.
[467] Gabhann, J.N., Higgs, R., Brennan, K., Thomas, W., Damen, J.E., Ben Larbi, N., Krystal, G. and Jefferies, C.A. (2010). Absence of SHIP-1 results in constitutive phosphorylation of tank-binding kinase 1 and enhanced TLR3-dependent IFN-beta production. J Immunol 184, 2314-20.
[468] Cox, D., Dale, B.M., Kashiwada, M., Helgason, C.D. and Greenberg, S. (2001). A regulatory role for Src homology 2 domain-containing inositol 5'-phosphatase (SHIP) in phagocytosis mediated by Fc gamma receptors and complement receptor 3 (alpha(M)beta(2); CD11b/CD18). J Exp Med 193, 61-71.
[469] Tiwari, S., Choi, H.P., Matsuzawa, T., Pypaert, M. and MacMicking, J.D. (2009). Targeting of the GTPase Irgm1 to the phagosomal membrane via PtdIns(3,4)P(2) and PtdIns(3,4,5)P(3) promotes immunity to mycobacteria. Nat Immunol 10, 907-17.
[470] Kamen, L.A., Levinsohn, J., Cadwallader, A., Tridandapani, S. and Swanson, J.A. (2008). SHIP-1 increases early oxidative burst and regulates phagosome maturation in macrophages. J Immunol 180, 7497-505.
[471] Valderrama-Carvajal, H., Cocolakis, E., Lacerte, A., Lee, E.H., Krystal, G., Ali, S. and Lebrun, J.J. (2002). Activin/TGF-beta induce apoptosis through Smad-dependent expression of the lipid phosphatase SHIP. Nat Cell Biol 4, 963-9.
[472] Costinean, S., Sandhu, S.K., Pedersen, I.M., Tili, E. and Trotta, R. (2009). Src homology 2 domain–containing inositol-5-phosphatase and CCAAT enhancer-binding protein β are targeted by miR-155 in B cells of Eμ-MiR-155 …. Blood
[473] Ruschmann, J. *et al.* (2010). Tyrosine phosphorylation of SHIP promotes its proteasomal degradation. Exp Hematol 38, 392-402, 402.e1.
[474] Zhang, J., Ravichandran, K.S. and Garrison, J.C. (2010). A key role for the phosphorylation of Ser440 by the cyclic AMP-dependent protein kinase in regulating the activity of the Src homology 2 domain-containing Inositol 5'-phosphatase (SHIP1). J Biol Chem 285, 34839-49.
[475] Zhang, J., Walk, S.F., Ravichandran, K.S. and Garrison, J.C. (2009). Regulation of the Src Homology 2 Domain-containing Inositol 5. The Jornal of Biological Chemistry 284, 20070-20078.

[476] Mukherjee, O. *et al.* (2012). The SH2-domain of SHIP1 interacts with the SHIP1 C-terminus: impact on SHIP1/Ig-α interaction. Biochimica et biophysica acta 1823, 206-214.
[477] Yang, L., Williams, D.E., Mui, A., Ong, C., Krystal, G., van Soest, R. and Andersen, R.J. (2005). Synthesis of pelorol and analogues: activators of the inositol 5-phosphatase SHIP. Org Lett 7, 1073-6.
[478] Kennah, M., Yau, T.Y., Nodwell, M., Krystal, G., Andersen, R.J., Ong, C.J. and Mui, A.L.F. (2009). Activation of SHIP via a small molecule agonist kills multiple myeloma cells. Experimental Hematology 37, 1274-1283.
[479] Williams, D.E., Amlani, A., Dewi, A.S., Patrick, B.O., van Ofwegen, L., Mui, A.L. and Andersen, R.J. (2010). Australin E Isolated from the Soft Coral Cladiella sp. Collected in Pohnpei Activates the Inositol 5-Phosphatase SHIP1. Australian Journal of Chemistry 63, 895-900.
[480] Li, D., Carr, G., Zhang, Y., Williams, D.E., Amlani, A., Bottriell, H., Mui, A.L. and Andersen, R.J. (2011). Turnagainolides A and B, cyclic depsipeptides produced in culture by a Bacillus sp.: isolation, structure elucidation, and synthesis. J Nat Prod 74, 1093-9.
[481] Brooks, R., Fuhler, G.M., Iyer, S., Smith, M.J., Park, M.Y., Paraiso, K.H., Engelman, R.W. and Kerr, W.G. (2010). SHIP1 inhibition increases immunoregulatory capacity and triggers apoptosis of hematopoietic cancer cells. J Immunol 184, 3582-9.
[482] Viernes, D.R., Choi, L.B., Kerr, W.G. and Chisholm, J.D. (2014). Discovery and development of small molecule SHIP phosphatase modulators. Med Res Rev 34, 795-824.
[483] Brauer, H., Strauss, J., Wegner, W., Müller-Tidow, C., Horstmann, M. and Jücker, M. (2012). Leukemia-associated mutations in SHIP1 inhibit its enzymatic activity, interaction with the GM-CSF receptor and Grb2, and its ability to inactivate PI3K/AKT signaling. Cellular Signalling 24, 2095-2101.
[484] Lo, T.C.T., Barnhill, L.M., Kim, Y., Nakae, E.A., Yu, A.L. and Diccianni, M.B. (2009). Inactivation of SHIP1 in T-cell acute lymphoblastic leukemia due to mutation and extensive alternative splicing. Leukemia Research 33, 1562-1566.
[485] Franke, T.F., Kaplan, D.R., Cantley, L.C. and Toker, A. (1997). Direct regulation of the Akt proto-oncogene product by phosphatidylinositol-3,4-bisphosphate. Science 275, 665-8.
[486] Scheid, M.P. *et al.* (2002). Phosphatidylinositol (3,4,5)P3 is essential but not sufficient for protein kinase B (PKB) activation; phosphatidylinositol (3,4)P2 is required for PKB phosphorylation at Ser-473: studies using cells from SH2-containing inositol-5-phosphatase knockout mice. J Biol Chem 277, 9027-35.
[487] Ma, K., Cheung, S.M., Marshall, A.J. and Duronio, V. (2008). PI(3,4,5)P3 and PI(3,4)P2 levels correlate with PKB/akt phosphorylation at Thr308 and Ser473, respectively; PI(3,4)P2 levels determine PKB activity. Cell Signal 20, 684-94.
[488] Jain, S.K., Susa, M., Keeler, M.L., Carlesso, N., Druker, B. and Varticovski, L. (1996). PI 3-kinase activation in BCR/abl-transformed hematopoietic cells does not require interaction of p85 SH2 domains with p210 BCR/abl. Blood 88, 1542-50.
[489] Agoulnik, I.U., Hodgson, M.C., Bowden, W.A. and Ittmann, M.M. (2011). INPP4B: the new kid on the PI3K block. Oncotarget 2, 321-8.
[490] Landego, I., Jayachandran, N., Wullschleger, S., Zhang, T.T., Gibson, I.W., Miller, A., Alessi, D.R. and Marshall, A.J. (2012). Interaction of TAPP adapter proteins with phosphatidylinositol (3,4)-bisphosphate regulates B-cell activation and autoantibody production. Eur J Immunol 42, 2760-70.
[491] Hogan, A., Yakubchyk, Y., Chabot, J., Obagi, C., Daher, E., Maekawa, K. and Gee, S.H. (2004). The phosphoinositol 3,4-bisphosphate-binding protein TAPP1 interacts with syntrophins and regulates actin cytoskeletal organization. J Biol Chem 279, 53717-24.

[492] Cheung, S.M., Kornelson, J.C., Al-Alwan, M. and Marshall, A.J. (2007). Regulation of phosphoinositide 3-kinase signaling by oxidants: hydrogen peroxide selectively enhances immunoreceptor-induced recruitment of phosphatidylinositol (3,4) bisphosphate-binding PH domain proteins. Cell Signal 19, 902-12.
[493] Pauls, S.D., Lafarge, S.T., Landego, I., Zhang, T. and Marshall, A.J. (2012). The phosphoinositide 3-kinase signaling pathway in normal and malignant B cells: activation mechanisms, regulation and impact on cellular functions. Front Immunol 3, 224.
[494] Kurokawa, T., Takasuga, S., Sakata, S., Yamaguchi, S., Horie, S., Homma, K.J., Sasaki, T. and Okamura, Y. (2012). 3' Phosphatase activity toward phosphatidylinositol 3,4-bisphosphate [PI(3,4)P2] by voltage-sensing phosphatase (VSP). Proc Natl Acad Sci U S A 109, 10089-94.
[495] Leverrier, Y., Okkenhaug, K., Sawyer, C., Bilancio, A., Vanhaesebroeck, B. and Ridley, A.J. (2003). Class I phosphoinositide 3-kinase p110beta is required for apoptotic cell and Fcgamma receptor-mediated phagocytosis by macrophages. J Biol Chem 278, 38437-42.
[496] Hou, S., Pauls, S.D., Liu, P. and Marshall, A.J. (2010). The PH domain adaptor protein Bam32/DAPP1 functions in mast cells to restrain FcεRI-induced calcium flux and granule release. Mol Immunol 48, 89-97.
[497] Li, H. and Marshall, A.J. (2015). Phosphatidylinositol (3,4) bisphosphate-specific phosphatases and effector proteins: A distinct branch of PI3K signaling. Cell Signal 27, 1789-98.
[498] Li, H. *et al.* (2016). Phosphatidylinositol-3,4-Bisphosphate and Its Binding Protein Lamellipodin Regulate Chemotaxis of Malignant B Lymphocytes. J Immunol 196, 586-95.
[499] Kerr, W.G., Park, M.Y., Maubert, M. and Engelman, R.W. (2011). SHIP deficiency causes Crohn's disease-like ileitis. Gut 60, 177-88.
[500] McLarren, K.W. *et al.* (2011). SHIP-deficient mice develop spontaneous intestinal inflammation and arginase-dependent fibrosis. Am J Pathol 179, 180-8.
[501] Barrett, J.C. *et al.* (2008). Genome-wide association defines more than 30 distinct susceptibility loci for Crohn's disease. Nat Genet 40, 955-62.
[502] Kerr, W., Fernandes, S., Middleton, F., Chisholm, J. and Ryan, J. (2016). P-176 SHIP1 Deficiency in Human IBD: Molecular Basis, Prognosis and Agonist Development. Inflammatory Bowel Diseases 22, S63.
[503] Stenton, G.R. *et al.* (2013). Characterization of AQX-1125, a small-molecule SHIP1 activator: Part 2. Efficacy studies in allergic and pulmonary inflammation models in vivo. Br J Pharmacol 168, 1519-29.
[504] Leaker, B.R., Barnes, P.J., O'Connor, B.J., Ali, F.Y., Tam, P., Neville, J., Mackenzie, L.F. and MacRury, T. (2014). The effects of the novel SHIP1 activator AQX-1125 on allergen-induced responses in mild-to-moderate asthma. Clin Exp Allergy 44, 1146-53.
[505] Nickel, J.C., Egerdie, B., Davis, E., Evans, R., Mackenzie, L. and Shrewsbury, S.B. (2016). A Phase II Study of Efficacy and Safety of a Novel, Oral SHIP1 Activator, AQX-1125, in Subjects with Moderate to Severe Interstitial Cystitis/Bladder Pain Syndrome (IC/BPS). J Urol
[506] Watanabe, S., Mui, A.L., Muto, A., Chen, J.X., Hayashida, K., Yokota, T., Miyajima, A. and Arai, K. (1993). Reconstituted human granulocyte-macrophage colony-stimulating factor receptor transduces growth-promoting signals in mouse NIH 3T3 cells: comparison with signalling in BA/F3 pro-B cells. Mol Cell Biol 13, 1440-8.
[507] Segura, M.M., Garnier, A., Durocher, Y., Ansorge, S. and Kamen, A. (2010). New protocol for lentiviral vector mass production. Methods Mol Biol 614, 39-52.
[508] Kabsch, W. (2010). XDS. Acta Crystallogr D Biol Crystallogr 66, 125-32.
[509] Canutescu, A.A., Shelenkov, A.A. and Dunbrack, R.L. (2003). A graph-theory algorithm for rapid protein side-chain prediction. Protein Sci 12, 2001-14.

[510] McCoy, A.J. (2007). Solving structures of protein complexes by molecular replacement with Phaser. Acta Crystallogr D Biol Crystallogr 63, 32-41.
[511] Emsley, P. and Cowtan, K. (2004). Coot: model-building tools for molecular graphics. Acta Crystallogr D Biol Crystallogr 60, 2126-32.
[512] Murshudov, G.N. *et al.* (2011). REFMAC5 for the refinement of macromolecular crystal structures. Acta Crystallogr D Biol Crystallogr 67, 355-67.
[513] Langer, G., Cohen, S.X., Lamzin, V.S. and Perrakis, A. (2008). Automated macromolecular model building for X-ray crystallography using ARP/wARP version 7. Nat Protoc 3, 1171-9.
[514] Lee, R.C., Feinbaum, R.L. and Ambros, V. (1993). The C. elegans heterochronic gene lin-4 encodes small RNAs with antisense complementarity to lin-14. Cell 75, 843-54.
[515] Ruvkun, G. (2001). Molecular biology. Glimpses of a tiny RNA world. Science 294, 797-9.
[516] Liu, G., Friggeri, A., Yang, Y., Park, Y.J., Tsuruta, Y. and Abraham, E. (2009). miR-147, a microRNA that is induced upon Toll-like receptor stimulation, regulates murine macrophage inflammatory responses. Proc Natl Acad Sci U S A 106, 15819-24.
[517] Bazzoni, F. *et al.* (2009). Induction and regulatory function of miR-9 in human monocytes and neutrophils exposed to proinflammatory signals. Proc Natl Acad Sci U S A 106, 5282-7.
[518] Jennewein, C., von Knethen, A., Schmid, T. and Brüne, B. (2010). MicroRNA-27b contributes to lipopolysaccharide-mediated peroxisome proliferator-activated receptor gamma (PPARgamma) mRNA destabilization. J Biol Chem 285, 11846-53.
[519] Qi, J., Qiao, Y., Wang, P., Li, S., Zhao, W. and Gao, C. (2012). microRNA-210 negatively regulates LPS-induced production of proinflammatory cytokines by targeting NF-κB1 in murine macrophages. FEBS Lett 586, 1201-7.
[520] Androulidaki, A. *et al.* (2009). The Kinase Akt1 Controls Macrophage Response to Lipopolysaccharide by Regulating MicroRNAs. Immunity 31, 220-231.
[521] Chen, Q., Wang, H., Liu, Y., Song, Y., Lai, L., Han, Q., Cao, X. and Wang, Q. (2012). Inducible microRNA-223 down-regulation promotes TLR-triggered IL-6 and IL-1β production in macrophages by targeting STAT3. PLoS One 7, e42971.
[522] Liu, Y., Chen, Q., Song, Y., Lai, L., Wang, J., Yu, H., Cao, X. and Wang, Q. (2011). MicroRNA-98 negatively regulates IL-10 production and endotoxin tolerance in macrophages after LPS stimulation. FEBS Letters 585, 1963-1968.
[523] Quinn, S.R. and O'Neill, L.A. (2011). A trio of microRNAs that control Toll-like receptor signalling. Int Immunol 23, 421-5.
[524] Nakagawa, R. *et al.* (2002). SOCS-1 participates in negative regulation of LPS responses. Immunity 17, 677-87.
[525] Kinjyo, I. *et al.* (2002). SOCS1/JAB is a negative regulator of LPS-induced macrophage activation. Immunity 17, 583-91.
[526] Sachithanandan, N., Graham, K.L., Galic, S., Honeyman, J.E., Fynch, S.L., Hewitt, K.A., Steinberg, G.R. and Kay, T.W. (2011). Macrophage deletion of SOCS1 increases sensitivity to LPS and palmitic acid and results in systemic inflammation and hepatic insulin resistance. Diabetes 60, 2023-31.
[527] Tomaselli, S., Bonamassa, B., Alisi, A., Nobili, V., Locatelli, F. and Gallo, A. (2013). ADAR enzyme and miRNA story: a nucleotide that can make the difference. International journal of molecular sciences 14, 22796-22816.
[528] Nishikura, K. (2010). Functions and regulation of RNA editing by ADAR deaminases. Annual review of biochemistry 79, 321-349.
[529] Briata, P. *et al.* (2012). PI3K/AKT signaling determines a dynamic switch between distinct KSRP functions favoring skeletal myogenesis. Cell Death Differ 19, 478-87.

[530] Tamassia, N. *et al.* (2010). Uncovering an IL-10-dependent NF-kappaB recruitment to the IL-1ra promoter that is impaired in STAT3 functionally defective patients. FASEB J 24, 1365-75.
[531] Papouli, E., Defais, M. and Larminat, F. (2002). Overexpression of metallothionein-II sensitizes rodent cells to apoptosis induced by DNA cross-linking agent through inhibition of NF-kappa B activation. J Biol Chem 277, 4764-9.
[532] Brasier, A.R., Lu, M., Hai, T., Lu, Y. and Boldogh, I. (2001). NF-kappa B-inducible BCL-3 expression is an autoregulatory loop controlling nuclear p50/NF-kappa B1 residence. J Biol Chem 276, 32080-93.
[533] Lu, B., Yu, H., Chow, C., Li, B., Zheng, W., Davis, R.J. and Flavell, R.A. (2001). GADD45gamma mediates the activation of the p38 and JNK MAP kinase pathways and cytokine production in effector TH1 cells. Immunity 14, 583-90.
[534] Salmeron, A., Ahmad, T.B., Carlile, G.W., Pappin, D., Narsimhan, R.P. and Ley, S.C. (1996). Activation of MEK-1 and SEK-1 by Tpl-2 proto-oncoprotein, a novel MAP kinase kinase kinase. EMBO J 15, 817-26.
[535] Riley, J.K., Takeda, K., Akira, S. and Schreiber, R.D. (1999). Interleukin-10 receptor signaling through the JAK-STAT pathway. Requirement for two distinct receptor-derived signals for anti-inflammatory action. Journal of Biological Chemistry 274, 16513-16521.
[536] Blom, N., Gammeltoft, S. and Brunak, S. (1999). Sequence and structure-based prediction of eukaryotic protein phosphorylation sites. J Mol Biol 294, 1351-62.
[537] Prilusky, J., Felder, C.E., Zeev-Ben-Mordehai, T., Rydberg, E.H., Man, O., Beckmann, J.S., Silman, I. and Sussman, J.L. (2005). FoldIndex: a simple tool to predict whether a given protein sequence is intrinsically unfolded. Bioinformatics 21, 3435-8.
[538] Akerström, B., Lögdberg, L., Berggård, T., Osmark, P. and Lindqvist, A. (2000). alpha(1)-Microglobulin: a yellow-brown lipocalin. Biochimica et biophysica acta 1482, 172-184.
[539] Pugia, M.J. and Lott, J.A. (2005). Pathophysiology and diagnostic value of urinary trypsin inhibitors. Clin Chem Lab Med 43, 1-16.
[540] Aguiló, N., Uranga, S., Marinova, D., Martín, C. and Pardo, J. (2014). Bim is a crucial regulator of apoptosis induced by Mycobacterium tuberculosis. Cell Death Dis 5, e1343.
[541] Kirschnek, S., Ying, S., Fischer, S.F., Häcker, H., Villunger, A., Hochrein, H. and Häcker, G. (2005). Phagocytosis-induced apoptosis in macrophages is mediated by up-regulation and activation of the Bcl-2 homology domain 3-only protein Bim. The Journal of Immunology 174, 671-679.
[542] Schaale, K., Neumann, J., Schneider, D., Ehlers, S. and Reiling, N. (2011). Wnt signaling in macrophages: augmenting and inhibiting mycobacteria-induced inflammatory responses. Eur J Cell Biol 90, 553-9.
[543] Said, E.A. *et al.* (2010). Programmed death-1-induced interleukin-10 production by monocytes impairs CD4+ T cell activation during HIV infection. Nat Med 16, 452-9.
[544] Lattin, J.E. *et al.* (2008). Expression analysis of G Protein-Coupled Receptors in mouse macrophages. Immunome Res 4, 5.
[545] Imielinski, M. *et al.* (2009). Common variants at five new loci associated with early-onset inflammatory bowel disease. Nat Genet 41, 1335-40.
[546] Chen, E., Staudt, L.M. and Green, A.R. (2012). Janus kinase deregulation in leukemia and lymphoma. Immunity 36, 529-41.
[547] Xu, W. *et al.* (2007). Epithelial cells trigger frontline immunoglobulin class switching through a pathway regulated by the inhibitor SLPI. Nat Immunol 8, 294-303.
[548] Xia, J., Benner, M.J. and Hancock, R.E.W. (2014). NetworkAnalyst--integrative approaches for protein-protein interaction network analysis and visual exploration. Nucleic acids research 42, W167-74.

[549] Chen, E., Staudt, L.M. and Green, A.R. (2012). Janus kinase deregulation in leukemia and lymphoma. Immunity 36, 529-541.
[550] Xu, Y., Schnorrer, P., Proietto, A., Kowalski, G., Febbraio, M.A., Acha-Orbea, H., Dickins, R.A. and Villadangos, J.A. (2011). IL-10 controls cystatin C synthesis and blood concentration in response to inflammation through regulation of IFN regulatory factor 8 expression. Journal of immunology (Baltimore, Md. : 1950) 186, 3666-3673.
[551] Aoki, Y., Feldman, G.M. and Tosato, G. (2003). Inhibition of STAT3 signaling induces apoptosis and decreases survivin expression in primary effusion lymphoma. Blood 101, 1535-1542.
[552] Liu, H., Ma, Y., Cole, S.M., Zander, C., Chen, K.-H., Karras, J. and Pope, R.M. (2003). Serine phosphorylation of STAT3 is essential for Mcl-1 expression and macrophage survival. Blood 102, 344-352.
[553] Li, Y. *et al.* (2008). Extracellular Nampt promotes macrophage survival via a nonenzymatic interleukin-6/STAT3 signaling mechanism. Journal of Biological Chemistry 283, 34833-34843.
[554] Cuesta, N., Nhu, Q.M., Zudaire, E., Polumuri, S., Cuttitta, F. and Vogel, S.N. (2007). IFN regulatory factor-2 regulates macrophage apoptosis through a STAT1/3- and caspase-1-dependent mechanism. The Journal of Immunology 178, 3602-3611.
[555] Lioubin, M.N., Algate, P.A., Tsai, S., Carlberg, K., Aebersold, A. and Rohrschneider, L.R. (1996). p150Ship, a signal transduction molecule with inositol polyphosphate-5-phosphatase activity. Genes Dev 10, 1084-95.
[556] Liu, L., Damen, J.E., Hughes, M.R., Babic, I., Jirik, F.R. and Krystal, G. (1997). The Src homology 2 (SH2) domain of SH2-containing inositol phosphatase (SHIP) is essential for tyrosine phosphorylation of SHIP, its association with Shc, and its induction of apoptosis. Journal of Biological Chemistry 272, 8983-8988.
[557] Gardai, S., Whitlock, B.B., Helgason, C., Ambruso, D., Fadok, V., Bratton, D. and Henson, P.M. (2002). Activation of SHIP by NADPH oxidase-stimulated Lyn leads to enhanced apoptosis in neutrophils. J Biol Chem 277, 5236-46.
[558] Peng, Q., Malhotra, S., Torchia, J.A., Kerr, W.G., Coggeshall, K.M. and Humphrey, M.B. (2010). TREM2- and DAP12-dependent activation of PI3K requires DAP10 and is inhibited by SHIP1. Sci Signal 3, ra38.
[559] Park, M.Y., Srivastava, N., Sudan, R., Viernes, D.R., Chisholm, J.D., Engelman, R.W. and Kerr, W.G. (2014). Impaired T-cell survival promotes mucosal inflammatory disease in SHIP1-deficient mice. Mucosal Immunol 7, 1429-39.
[560] Gloire, G., Erneux, C. and Piette, J. (2007). The role of SHIP1 in T-lymphocyte life and death. Biochem Soc Trans 35, 277-80.
[561] Wang, Z.Q., Bapat, A.S., Rayanade, R.J., Dagtas, A.S. and Hoffmann, M.K. (2001). Interleukin-10 induces macrophage apoptosis and expression of CD16 (FcgammaRIII) whose engagement blocks the cell death programme and facilitates differentiation. Immunology 102, 331-7.
[562] Martin, C., Espaillat, M.P. and Santiago-Schwarz, F. (2015). IL-10 restricts dendritic cell (DC) growth at the monocyte-to-monocyte-derived DC interface by disrupting anti-apoptotic and cytoprotective autophagic molecular machinery. Immunologic Research 63, 131-143.
[563] Bailey, D.P., Kashyap, M., Bouton, L.A., Murray, P.J. and Ryan, J.J. (2006). Interleukin-10 induces apoptosis in developing mast cells and macrophages. Journal of leukocyte biology 80, 581-589.
[564] Yang, H. and Chen, S.C. (2011). The effect of interleukin-10 on apoptosis in macrophages stimulated by oxLDL. Eur J Pharmacol 657, 126-30.
[565] Arai, T., Hiromatsu, K., Nishimura, H., Kimura, Y., Kobayashi, N., Ishida, H., Nimura, Y. and Yoshikai, Y. (1995). Endogenous interleukin 10 prevents apoptosis in macrophages

during Salmonella infection. Biochemical and Biophysical Research Communications 213, 600-607.
[566] Rojas, M., Olivier, M., Gros, P., Barrera, L.F. and García, L.F. (1999). TNF-alpha and IL-10 modulate the induction of apoptosis by virulent Mycobacterium tuberculosis in murine macrophages. The Journal of Immunology 162, 6122-6131.
[567] Weber-Nordt, R.M., Henschler, R., Schott, E., Wehinger, J., Behringer, D., Mertelsmann, R. and Finke, J. (1996). Interleukin-10 increases Bcl-2 expression and survival in primary human CD34+ hematopoietic progenitor cells. Blood 88, 2549-2558.
[568] Halvorsen, B. *et al.* (2005). Interleukin-10 enhances the oxidized LDL-induced foam cell formation of macrophages by antiapoptotic mechanisms. J Lipid Res 46, 211-9.
[569] Chen, E.Y., Tan, C.M., Kou, Y., Duan, Q., Wang, Z., Meirelles, G.V., Clark, N.R. and Ma'ayan, A. (2013). Enrichr: interactive and collaborative HTML5 gene list enrichment analysis tool. BMC Bioinformatics 14, 128.
[570] Chen, M., Capps, C., Willerson, J.T. and Zoldhelyi, P. (2002). E2F-1 regulates nuclear factor-kappaB activity and cell adhesion: potential antiinflammatory activity of the transcription factor E2F-1. Circulation 106, 2707-13.
[571] Fang, F. *et al.* (2010). Transcription factor E2F1 suppresses dendritic cell maturation. J Immunol 184, 6084-91.
[572] Kundu, M., Guermah, M., Roeder, R.G., Amini, S. and Khalili, K. (1997). Interaction between cell cycle regulator, E2F-1, and NF-kappaB mediates repression of HIV-1 gene transcription. J Biol Chem 272, 29468-74.
[573] Tanaka, H. *et al.* (2002). E2F1 and c-Myc potentiate apoptosis through inhibition of NF-kappaB activity that facilitates MnSOD-mediated ROS elimination. Mol Cell 9, 1017-29.
[574] Lim, C.A. *et al.* (2007). Genome-wide mapping of RELA(p65) binding identifies E2F1 as a transcriptional activator recruited by NF-kappaB upon TLR4 activation. Mol Cell 27, 622-35.
[575] Xu, Y., Jin, H., Yang, X., Wang, L., Su, L., Liu, K., Gu, Q. and Xu, X. (2014). MicroRNA-93 inhibits inflammatory cytokine production in LPS-stimulated murine macrophages by targeting IRAK4. FEBS Lett 588, 1692-8.
[576] Xie, W., Li, M., Xu, N., Lv, Q., Huang, N., He, J. and Zhang, Y. (2013). MiR-181a regulates inflammation responses in monocytes and macrophages. PLoS One 8, e58639.
[577] Zhang, W., Shen, X., Xie, L., Chu, M. and Ma, Y. (2015). MicroRNA-181b regulates endotoxin tolerance by targeting IL-6 in macrophage RAW264.7 cells. J Inflamm (Lond) 12, 18.
[578] Hutchison, E.R. *et al.* (2013). Evidence for miR-181 involvement in neuroinflammatory responses of astrocytes. Glia 61, 1018-28.
[579] Li, Q.Q. *et al.* (2011). Involvement of NF-κB/miR-448 regulatory feedback loop in chemotherapy-induced epithelial-mesenchymal transition of breast cancer cells. Cell Death Differ 18, 16-25.
[580] Pedersen, I.M., Cheng, G., Wieland, S., Volinia, S., Croce, C.M., Chisari, F.V. and David, M. (2007). Interferon modulation of cellular microRNAs as an antiviral mechanism. Nature 449, 919-22.
[581] Yasukawa, H. *et al.* (2003). IL-6 induces an anti-inflammatory response in the absence of SOCS3 in macrophages. Nature Immunology 4, 551-556.
[582] Niemand, C., Nimmesgern, A., Haan, S., Fischer, P., Schaper, F., Rossaint, R., Heinrich, P.C. and Müller-Newen, G. (2003). Activation of STAT3 by IL-6 and IL-10 in primary human macrophages is differentially modulated by suppressor of cytokine signaling 3. The Journal of Immunology 170, 3263-3272.
[583] Murray, P.J. (2006). Understanding and exploiting the endogenous interleukin-10/STAT3-mediated anti-inflammatory response. Curr Opin Pharmacol 6, 379-86.

[584] Williams, L., Jarai, G., Smith, A. and Finan, P. (2002). IL-10 expression profiling in human monocytes. Journal of leukocyte biology 72, 800-809.
[585] Antoniv, T.T., Park-Min, K.-H. and Ivashkiv, L.B. (2005). Kinetics of IL-10-induced gene expression in human macrophages. Immunobiology 210, 87-95.
[586] Divorty, N., Mackenzie, A.E., Nicklin, S.A. and Milligan, G. (2015). G protein-coupled receptor 35: an emerging target in inflammatory and cardiovascular disease. Frontiers in pharmacology 6, 41.
[587] Imielinski, M. *et al.* (2009). Common variants at five new loci associated with early-onset inflammatory bowel disease. Nature genetics 41, 1335-1340.
[588] Horikawa, Y. *et al.* (2000). Genetic variation in the gene encoding calpain-10 is associated with type 2 diabetes mellitus. Nat Genet 26, 163-75.
[589] Sun, Y.V., Bielak, L.F., Peyser, P.A., Turner, S.T., Sheedy, P.F., Boerwinkle, E. and Kardia, S.L. (2008). Application of machine learning algorithms to predict coronary artery calcification with a sibship-based design. Genet Epidemiol 32, 350-60.
[590] Zhao, P. *et al.* (2010). Targeting of the orphan receptor GPR35 by pamoic acid: a potent activator of extracellular signal-regulated kinase and β-arrestin2 with antinociceptive activity. Mol Pharmacol 78, 560-8.
[591] Wang, J., Simonavicius, N., Wu, X., Swaminath, G., Reagan, J., Tian, H. and Ling, L. (2006). Kynurenic acid as a ligand for orphan G protein-coupled receptor GPR35. J Biol Chem 281, 22021-8.
[592] Taniguchi, Y., Tonai-Kachi, H. and Shinjo, K. (2006). Zaprinast, a well-known cyclic guanosine monophosphate-specific phosphodiesterase inhibitor, is an agonist for GPR35. FEBS Lett 580, 5003-8.
[593] Shore, D.M. and Reggio, P.H. (2015). The therapeutic potential of orphan GPCRs, GPR35 and GPR55. Front Pharmacol 6, 69.
[594] Iyoda, T. *et al.* (2014). A novel mechanism underlying the basic defensive response of macrophages against Mycobacterium infection. J Immunol 192, 4254-62.
[595] Häcker, G., Suttner, K., Harada, H. and Kirschnek, S. (2006). TLR-dependent Bim phosphorylation in macrophages is mediated by ERK and is connected to proteasomal degradation of the protein. Int Immunol 18, 1749-57.
[596] Carnero, A., Blanco-Aparicio, C., Renner, O., Link, W. and Leal, J.F.M. (2008). The PTEN/PI3K/AKT signalling pathway in cancer, therapeutic implications. Current cancer drug targets 8, 187-198.
[597] Gharbi, S.I., Zvelebil, M.J., Shuttleworth, S.J., Hancox, T., Saghir, N., Timms, J.F. and Waterfield, M.D. (2007). Exploring the specificity of the PI3K family inhibitor LY294002. Biochem J 404, 15-21.
[598] Davies, S.P., Reddy, H., Caivano, M. and Cohen, P. (2000). Specificity and mechanism of action of some commonly used protein kinase inhibitors. Biochem J 351, 95-105.
[599] Liu, Y., Shreder, K.R., Gai, W., Corral, S., Ferris, D.K. and Rosenblum, J.S. (2005). Wortmannin, a widely used phosphoinositide 3-kinase inhibitor, also potently inhibits mammalian polo-like kinase. Chem Biol 12, 99-107.
[600] Rückle, T., Schwarz, M.K. and Rommel, C. (2006). PI3Kgamma inhibition: towards an 'aspirin of the 21st century'? Nat Rev Drug Discov 5, 903-18.
[601] Thorpe, L.M., Yuzugullu, H. and Zhao, J.J. (2015). PI3K in cancer: divergent roles of isoforms, modes of activation and therapeutic targeting. Nature reviews. Cancer 15, 7-24.
[602] Al-Alwan, M.M., Okkenhaug, K., Vanhaesebroeck, B., Hayflick, J.S. and Marshall, A.J. (2007). Requirement for phosphoinositide 3-kinase p110delta signaling in B cell antigen receptor-mediated antigen presentation. J Immunol 178, 2328-35.
[603] Sly, L.M. *et al.* (2009). SHIP prevents lipopolysaccharide from triggering an antiviral response in mice. Blood 113, 2945-54.

[604] Papakonstanti, E.A. *et al.* (2008). Distinct roles of class IA PI3K isoforms in primary and immortalised macrophages. J Cell Sci 121, 4124-33.
[605] Whisstock, J.C., Romero, S., Gurung, R., Nandurkar, H., Ooms, L.M., Bottomley, S.P. and Mitchell, C.A. (2000). The Inositol Polyphosphate 5-Phosphatases and the Apurinic/Apyrimidinic Base Excision Repair Endonucleases Share a Common Mechanism for Catalysis. Journal of Biological Chemistry 275, 37055-37061.
[606] Fox, J.D. and Waugh, D.S. (2003). Maltose-binding protein as a solubility enhancer. Methods Mol Biol 205, 99-117.
[607] Trésaugues, L. *et al.* (2014). Structural Basis for Phosphoinositide Substrate Recognition, Catalysis, and Membrane Interactions in Human Inositol Polyphosphate 5-Phosphatases. 22, 744-755.
[608] Aman, M.J., Walk, S.F., March, M.E., Su, H.P., Carver, D.J. and Ravichandran, K.S. (2000). Essential role for the C-terminal noncatalytic region of SHIP in FcgammaRIIB1-mediated inhibitory signaling. Molecular and cellular biology 20, 3576-3589.
[609] Derewenda, Z.S. (2004). Rational protein crystallization by mutational surface engineering. Structure 12, 529-35.
[610] Goldschmidt, L., Cooper, D.R., Derewenda, Z.S. and Eisenberg, D. (2007). Toward rational protein crystallization: A Web server for the design of crystallizable protein variants. Protein Sci 16, 1569-76.
[611] Sievers, F. *et al.* (2011). Fast, scalable generation of high-quality protein multiple sequence alignments using Clustal Omega. Mol Syst Biol 7, 539.
[612] Erneux, C., Govaerts, C., Communi, D. and Pesesse, X. (1998). The diversity and possible functions of the inositol polyphosphate 5-phosphatases. Biochimica et biophysica acta 1436, 185-199.
[613] Schmid, A.C., Wise, H.M., Mitchell, C.A., Nussbaum, R. and Woscholski, R. (2004). Type II phosphoinositide 5-phosphatases have unique sensitivities towards fatty acid composition and head group phosphorylation. FEBS Letters 576, 9-13.
[614] Kim, Y.J., Jahan, N. and Bahk, Y.Y. (2013). Biochemistry and structure of phosphoinositide phosphatases. BMB Rep 46, 1-8.
[615] Chi, Y. *et al.* (2004). Comparative mechanistic and substrate specificity study of inositol polyphosphate 5-phosphatase Schizosaccharomyces pombe Synaptojanin and SHIP2. J Biol Chem 279, 44987-95.
[616] Mills, S.J. *et al.* (2012). A synthetic polyphosphoinositide headgroup surrogate in complex with SHIP2 provides a rationale for drug discovery. ACS Chem Biol 7, 822-8.
[617] Majerus, P.W., Kisseleva, M.V. and Norris, F.A. (1999). The role of phosphatases in inositol signaling reactions. J Biol Chem 274, 10669-72.
[618] Madej, T., Lanczycki, C.J., Zhang, D., Thiessen, P.A., Geer, R.C., Marchler-Bauer, A. and Bryant, S.H. (2014). MMDB and VAST+: tracking structural similarities between macromolecular complexes. Nucleic Acids Res 42, D297-303.
[619] Xu, J., Bacaj, T., Zhou, A., Tomchick, D.R., Südhof, T.C. and Rizo, J. (2014). Structure and Ca2+-Binding Properties of the Tandem C2 Domains of E-Syt2. Structure/Folding and Design 22, 269-280.
[620] Rizo, J. and Südhof, T.C. (1998). C2-domains, structure and function of a universal Ca2+-binding domain. J Biol Chem 273, 15879-82.
[621] Corbalan-Garcia, S., Garcia-Garcia, J., Rodriguez-Alfaro, J.A. and Gomez-Fernandez, J.C. (2003). A New Phosphatidylinositol 4,5-Bisphosphate-binding Site Located in the C2 Domain of Protein Kinase C. Journal of Biological Chemistry 278, 4972-4980.
[622] Kuo, W., Herrick, D.Z., Ellena, J.F. and Cafiso, D.S. (2009). The calcium-dependent and calcium-independent membrane binding of synaptotagmin 1: two modes of C2B binding. J Mol Biol 387, 284-94.

[623] Padmanarayana, M., Hams, N., Speight, L.C., Petersson, E.J., Mehl, R.A. and Johnson, C.P. (2014). Characterization of the lipid binding properties of Otoferlin reveals specific interactions between PI(4,5)P2 and the C2C and C2F domains. Biochemistry 53, 5023-33.
[624] Therrien, C., Di Fulvio, S., Pickles, S. and Sinnreich, M. (2009). Characterization of lipid binding specificities of dysferlin C2 domains reveals novel interactions with phosphoinositides. Biochemistry 48, 2377-84.
[625] Domin, J., Gaidarov, I., Smith, M.E., Keen, J.H. and Waterfield, M.D. (2000). The class II phosphoinositide 3-kinase PI3K-C2alpha is concentrated in the trans-Golgi network and present in clathrin-coated vesicles. J Biol Chem 275, 11943-50.
[626] Das, S., Dixon, J.E. and Cho, W. (2003). Membrane-binding and activation mechanism of PTEN. Proc Natl Acad Sci U S A 100, 7491-6.
[627] Schiavo, G., Gu, Q.M., Prestwich, G.D., Söllner, T.H. and Rothman, J.E. (1996). Calcium-dependent switching of the specificity of phosphoinositide binding to synaptotagmin. Proc Natl Acad Sci U S A 93, 13327-32.
[628] Chung, S.H., Song, W.J., Kim, K., Bednarski, J.J., Chen, J., Prestwich, G.D. and Holz, R.W. (1998). The C2 domains of Rabphilin3A specifically bind phosphatidylinositol 4,5-bisphosphate containing vesicles in a Ca2+-dependent manner. In vitro characteristics and possible significance. J Biol Chem 273, 10240-8.
[629] Guerrero-Valero, M., Ferrer-Orta, C., Querol-Audí, J., Marin-Vicente, C., Fita, I., Gómez-Fernández, J.C., Verdaguer, N. and Corbalán-García, S. (2009). Structural and mechanistic insights into the association of PKCalpha-C2 domain to PtdIns(4,5)P2. Proceedings of the National Academy of Sciences of the United States of America 106, 6603-6607.
[630] Corbalan-Garcia, S. and Gómez-Fernández, J.C. (2014). Signaling through C2 domains: more than one lipid target. Biochim Biophys Acta 1838, 1536-47.
[631] Krissinel, E. and Henrick, K. (2007). Inference of macromolecular assemblies from crystalline state. J Mol Biol 372, 774-97.
[632] Munuganti, R.S. *et al.* (2014). Identification of a potent antiandrogen that targets the BF3 site of the androgen receptor and inhibits enzalutamide-resistant prostate cancer. Chem Biol 21, 1476-85.
[633] Dowler, S., Kular, G. and Alessi, D.R. (2002). Protein lipid overlay assay. Sci STKE 2002, pl6.
[634] Lemmon, M.A., Ferguson, K.M., O'Brien, R., Sigler, P.B. and Schlessinger, J. (1995). Specific and high-affinity binding of inositol phosphates to an isolated pleckstrin homology domain. Proc Natl Acad Sci U S A 92, 10472-6.
[635] Sánchez-Bautista, S., Marín-Vicente, C., Gómez-Fernández, J.C. and Corbalán-García, S. (2006). The C2 domain of PKCalpha is a Ca2+ -dependent PtdIns(4,5)P2 sensing domain: a new insight into an old pathway. J Mol Biol 362, 901-14.
[636] Narayan, K. and Lemmon, M.A. (2006). Determining selectivity of phosphoinositide-binding domains. Methods 39, 122-33.
[637] Chao, H., Martin, G.G., Russell, W.K., Waghela, S.D., Russell, D.H., Schroeder, F. and Kier, A.B. (2002). Membrane charge and curvature determine interaction with acyl-CoA binding protein (ACBP) and fatty acyl-CoA targeting. Biochemistry 41, 10540-53.
[638] Suwa, A. *et al.* (2009). Discovery and functional characterization of a novel small molecule inhibitor of the intracellular phosphatase, SHIP2. Br J Pharmacol 158, 879-87.
[639] Lee, J.O. *et al.* (1999). Crystal structure of the PTEN tumor suppressor: implications for its phosphoinositide phosphatase activity and membrane association. Cell 99, 323-334.
[640] Tsujishita, Y., Guo, S., Stolz, L.E., York, J.D. and Hurley, J.H. (2001). Specificity determinants in phosphoinositide dephosphorylation: crystal structure of an archetypal inositol polyphosphate 5-phosphatase. Cell 105, 379-389.

[641] Fatatis, A. and Russell, J.T. (1992). Spontaneous changes in intracellular calcium concentration in type I astrocytes from rat cerebral cortex in primary culture. Glia 5, 95-104.
[642] Danciu, T.E., Adam, R.M., Naruse, K., Freeman, M.R. and Hauschka, P.V. (2003). Calcium regulates the PI3K-Akt pathway in stretched osteoblasts. FEBS Lett 536, 193-7.
[643] Liu, Z.M., Chen, G.G., Vlantis, A.C., Tse, G.M., Shum, C.K. and van Hasselt, C.A. (2007). Calcium-mediated activation of PI3K and p53 leads to apoptosis in thyroid carcinoma cells. Cell Mol Life Sci 64, 1428-36.
[644] Konc, J., Lešnik, S. and Janežič, D. (2015). Modeling enzyme-ligand binding in drug discovery. J Cheminform 7, 48.
[645] Law, V. *et al.* (2014). DrugBank 4.0: shedding new light on drug metabolism. Nucleic Acids Res 42, D1091-7.
[646] Koseki, Y., Kinjo, T., Kobayashi, M. and Aoki, S. (2013). Identification of novel antimycobacterial chemical agents through the in silico multi-conformational structure-based drug screening of a large-scale chemical library. Eur J Med Chem 60, 333-9.
[647] Lindsley, J.E. and Rutter, J. (2006). Whence cometh the allosterome? Proc Natl Acad Sci U S A 103, 10533-5.
[648] Lee, D.W. *et al.* (2012). Loss of SHIP-1 protein expression in high-risk myelodysplastic syndromes is associated with miR-210 and miR-155. Oncogene 31, 4085-94.
[649] Pencik, J. *et al.* (2015). STAT3 regulated ARF expression suppresses prostate cancer metastasis. Nat Commun 6, 7736.
[650] Lee, H. *et al.* (2012). Acetylated STAT3 is crucial for methylation of tumor-suppressor gene promoters and inhibition by resveratrol results in demethylation. Proc Natl Acad Sci U S A 109, 7765-9.
[651] Li, J. *et al.* (2013). STAT3 acetylation-induced promoter methylation is associated with downregulation of the ARHI tumor-suppressor gene in ovarian cancer. Oncol Rep 30, 165-70.
[652] Yang, J., Liao, X., Agarwal, M.K., Barnes, L., Auron, P.E. and Stark, G.R. (2007). Unphosphorylated STAT3 accumulates in response to IL-6 and activates transcription by binding to NFkappaB. Genes Dev 21, 1396-408.
[653] Peña, G., Cai, B., Liu, J., van der Zanden, E.P., Deitch, E.A., de Jonge, W.J. and Ulloa, L. (2010). Unphosphorylated STAT3 modulates alpha 7 nicotinic receptor signaling and cytokine production in sepsis. Eur J Immunol 40, 2580-9.
[654] Timofeeva, O.A. *et al.* (2012). Mechanisms of unphosphorylated STAT3 transcription factor binding to DNA. J Biol Chem 287, 14192-200.
[655] Yoshida, Y., Kumar, A., Koyama, Y., Peng, H., Arman, A., Boch, J.A. and Auron, P.E. (2004). Interleukin 1 activates STAT3/nuclear factor-kappaB cross-talk via a unique TRAF6- and p65-dependent mechanism. J Biol Chem 279, 1768-76.
[656] Huang, J.C. *et al.* (2007). Using expression profiling data to identify human microRNA targets. Nat Methods 4, 1045-9.

Appendices

Table A.1: Primers used in qPCR

Name	Primer Sequence
18S Fwd	CAAGACGGACCAGAGCGAAA
18S Rev	GGCGGGTCATGGGAATAAC
Abcb1b Fwd	CTGTTGGCGTATTTGGGATGT
Abcb1b Rev	CAGCATCAAGAGGGGAAGTAATG
ambp Fwd	CTGCGTCAACACTGCCAGATA
ambp Rev	CTTGTCCTTAATGCGGCTCAG
Arid5a Fwd	CCACTCACGGGTGCTAGTAG
Arid5a Rev	GGGGACTGTCTTGAATGTCCT
Bcl2l11 Fwd	CCCGGAGATACGGATTGCAC
Bcl2l11 Rev	GCCTCGCGGTAATCATTTGC
bcl3 Fwd	CCGGAGGCCCTTTACTACCA
bcl3 Rev	GGAGTAGGGGTGAGTAGGCAG
ccl2 Fwd	TTAAAAACCTGGATCGGAACCAA
ccl2 Rev	GCATTAGCTTCAGATTTACGGGT
ccl3 Fwd	TTCTCTGTACCATGACACTCTGC
ccl3 Rev	CGTGGAATCTTCCGGCTGTAG
Ccnd2 Fwd	GAGTGGGAACTGGTAGTGTTG
Ccnd2 Rev	CGCACAGAGCGATGAAGGT
Cd274 Fwd	GCTCCAAAGGACTTGTACGTG
Cd274 Rev	TGATCTGAAGGGCAGCATTTC
Crlf2 Fwd	GAGTTCCGTTATGGCACTGG
Crlf2 Rev	GCTGCCTAGCCTTAAACACCA
cxcl1 Fwd	CTGGGATTCACCTCAAGAACATC
cxcl1 Rev	CAGGGTCAAGGCAAGCCTC
Cxcl2 Fwd	CCAACCACCAGGCTACAGG
Cxcl2 Rev	GCGTCACACTCAAGCTCTG
Dpm1 Fwd	CCCACCTACAACGAACGGG
Dpm1 Rev	CAGCTTTTTCTCTCGTGGTCTTA
egr1 Fwd	TCGGCTCCTTTCCTCACTCA
egr1 Rev	CTCATAGGGTTGTTCGCTCGG
Ewsr1 Fwd	CCCACTGGTTATAGCACTCCA
Ewsr1 Rev	CAGTCTGAGCTGCGTAAGAGG
Fzd7 Fwd	AGACCCACCTTTCACTGCG
Fzd7 Rev	AAGTACATGAGGCCGTTAGCA
Gpr35 Fwd	ACAACCTGTAACAGCACCCTC
Gpr35 Rev	GCGATAGCAGAATACCCAGAGT
icam1 Fwd	GTGATGCTCAGGTATCCATCCA
icam1 Rev	CACAGTTCTCAAAGCACAGCG
Id3 Fwd	CTGTCGGAACGTAGCCTGG
Id3 Rev	GTGGTTCATGTCGTCCAAGAG
il4ra Fwd	TCTGCATCCCGTTGTTTTGC
il4ra Rev	GCACCTGTGCATCCTGAATG
Impact Fwd	GTGAAGAAATCGAAGCAATGGC
Impact Rev	GGTACTCACTTGGCAACATCA
Irf8 Fwd	CGGGGCTGATCTGGGAAAAT
Irf8 Rev	CACAGCGTAACCTCGTCTTC
junB Fwd	TCACGACGACTCTTACGCAG

Name	Primer Sequence
junB Rev	CCTTGAGACCCCGATAGGGA
Lrp1 Fwd	ACTATGGATGCCCCTAAAACTTG
Lrp1 Rev	GCAATCTCTTTCACCGTCACA
map3k8 Fwd	ATGGAGTACATGAGCACTGGA
map3k8 Rev	GGCTCTTCACTTGCATAAAGGTT
marcksl1 Fwd	CAATGGAGACTTAACCCCCAAG
marcksl1 Rev	GGCCACTCAATTTGAAAGGCT
mGAPDH Fwd	AATGTGTCCGTCGTGGATCT
mGAPDH Rev	GCTTCACCACCTTCTTGATGT
nfil3 Fwd	GAACTCTGCCTTAGCTGAGGT
nfil3 Rev	ATTCCCGTTTTCTCCGACACG
nfkbia Fwd	TGAAGGACGAGGAGTACGAGC
nfkbia Rev	TTCGTGGATGATTGCCAAGTG
nfkbiz Fwd	GCTCCGACTCCTCCGATTTC
nfkbiz Rev	GAGTTCTTCACGCGAACACC
nucks1 Fwd	TCTCGGCCTGTCAGAAATAGG
nucks1 Rev	GGGGAGATGACCGAATCTTCTTA
peli1 Fwd	GCCCCAGTAAAATATGGCGAA
peli1 Rev	CCCCATTTGCCTTAGGTCTTT
pim1 Fwd	CTGGAGTCGCAGTACCAGG
pim1 Rev	CAGTTCTCCCCAATCGGAAATC
Prdx6 Fwd	CGCCAGAGTTTGCCAAGAG
Prdx6 Rev	TCCGTGGGTGTTTCACCATTG
Pre-mmu-155 Fwd	GCTAATTGTGATAGGGGTTTTGG
Pre-mmu-155 Rev	GTTAATGCTAACAGGTAGGAGTC
Pri-mmu-155 Fwd	GACACAAGGCCTGTTACTAGCAC
Pri-mmu-155 Rev	GTCTGACATCTACGTTCATCCAGC
Psmc5 Fwd	AACTTGACCAGGGGGATCAAC
Psmc5 Rev	AGTCCTCCTGAGTGACGTGG
Ptger4 Fwd	ACCATTCCTAGATCGAACCGT
Ptger4 Rev	CACCACCCCGAAGATGAACAT
Rgs2 Fwd	GAGAAAATGAAGCGGACACTCT
Rgs2 Rev	GCAGCCAGCCCATATTTACTG
Rnf216 Fwd	GCCCATCCTCTAGGAGAGCTT
Rnf216 Rev	CCGTTTCTTTCACTAACAGTGGA
Sbno2 Fwd	CATCCAGCTACAGAACCGACT
Sbno2 Rev	GAACCCACGAACTGTTGGTTT
sod2 Fwd	CAGACCTGCCTTACGACTATGG
sod2 Rev	CTCGGTGGCGTTGAGATTGTT
Tfam Fwd	ATTCCGAAGTGTTTTTCCAGCA
Tfam Rev	TCTGAAAGTTTTGCATCTGGGT
Tnf Fwd	TCTTCTCATTCCTGCTTGTGG
Tnf Rev	GGTCTGGGCCATAGAACTGA
tnfsf9 Fwd	CGGCGCTCCTCAGAGATAC
tnfsf9 Rev	ATCCCGAACATTAACCGCAGG
Tor1a Fwd	GAGCCCATCAGCCTGAGTC
Tor1a Rev	AAACCAGACACGGCGTTTAGG

Table A.2: Site-directed mutagenesis primers

Residue numbering of mouse SHIP1 sequence is based on the RefSeq entry with accession number of NP_034696.

Name	Sequence	Description
SHIP1-Y190F SDM Fwd	AAGCCATCCAGGATTTCCTGAGCAC TCAGCTCC	Potential tyrosine phosphorylation site
SHIP1-Y190F SDM Rev	AGCTGAGTGCTCAGGAAATCCTGG ATGGCTTTC	
SHIP770to773 SDM Fwd	AGAGTCAGGAAGGAGCGAATGCAG CGGGAAGTGAAGGAGAG	Surface Entropy Reduction Mutations
SHIP770to773 SDM Rev	CTCTCCTTCACTTCCCGCTGCATTC GCTCCTTCCTGACTCTTG	
SHIP1-L573A SDM Fwd	CCTGGGAGACAAGAAGGCAAGCCC ATTTAACATCAC	Potential AQX-MN100 binding site
SHIP1-L573A SDM Rev	GTGATGTTAAATGGGCTTGCCTTCT TGTCTCCCAGG	
SHIP1-Y683A SDM Fwd	AGTCCTCTGGAAGTCTGCACCGCTG GTGCATGTG	Potential AQX-MN100 binding site
SHIP1-Y683A SDM Rev	CACATGCACCAGCGGTGCAGACTT CCAGAGGAC	
SHIP1-S758A SDM Fwd	ACTTGGAGTTCCACTCAGCCTGCTT AGAGAGTTTTG	Potential AQX-MN100 binding site
SHIP1-S758A SDM Rev	ACAAAACTCTCTAAGCAGGCTGAG TGGAACTCCAAG	
SHIP1-H635A SDM Fwd	ACCAGAAGGTCTTCCTGGCCTTTGA GGAGGAAGAG	Potential AQX-MN100 binding site
SHIP1-H635A SDM Rev	CTCTTCCTCCTCAAAGGCCAGGAAG ACCTTCTGG	
SHIP1-H580A SDM Fwd	CCATTTAACATCACCGCCCGCTTCA CCCACCTC	Potential AQX-MN100 binding site
SHIP1-H580A SDM Rev	AGGTGGGTGAAGCGGGCGGTGATG TTAAATGG	
SHIP1-H704A Fwd	CATCATGACGAGTGACGCCAGCCC TGTCTTTGCC	Potential AQX-MN100 binding site
SHIP1-H704A Rev	GGCAAAGACAGGGCTGGCGTCACT CGTCATGATG	
SHIP1-D590A Fwd	TCTTCTGGCTTGGGGCTCTCAACTA CCGCGTG	Potential AQX-MN100 binding site
SHIP1-D590A Rev	ACGCGGTAGTTGAGAGCCCCAAGC CAGAAGAG	

Table A.3: Ligase-independent cloning primers

Residue numbering of mouse SHIP1 sequence is based on the RefSeq entry with accession number of NP_034696.

Name	Sequence	Description
SHIP 402 LIC Fwd	TTACTTCCAATCCAATGCACCAGAG CCTGACATGATCACCATC	Forward primer for both PAC1 and PAC2
SHIP857 LIC Rev	TTATCCACTTCCAATGTTATTACTGC AGCTTAATCTCTCCCCTG	Reverse primer for PAC2
SHIP861 LIC Rev	TTATCCACTTCCAATGTTATTAGCCC TGGGAGGTCTGCAGC	Reverse primer for PAC1

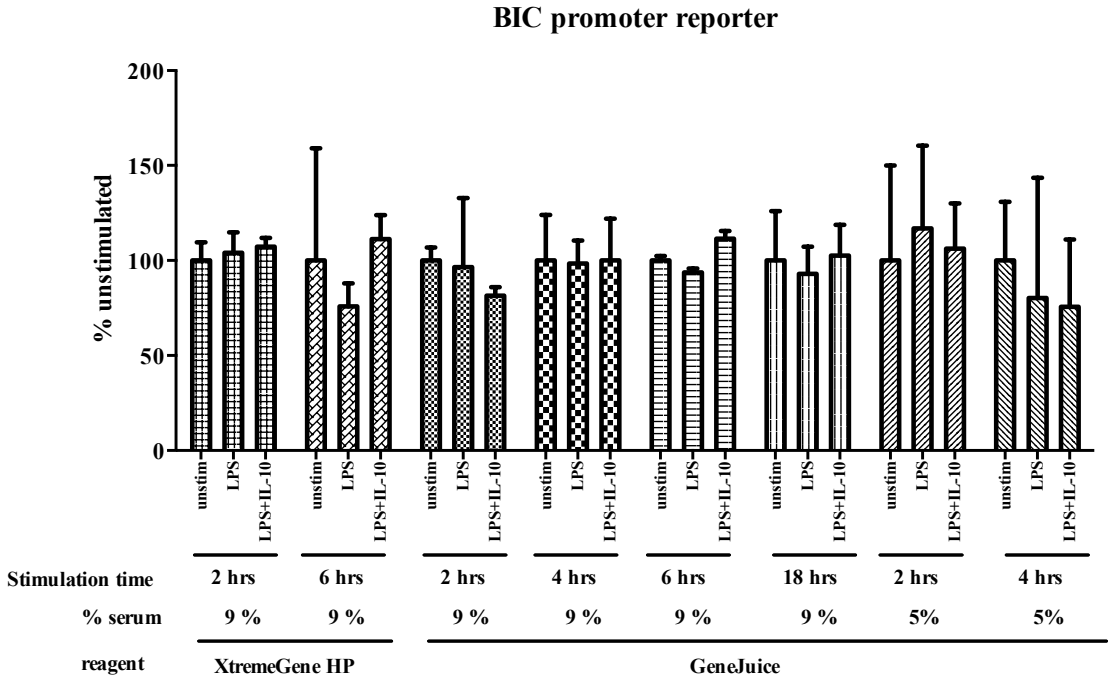

Figure A.1 The BIC promoter reporter is unresponsive to LPS and IL-10.

The BIC promoter reporter constructs were transfected into RAW264.7 cells using either XtremeGene HP transfection reagent or GeneJuice transfection reagent according to the manufacturer's instructions. Cells were then rested in medium containing 9% or 5% serum for 24-48 hours before stimulation for the indicated time. Luciferase activity was measure with Dual-Glo Luciferase Assay System, and plotted as % of the unstimulated samples.

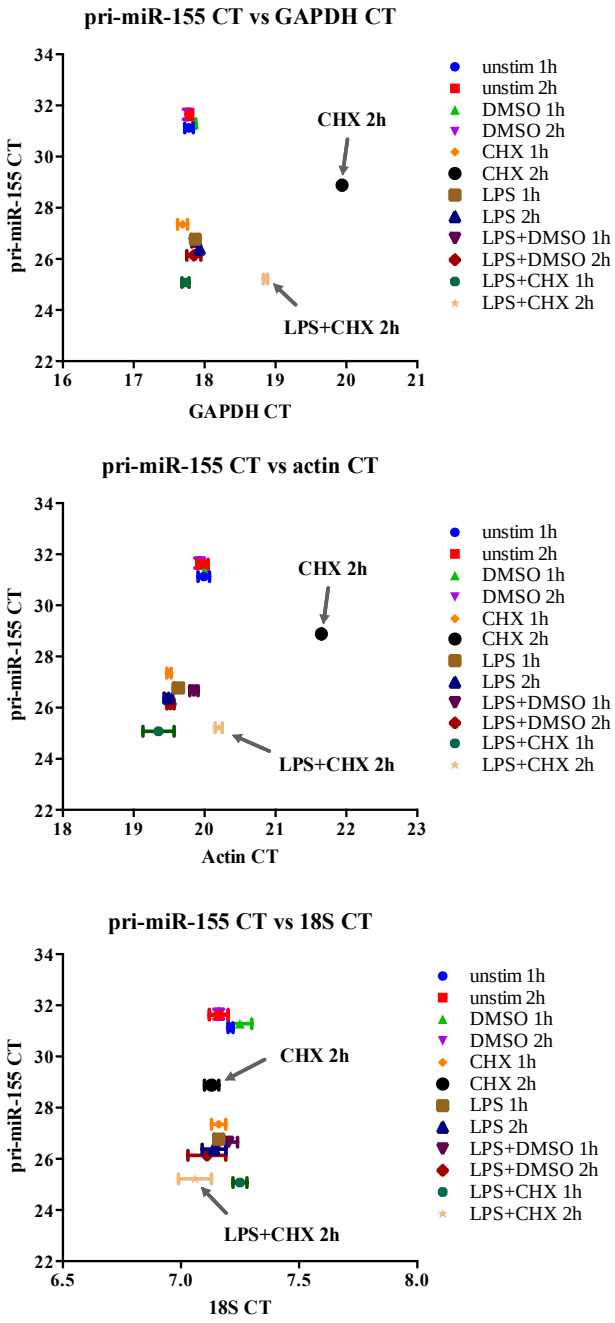

Figure A.2 CHX treatment alters the expression level of GAPDH and actin, but not that of 18S rRNA.

RAW264.7 cells were treated with DMSO, CHX, ActD, LPS or LPS+CHX for 1 or 2 hours prior to RNA extraction and determination of pri-miR-155, GAPDH, actin and 18S rRNA levels by real time PCR. Raw Ct values of pri-miR-155 were plotted against those of each normalization control.

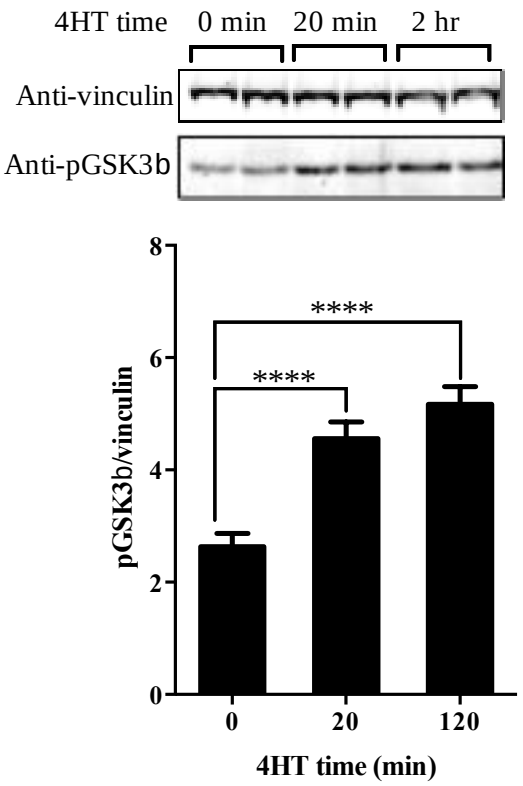

Figure A.3 4-HT treatment in the AKT-ER cells increases phosphorylation of GSK3β.

AKT-ER cells were either untreated or treated with 150 nM 4-HT for 20 minutes or 2 hours prior to immunoblotting analysis for phospho-GSK3β (pGSK3β) and vinculin (loading control).

Table A.4: Results of SERp server

Residue numbering of mouse SHIP1 sequence is based on the RefSeq entry with accession number of NP_034696.

Cluster	Suggested Mutation	Description
Cluster A:	E 637 => A	Residues 637 - 639: EEEE SERp Score: 7.77
	E 638 => A	
	E 639 => A	
Cluster B:	E 550 => A	Residues 550 - 552: EKK SERp Score: 5.86
	K 551 => A	
	K 552 => A	
Cluster C:	E 770 => A	Residues 770 - 773: QEGENEEGSEGE SERp Score: 5.85
	E 772 => A	
	E 773 => A	